Hypoxic Regions in Mesothelioma Likely Modulate Cross-Talk between Tumour Cells, Macrophages and Endothelial Cells and Regulate Responses to Immunotherapy

Abdulwahed Alrehaily

This thesis is presented
for the
Degree of Doctor of Philosophy
of
Curtin University

March 2021

DECLARATION

To the best of my knowledge and belief this contains no material previously published by any other person except where due acknowledgement has been made. This thesis contains no material which has been accepted for the award of any other degree or diploma in any university.

Human Ethics The research presented and reported in this thesis was conducted in accordance with the National Health and Medical Research Council National Statement on Ethical Conduct in Human Research (2007) – updated March 2017. The proposed research study received human research ethics approval from the Curtin University Human Research Ethics Committee (EC00262), Approval Number # HRE2017-0823.

Signature:
Date:

ABSTRACT

Mesothelioma is an aggressive tumour that can develop decades after exposure to asbestos. Hypoxia is a hallmark of locally advancedsolid tumours and is recognized as a key determinant of tumour aggressiveness (1). It has been reported that significant regions of hypoxia are formed in human malignant mesothelioma (HMM) as the tumour progresses (2, 3), which augments the aggressive phenotypes of HMM (4). Tumour hypoxia plays a fundamental role in macrophage recruitment and accumulation within the hypoxic regions of tumours (5). Solid tumours, including mesothelioma tumours, develop their own vascular system to support their growth and metastasis (6). The newly formed tumour blood vessels represent poorly functional vasculature, enforcing a hypoxic environment within tumours (7). Our group has shown that the intra-tumoural injection of Interleukin-2 (IL-2) or an agonistanti-CD40 antibody (α-CD40) alone can shrink small, but not large, mesothelioma tumours (8, 9). However, our group also found that the intra-tumoural injection of IL-2 combined with α-CD40 induced curative regression of large tumours (8-10), therefore, the effect of IL-2/α-CD40 on mesothelioma cells, macrophages and endothelial cells under hypoxia was examined in this thesis. Furthermore, VTX-2337 has been shown to activate immune cells via TLRand has been assessed in a phase I oncology trial and was therefore also tested in this thesis(11, 12).

This project's overall hypotheses was that the effect of the dynamic properties of the human mesothelioma microenvironment could be represented by studying the crosstalk between mesothelioma tumour cells, macrophages and endothelial cells (ECs) under hypoxic and normoxic conditions. It was further hypothesised that these cells' responses to immunotherapies involving IL-2, α-CD40 and VTX-2337 could be better understood by developing a 3D spheroid tumour model incorporating the three cell types (mesothelioma cells, macrophages and ECs). It was hoped that this organoid approach would reproduce the in-vivo tumour microenvironment and reveal novel immune/EC-mediated therapeutic approaches for treating mesothelioma. Whilst considerable progress in developing solid 3D human and murine spheroid tumour

models aiming to incorporate the three cell types was achieved, a major hurdle proved to be maintaining the viability of the ECs (human umbilical vein endothelial cells (HUVECs) – a problem which had not been solved at the time this thesis was written. The 3D work was stopped due to time and budget constraints; this is addressed in chapter 6. Therefore, the study was continued using a 2D model under two in vitro conditions – normoxia (20% O_2) and hypoxia (2% O_2). The aim was to determine changes that may occur in these two environments (that are both seen in tumour microenvironments, sometimes simultaneously) and avoid models that are only conducted at atmospheric conditions (21% O_2) and do not simulate the real tumour microenvironment(13). Therefore, the aims of the project are:

- To assess the effect of hypoxia on human macrophage subsets (MØ, M1 and M2) and endothelial cells (human umbilical vein endothelial cells, HUVECs). Cells were grown in a hypoxic environment and compared to their normoxic controls using multiparameter staining and flow cytometry.
- To investigate the effect of mesothelioma-derived factors on macrophage subsets (MØ, M1 and M2). Human monocyte-derived macrophages were incubated under hypoxic conditions with mesothelioma-derived factors also generated under hypoxia, and compared to the normoxic mesothelioma model, in which mesothelioma-derived molecules were generated under normoxia and macrophages differentiated from monocytes under normoxia using multiparameter staining and flow cytometry.
- To investigate the effect of mesothelioma-derived factors on ECs under normoxic versus hypoxic conditions. HUVECs were incubated in hypoxic conditions with mesothelioma-derived factors generated under hypoxia, and compared to the normoxic mesothelioma model, in which the mesothelioma-derived molecules were generate under normoxia, using multiparameter staining and flow cytometry.
- To investigate the cross talk between macrophages and HUVECs under normoxia and hypoxia, HUVECs were exposed to supernatants collected from

macrophage subsets (MØ, M1 and M2) under their relative conditions examined for changes using multiparameter staining and flow cytometry.

- To assess molecular alterations in macrophages and ECs in response to 24 hour exposure to IL-2, α-CD40, IL-2/α-CD40 or VTX-2337 under normoxic versus hypoxic conditions using multiparameter staining and flow cytometry.
- To assess the effect of supernatant from mesothelioma-exposed macrophages treated with IL-2, α-CD40, IL-2/α-CD40 and VTX-2337on ECs under normoxic versus hypoxic conditions using multiparameter staining and flow cytometry.
- To use an *in silico* approach to confirm in vivo expression of target genes among human cancers including mesothelioma.
- To use an *in silico* approach to identify possible mechanisms for upregulation of molecules seen in mesothelioma-exposed ECs and macrophages under hypoxia by identifying functionally active hypoxia response elements (HREs) in promoter regions of the target genes; identifying hypoxia related transcription factors binding sites (TFBSs), and determining the role of hypoxia related transcription factors; and analysing relevant signalling pathways.

The comparison of the in vitro results between normoxic and hypoxic 2D cell culture monolayers should aid translational studies on macrophage profiling, vessel-wall injury and treatment effects in healthy and diseased (mesothelioma) human tissues. This work demonstrated the importance of choosing the appropriate in-vitro environment in which to study tumours, where oxygen levels affect mesothelioma tumour cells, macrophages and endothelial cells. The data highlighted the complexity of the potential crosstalk between mesothelioma cells, macrophages and ECs under two different oxygenation levels, especially when considering that a single tumour microenvironment can contain both hypoxic and normoxic regions. This becomes more complicated when attempting to dissect the effect of responses to stimuli, such as LPS/IFN-γ, IL-4/IL-13, IL-2 +/- anti-CD40 and VTX-2337.

The impact on macrophages includes modulating their capacity for T cell stimulation via decreased HLA-DR antigen presentation, decreased or increased co-stimulatory (CD40, CD80 and CD86) and co-inhibitory (CD39, A2A-R, PD-L1 and Gal-9) pathway

activity, and modification of their bioenergetic profiles towards high OXPHOS, associated with high ATP production, yet simultaneously maintaining glycolysis. However, with inadequate oxygen availability, macrophages decrease mitochondrial ATP production through OXPHOS but maintain their glycolytic rate. The hypoxic environment proved to be harsh on macrophages, as their responses to LPS/IFN-γ were compromised in comparison to those seen under normoxia, which may contribute to their poor responses to stimuli, downregulated mitochondrial respiratory activity and ATP production.

Hypoxia plays a major role directly and indirectly on ECs by modifying molecules secreted by macrophages, thereby affecting ECs. The effect on ECs demonstrated potentially increased vascular permeability, leukocyte extravasation and potential metastatic activity as hypoxia lead to increased expression of CD309, CD54 and CD105. While indirect hypoxia effects include modulating soluble factors secreted by macrophages which in turn modulate ECs expression of CD144 (VE-cadherin). This study also demonstrates that normoxic and hypoxic tumour-derived factors can modify the functional status of ECs. Under normoxia, only CD54 increased, with CD309, CD146, CD144 and CD105 remaining unchanged in response to tumour derived factors; however, hypoxia led to the upregulation of CD309, CD146, CD105 and CD54.

The *in silico* study confirmed in vivo gene expression of the target molecules of interest (HLADR, CD206, CD309, CD54, CD40, CD144, A2A-R, CD105, CD163, CD80, Gal-9, CD39, CD86, PDL-1, and CD146) in human mesothelioma. The *silico* study also showed that HREs could not account for elevated expression of CD309, CD54, CD105 and CD146 on ECs or macrophages under hypoxic conditions, as there were no functionally active HREs in promoter regions of genes for these molecules. However, hypoxia related TFBSs in promoter regions of the upregulated genes under hypoxia in mesothelioma were identified. The presence of binding sites for essential TFs related to hypoxia in the VEGFR2, CD54, CD105 and PD-L1 genes on ECs and/or macrophages provides a plausible underlying mechanism for their upregulation in the

hypoxic mesothelioma microenvironment. These findings may help identify novel targets and possible combination treatments for mesothelioma.

ACKNOWLEDGEMENTS

First, I would like to express my sincere gratitude to my supervisors, Associate Professor Delia Nelson and Dr. Connie Jackaman, for their invaluable guidance and continuous encouragement and support throughout the duration of this project. Your enthusiasm, scientific knowledge and expertise in tumour immunology have been invaluable and truly helped me in the field.

I would also like to extend my deepest gratitude to Associate Professor Elizabeth Watkin, the chairperson of my thesis committee, for her help and support.

I would also like to express my sincere thanks to Dr. Munazzah Tasleem for her guidance, teaching and sharing her experiences in bioinformatics.

Extended thanks go to current and previous members of the Nelson laboratory group, Joanne, Audrey, Lelinh, Wei Khei and Stephen Proksch. I greatly appreciate the support, friendship, laughter and memorable moments over the years. More specifically, I would like to thank Sheeraz. I am so glad to have had you by my side throughout this journey. It has been so much fun sharing a desk with you and working side by side in the lab. Thank you for making me smile, helping me overcome challenges and always being there.

I am also extremely grateful to Jeanne Edmands for her amazing help in training me on flow cytometry, panel design and data analysis. Thank you for your kindness and friendship.

I want to express my deep gratitude to Steve Broomfield for his friendship and for allowing me to share his hypoxia incubator.

Some special words of gratitude go to my friends Mohammed Yaro and Sam Siem, with whom I have shared moments of deep anxiety but also joyous excitement. Thanks to you both for the memorable moments we have had and the laughs we have shared.

Last, but certainly not least, I would like to express my deepest gratitude and special words of thanks to my family for their warm love, continued patience, encouragement and endless support.

TABLE OF CONTENTS

LIST OF FIGURES

LIST OF TABLES

LIST OF ABBREVIATIONS

A2AR	Adenosine receptor 2
ADP	Adenosine diphosphate
APCs	Antigen presenting cells
ATP	Adenosine triphosphate
BM	Bone marrow
CSFR-1	Colony stimulating factor receptor 1
CTLA-4	Cytotoxic T-lymphocyte-associated protein 4
CXCL	C-X-C motif chemokine ligand
DMSO	Dimethyl sulfoxide
EDTA	Ethylenediaminetetraacetic acid
ETC	Electron transport chain
FCS	Fetal calf serum
G-CSF	Granulocyte-colony stimulating factor
Gal-9	Galectin-9
GM-CSF	Granulocyte-macrophage colony-stimulating factor
GPT	Glutamic pyruvic transaminase
HLA-DR	Human Leukocyte Antigen
HREs	Hypoxia response elements
HUVECs	Human umbilical vein endothelial cells
IFN-γ	Interferon-γ
IL	Interleukin
IL-2/CD40	Interleukin-2 combined with agonist anti-CD40 antibody
JAK2	Janus kinase
LDH	Lactate Dehydrogenase
LPS	Lipopolysaccharides
M-CSF	Macrophage colony-stimulating factor
MHC	Major histocompatibility complex
MMPs	Matrix metalloproteinases
MCTS	Multicellular tumour spheroid

NADH	Nicotinamide adenine dinucleotide
NF-κB	Nuclear factor-kappa B
OCR	Oxygen consumption rate
OXPHOS	Oxidative phosphorylation
PAMPs	Pathogen-associated molecular patterns
PBMCs	Peripheral blood mononuclear cells
PBS	Phosphate-buffered saline
PD-1	Programmed cell death protein 1
PD-L1	Programmed death-ligand 1
PK	Pyruvate kinase
PPP	Pentose phosphate pathway
PRRs	Pattern recognition receptors
ROS	Reactive oxygen species
STAT	Signal transducer and activation of transcription
TAMs	Tumour-associated macrophages
TCM	Tumour-conditioned media
TCM-CM	TCM-conditioned macrophages
TCM-CM1	TCM-conditioned M1 macrophages
TCM-CM2	TCM-conditioned M2 macrophages
TCR	T cell receptor
TFBSs	Transcription factors binding sites
TGF	Transforming growth factor
TIM-3	T cell immunoglobulin and mucin-domain containing-3
TLR	Toll-like receptor
TNF	Tumour necrosis factor
Treg	Regulatory T cell
VEGF	Vascular endothelial growth factor

CHAPTER 1
INTRODUCTION

1.1 Mesothelioma

Mesothelioma is a rare, aggressive cancer that affects serosal membranes and is primarily caused by exposure to asbestos. Pathologically, mesothelioma develops from the transformation of mesothelial cells. Mesothelial cells form the serosa membrane, a layer that comprises the linings of body cavities such as the heart sac (pericardium), thoracic cavity (pleura), the abdominal cavity (peritoneum) and the tunica vaginalis of the testes (14). The development of mesothelioma is primarily associated with the inhalation of asbestos fibres. More than 80% of all mesotheliomas originate in the pleural area. Once asbestos fibres are inhaled and reach the pleural cavity, they are able to directly injure mesothelial cells to induce tumour development (15). This induction can occur by fibres penetrating the lungs and crossing into the pleural cavity, resulting in pleural irritation. The fibres are also capable of damaging mesothelial cell chromosomes by piercing their mitotic spindles. They may also promote local inflammation that generates reactive oxygen species (ROS), which can damage DNA and activate proto-oncogenes (16, 17). Currently, the incidence of malignant mesothelioma (MM) worldwide is rising. Even though asbestos has been prohibited in most western countries, incidences of mesothelioma have continued to rise due to its long latency period of about 20 years. Some studies have even shown that this period can extend to 70 years. The latency period is the period between initial asbestos exposure and clinically detectable mesothelioma (16, 18, 19). For example, in Australia, the annual mesothelioma incidence rate between 1982 and 2009 increased from 156 to 666 (20).

Diagnosis of mesothelioma cancer is first conducted through a chest X-ray to identify the presence of a pleural effusion or any pleural thickening. Further imaging follows using a CT scan, and cytological and histological studies of the pleural fluid and extracted biopsies are conducted (21).

There are three histological categories of mesothelioma: sarcomatoid mesothelioma, which occur as spindle cell morphologies in 20% of mesotheliomas; epithelioid mesothelioma, which constitute around 60% of mesotheliomas; and biphasic mesothelioma, which constitute 20% of mesotheliomas. Biphasic mesotheliomas have a combination of sarcomatoid and epithelioid histologies and are commonly termed Biphasic-E or Biphasic-S, depending on the predominant histology (sarcomatoid or epithelioid cells) (22, 23). The median survival rates of patients diagnosed with mesothelioma depends on the histological subtype. For instance, pure epithelioid histologies allow for a longer survival of around 12-27 months post diagnosis. In contrast, sarcomatoid histologies have the shortest endurance rate of 7-18 months, while biphasic tumours occur with a transitional outcome of around 8-21 months (23).

1.1.1 Hypoxic environment of mesothelioma

In solid tumours including mesothelioma, hypoxia is created when oxygen levels required by proliferating tumour cells surpasses the amount of oxygen that the tumour receives through the bloodstream (24). Different studies have shown that hypoxia in human malignant mesothelioma (HMM) is a major barrier to effective mesothelioma treatment because hypoxic tumour cells tend to be resistant to chemotherapy and radiation through inhibition of apoptosis (4, 24). Hypoxia also enhances mesothelioma cell survival, migration and invasion (4).

1.1.2 Current treatments

Currently, there is no curative therapy for MM. Thus, the goals of current treatment are to reduce patients' symptoms, extend life expectancy and improve quality of life. Chemotherapy, surgery and immunotherapy represent current treatment options available for mesothelioma patients (15, 23).

1.1.2.1 Chemotherapy

Combination chemotherapy, which includes antifolate and platinum regimens, has been established for the treatment of mesothelioma. Pemetrexed plus cisplatin is the currently

approved regimen with Phase III studies showing a 45.5% tumour response rate with improvements in progression-free survival of about 6.1 months, overall survival of 13.3 months, and improvements in cancer-associated symptoms. Nonetheless, the benefits of the therapy are limited and survival is estimated to be prolonged by a few months (15, 23).

1.1.2.2 Surgery

Debulking surgery is a procedure that involves removal of a portion of the lung, the pleura, the pericardium and the diaphragm. However, because mesothelioma tumours grow diffusely, they are difficult to totally resect (15). Although extrapleural pneumonectomy procedures have largely been abandoned due to their poor results, as shown by the Mesothelioma and Radical Surgery (MARS) trial, they are considered a treatment therapy in North America. Furthermore, while randomised trials on extended pleurectomy decortication are currently being conducted in the United Kingdom, the procedure remains controversial elsewhere (23).

1.1.2.3 Multimodal approaches

As the aim of surgery in mesothelioma patients is to reduce the number of cancer cells, some residual tumour tissue is generally left behind. Multimodal approaches, which involve surgery combined with chemotherapy, are other options used to eliminate remaining tumour cells (15).

1.1.2.4 Radiotherapy

Although radiotherapy can relieve pain, there is no evidence that it is effective alone, as MM is not sensitive to it. In some cases, radiotherapy can be used as part of a multimodal approach by combining it with surgery and/or chemotherapy (15).

1.1.2.5 Immunotherapy

As mentioned before, the prognosis of mesothelioma patients remains poor. This has triggered studies on the application of immunotherapy in the treatment of mesothelioma (25). There is data suggesting that immune modulation in mesothelioma patients can be beneficial (26). The induction of immune responses is not a new method in cancer. For

instance, the first attempt was by William Coley over a century ago who injected inoperable sarcoma patients with streptococci (27). Around 10% of these cases experienced tumour regression (28). Cancer immunotherapy mainly involves use of compounds to promote killing of tumour cells by the host's immune response (28, 29). Our group has shown that administration of Interleukin-2 (IL-2) or an agonist anti-CD40 antibody when used as single drugs into tumours can cure small murine mesothelioma tumours (8, 9), while the IL-2/α-CD40 combination induces regression of larger mesothelioma tumours (8, 10). Furthermore, IL-2-/CD40-activated macrophages rescued production of IFN-γ by T cells from geriatric mice. Therefore, targeting macrophages using IL-2/α-CD40 may improve innate, as well, as T-cell immunity (30). Furthermore, VTX-2337 has been assessed in a phase I oncology trial (12). Both approaches will be explored in this thesis.

1.1.2.5.1 Interleukin-2 (IL-2)

IL-2 is involved in the propagation and differentiation of immune cells (31, 32). IL-2 resembles granulocyte-macrophage colony-stimulating factor (GM-CSF) and IL-4 in structure, as they are 15.5 kDa glycosylated proteins (33, 34). IL-2 is mainly produced by $CD4^+$ T helper cells and stimulates the growth and differentiation of T and B cells, and the proliferation and activity of cytotoxic T cells (32). The growth of some human tumour cells is inhibited by IL-2 (35). IL-2 biological activity occurs via interaction with its cognate receptor, which consists of three subunits: IL-2Rα (CD25), IL-2Rβ (CD122) and γc (CD132) (31). Whilst a number of human clinical trials have shown that IL-2 can promote anti-cancer activity, systemic IL-2 administration can be toxic. However, when locally applied, it has been seen in pre-clinical trials to be safe and effective in cancer treatment, including for mesothelioma. For instance, IL-2 administration in mice with small flank tumours at the beginning of treatment results in increased survival. However, for larger tumours, the rate of survival did not increase (9).

1.1.2.5.2 Anti-CD40 antibody

CD40 was first identified on B cells and was known as a B cell growth activator (36, 37). CD40 is a 48 kDa transmembrane glycoprotein receptor and is a member of the tumour necrosis factor receptor superfamily (TNFRSF) (38). CD40 is also found on other antigen presenting cells (APCs) such as DCs and macrophages and non-immune cells including epithelial and endothelial cells. CD40 can be found on activated T cells, as well as some tumour cells (39-41). CD154 (also known as Bp35, CD40L, TRAP or T-BAM) is the ligand for CD40. CD154 is a 34–39 kDa type II integral membrane protein. CD40L can be expressed in various cells, such as monocytes, platelets, activated T cells, ECs, basophils, activated human dendritic cells (DCs) and eosinophils (42). Agonist anti-CD40 antibody generates a number of changes when targeted into the tumour bed (43). For example, CD40-activated tumour blood vessels become permissive to T cell migration and DC emigration (43). However, CD40-activated ECs have also been shown to promote tumour neoangiogenesis in a murine model of mammary carcinoma (43, 44).

1.1.2.5.3 Toll-like receptors (TLRs)

TLRs are a family of proteins that recognize different pathogen-associated molecular patterns (PAMPS) as well as damage-associated molecular patterns (PAMPs and DAMPs) and provide the initial defence against pathogens (45, 46). Upon recognition, TLRs activate inflammatory responses via NF-kB that acts as a switch for inflammation and is involved in tumour development associated with chronic inflammation (47). Once TLRs are engaged, various cell populations are activated and cytokine and inflammatory mediator production is upregulated, leading to immune responses (12). TLR3, 7, 8 and 9 induce protective immune responses by detecting viral and bacterial nucleic acids. These TLRs have been linked to RNA detection (48). TLR8 is expressed primarily in macrophages or monocytes, neutrophils and myeloid dendritic cells. A new TLR8 agonist, known as Motolimod (formerly known as VTX-2337) activates monocytes, Natural Killer (NK) cells and DCs, increases cytolytic activity and IFN-γ production (49). VTX-2337 may help shift the TAM phenotype from M2 towards M1.

1.2 Tumour Immunity

1.2.1 The immune system

The immune system is a defence mechanism whose main function is to protect the body by recognising non-self "infectious organisms", such as viruses, bacteria, parasites and fungi, and altered-self "transformed cells", such as tumour cells. Molecules that can be recognised by the immune system are known as antigens, and the ability of the body to resist these invaders is referred to as immunity. The immune system is made up of complex interconnections of molecules, cells, tissues and organs. There are two major types of immunity: innate immunity and adaptive immunity (50).

1.2.1.1 The innate immune system

The innate immune system responds rapidly to tissue destruction and infection and is highly selective in recognising pathogens. The innate system includes epithelia, which are the first line of defence in fighting pathogens. Innate immunity is acquired naturally by the host and does not require antigen sensitisation since it is acquired at birth and remains active throughout the person's life. It is comprised mainly of a wide array of cells, including macrophages/monocytes, NK cells and DCs, as well as several plasma proteins, such as the complement system. Its mechanism of action occurs when an infectious agent penetrates the body's physical and chemical barriers, such as epithelial tissue, whereupon pattern recognition receptors (PRRs) detect specific molecular structures. These structures or PAMPs, vary depending on the type of pathogen. For instance, bacterial PAMPs mainly comprise of lipoteichoic acids, lipopolysaccharides (LPS) and peptidoglycan. β-glucan, the most abundant fungal cell wall polysaccharide, and unmethylated CpG motifs found in the nucleic acid of bacteria and viruses, can also be recognised. Once a pathogen is recognised by PRRs such as toll-like receptors (TLRs), immune cells are activated leading to pathogen uptake by phagocytic cells such as neutrophils, macrophages and DCs. In addition, activated immune cells secrete pro-inflammatory chemokines and cytokines resulting in the activation and recruitment of other immune cells within the host (51).

1.2.1.2 The adaptive immune system

Unlike innate immunity, adaptive immunity develops throughout an individual's life and during the priming phase exhibits delayed responses towards pathogens. It develops upon exposure to pathogens including when a person is immunised through vaccinations. Adaptive immunity involves specialised T and B lymphocytes, which recognise many types of antigens. B cells are derived from B cell progenitors in the bone marrow and their maturation is accompanied by expression of membrane-bound immunoglobulins, called B cell receptors (BCRs). Activation of B cells upon an antigen binding the BCRs leads to their differentiation into memory or antibody-secreting plasma cells. On the other hand, T lymphocyte precursors migrate from the bone marrow to the thymus, where they complete their antigen-independent maturation into functional T cells. These lymphocytes contain T cell receptors (TCRs), which recognise antigens displayed as peptides by major histocompatibility complex (MHC) molecules on the surface of tissue cells. T cells are divided into two subsets, namely $CD4^+$ and $CD8^+$ T cells. The former recognises antigens embedded in MHC class II molecules, while $CD8^+$ T cellsrecognise antigens in MHC class I molecules. For full activation of T cells to occur, additional costimulatory signals via molecules such as CD80, CD86 and CD40 must occur. Along with MHC molecules, these costimulatory signals are mainly displayed by APCs (52, 53), with professional APCs being macrophages, B cells and DCs.

1.2.2 Tumour immunology

The local microenvironment of a cancer contains immune cell subsets which have the ability to prompt anti-tumour responses (54). Even though the immune system can recognise and eliminate abnormal cells, cancer is a very common disease with around 38% of women and 39% of men diagnosed with cancer at some point in their lives (55). This is a clear indication that the body's immune responses against tumours is insufficient and cannot destroy tumours completely.

The inability of the immune system to completely destroy tumours can be attributed to several factors. First, some subsets of immune cells promote tumour development. Additionally, the induction of immunosuppressive tumour microenvironments through

conditions, such as hypoxia or secretion of suppressive factors, can assist tumours to evade immune destruction (56). Furthermore, the immune system may facilitate tumour progression by modifying their immunogenic phenotypes during cancer development through a concept referred to as cancer immunoediting (57, 58). Indeed, avoiding immune destruction is recognised as one of the hallmarks of cancer (59).

There are three phases of tumour outgrowth: elimination, equilibrium and escape. These are referred to as the "three Es" of immunoediting. Elimination, the first phase, involves recognition and elimination or control of tumour growth by the immune system. In equilibrium, the second phase, selection and/or promotion of tumour cell variants due to their inherent genetic instability occurs, leading to an increased capacity to survive immune attack. The third phase, known as the escape phase, refers to the final outgrowth of tumours. During this time, immunologically sculpted tumours begin to grow progressively and produce cells that are resistant to immune effector cells (59-61). Evidence has accumulated that during neoplastic programming, cancer cells recruit and re-educate immune cells to become active collaborators in the process (62).

1.2.3 Macrophages

Macrophages were first described by Elie Metchnikoff in the 19th century as phagocytic cells that have the ability to engulf and destroy pathogens such as bacteria (63). The origin of macrophages is a topic of a debate that many researchers have investigated. For instance, it has been opined that macrophages originate from the circulating adult precursor cells referred to as monocytes, which are produced from bone marrow that later differentiate into macrophages upon entry into tissues. Ginhoux et al. (2010) argued that recruitment of tissue macrophages occurs during embryonic development, after which they persist into adulthood independent of input by blood monocytes (64, 65).

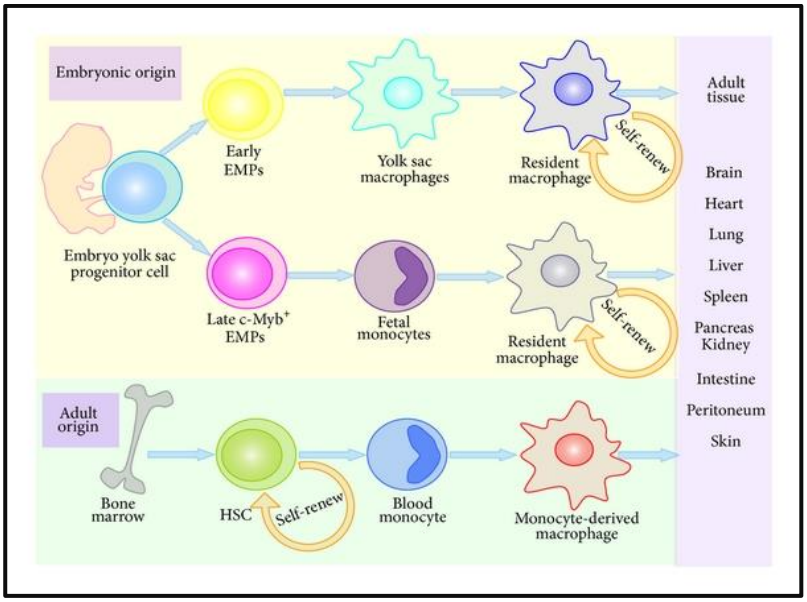

Figure 1. 1 The origin and development of tissue-resident macrophages (66)

The diversity or heterogeneity of tissue macrophages is proposed to be dependent on the tissue microenvironment. Heterogenicity also includes differences in functional specialisations. For instance, macrophages may differentiate to attain a functional specialisation that is driven by tissue-specific signals. Therefore, resident macrophages are referred to as microglia (brain), osteoclasts (bone), alveolar macrophages (lung), Langerhans cells (dermis), Kupffer cells (liver) and histiocytes (interstitial connective tissue) (67) (see Figure 1.1 (66). It is important to note that the tissue differentiation of these macrophages is both functional and phenotypical. However, this differentiation is not end-stage because tissue macrophages still retain the capacity to proliferate alongside functional plasticity. Macrophage activation refers to the process through which the morphology and functional activity of macrophages is altered after engagement of PRRs. This response is mainly influenced by cytokines and involves enlargement of resting macrophages, making them more motile. These macrophages also increase MHC class II proteins on their surface, have more lysosomes and lysosomal enzymes and increased phagocytic activity, among other properties (68). Based on their activation status, macrophages can be classified into classically-activated pro-inflammatory macrophages (M1-like) or alternatively-activated anti-inflammatory macrophages (M2-like). M1 macrophages are induced by microbial

products, including LPS and/or cytokines, such as tumour necrosis factor alpha (TNF), interferon-γ (IFN-γ) and granulocyte-macrophage colony-stimulating factor (GM-CSF) and amongst other functions promote tumour destruction. In contrast, activation of M2 macrophages is mainly regulated by glucocorticoids interleukin-4 (IL-4), IL-13 and IL-10 (69)however, these M2 cells can promote tumour development (see Figure 1.2 (70)).

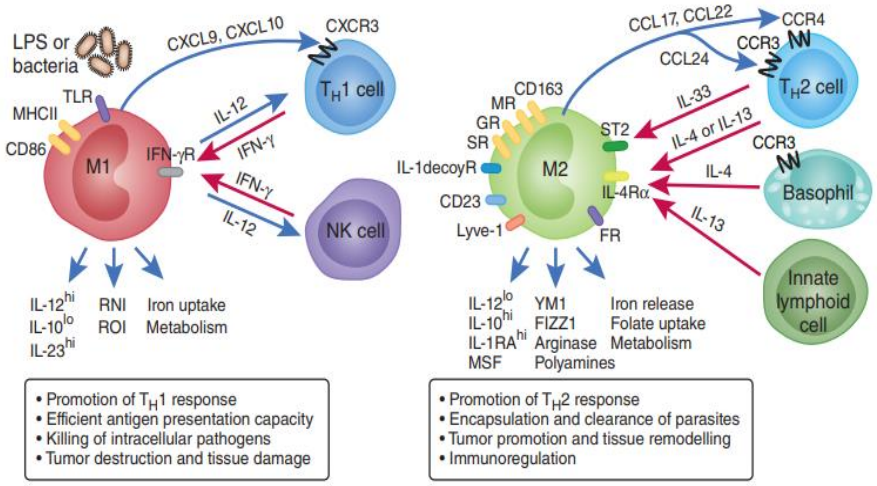

Figure 1. 2 Schematic and polarisation of macrophage activation by lymphoid cells (70)

1.2.3.1 Macrophage expression of activation markers

Signals from APCs, including macrophages, are required to activate T cells (71). The first signal required is antigenic peptide presented on MHC class I and II molecules to the TCR. MHC II, also called human leukocyte antigen-DR (HLA-DR), is a cell-surface glycoprotein that presents peptide antigens to $CD4^+$ TCRs leading to the coordination and regulation of effector or regulator cells (71-73). For full T cell activation, costimulatory signals include engaging the T cell co-stimulator, CD28, by its ligands that are members of the B7 family, i.e. B7-1 and B7-2 (also called CD80 and CD86 respectively); CD40 ligand (CD40L):CD40 interactions are also required (74). CD40 is a member of the tumour necrosis factor super family. It is a 48-kDa type I transmembrane protein and interacts with CD40L (CD154) on T cells (75). The CD40-CD40L axis is necessary in the delivery of T cell help for CTL priming (39) and plays

a key role for tumour rejection mediated by $CD8^+$ effector cytotoxic T lymphocytes (CTLs)(76). This is because upon CD40 ligation, APCs upregulate costimulatory molecules such as CD80 and CD86 (75). Macrophages activated via agonist anti-CD40 antibody also exhibit direct tumoricidal activity against B16 melanoma cells, through TNFα and NO secretion (77).

CD80, a 55 kDa type I hydrophobic transmembrane glycoprotein, and CD86, a 70kDa type 1 membrane glycoprotein, are members of the immunoglobulin supergene family (IgSF). Macrophages have been reported to express low basal levels of CD80 and moderate basal levels of CD86 (78). Expression of both molecules increases rapidly after stimulation via GM-CSF, CD40, IFN-γ, IFN-α and LPS; however, cytokines such as IL-4 and IL-10 may inhibit their expression (72, 79). After CD80/CD86-CD28 interactions, CD28 provides an essential costimulatory signal that induces T cell activation, proliferation, and differentiation to acquire effector functions (73, 80). This interaction also triggers T cells to produce IFN-γ and IL-2 (81). After T-cell activation, CTLA-4 surface expression is upregulated rendering it available for binding to CD86 or CD80 leading to inhibitory signals that prevent immune overactivation (80). CTLA-4 has a higher affinity for CD86 or CD80 and out-competes CD28 to inhibit IL-2 accumulation and restrict T cell transition from the G1 to the DNA Synthesis (S) phase (82, 83).

1.2.3.2 Macrophage expression of regulatory markers

Activation of immune checkpoint mechanisms can occur within the hypoxic tumour microenvironment to suppress local anti-tumour immune responses. Accumulating data have highlighted the impact of purinergic nucleotides such as adenosine in modulating the immune response (84, 85). In inflammation, adenosine triphosphate (ATP) the most studied purine, is actively released by immune cells in extracellular spaces (86). Local tumour-associated metabolic activity can regulate the recruitment and functional polarization of immune cells via ATP. ATP contributes to inflammation by binding P2 purinoreceptors, such as P2X7, on immune cells (87, 88). Most cell types, including macrophages, produce ATP following activation or stress. ATP attracts APCs, leading to enhanced anti-tumour responses (88). Extracellular ATP is rapidly hydrolysed by the

membrane-bound nucleotidase,CD39 (NTPDase1 nucleoside triphosphate diphosphohydrolase 1) into adenosine diphosphate (ADP) and adenosine monophosphate (AMP). The final step, the dephosphorisation of AMP, into adenosine, is activated by ecto-5'nucleotidase, or CD73 (84, 88). Adenosine can inhibit immune cells (88). Among adenosine receptors, such as A1, A2A, A2B and A3, the 2A receptor is the highest affinity receptor (89) and plays a significant role in reducing inflammation and tissue damage (88). The presence of adenosine in tumours is a critical metabolic immune checkpoint that impairs anti-tumour immune responses (90).

Ectonucleotidase and adenosine production can be controlled by the microenvironment. For example, hypoxia contributes to increasing the rate of extracellular adenosine accumulation by upregulating CD39, which leads to increased adenosine production (90). Furthermore, cytokines can control ectonucleotidase expression. For example, in tumours, IL-27 induces CD39 on local cells (88).Some cancer tissues increase extracellular adenosine, which directly promotes tumour progression which is further aided by its immunosuppressive functions on effector T cells whilst promoting regulatory T cells (Treg). High expression of extracellular adenosine in mesothelioma leads to tumour cell apoptosis but maintains tumour growth showing its importance in disease progression (87).

Programmed death ligand-1 (PD-L1, CD274 or B7-H1) is a type I transmembrane protein expressed by tumour cells, TAMs and T cells. Binding PD-L1 to PD-1 on activated T and B cells leads to immune suppression. In tumours, cytokines such as TNF-α and IFN-γ, and factors such as hypoxia increase PD-L1expression, which enhances interactions between PD-1 and PD-L1 and inhibits CTLs (91). In lung cancer, a poor prognostic value was associated with high intensity PD-L1 expression by macrophages(92). Galectin-9 (Gal-9) is another immune modulator belonging to the tandem-repeat subfamily of galectins (93, 94). Expression of Gal-9 has been detected in macrophages (95). T cell immunoglobulin mucin (Tim)-3 is a receptor expressed by Th1 cells and $CD8^+$ T CTLs(96). The binding of Gal-9 to Tim-3 induces apoptosis of Tcells and negatively regulates immune responses mediated by Tcells (96-98).

1.2.3.3 Macrophage expression of scavenger receptors

The main function of scavenger receptors is to recognize and remove modified lipoproteins (99). M1 and M2 macrophages express scavenger receptors such as CD163 and CD206; the former is a member of the cysteine-rich family class B (100) and the latter is a type 1 membrane glycoprotein mannose receptor (101). High CD163 and CD206 expression are used as markers for M2 (102, 103), whereas M1 macrophages increase CD80 and CD86 expression and decrease CD163 and CD206 expression (104).

CD163 expression is increased by M-CSF, IL-6, IL-10, IL-10, IL-12, corticosteroids and oxidative stress and decreased by IL-4, IFN-γ, TGF-, TNF-α, GM-CSF and LPS (105-107). During acute and chronic inflammation, CD163 is cleaved by the disintegrin and metalloproteinase 17 (ADAM17)/TNF-α–cleaving enzyme (TACE) into soluble CD163 (sCD163) (107), which can be induced by exposure to oxidative stress or an inflammatory stimulus such as LPS. Moreover, ADAM17 has been found to cause excessive TNF-α shedding with a similar increase in the sCD163 level (108). In addition to TNF-α, a positive correlation was seen between IL-6 and IL-10 with sCD163 concentrations (109). Although the mechanism of how sCD163 interacts with T-lymphocytes remains unclear, sCD163 proteins are known to be able to inhibit the proliferation of T-lymphocytes (110).

CD206 expression on the macrophage cell surface is downregulated by IFN-γ and LPS (111), whereas evoking macrophages with Th2 cytokines such as IL-4 and IL-13 upregulated CD206 expression (112, 113). Tumour-infiltrating macrophages in human pleural mesothelioma exhibit a high level of CD163 and CD206 (114).

1.2.3.4 Molecular mechanisms that regulate macrophage polarisation

Macrophage reprogramming and activation involves three different signalling pathways. The first is the cytokine signalling pathway, which uses JAK-STAT molecules. The second pathway involves microbial recognition receptors, such as TLRs. The last pathway uses immunoreceptors that signal through immunoreceptor tyrosine-based activation motifs (ITAMs). For instance, M1 stimuli such as IFN-γ and LPS trigger IFN-α/β, TLR-4 and IFN-γ receptors leading to activation of transcription

factors such as STAT1, NFκB and AP-1, resulting in transcription of M1-associated genes (115, 116). However, M2 stimulation of IL-4Rα through IL-4/13 results in activation of STAT6, which regulates expression of M2-associated genes (116, 117). Furthermore, activation of kinases, such as Syk and PI3K, as well as expression of certain molecules, such as prostaglandin E and IL-10, occur as a result of the FcγR, an ITAM-containing receptor, triggered by immune complexes (116).

1.2.3.5 Tumour-associated macrophages

Macrophages in tumours are referred to as tumour-associated macrophages (TAMs). Up to 60% of the tumour stroma can be comprised of TAMs (118). As mentioned above, a key characteristic of macrophages is their plasticity, which allows them to either fight or aid tumours, depending on their microenvironment (119). TAMs may play a substantial role linking inflammation with cancer. This is because TAMs contribute to the proliferation, invasion and metastasis of tumour cells. TAMs can also stimulate tumour angiogenesis, obstruct anti-tumour immune responses mediated by T cells and promote tumour progression. Therefore, macrophages are considered a double-edged sword in the tumour microenvironment (119, 120). The concept of macrophages differentiation highlights the two types of macrophages mentioned above; M1 and M2 macrophages, however it is now recognised that these two functional and phenotypic states represent the end stages of a spectrum of macrophage sub-types. This classification has also been applied for TAMs i.e. M1 TAM and M2 TAMs. These two types have several effects and influence the tumour microenvironment differently. For instance, M1 TAMs are pro-inflammatory, anti-angiogenic and anti-tumour. In contrast, M2 TAMs are anti-inflammatory and involved in angiogenesis, immunosuppression and are pro-tumour growth. Therefore, M2 TAMs are more pro-tumoural than M1 TAMs and contribute significantly to disease progression.

Several researchers have argued that due to the heterogeneity of TAMs, many types of macrophage subpopulations can exist within a M1-to-M2 spectrum (121, 122). For example, in the early phases of tumour development most TAMs have more M1-like

phenotypes; however, in the later stages of development, this shifts in favour of M2-like phenotypes (122-124).

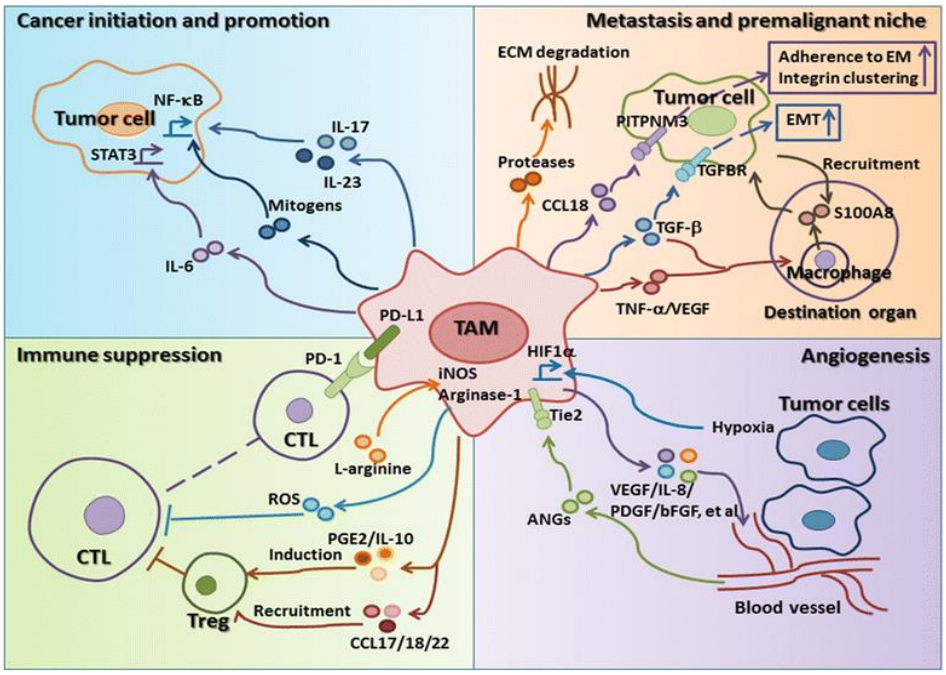

Figure 1. 3 Tumour-associated macrophages (TAMs) play a major role in tumour progression through their promotion of tumour growth, angiogenesis, metastasis and immunosuppression (125)

Studies have shown that high levels of TAMs are associated with poor prognoses in several cancers (126, 127). In addition, overexpression of M-CSF, which is responsible for the regulation of macrophage proliferation, differentiation and survival, is also associated with poor prognoses of some types of cancer (128, 129). Furthermore, it should be noted that most TAMs closely resemble M2 phenotypes. Also, the functional polarisation of these macrophages is due mainly to the absence of M1 signals, such as bacterial components and IFN-γ in the tumour microenvironment. Moreover, abundant M2 polarising factors in this microenvironment drive macrophage differentiation to express high IL-10 but not IL-12. Accordingly, secretion of IL-10 by TAM prevents the differentiation of monocytes into DCs and shifts monocyte differentiation to macrophages (130). Studies on murine TAMs have shown that defective NFκB

activation in response to M1 signals correlates with impaired production of NF-kB-dependent inflammatory cytokines such as TNF-α, IL-1β, IL-6 and IL-12 (131). Additionally, TAMs have been observed as poor producers of nitric oxide (NO) due to their low expression of inducible nitric oxide synthase (iNOS) and subsequent secretion of low levels of reactive species of oxygen (ROS) (132). Moreover, TAMs demonstrate M2 pro-tumoural functions (e.g. tumour progression, angiogenesis, invasion and metastasis) and skew away from pro-inflammatory responses and adaptive immunity (Figure 1.3 (125)).

1.2.3.5.1 The origin of TAMs

There are two theories regarding the origin of TAMs. The first is that blood monocytes are recruited into the tumour microenvironment, after which they differentiate into macrophages. The second is that TAMs originate from recruitment of tissue-resident macrophages (133).

1.2.3.5.2 Suppression of adaptive immunity

Unlike macrophages from healthy tissues, TAMs display a diminished capacity to destroy tumour cells(134). TAMs mediate suppression directly via cell-to-cell interactions and indirectly by secretion of chemokines and cytokinesthat create an immunosuppressive environment (135). Therefore, significant IL-10 activity and a defective NFκB pathway result in production of low levels of stimulatory cytokines, such as IL-12, IL-1 and TNF-α, which further decrease anti-tumour immune responses (131). In addition to the fact that TAMs are poor APCs, Mantovani and colleagues showed that TAMs have a high potential to suppress T cell activation and proliferation through transforming growth factor beta (TGF-β) and IL-10 (136). Furthermore, TAMs evade immune responses via secretion of chemokines, including Chemokine (C-C motif) ligand (CCL) 17 and CCL22 that recruit Tregs to the tumour microenvironment, which abolish anti-tumoural T cell responses (137). Moreover, macrophages in murine lung carcinoma models have been observed to produce arginase, resulting in impaired T cell function within tumours (138). On the other hand, direct contact between cells within a tumour microenvironment weakens the immune system by expressing immune

checkpoint ligands to immune checkpoint receptors, which inhibit immune cell function and allow tumours to evade anti-tumour immune responses. Additionally, it has been confirmed that macrophages express some of these immune checkpoint ligands, for instance, programmed death ligand-1 (PDL-1), which binds to PD-1 on T cells, triggering a reduction in T cell effector activity. In a study by Winograd and colleagues using a genetically engineered KPC mouse model of pancreatic ductal adenocarcinoma (PDAC), TAMs were found to express very high levels of PDL-1 (139).

1.2.3.5.3 The role of TAMs in angiogenesis

Many studies have established that in order for malignant tumours to grow and spread, they require angiogenesis. Angiogenesis refers to the physiological process that involves the formation of new blood vessels from pre-existing ones. Therefore, angiogenesis in tumours revolves around abnormal tumour vascularisation. Tumour vascularisation is a complex process that involves the interaction of tumours with their surrounding stroma, in addition to other diverse factors that regulate angiogenesis. This process is a vital in tumours, as it contributes to disease progression, nutrient and oxygen supply to tumour cells, as well as aiding metastatic spread (140). In addition, most cancers and cancer models have shown increased tissue vascular density inside and around tumours during transformation to the malignant state, providing a door for metastatic cells to enter the general circulation (141, 142). Although many types of cells contribute to angiogenesis TAMs are a major player. Studies have shown that the infiltration of TAMs is closely associated with increased angiogenesis. For instance, Leek et al. (1996) confirmed this in the study they conducted on breast carcinomas (143). Their findings are analogous to studies conducted by Saji et al. (2001), Koide et al. (2004) and Ohta et al. (2003)(144-146). In addition, TAMs also enhance tumour revascularisation in response to cytotoxic therapy, such as radiotherapy, resulting in cancer relapse. This means that they contribute to the resistance of tumours to therapies (147). A subpopulation of TAMs are recruited to avascular regions within tumours in response to chemoattractant molecules secreted by tumour cells (148). These TAMs play an essential role in tumour angiogenesis through production of multiple pro-

angiogenic factors, including platelet-derived growth factor (PDGF), vascular endothelial growth factor (VEGF), TGF-β and fibroblast growth factor (FGF). In human cervical cancer, TAMs promote lymph angiogenesis as well as the formation of lymphatic metastasis through the release of VEGF (149). In lung cancer, TAMs produce PDGF, which supports tumour progression (150). Production of chemokines is another feature of proangiogenic TAMs. Studies show that secretion of CXCL1, CCL2, CCL5, CXCL12, CXCL8 and CXCL13 contribute to angiogenic processes such as neovascularisation (151-153). Furthermore, TAMs that reside within avascular regions with low oxygen levels support production of pro-angiogenic factors,as hypoxia activates a pro-angiogenic program regulated by Hypoxia inducible factor (HIF)-1 and HIF-2 transcription factors. This induces expression of pro-angiogenic factors, including VEGF, CXCL8, CXCL12 and FGF, intensifying angiogenic responses (154).

1.2.3.5.4 Matrix remodelling and metastasis

TAMs have been shown to play a significant role in tumour cell migration, invasion and metastasis via expression of extracellular matrix (ECM)-remodelling enzymes in response to cytokines from tumour cells. The main ECM enzymes secreted by TAMs include matrix metalloproteinases (MMPs) 1,2, 9, 12 and 14; lysosomal enzymes; cathepsins B, S, C, L and Z; and serine proteases (155). Additionally, chemokines such as CCL5 and factors such as VEGF, IL-1β and TNF-α increase MMP expression, which result in tumour cell invasion and metastasis (156, 157).

1.2.3.5.5 TAMs in malignant mesothelioma

Malignant pleural mesothelioma is the most common form of mesothelioma associated with exposure to asbestos. Once the pleural cavity comes into contact with asbestos fibres, macrophage recruitment and activation occur in an attempt to remove the fibres. Failure to clear these fibres results in chronic inflammation as well as free radical secretion, leading to genotoxic damage and transformation of normal mesothelial cells to malignant ones (mesothelioma) in a process called frustrated phagocytosis (158, 159). Therefore, it has been opined that the abundance of TAMs in

the MM microenvironment plays a significant role in mesothelioma tumour biology. Additionally, both normal and established human mesothelial cell lines produce cytokines, including IL-6, G-CSF, GM-CSF and IL-8, which recruit monocytes to tumours. These monocytes then differentiate into macrophages (160, 161). Therefore, a large number of circulating monocytes is associated with poor prognosis and survival among mesothelioma patients. Burt et al. investigated the prognostic significance of circulating blood monocytes and TAMs in 667 pleural mesothelioma patients who underwent cytoreductive surgery between 1989 and 2009. The data showed that a large number of TAMs is associated with poor survival in non-epithelial malignant pleural mesothelioma (MPM) patients. Moreover, these TAMs resembled M2-like phenotypes with high expression of CD163 and CD206. Thus, due to the high densities of macrophages in mesothelioma, any therapeutic target that includes manipulation of TAMs may represent a promising strategy (114). This becomes particularly important as polarisation of macrophages can alter the sensitivity of the mesothelioma microenvironment (including tumours cells) to chemotherapy and other therapeutic approaches (162, 163).

1.2.3.5.6 The effect of hypoxia on macrophages

The term "hypoxia" describes a state of oxygen insufficiency that can be experienced in tumours, wounds and even normal tissues (164). Hypoxia develops within certain areas of tumours as a result of inadequate perfusion of the vascular network and is attributed to the development of blood vessels that are both disorganised and immature (1). Tumour hypoxia is thought to affect macrophages in diverse ways; for instance, it regulates the activation and polarisation of macrophages towards the pro-angiogenic phenotype via IL-10-activated pathways (165, 166). It is important to note that hypoxia carries out this function alongside various signals derived from tumour and stromal cells. Also, hypoxia regulates the mobilisation of macrophages into tumour tissues via release of higher quantities of VEGF, endothelial cell monocyte-activating polypeptide-II (EMAP-II), stromal cell-derived factor 1α (SDF1α), semaphorin 3A (SEMA3A), eotaxin, endothelin and oncosatin M, which enhance the migration of macrophages to these hypoxic areas. Additionally, hypoxia

restrains macrophages by decreasing their mobility through increasing the quantity of mitogen-activated protein kinase (MAPK) phosphatase 1 (MPK1) enzymes. Decreased macrophage mobility terminates the possibility of macrophages to respond to chemo-attractants and leads to the accumulation of macrophages in hypoxic/necrotic regions (165). Tumour-induced changes in macrophage phenotype and function may be due to their metabolic modification or reprogramming.

1.3 Cellular Respiration

Cellular respiration refers to the metabolic reactions and processes that occur in cells by which biochemical energy from nutrients is converted into adenosine triphosphate (ATP). Nutrients that are commonly used by cells in cellular respiration include glucose (from carbohydrates), small peptides and amino acids (from protein) and fatty acids (from lipids), and a common oxidising agent (electron acceptor) is molecular oxygen (O_2). Trapped and stored energy in the form of ATP is released when required to drive other processes that require energy, such as the biosynthesis, transportation or locomotion of molecules across cell membranes. The most significant pathways involved in cellular respiration are glycolysis and oxidative metabolism. Glycolysis takes place within the cell's cytosol where glycolytic enzymes are found and by which glucose is converted into pyruvate to give a small net energy (167). The oxidative phosphorylation (OXPHOS) system is located in the mitochondria, and the process of OXPHOS produces large amounts of ATP. During this process, an exchange of protons creates an electrochemical gradient across the membrane that allows for ATPproduction (168). Cancer cells and immune cells can switch metabolic states to facilitate their survival, proliferation and behaviour in a process referred to as metabolic reprogramming (169) (Figure 1.4).

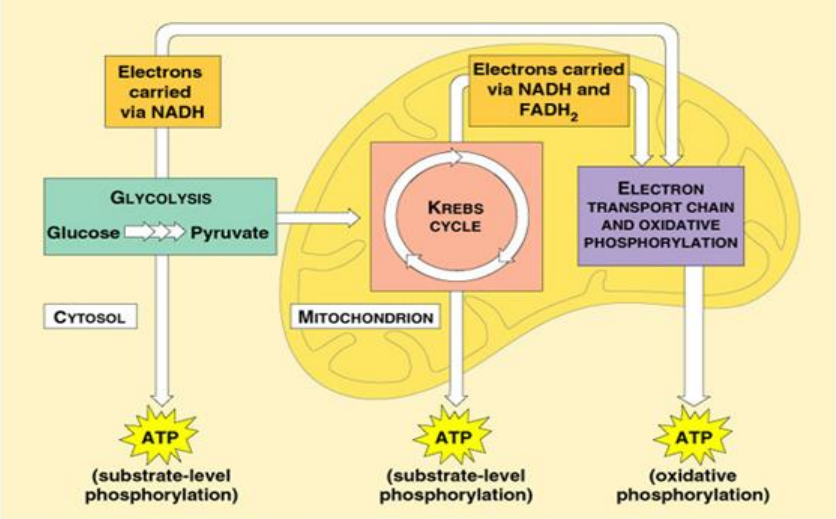

Figure 1. 4 Cellular respiration

1.3.1 Metabolic reprogramming of cancer cells

In the 1920s, Otto Warburg and colleagues discovered a metabolic distinction between normal and tumour cells in a phenomenon called “the Warburg effect”. The Warburg effect, also known as aerobic glycolysis, suggests that cancer cells prefer to produce ATP via glycolysis instead of OXPHOS, even in the presence of oxygen. As part of the Warburg effect, the partial suppression of oxidative metabolism in cancer cells is believed to be caused mainly by mitochondrial dysfunction (170, 171). Furthermore, it has long been recognised that cancer cells’ glycolytic phenotypes are closely connected to defective mitochondrial OXPHOS(170). In cancer cells, glucose metabolism is mainly characterised by two major biochemical events: (i) aerobic glycolysis, and (ii) increased glucose cellular uptake (172, 173). In normal cells, glucose is broken down aerobically and further metabolised through the tricarboxylic acid cycle (TCA) and OXPHOS in mitochondria. However, cancer cells often shunt glucose away from the TCA and metabolise it primarily through the fermentative pathway, ending in lactateproduction (174, 175). Oncogenic transformation in glucose-addicted cancer cells causes upregulation of glucose transporters (e.g. GLUT1 and GLUT3), thus mediating increased glucose uptake, which in turn increases the rate of glucose metabolism (173). A higher glycolytic rate in cancer cells was found to be anti-

apoptotic and associated with resistance to chemotherapy. For example, upregulation of GLUT1 and HIF-1 has shown to be resistant to chemotherapeutics in acute myeloid leukaemia (173, 176). Additionally, under hypoxic conditions, increased expression of glycolytic enzymes, such as hexokinaseII (HKII), phosphofructokinase (PFK) and lactate dehydrogenase (LDH), has been linked to chemotherapy resistance due to reduced apoptosis (170). Moreover, LDH-A(LDHA) has been demonstrated to provide resistance to paclitaxel/trastuzumab in breast cancer patients and the pyruvate dehydrogenase kinase (PDK) isoform PDK3 is correlated with hypoxia-induced drug resistance in colon and cervical cancer patients (177).

1.3.2 Metabolic reprogramming of macrophages

1.3.2.1 Metabolic reprogramming of M1 and M2 macrophages

Briefly, M1 macrophages activated with LPS or IFNγ are associated with a metabolic switch from OXPHOS to aerobic glycolysis, displaying a rapid activation of aerobic glycolysis followed by a reduction in OXPHOS and attenuated TCA cycle activities leading to ROS production (178, 179). Thus, M1 macrophage metabolism displays upregulated glycolysis, which involves an increase in glucose uptake as well as the conversion of pyruvate to lactate. In contrast, activated M2 macrophages are characterised by decreased glycolysis since they use OXPHOS as the main means to generate ATP generation (177). Additionally, the metabolic switch that leads to elevated aerobic glycolysis experienced by most cancer and immune cells is considered a hallmark of their ability to sustain viability and promote inflammatory activity (178, 180). Inhibition of this shift results in blockage of the M1 phenotype and decreases pro-inflammatory cytokine/chemokine production (178, 180).

1.3.2.2 Metabolic reprogramming of TAM

The metabolic features of TAMs have always been considered complicated, as they display complex forms of metabolic change. Although it has been suggested that TAMs are M2-like, many studies have demonstrated that, like M1 macrophages, TAMs have a high glycolytic rate (181, 182). On the other hand, TAMs have shown increased OXPHOS, even with a broken TCA cycle (182). Therefore, the metabolic features of

TAMs demonstrate that TAMs do not reflect the strictness of the M1 and M2 paradigms. Moreover, a tumour's microenvironmental factors can create different TAMs with different metabolic programs and phenotypes, such as hypoxia, depending on the area within the tumour they occupy (182). Importantly, the glycolytic pathway in TAMs is upregulated via the Akt/mTOR signalling pathway and stabilisation of HIF-1α, which has been proven to be associated with the pro-inflammatory M1 macrophage phenotype (182, 183). Accordingly, HIF-1α expression can be regulated by a different classical pathway i.e. NF-κB, which mediates pro-inflammatory cytokine expression, and other mediators, such as glycolytic enzymes and glucose transporters of the M1 phenotype. In contrast, HIF-2α expression is regulated independently from NF-κB and is correlated with an alternative pathway activation (184). Furthermore, it has been found that TNF-α secreted by TAMs enhances tumour cell glycolysis, whereas TAMs facilitate tumour hypoxia via increased AMP-activated protein kinase expression and peroxisome proliferator-activated receptor gamma coactivator 1-alpha (PGC-1α) upregulation (185).

1.4 Tumour Neovascularisation

1.4.1 Angiogenesis and vasculogenesis

The network of veins, capillaries and arteries in the body is called the vascular system and is essential for maintaining homeostasis (186). The functions of all tissues in the body require a blood supply. This blood supply depends solely upon ECs that line the interior of blood vessels. Endothelial cells form a network of blood vessels that extend to all parts of the body and assist in tissue growth, wound healing and repair. Every blood vessel, large or small, must have an endothelial lining as these cells control the transport of material and white blood cells to tissues. Blood vessels are formed by two processes: angiogenesis and vasculogenesis. The process in which ECs derived from precursor endothelial cells or angioblasts form de novo networks of vessels is known as vasculogenesis (187). Vasculogenesis occurs with formation of the initial primitive vascular network, including the heart and yolk sac, during embryogenesis (188). In contrast, angiogenesis is the formation of new vessels from existing ones. Angiogenesis can modify and expand the vascular network and construct new veins and arteries from

the microcirculation. Angiogenesis involves two vital dynamic mechanisms in the formation of new blood vessels: intussusception and sprouting (188, 189).

1.4.1.1 Intussusceptive angiogenesis

Intussusceptive angiogenesis, also known as splitting angiogenesis, non-sprouting angiogenesis or inverse sprouting angiogenesis, occurs when new blood vessels are formed through the formation of multiple transluminal tissue pillars. The pillars that arise are reshaped and fused, leading to a "splitting" of the pre-existing vessel into two segments. The endothelial cells form protrusions towards the vessel lumen, leading to the formation of these trans-capillary, or intussusceptive, pillars (189).

1.4.1.2 Sprouting angiogenesis

In adulthood, most blood vessels remain at rest, with the exception of those in the placenta during pregnancy (190). During the process of sprouting angiogenesis, the capillary originates just like pseudopodia and forms a hollow tube called a capillary sprout that grows continuously until it touches another capillary. Then, the two capillaries connect, and blood starts flowing. Endothelial cells in arteries and veins have specific receptors to enable this highly organised and integrated system (191).

1.4.1.3 Tumour angiogenesis

The tumour microenvironment consists of normal cells, such as fibroblasts and ECs, and cells that are recruited from the bloodstream such as monocytes/macrophages, neutrophils and T and B cells (192). In 1971, Judah, Folkman and co-workers proposed that cancer cells can grow in two different environments: in the presence of blood circulation (vascular phase) and in the absence of blood circulation (avascular phase). In the avascular phase, the tumour mass cannot exceed a size of 1-2 mm^3 without angiogenesis, as up to this point, cells can obtain the necessary oxygen and nutrient supplies from nearby capillaries. Further growth and survival beyond this size is severely limited by oxygen and nutrient supply as well as waste removal, which increases the tumour's need to build their own vasculature (vascular phase) (193, 194). If there is no vascular support, the tumour may enter into an apoptotic phase or become

necrotic, suggesting that angiogenesis is an important factor in tumour growth and progression (195). In the vascular phase, thebasement membrane is disrupted, and cells experience hypoxia. The process of tumour angiogenesis is complex, as it depends on the coordination of many factors, including specifications of tips and stalks of endothelial cells (TECs; that lead to capillary growth), basement membrane degradation, EC activation and migration to hypoxic regions, followed by their proliferation and formation of the capillary network (196).

Mechanisms of tumour angiogenesis and/or vascularisation include vasculogenesis (described on page 23), sprouting (described on page 23), intussusception (described on page 23), as well as co-option and vasculogenic mimicry. Vasculogenic mimicry is a process in which tumour cells undergo dedifferentiation to mimic endothelial-like properties(194). Aggressive tumours follow this process and form tube-like structures containing cells that have differentiated into endothelial phenotypes. Certain tumours (e.g. in lungs and brain) grow during the avascular phase around existing blood vessels without starting the process of angiogenesis; this is called vessel co-option (Figure 1.5) (194).

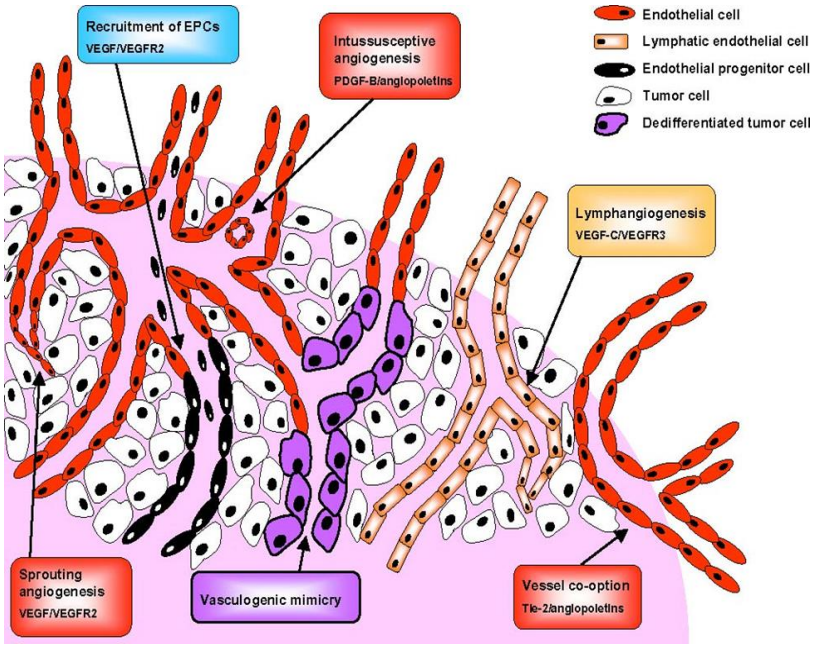

Figure 1. 5 Mode of tumour vessel formation (133)

1.4.2 Tumour blood vessels

Disorganised vasculature is considered a hallmark of tumour development that arises from an imbalance of pro- and anti-angiogenic signalling within tumours (197). Jain and co-workers (2008) described vessel architecture and function in tumours (198, 199). These vessels have different morphological and physiological characteristics than normal blood vessels in that they are characterised by chaotic, aberrative, tortuous, dilated and hyper-permeable vessels (125,126). Defects in blood vessels can lead to spatial and temporal variations in tumour blood flow, increased tumour interstitial fluid pressure (IFP), hypoxia and high acidity (198) in the tumour microenvironment. Negative consequences of alterations include changes to blood vessel diameter, which leads to uneven blood flow in one direction and possible static flow at one or more site. Open vessels in tumours cannot be continuously perfused, therefore blood flows along different paths (200). These blood vessels are often found less in the centre of the tumour. The endothelia of tumour vessels are also defective; for instance, they may have junctions that are poorly connected or scattered pericyte coverage. Tight junctions play a critical role in the movement of ions across the paracellular space and the absence of tight junctions leads to vessel leakiness,less nutrients and oxygen supply to cells (201). Thus, tumours have low blood flow, high blood leakage and poor perfusion, thereby generating an increase in interstitial pressure, hypoxia, starvation and acidosis in the local microenvironment. Irregular blood flow within a tumour can affect the delivery of drugs. Furthermore, increased vascular permeability enhances transmigration of immune cells, including monocytes, from blood vessels into the tissue (202). Also, a hypoxic environment can cause gene alterations in cancerous cells and mediate their migration to healthy tissue. Furthermore, an acidic environment can impair the ability of immune cells to target cancer cells and induces resistance to chemotherapy and radiation (203) (Figure 1.6) (204).

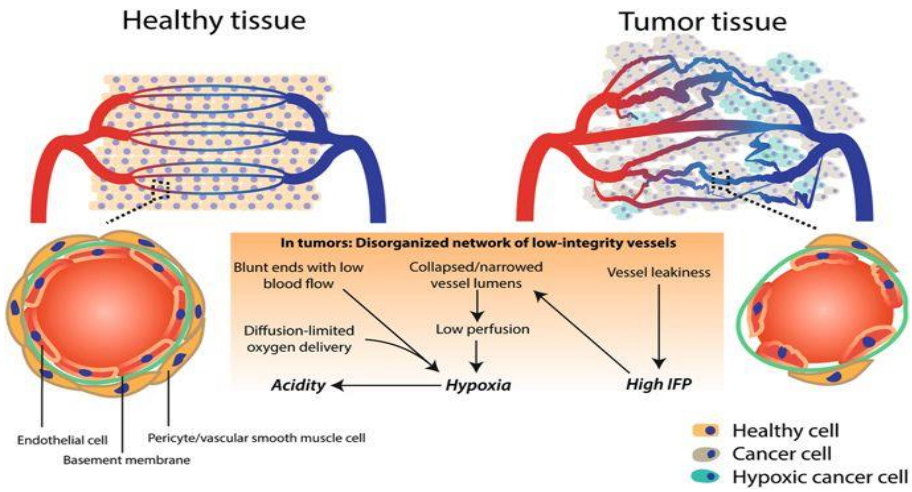

Figure 1.6 The role of abnormal vasculature in shaping the tumour microenvironment(144)

1.5 Project Hypothesis

Asbestos-induced abnormalities in mesothelial cells are the triggers that create new dynamic tissue-like organs, i.e. mesothelioma tumour masses. Molecules secreted by transformed mesothelioma cells likely affect the phenotype and function of neighbouring cells including tumour-associated macrophages and ECs that influence organisation of the resulting tumour microenvironment. This mesothelioma/macrophage/EC axis might be further modified by tumour oxygenation, in particular hypoxia, and will be addressed in this project. TAMs and tumour-associated ECs may directly interact with each other and this cross-talk may modify macrophage and EC activation, proliferation and function. Again, tumour oxygenation could influence the outcomes of this cross-talk and will be addressed in this project. Our laboratory has promising pre-clinical data showing that an IL-2/CD40-based immunotherapy can induce regression of large mesothelioma tumours in mice. However, its effect in humans is not yet clear, particularly if there are significant hypoxic regions. VTX-2337 also showed promising results in preclinical models and represents a possible alternative therapy used alone or in combination with IL-2/CD40.

On average, under 8% of results from animal models are successfully translated to human clinical cancer trials. Animal models are constrained in their capacity to imitate the intricacies of human carcinogenesis, physiology, and development. Thus, the safety and viability of a specific novel therapy found in animal experiments will not necessarily hold true in human trials (205). However, this primary concern may be addressed by in vitro models which better imitate in vivo human tumours. Such models are helpful in early-stage drug development and reduce the number of animals used for laboratory experimentation (206-208). There is expanding enthusiasm for using 3D spheroid models, or organoids, to show malignant growth and tissue biology, quickening the implementation of research results in clinical practice. The 3D microenvironment can powerfully impersonate the various cell heterogeneities of in vivo settings (209). Of such models, the multicellular tumour spheroid (MCTS) model is capable, not only of reproducing the harsh conditions in poorly vascularised tumours, but also of assessing compound (drug) infiltration properties (210-212).

This project's overall hypotheses was that the effect of the dynamic properties of the human mesothelioma microenvironment could be represented by studying the crosstalk (mediated by soluble factors) between mesothelioma tumour cells, macrophages and endothelial cells (ECs) under hypoxic and normoxic conditions. It was further hypothesised that these cells' responses to IL-2, α-CD40 and VTX-2337 could be better understood by developing a 3D spheroid tumour model incorporating the three cell types (mesothelioma cells, macrophages and ECs). It was hoped that this organoid approach would reproduce the in-vivo tumour microenvironment and reveal novel immune/EC-mediated therapeutic approaches for treating mesothelioma.

To address the project's hypothesis, the following aims were addressed:

Aim #1: To assess the ability of healthy, non-mesothelioma exposed human macrophages to polarise into pro-inflammatory M1-like cells characterized by high CD80 and low CD206 expression or anti-inflammatory M2-like cells defined as high CD206 (using monocyte-derived macrophages), and to measure molecular changes to healthy ECs (using human umbilical vein endothelial cells, HUVECs), under hypoxic

(2% O_2) versus normoxic (20% O_2) conditions (measured using multiparameter staining and flow cytometry).

Aim #2: To investigate the effect of mesothelioma-derived factors (using tumour conditioned media from human JU77 mesothelioma cells) on the ability of human macrophages to polarise into M1-like or M2-like cells incubated under hypoxic versus normoxic conditions. Note that mesothelioma-derived molecules were matched by being generated under normoxic and hypoxic conditions. The same tests were used as for Aim #1.

Aim #3: To investigate the effect of JU77 mesothelioma-derived factors on ECs under hypoxic versus normoxic conditions measuring measuring CD309, CD54, CD105, CD144, and CD146, using multiparameter staining and flow cytometry.

Aim #4: To investigate the effects of cross talk between healthy and JU77 mesothelioma-exposed macrophages and HUVECs incubated under normoxic and hypoxic conditions measuring CD309, CD54, CD105, CD144, and CD146, using multiparameter staining and flow cytometry.

Aim #5: To assess the effect of immunotherapy on mesothelioma-exposed macrophages by measuring molecular alterations in Ju77-exposed macrophages in response to 24 hours exposure to IL-2, α-CD40, IL-2/α-CD40 or VTX-2337 under normoxic and hypoxic conditions measuring HLADR, CD206, CD309, CD54, CD40, CD144, A2A-R, CD105, CD163, CD80, Gal-9, CD39, CD86, PDL-1, and, CD146, using multiparameter staining and flow cytometry.

Aim #6: To assess the effect of IL-2, α-CD40, IL-2/α-CD40 and VTX-2337 on healthy and mesothelioma-exposed ECs under normoxic and hypoxic conditions measuring CD309, CD54, CD105, CD144, and CD146, using multiparameter staining and flow cytometry

Aim #7: To assess the effect of supernatant from mesothelioma-exposed macrophages treated with IL-2, α-CD40, IL-2/α-CD40 and VTX-2337 on ECs under normoxic versus hypoxic conditions measuring CD309, CD54, CD105, CD144 and CD146 using multiparameter staining and flow cytometry.

Aim #8: To attempt to validate *in vitro* findings using an *in silico* approach to:

- Confirm expression of the target genes (HLADR, CD206, CD309, CD54, CD40, CD144, A2A-R, CD105, CD163, CD80, Gal-9, CD39, CD86, PDL-1, and CD146) in human mesothelioma.
- Identify functionally active HREs in the promoter regions of target genes.
- Identify hypoxia related transcription factors binding sites
- Identify possible mechanisms for upregulation of molecules seen in mesothelioma-exposed ECs and macrophages under hypoxia by analysing signalling pathways to identify the role of hypoxia related transcription factors.

Two experimental approaches were planned: 2D and 3D in vitro cell culture models. In traditional, 2D cell culture conditions, cells were plated on a flat surface and, therefore, had a flat shape. Macrophages were exposed to mesothelioma-derived factors, while ECs were exposed to mesothelioma-derived factors or macrophage-derived molecules in normoxic and hypoxic environments. In 3D cell culture conditions, the aim was to develop a spheroid model that would enable direct, cell-to-cell communication by incorporating mesothelioma cells, macrophages and ECs in ultra-low adhesion round-bottom plates,as described in chapter 6.

CHAPTER 2
MATERIALS AND METHODS

2.1 Human Ethics

This study has been approved by the Curtin University Human Research Ethics Committee (approval number HRE2017-0823).

2.2 Recruitment of Volunteers

Twenty healthy young volunteers (21–37 years of age) were recruited via word-of-mouth within and outside Curtin University and in collaboration with Dr. P. Methoram's research group, whose focus is platelets leaving the buffy coat available for others. All volunteers were provided with an information sheet prior to participating in the study. Their health status was assessed via a questionnaire detailing current and past medical conditions, current medications, family disease history, smoking status and asbestos exposure status (Appendix A). Any volunteer who previously or currently had cancer or who suffered from severe immune disorders, such as autoimmune disorders, were excluded from the study.Before blood collection, eligible donors were required to sign a consent form to participate in the study. The experiments were repeated at least 8 times using different donors (12 times per normoxic naive macrophages (MØ), 10 times per hypoxic macrophages MØ, 12 times per normoxic tumour-conditioned macrophages (TCM-CM), 10 times per hypoxic TCM-CM, and 8 times for all other conditions).

2.3 Cell Culture and Maintenance

2.3.1 The JU77 human mesothelioma cell line

The malignant mesothelioma JU77 cell line is an adherent cell line that was generated from the pleural effusion of a patient with a confirmed disease diagnosis (213). JU77 cells were maintained in complete RPMI (Life Technologies, USA) media containing 10 % FCS (Thermo Fisher Scientific, USA), 1% glutamax, 50 μM 2-mercaptoethanol (2-ME, Life Technologies, USA), 100 U/ml Penicillin (Life Technologies, USA) and 50 mg/ml Streptomycin (Life Technologies, USA). JU77 cells were cultured in a 37º C

and 5 % CO2 humidified incubator until 80-90 % confluent. Cells were then washed twice using warm phosphate-buffered saline (PBS; Life Technologies). Next, cells were incubated with a new warmPBS to detach cells from tissue culture flasks. The cell suspension was transferred to a new tube, centrifuged at 1,200 rpm for 5 min. Pelleted cells were resuspended in complete RPMI and cultured into new tissue culture flasks or plates (Beckton Dickinson, California, USA).

2.3.1.1 Collection of mesothelioma tumour-conditioned media

To generate tumour-conditioned media (TCM), JU77 mesothelioma cells were grown under two oxygen conditions, 2% oxygen (a hypoxic environment) or 20% oxygen (a normoxic environment) until confluent. Cell-free supernatants were collected from using centrifugation at 1200 rpm for 5 min and stored at −80º C until needed.

2.3.1.2 Cryopreservation of cells

Cells were resuspended in a cryopreservation solution (90% FCS and 10% dimethyl sulfoxide; DMSO; Sigma-Aldrich, (214) at 2 x 10^6 cells/ml and transferred into cryogenic vials (Nunc/ThermoScientific) for storage at −80°C.

2.3.1.3 Thawing cells

Cells stored at −80°C were warmed quickly by immersion in a 37°C water bath, then rapidly transferred to 15 ml tubes containing 9 ml complete RPMI medium and centrifuged at 1200 rpm for 5 min to remove the cryoprotective agent. The supernatant was discarded, and cells resuspended in a complete medium and transferred to tissue culture flasks, for incubation at 37°C in a 5% CO_2 atmosphere.

2.3.2 Primary human macrophages

2.3.2.1 Blood sample collection

Via mid-arm venepuncture, whole blood samples (50 ml) from healthy volunteers were divided into five 10 ml dipotassium ethylenediaminetetraacetic acid (K_2 EDTA) BD vacutainer tubes (Beckton Dickinson) and transported to the laboratory for immediate

processing. K_2 EDTA was used to block the coagulation cascade by chelating calcium ions (215).

2.3.2.2 Isolation of peripheral blood mononuclear cells (PBMCs)

Whole blood samples (50 ml) collected as described were distributed evenly into two 50 ml centrifuge tubes. To each 25 ml of blood, 10 ml of PBS solution containing 2 mM EDTA (Sigma-Aldrich, USA) was added. Then, 35 ml of diluted blood was layered over 15 ml of a density gradient medium, Ficoll-Paque^{TM} Plus (GE Healthcare, New South Wales, Australia) and centrifuged at 400 g for 40 min at 20º C without acceleration or brakes. Following centrifugation, the PBMC layer or buffy coat (at the interphase) was carefully transferred to a 50 ml tube and resuspended in 50 ml of PBS/2 mM EDTA for centrifugation at 300 g for 10 min at 20°C with acceleration and brakes. For the second and third washes, cells were resuspended in 50 ml of PBS/2 mM EDTA and centrifuged at 200 g for 10 min at 20°C with acceleration and brakes. A final wash was performed at 120 g to remove any remaining platelets.

2.3.2.3 Isolation of monocytes

After the final wash, the supernatant was discarded, and cell pellets resuspended in RPMI media ($5X10^6$ cells/well) and cells seeded into six-well flat-bottom BD Falcon cell culture plates (in 2 ml of RMPI media/well; Beckton Dickinson). Cells were incubated for 2-3 hrs at 37º C in 5% CO_2 to allow monocytes to adhere to the bottom of the plate, whilst lymphocytes remain non-adherent. Media containing non-adherent lymphocytes were removed to leave behind a predominantly adherent monocyte population in the plate.

2.3.3 3 In-vitro generation of macrophages and tumour-conditioned macrophages

Human monocytes were cultured in 2 ml of complete RPMI-1640 medium and incubated with 50 ng/ml of human recombinant macrophage colony-stimulating factor (M-CSF) for 7 days to differentiate monocytes into macrophages. Media containing M-CSF was replaced on day 3 and day 6. To mimic the tumour microenvironment and generate tumour-conditioned macrophages, monocytes were cultured in a (50:50)

medium consisting of 1 ml of complete RPMI-1640 medium and 1 ml of TCM with 50 ng/ml hM-CSF for 7 days. Please note that for hypoxic studies, monocytes were differentiated under a hypoxic environment, and hypoxic TCM was used.

2.3.3.1 Stimulation of macrophages

On Day 7, samples and control media were replenished with new media and different stimuli added. The stimuli are shown in Table 1 and include lipopolysaccharide (LPS)/ interferon gamma (IFN-γ), interleukin (IL)-4/IL-13, IL-2, anti-CD40 antibody, IL-2/anti-CD40 and VTX-2337(TLR8 agonist).

Table 2. 1 Stimuli used in this study

Stimuli	Concentration	Supplier
LPS	1 μg/ml	Sigma-Aldrich
IFN-γ	200 ng/ml	Shenandoah Biotechnology
IL-4	10 ng/ml	Shenandoah Biotechnology
IL-13	10 ng/ml	Shenandoah Biotechnology
IL-2	1 μg/ml	PeproTech
anti-CD40 (CP-870,893 hIgG2)	1 μg/ml	Supplied by Professor Martin Glennie and Dr. Ann White
VTX-2337	10 μM	Sapphire Bioscience
DMSO	10 μM	Sigma-Aldrich

2.3.3.2 Collection of macrophages and TCM-conditioned macrophage supernatant

After 24 h, supernatants were transferred to 15 ml tubes and centrifuged to pellet cells and cellular debris. Then, supernatants were aliquoted and stored at -80°C until needed. To detach macrophages from the bottom of the plate, cells were washed with pre-warmed PBS to remove residual media, and the supernatant discarded. Then, cells were incubated with 2 ml of pre-warmed PBS in a humidified incubator at 37°C in 5% CO_2 for 10 min to detach cells from plate. Cell suspensions were centrifuged for 5 min at 1200 rpm.

2.3.4 Human umbilical vein endothelial cells (HUVECs)

Human umbilical vein endothelial cells (HUVECs) were obtained from the American Type Culture Collection (Manassas, VA, USA). These cells are derived by the perfusion of donor umbilical veins and are the most widespread *in vitro* model for the study of endothelial cell regulation and their responses to different stimuli (216). The first isolation of endothelial cells from a human umbilical vein by perfusion was in 1973 (216).

2.3.4.1 Passaging HUVEC cell lines

HUVECs were grown in HUVEC media containing endothelial cell basal medium (EBM; Lonza) supplemented with ascorbic acid (Lonza), hydrocortisone (Lonza), bovine brain extract (BBE; Lonza), foetal bovine serum (FBS, Lonza), gentamicin/amphotericin-b (GA, Lonza) and human epidermal growth factor (hEGF, Lonza) in tissue culture flasks. Once cells reached 80–90% confluency, HUVECs were subcultured using warm PBS to dislodge cells (as described previously) and resuspended in HUVEC media. Then, HUVECs were seeded in tissue culture flasks and incubated in a humidified 5% CO_2 incubator at 37°C.

2.3.4.2 In-vitro generation of TCM-conditioned HUVECs

Once passaged HUVECs reached 80–90% confluency in a six-well plate, 3 x 10^5 cells/well were seeded in 2 ml of HUVEC media and incubated in a humidified 5% CO_2 incubator at 37°C for 24 h to allow them to adhere to the plate. After 24 h, the media was replaced with either 2 ml of 100% HUVEC media or a 50:50 mixture of medium consisting of 1 ml of HUVEC media and 1 ml of TCM. Cells were then incubated for 48 h to generate TCM-conditioned HUVECs. Please note that passage 6 HUVECs were used for all experiments to ensure consistency.

2.3.4.3 Stimulation of HUVECs

On day 3, media was replenished and stimuli as per Table 1 added.

2.3.4.4 Collection of HUVECs and TCM-conditioned HUVEC supernatant

Supernatant was collected using the same method as per macrophage supernatant collection described in section 2.3.2.6.

2.3.4.5 Thawing HUVECs

Cryopreserved HUVECs were stored in liquid nitrogen and HUVECs vials were dipped into a 37°C water bath to enable rapid thawing (< 1 minute). Thawed cells were diluted using 1 ml of pre-warmed supplemented medium. Next, HUVECswere transferred to 15 ml tubes at 1.25 x 10^4 viable cells/ml using supplemented medium. Finally, 5 ml of cell suspension was added to each 25 cm^2 culture flask for incubation at 37°C in a 5% CO_2 atmosphere.

2.4 Cell Viability and Counting

To calculate the number of dead and viable cells/ml for all cells, trypan blue staining was used. To do this, 10 µl of cell suspension and 10 µl of 0.4% trypan blue solution (Sigma-Aldrich, USA) were mixed gently. Then, the trypan blue-treated cell suspension was loaded onto a glass hemocytometer. A 10X objective of Nikon Tie microscope (Tokyo, Japan) was used to count the number of cells in each set of 16 corner squares of the grid lines of the hemocytometer. Cell number = average cell count/square x dilution factor x 10,000 x volume.

2.5 Staining Macrophage Cells and HUVECs for FACS Analysis

Flow cytometry was performed using a BD LRS Fortessa.

2.5.1 Staining and gating strategy to identify and characterise macrophages

To setup the instrument and for analysis, negative controls (unstained cells), a single stained fluorescence sample for every molecule and fluorescence minus one (FMO) controls were used. FMO controls were tested for each fluorochrome during optimisation of staining (data not shown) and for subsequent experiments CD80 (Alexa Fluor647) and Galectin-9 (Gal-9) (PerCP/Cyanine5.5) were included. The unstained and single stained fluorescent controls were used for setting compensation to correct

the spill over between the channels. The single stained fluorescent controls were also used to identify the positive populations of CD40 (Brilliant Violet 421), CD80 (Alexa Fluor647), HLA-DR (Brilliant Violet 650), CD39 (Brilliant Violet 510), CD11b (Brilliant Violet 711), CD206 (Alexa Fluor 488), CD163 (Brilliant Violet 605), Adenosine-A2A-receptor (A2A-R) (PE) and to identify live cells via Fixable Viability Stain (FVS700). The CD80 and Gal-9 FMO controls were used to identify CD80 and Gal-9 positive populations, respectively. Note that PDL-1 was stained in a separate panel with FVS700.

Table 2. 2 Anti-human antibodies used in this study to identify and characterise macrophages

Antigen	Fluorochrome	Clone	Isotype	Supplier	Dilution	Antibody concentration
Extracellular antigens/markers						
CD40	Brilliant Violet 421	5C3	Mouse IgG1, κ	Biolegend	1:100	0.00025 μg/μl
CD86	PE/Dazzle 594	IT2.2	Mouse IgG2b, κ	Biolegend	1:100	0.001 μg/μl
HLA-DR	Brilliant Violet 650	L243	Mouse IgG2a, κ	Biolegend	1:200	0.0005 μg/μl
CD39	Brilliant Violet 510	TU66	Mouse IgG2b, κ	BD Biosciences	1:100	0.002 μg/μl
CD80	Alexa Fluor647	2D10	Mouse IgG1, κ	Biolegend	1:100	0.004 μg/μl
CD11b	Brilliant Violet 711	ICRF44	Mouse IgG1, κ	Biolegend	1:100	0.001 μg/μl
CD206	Alexa Fluor 488	15-2	Mouse IgG1, κ	Biolegend	1:200	0.002 μg/μl
CD163	Brilliant Violet 605	GHI/61	Mouse IgG1, κ	Biolegend	1:100	0.0015 μg/μl
PD-L1	PE-Cy7	29E.2A3	Mouse IgG2b	Biolegend	1:500	0.0002
Intracellular antigens/markers						
A2A-R	PE	7F6-G5-A2	Mouse IgG2a	Santa Cruz Biotechnology	1:100	0.002 μg/μl
Gal-9	PerCP/Cyanine5.5	9M1-3	Mouse IgG1, κ	Biolegend	1:100	0.001 μg/μl
FVS700	---	N/A	N/A	BD Biosciences	1:1200	----

Table 2. 3 Molecules examined in this study

Molecule	Function
CD40	Engagement of CD40 by its ligand CD154 plays a major role in providing costimulation for T cell activation (217).
CD86	Engagement of CD86 with CD28 leads to T-cell activation, survival and cytokine production, or immune regulation with cytotoxic T-lymphocyte-associated protein 4 (CTLA-4) engagement (81).
HLA-DR	Mediates antigen presentation to CD4-positive T cells (218).
CD39	Responsible for the breakdown of ATP to immunosuppressive adenosine (89).
CD80	Engagement of CD86 with CD28 leads to T-cell activation, survival and cytokine production or immune regulation with CTLA-4 engagement (81).
CD11b	Plays a role in cellular adhesion and cell-cell interactions (89).
CD206	A scavenger receptor (219).
CD163	A scavenger receptor (219).
PD-L1	Engagement of PD-L1 with PD-1 leads to inhibition of T cell proliferation and cytokine production (220).
A2A-R	Binding with adenosine leads to immunoregulation (221).
Galectin-9	Binding TIM-3 on $CD8^+$ and $CD4^+$ cells induces apoptosis and promotes Tregs (222).

2.5.2 Staining and gating strategy to identify and characterise HUVECs

To study HUVECs, controls included unstained cells, a single stained fluorescence sample for every molecule and fluorescence minus one (FMO) controls for FVS700 and CD144 (PerCP/Cyanine5.5). The unstained and single stained fluorescence samples were used for setting compensation to correct spill over between channels. Single stained fluorescent controls also were used to identify positive populations expressing CD146 (BUV395), CD54 (Brilliant Violet 650), CD309 (Brilliant Violet 510), CD62E (Brilliant Violet 421), CD105 (PE/Cy7), CD31 (Brilliant Violet 711), and CD321 (PE). The CD144 and FVS700 FMO controls were used to identify CD144 positive populations and negative populations (live cells), respectively.

Table 2. 4 Anti-human antibodies used in this study to identify and characterise HUVECs

Antigen	Fluorochrome	Clone	Isotype	Supplier	Dilution	Antibody concentration
CD31	Brilliant Violet 711	WM59	Mouse IgG1, κ	BD Biosciences	1:500	0.0004 μg/μl
CD54	Brilliant Violet 650	HA58	Mouse IgG1, κ	BD Biosciences	1:200	0.001 μg/μl
CD62E	BV421	68-5H11	Mouse IgG1, κ	BD Biosciences	1:200	0.001 μg/μl
CD105	PE/Cy7	43A3	Mouse IgG1, κ	Biolegend	1:500	0.0004 μg/μl
CD144	PerCP-Cy5.5	55-7H1	Mouse IgG1, κ	BD Biosciences	1:100	0.002 μg/μl
CD146	BUV395	P1H12	Mouse IgG1, k	BD Biosciences	1:200	0.001 μg/μl
CD309	Brilliant Violet 510	TU66	Mouse IgG2b, κ	Biolegend	1:100	0.00025 μg/μl
CD321	PE	M.Ab.F11	Mouse IgG1, κ	BD Biosciences	1:100	0.002 μg/μl
FVS700	---	N/A	N/A	BD Biosciences	1:1200	----

Table 2. 5 Molecules examined in this study

Molecule	Function
CD31	Is involved in cell adhesion and leukocyte diapedesis (223).
CD54	Plays a role in cell migration (224), cell-cell adhesion, lymphocyte activation and leukocyte trafficking, (225, 226).
CD62E	Plays an important role in leucocyte rolling, angiogenesis and tumor metastasis (227).
CD105	Important accessory receptor to transforming growth factor beta (TGF-β) (228).
CD144	a master regulator on endothelial cell–cell junctions which coordinates the opening and closing of the endothelial barrier, thus control permeability changes (229)
CD146	Is involved in heterophilic cell adhesion and in the control of leukocyte extravasation (230).
CD 309	VEGFR2 regulates endothelial migration and proliferation as well as mediates vascular permeability (231)
CD 321	JAM-A is implicated in several processes including leukocyte migration, cell–cell adhesion, angiogenesis, (232, 233)

2.6 Metabolic Activity Assays

After 24 h stimulation, basal oxygen consumption rate (OCR) and extracellular acidification rate/proton production rate (ECAR/PPR) measurements were undertaken using a Seahorse XF96 extracellular flux analyser (Seahorse Bioscience, North

Billerica, MA). To measure OCR, cells were seeded at 70,000/well (XF96 plate) in a base medium of Dulbecco's modified eagle's medium (DMEM; Sigma) containing 10% FBS, 2.5 mM glucose, 2 mM L-glutamax, 1 mM sodium pyruvate and 0.3% phenol red. OCR measurements were taken before and following each injection of 1 μM oligomycin, an ATP synthase inhibitor (234), 1 μM fluoro-carbonyl cyanide phenylhydrazone (FCCP) (Enzo), a mitochondrial electron transport chain uncoupler (235) and 1 μM rotenone, a mitochondrial complex I inhibitor + 1 μM antimycin A, a complex III inhibitor (236). To measure ECAR, cells were incubated in the base assay medium without glucose and ECAR measurements carried out prior to the addition of glucose and following each injection of 25 mM glucose, 1 μM oligomycin and 100 mM 2-deoxy-glucose (2-DG), a glycolytic inhibitor (237).

2.7 Data Analysis

Statistical analyses were conducted using GraphPad Prism v7 (GraphPad Software Inc, California, USA). Comparisons to determine statistical differences between two groups were made using the Mann–Whitney test and between greater than two groups using two-way ANOVA. To determine significance, the probability value (p-value) was set at less than 0.05. Agilent Seahorse Wave Desktop software was used to analyse the metabolic profiles generated by Seahorse XF96.

CHAPTER 3
ASSESSING MACROPHAGE PHENOTYPIC AND BIOENERGETIC PROGRAMMING UNDER NORMOXIC VERSUS HYPOXIC TUMOUR CONDITIONS

3.1 Introduction

Macrophages represent a heterogeneous cell population that demonstrate plasticity, possessing the ability to adapt their function in response to microenvironmental stimuli. In numerous human cancers abundant macrophage infiltration in tumours has been considered an important prognostic factor (238, 239). Although macrophages are abundant in epithelial and non-epithelial mesothelioma (114, 240, 241), Burt et al. showed that higher densities of tumour-infiltrating macrophages are associated with poor survival in patients after surgery in patients with non-epithelioid MPM (114).

Within cancerous tissue, macrophages are educated by the tumour microenvironment to assist tumour progression by adopting proangiogenic tumour-promoting (M2-like) macrophages features (242). Furthermore, oxygen is vital for living cells, yet in many tumours, oxygen levels are between 1%–2% O_2(243). This hypoxic environment can affect cancer cells and immune cells. Indeed, tumour hypoxia is thought to play a pivotal role in the reprogramming of macrophages, as hypoxic TAMs become anti-inflammatory and start releasing proangiogenic factors (244, 245). What is less clear is if the hypoxic environment is the direct cause of macrophage reprogramming, or if an indirect mechanism exists that involves cross-talk between hypoxic-modulated cancer cells and hypoxic-modulated macrophages.

In-vitro mesothelioma tumour models were developed for this thesis to determine differences between the influence of normoxic and hypoxic environments. To mimic the scenario of monocytes being recruited into hypoxic regions of mesothelioma tumours, the effect of hypoxic-induced mesothelioma-derived factors on monocyte-derived macrophages generated under hypoxic conditions was examined. A similar approach was used with mesothelioma cells and monocyte-derived macrophages

cultured under normoxic conditions. To our knowledge, no in-vitro studies have assessed differences between normoxic and hypoxic mesothelioma tumour models.

Therefore, work in this chapter aimed to compare interactions between mesothelioma tumour cells and macrophages in normoxic (20% O_2) versus hypoxic (2% O_2) environments. Human mesothelioma JU77 cells were cultured under both conditions and tumour-conditioned media (TCM) collected. Human monocytes were differentiated using macrophage colony-stimulating factor (M-CSF), also known as colony stimulating factor 1 (CSF-1), into unpolarised MØ macrophages, M1 macrophages (using LPS/IFN-γ), M2 macrophages (using IL-4/IL-13) or tumour-exposed (using normoxic or hypoxic TCM) macrophages under both conditions (Figure 3.1). Changes to expression of molecules associated with macrophage function were assessed using flow cytometry (Figure 3.2), whilst changes to metabolic functionwere assessed using Seahorse technology.

3.2 Study characteristics

This study was approved by the Curtin University Human Research Ethics Committee (approval number HRE2017-0823). Healthy young volunteers (21–37 years of age) were recruited via word-of-mouth within and outside Curtin University and in collaboration with Dr. P. Methoram's research group, whose focus is platelets leaving the buffy coat available for others. All volunteers were provided with an information sheet prior to participating in the study. Volunteer health status was assessed via a questionnaire detailing their current and past medical conditions, current medications, family disease history, smoking status and asbestos exposure status (Appendix A). Any volunteer who previously or currently had cancer or who suffered from severe immune disorders, such as autoimmune disorders, were excluded from the study. Before blood collection, eligible donors were required to sign a consent form to participate in the study.

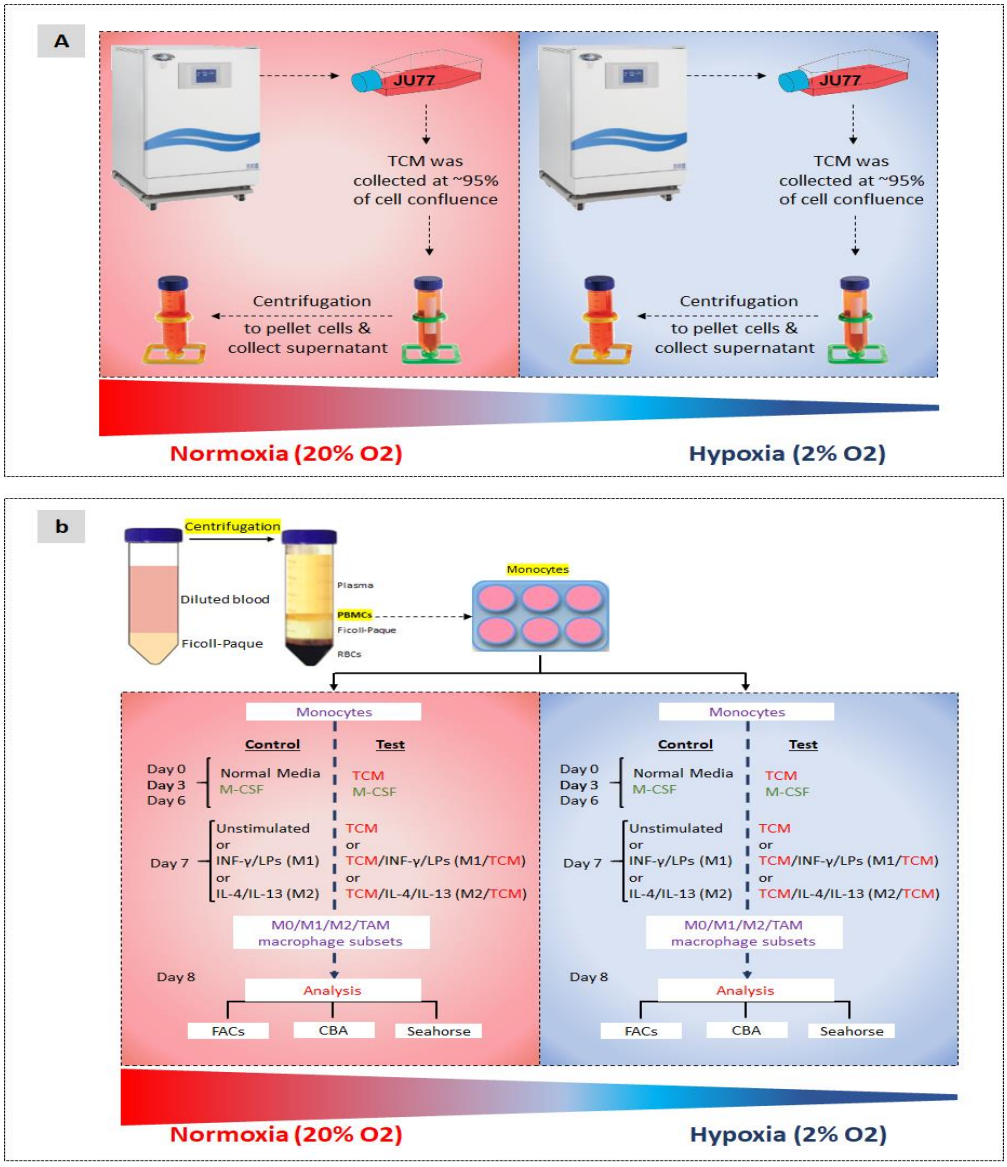

Figure 3. 1 Experimental design

(A) JU77 mesothelioma cells were grown under 20% oxygen (normoxia, shown as red) or 2% oxygen (hypoxia, shown as blue). Cell-free supernatants were isolated from tumour cell cultures using centrifugation at 1200 rpm for 5 minutes and stored at −80º C**. (B)** Human monocytes obtained from whole blood samples were cultured in 2 ml of complete RPMI-1640 medium with 50 ng/ml human M-CSF for 7 days to trigger the differentiation of monocytes into macrophages. To mimic the tumour microenvironment and generate tumour-conditioned macrophages,

monocytes were cultured in a 50:50 medium consisting of 1 ml of RPMI-1640 medium and 1 ml of TCM with 50 ng/ml M-CSF for 7 days. For hypoxic studies, monocytes were differentiated under a hypoxic environment and hypoxic TCM used. The same approach was used for normoxic experiments. On day 7, sample and control media were replaced with new media and stimuli added, including LPS (1 μg/ml)/IFN-γ (200 ng/ml) and IL-4 (10 ng/ml)/IL-13 (10 ng/ml).

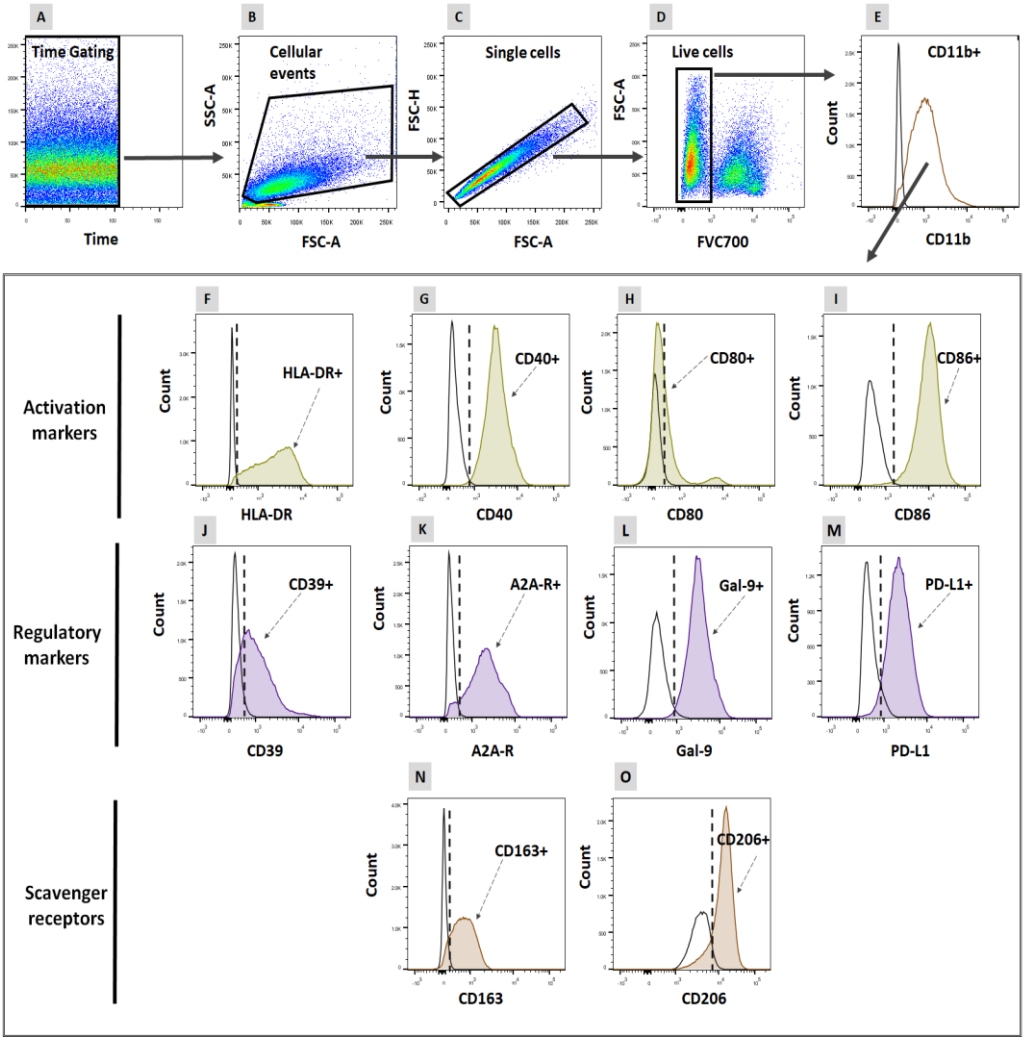

Figure 3. 2 Flow cytometric analysis of monocyte-derived macrophages

(A) FSC-A and time were used to exclude electronic noise. **(B)** FSC-A and SSC-A were used to gate cellular events based on size and granularity. **(C)** FSC-A and FSC-

H were used to eliminate doublets by gating on single cells. **(D)** A viability gate was used to eliminate dead cells stained with Fixable Viability Stain 700 (FVS700). **(E)** Live cells were analysed by gating on $CD11b^+$ macrophages for the activation markers HLA-DR **(F)**, CD40 **(G)**, CD80 **(H)** and CD86 **(I)**, the regulatory markers CD39 **(J)**, A2A-R **(K)**, Gal-9 **(L)** and PD-L1 **(M),** as well as for the scavenger receptors CD163 **(N)** and CD206 **(O)**. Figures (F-O) show coloured histograms (positive), overlaid onto open histograms (unstained cells).

3.3 Results

3.3.1 Evaluating the effect of mesothelioma on macrophages under normoxic and hypoxic conditions

3.3.1.1 Comparing the effect of normoxic versus hypoxic induced mesothelioma–derived factors on macrophage expression of activation markers

The aim of this study was to examine macrophage-mesothelioma cell interactions mediated by tumour-derived soluble factors collected under normoxic and hypoxic conditions and to evaluate changes to macrophage expression of HLA-DR, CD40, CD80 and CD86 at baseline and when stimulated with INF-γ+LPS or with IL-4+IL-13.

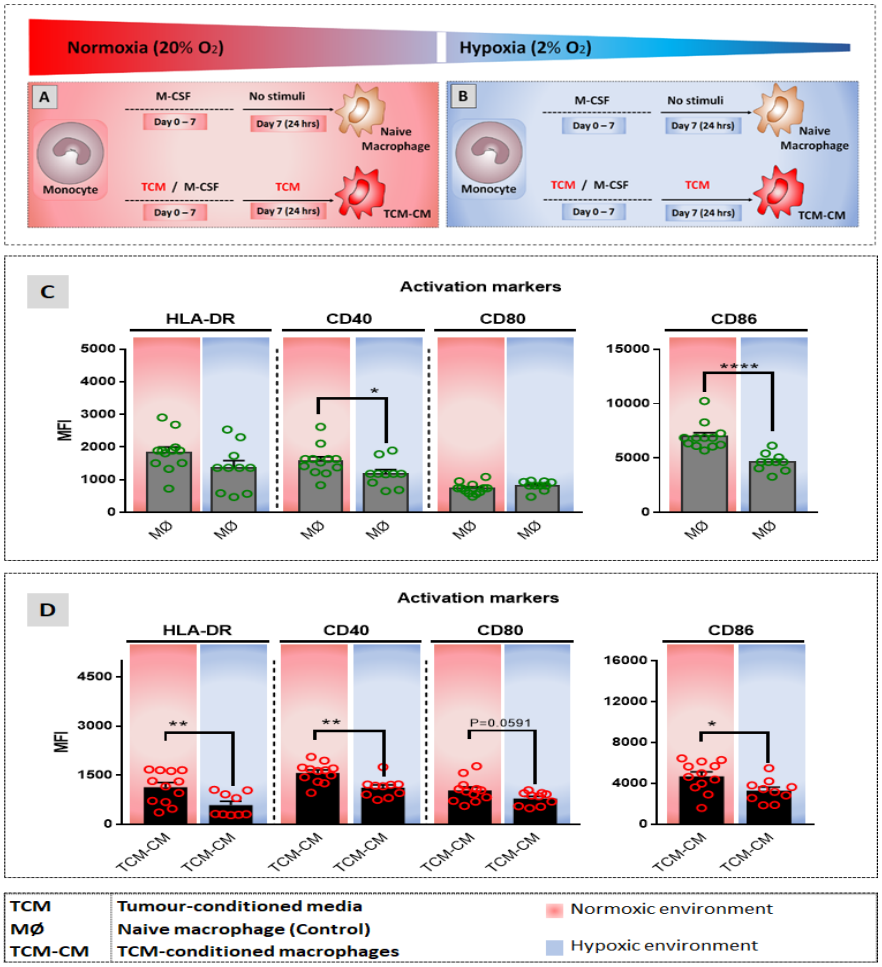

Figure 3.3 Hypoxia and hypoxic-exposed mesothelioma-derived factors reduce HLA-DR, CD40, CD80 and CD86 expression on macrophages

Human monocytes isolated from healthy donors (as described in Figure 3.1.B), were differentiated into mature macrophages using M-CSF under normoxic (A) and hypoxic (B) conditions. Similarly, tumour-conditioned macrophages were generated using M-CSF with or without TCM, under normoxic (A) and hypoxic (B) conditions. Cells were stained for activation markers (HLA-DR, CD40, CD80 and CD86) for flow cytometric analysis. Surface expression levels for HLA-DR, CD40, CD80 and CD86 (C and D) were quantified by flow cytometry and shown as median fluorescence intensity (MFI). Pooled data is expressed as mean ± standard error of the mean (SEM) in normoxic naive macrophages (MØ) (control) versus hypoxic macrophages MØ and normoxic tumour-conditioned macrophages (TCM-CM)

versus hypoxic (TCM-CM). P-values were determined using the Mann-Whitney test, * = $p < 0.05$, ** = $p < 0.005$, *** = $p < 0.0005$ **** = $p < 0.0001$, n = 12 replicates per normoxic condition, n = 10 replicates per hypoxic condition.

3.3.1.1.1 Hypoxia directly reduces CD40 and CD86 on macrophages

Naïve (non-tumour exposed) macrophages significantly decreased CD40 (Figure 3.3.C; $p = 0.02$) and CD86 expression (Figure 3.3.C; $p < 0.0001$) under hypoxic relative to normoxic conditions. In contrast, no differences were observed between normoxic and hypoxic macrophages in HLA-DR (Figure 3.3.C) and CD80 expression (Figure 3.3.C). These data show that oxygen deprivation can directly affect macrophage function.

3.3.1.1.2 Mesothelioma-derived factors generated under hypoxia further reduce HLA-DR, CD40 and CD86 expression on macrophages

Macrophages exposed to hypoxic TCM and cultured under hypoxic conditions demonstrate significantly lower expression levels of HLA-DR (Figure 3.3.D; $p = 0.009$), CD40 (Figure 3.3.D; $p = 0.002$) and CD86 (Figure 3.3.D; $p = 0.02$) relative to macrophages exposed to normoxic TCM and cultured under normoxic conditions. A decreasing trend was seen for CD80 expression in hypoxic TCM-conditioned macrophages relative to normoxic TCM-conditioned macrophages (Figure 3.3.D; $p = 0.06$). Taken together, the data show that macrophages adopt significantly different functions that are directly determined by oxygen levels and influenced by tumour cell responses to reduced oxygen. These data suggest that macrophages are significantly affected by the condition of the tumour cell and that oxygen levels also play a key role in determining their fate. Therefore, the data was further interrogated to determine the effects of normoxia-induced versus hypoxia-induced TCM on macrophages grown under normoxic and hypoxic conditions.

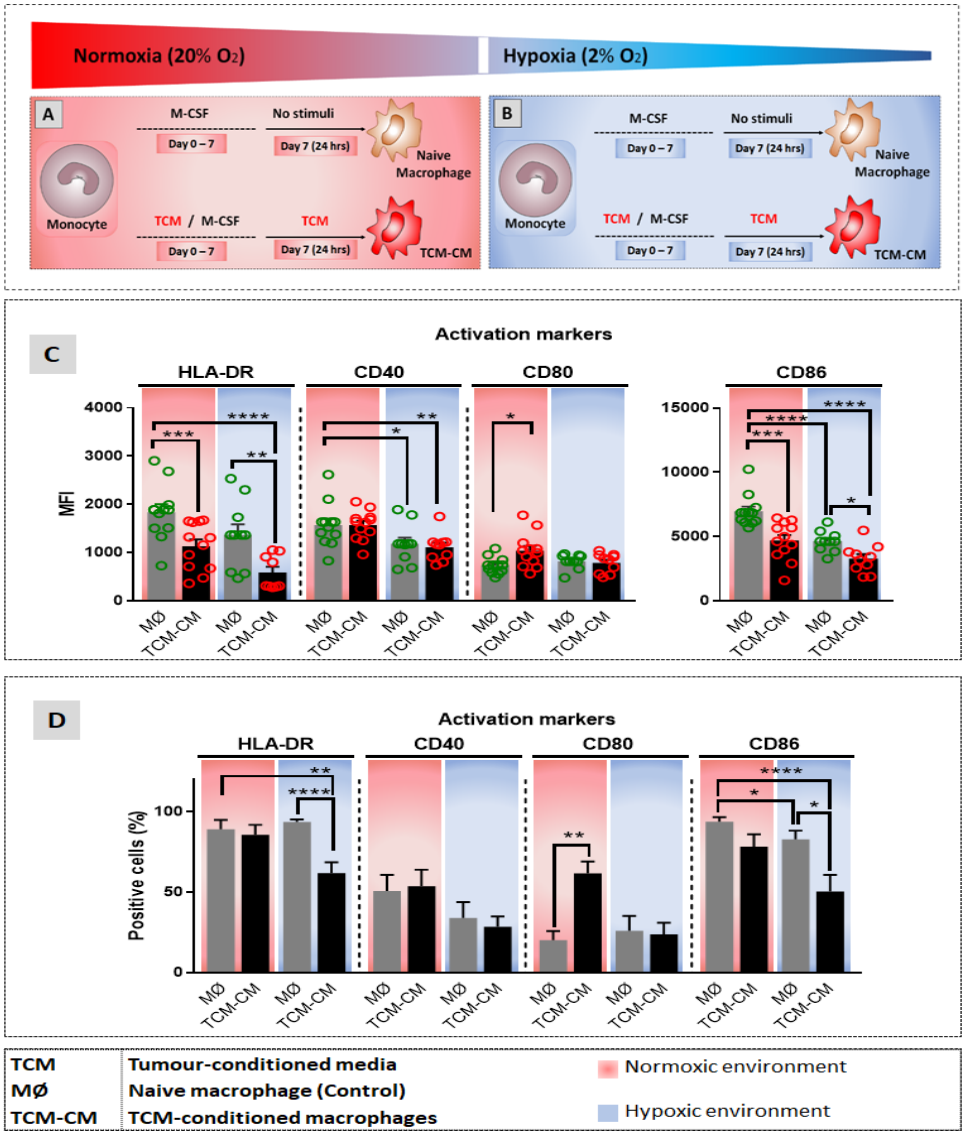

Figure 3.4 Oxygen levels modulate factors secreted by mesothelioma cells that affect macrophage expression of HLA-DR, CD40, CD80 and CD86

Normal macrophages and tumour-conditioned macrophages differentiated from monocytes under normoxic (A)and hypoxic (B) conditions were stained for HLA-DR, CD40, CD80 and CD86 for flow cytometric analysis. Pooled data of surface expression levels (MFI) (C) and percentages of positive cells (D) are expressed as mean ± SEM. P-values were determined using the Mann-Whitney test, * = $p < 0.05$, ** = $p < 0.005$, *** = $p < 0.0005$ **** = $p < 0.0001$, n=12 replicates per normoxic condition, n=10 replicates per hypoxic condition.

3.3.1.1.3 Regardless of oxygen levels, mesothelioma-derived factors down-regulate HLA-DR expression

Compared to naïve normoxic macrophage controls, HLA-DR expression levels (MFI) were significantly lower in normoxic TCM-conditioned macrophages (Figure 3.4.C; $p = 0.002$). There were no differences in HLA-DR expression between naïve normoxic macrophages and naïve hypoxic macrophages (Figure 3.4.C; $p = 0.065$). However, hypoxic TCM-conditioned macrophages had lower HLA-DR expression levels than normoxic controls (Figure 3.4.C; $p = 0.0001$), hypoxic controls (Figure 3.4.C; $p = 0.005$) and normoxic TCM-conditioned macrophages, as shown previously (Figure 3.3.D; $p = 0.009$). These data also showed that hypoxic TCM significantly lowered the percentage of HLA-DR^+ macrophages compared to normoxic (Figure 3.4.D; $p = 0.003$) and hypoxic controls (Figure 3.4.D; $p < 0.0001$). No differences were observed between normoxic controls and normoxic TCM-conditioned macrophages (Figure 3.4.D). These data suggest that mesothelioma derived factors reduce HLA-DR expression levels regardless of oxygen levels, and that factors generated when mesothelioma cells are under hypoxic conditions further reduce the proportion of HLA-DR^+ macrophages.

3.3.1.1.4 Hypoxia plays an essential role in decreasing CD40 on macrophages

No differences were observed in CD40 expression in normoxic TCM-conditioned macrophages compared to normoxic control macrophages (Figure 3.4.C). However, there was a significant decrease in hypoxic controls and TCM-conditioned macrophages compared to normoxic control macrophages (Figure 3.4.C; $p = 0.02$ and $p = 0.007$ respectively). No differences were seen between hypoxic controls and hypoxic TCM-conditioned macrophages (Figure 3.4.C). Note that the percentage of $CD40^+$ cells did not change in response to different oxygen levels and TCM (data not shown). These data suggest that CD40 downregulation on macrophages in tumours may be due to hypoxia.

3.3.1.1.5 Mesothelioma-derived factors generated under normoxia upregulate CD80 on macrophages

Normoxia-induced TCM significantly increased CD80 expression levels (MFI) and the percentage of $CD80^+$ cells relative to normoxic control macrophages (Figure 3.4.C; $p = 0.02$; Figure 3.4.D; $p = 0.001$ respectively); no differences were seen between hypoxic controls and hypoxic TCM-conditioned macrophages compared to normoxic control macrophages (Figure 3.4.C). Furthermore, no differences were seen between hypoxic and hypoxic TCM-conditioned macrophages in CD80 expression (Figure 3.4.C). These data suggest that normoxic-induced TCM contains molecules that increase CD80 expression.

3.3.1.1.6 Hypoxia, normoxic and hypoxic TCM downregulate CD86 expression on macrophages

CD86 expression levels (MFI) significantly decreased in normoxic TCM-conditioned macrophages (Figure 3.4.C; $p = 0.0003$), hypoxic controls (Figure 3.4.C; $p < 0.0001$) and hypoxic TCM-conditioned macrophages (Figure 3.4.C; $p < 0.0001$) compared to normoxic control macrophages. Further, hypoxic TCM-conditioned macrophages showed lower CD86 expression than hypoxic control macrophages (Figure 3.4.C; $p = 0.006$). Similarly, hypoxic and normoxic-induced TCM decreased the percentage of $CD86^+$ cells (Figure 3.4.D; $p = 0.05$) compared to normoxic controls. However, hypoxic TCM conditioned macrophages demonstrated the lowest percentage of $CD86^+$ cells compared to normoxic controls (Figure 3.4.D; $p = 0.0004$) and to hypoxic controls (Figure 3.4.D; $p = 0.04$). These data suggest that hypoxic TCMcontains molecules that lead to downregulation of CD86 expression on macrophages. Hypoxia further plays a major role in decreasing CD86 expression via a direct effect on macrophages. The effect would be reduced T cell activation.

3.3.1.1.7 How do normoxic and hypoxic tumour-conditioned macrophages respond to pro-inflammatory LPS/IFN-γ?

Next, the effect of proinflammatory stimuli LPS/IFN-γ on macrophages cultured with TCM under normoxic and hypoxic conditions was investigated. Note that no significant

changes were seen in HLA-DR surface expression when normoxic and hypoxic normal and TCM-conditioned macrophages were stimulated with LPS/IFN-γ (data not shown).

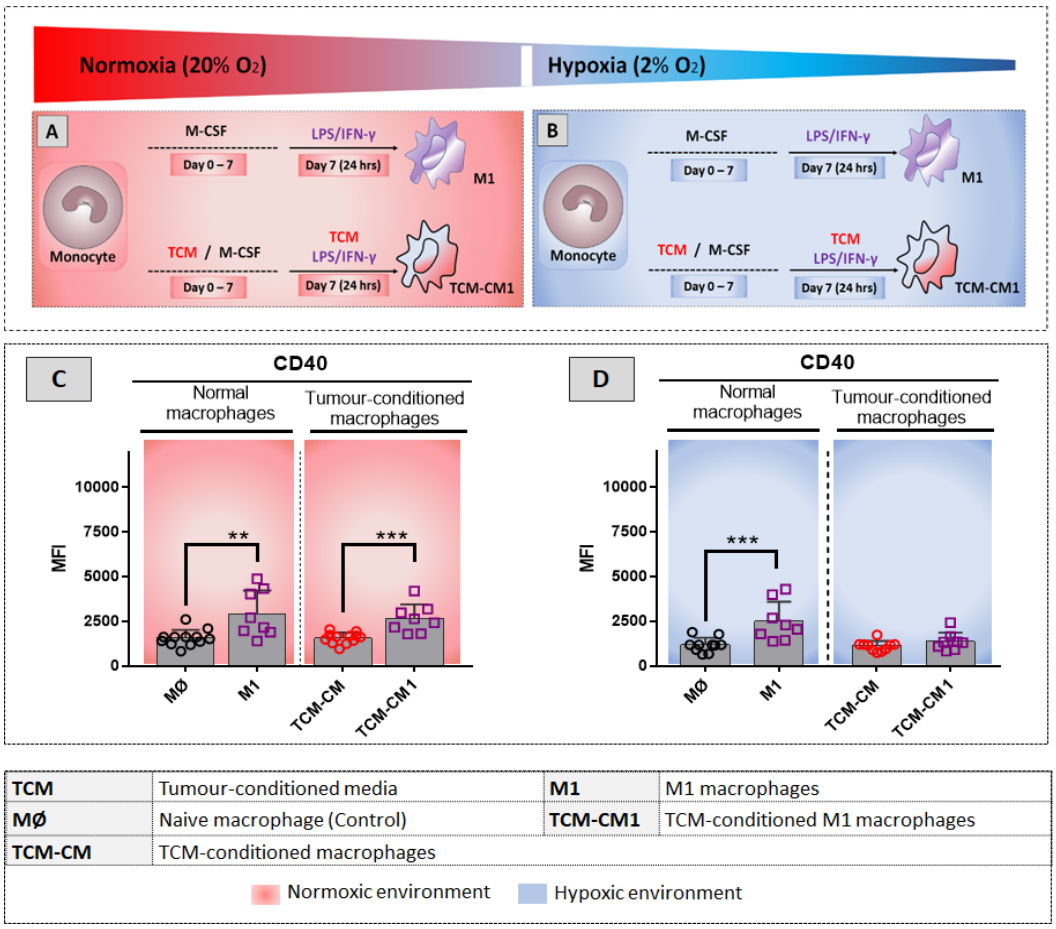

Figure 3.5 Effect of LPS/IFN-γ on macrophage CD40 expression under normoxic and hypoxic conditions

Normal and tumour-conditioned monocyte-derived macrophages stimulated with LPS/IFN-γ to generate M1 macrophages and tumour-conditioned M1 macrophages (TCM-CM1) at day 7 for 24 h, under normoxic (A) and hypoxic (B) conditions were stained for CD40 expression. Pooled MFI data (C and D) are expressed as mean ± SEM in normoxic naive macrophages (MØ) (control) versus normoxic M1, normoxic TCM-CM versus normoxic TCM-CM1, hypoxic naive macrophages (MØ) (control) versus hypoxic M1, hypoxic TCM-CM versus hypoxic TCM-CM1, hypoxic M1 versus hypoxic TCM-CM1 and normoxic TCM-CM1 versus hypoxic

TCM-CM1. P-values were determined using the Mann-Whitney test, * = $p < 0.05$, ** = $p < 0.005$, *** = $p < 0.0005$ **** = $p < 0.0001$, n=8 replicates per normoxic and hypoxic M1 and TCM-CM1 conditions.

3.3.1.1.7.1 Mesothelioma-derived factors generated under hypoxia inhibit the role of LPS/IFN-γ in upregulating CD40 expression

Stimulating macrophages with LPS/IFN-γ significantly increased CD40 expression in M1 macrophages versus naïve MØ macrophages (Figure 3.5.C; $p = 0.005$) and TCM-conditioned M1 macrophages versus TCM-conditioned macrophages (Figure 3.5.C; $p = 0.0007$) under normoxia. Further, M1 macrophages showed higher expression of CD40 compared to MØ macrophages (Figure 3.5.D; $p = 0.0002$) under hypoxia. However, LPS/IFN-γ could not increase CD40 expression under hypoxic tumour conditions (Figure 3.5.D) although the action of LPS/IFN-γ on normal macrophages under hypoxia ($p = 0.0002$) was higher than that on normal macrophages under normoxia ($p = 0.005$). The data implies that the ability of LPS/IFN-γto induce the CD40/CD154 costimulatory pathway in macrophages under hypoxia is compromised. This might also be seen as mesothelioma progresses into a hypoxic state.

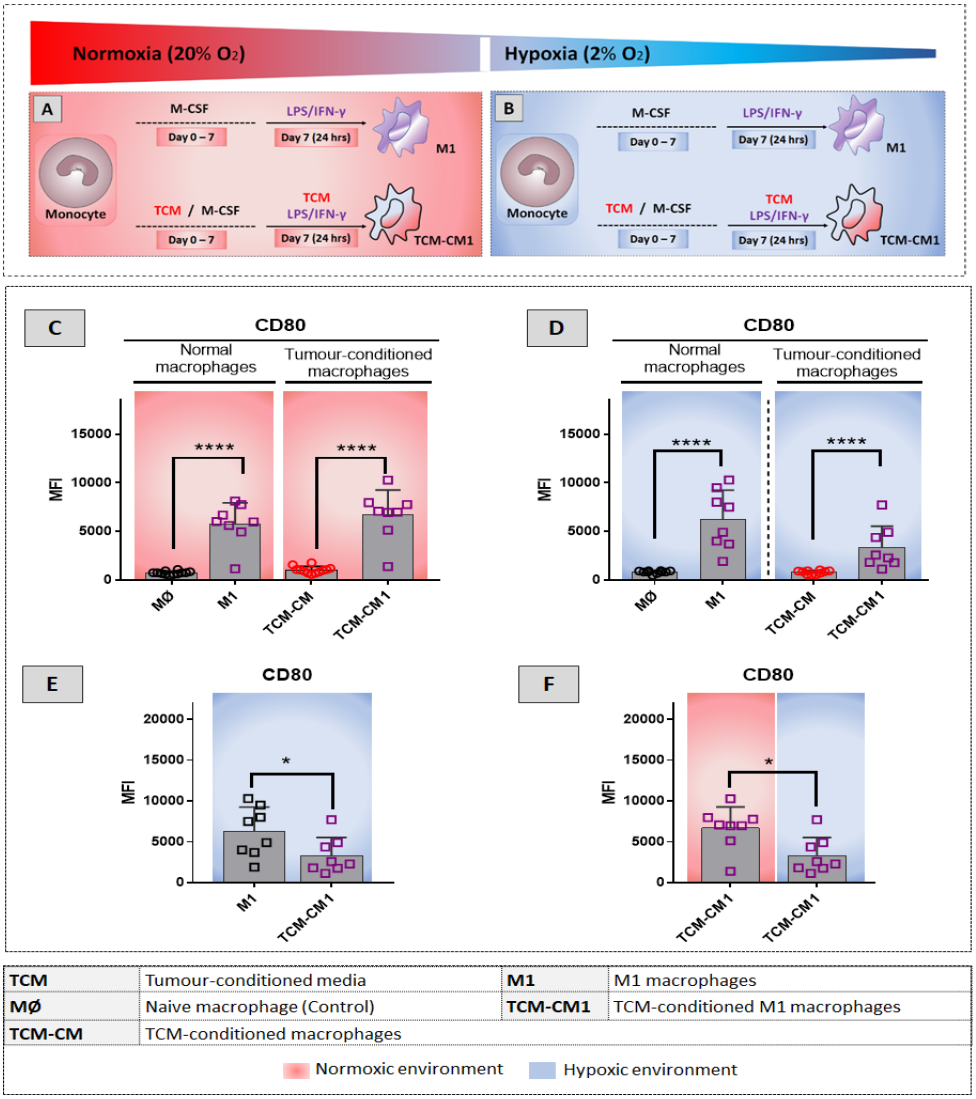

Figure 3.6 The effect of LPS/IFN-γ on macrophage CD80 expression under normoxic and hypoxic conditions

Normal and tumour-conditioned macrophages differentiated stimulated with LPS/IFN-γ to generate M1 macrophages and tumour-conditioned M1 macrophages (TCM-CM1), under normoxia (A) and hypoxia (B) were stained for CD80 for flow cytometric analysis. Pooled MFI data (C, D, E and F) are expressed as mean ± SEM. P-values were determined using the Mann-Whitney test, * = $p < 0.05$, ** = $p < 0.005$, *** = $p < 0.0005$ **** = $p < 0.0001$, n=8 replicates per normoxic, hypoxic M1 and TCM-CM1 conditions.

3.3.1.1.7.2 Hypoxic-exposed mesothelioma-derived factors attenuate the ability of LPS/IFN-γ to increase CD80 expression on macrophages

LPS/IFN-γ stimulation significantly upregulated CD80 surface expression in M1 macrophages compared to MØ macrophages, as expected (Figure 3.6.C; $p < 0.0001$) as well as in in TCM-conditioned M1 macrophages compared to TCM-conditioned macrophages (Figure 3.6.C; $p < 0.0001$) under normoxia. Similarly, under hypoxia LPS/IFN-γ upregulated CD80 expression in M1 macrophages compared to MØ macrophages (Figure 3.6.D; $p < 0.0001$) as well as in TCM-conditioned M1 macrophages compared to TCM-conditioned macrophages (Figure 3.6.D; $p < 0.0001$). Although LPS/IFN-γ stimulation was associated with a significant increase in CD80 in hypoxic M1 and TCM-conditioned M1 macrophages compared to controls, CD80 expression in TCM-conditioned M1 macrophages was significantly lower than in M1 macrophages (Figure 3.6.E; $p = 0.05$). Figure 3.6.F shows that hypoxic TCM-conditioned M1 macrophages expressed lower CD80 than normoxic TCM-conditioned M1 cells ($p = 0.03$), indicating that hypoxic TCM impairs the response of macrophages to LPS/IFN-γ.

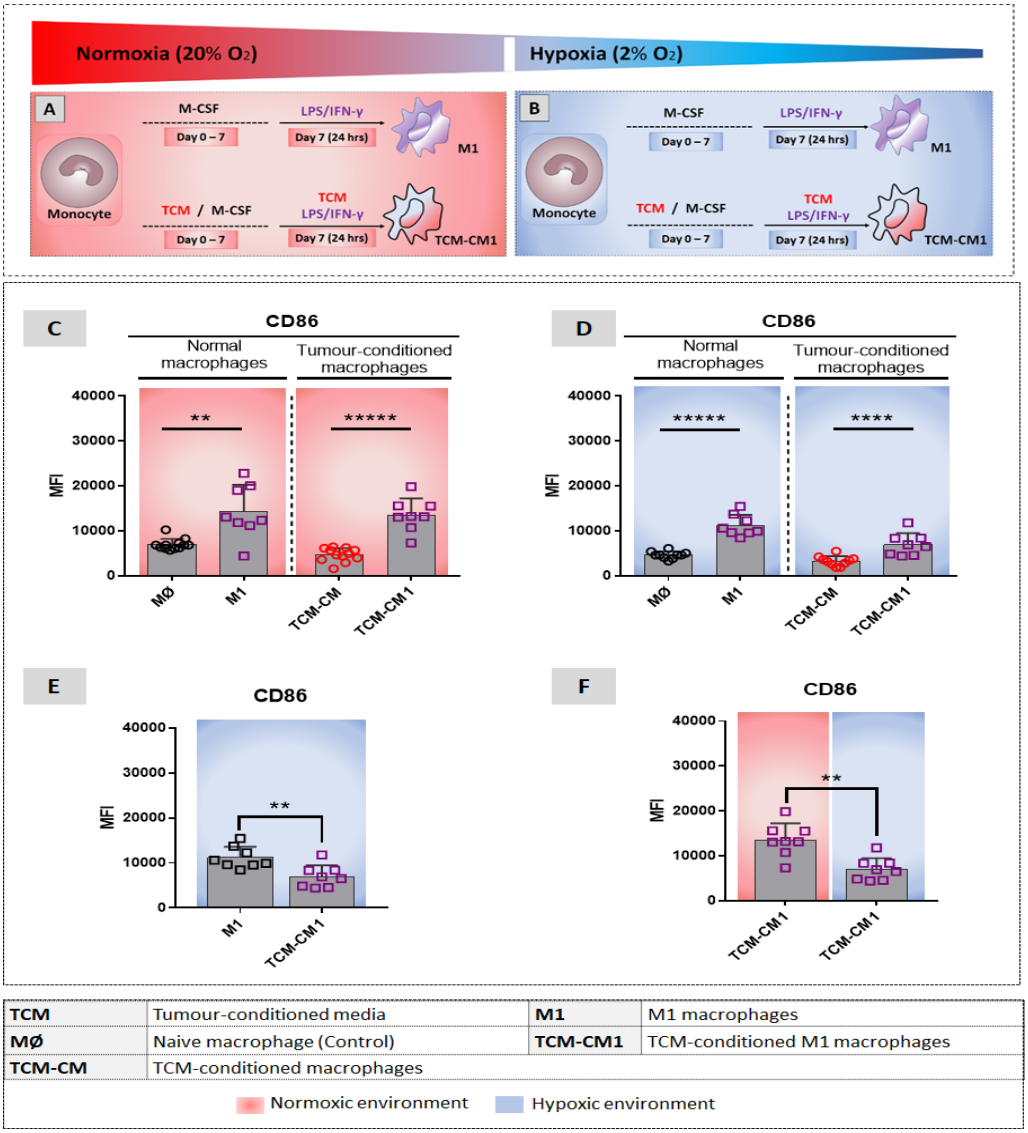

TCM	Tumour-conditioned media	**M1**	M1 macrophages
MØ	Naive macrophage (Control)	**TCM-CM1**	TCM-conditioned M1 macrophages
TCM-CM	TCM-conditioned macrophages		

Figure 3. 7 The effect of LPS/IFN-γ on macrophage CD86 expression under normoxic and hypoxic conditions

Normal and tumour-conditioned macrophages were stimulated with LPS/IFN-γ to generate M1 macrophages and tumour-conditioned M1 macrophages (TCM-CM1), under normoxic (A) and hypoxic (B) conditions and stained for CD86 for flow cytometric analysis. Pooled data of surface expression levels (MFI) (C, D, E and F) are expressed as mean ± SEM. P-values were determined using the Mann-Whitney test, * = $p < 0.05$, ** = $p < 0.005$, *** = $p < 0.0005$ **** = $p < 0.0001$, n=8 replicates per normoxic and hypoxic M1 and TCM-CM1 conditions.

3.3.1.1.7.3 Mesothelioma-derived factors generated under hypoxia attenuate the effect of LPS/IFN-γ in upregulating CD86 on macrophages

CD86 surface expression was significantly upregulated by LPS/IFN-γ in M1 macrophages compared to MØ macrophages (Figure 3.7.C; $p = 0.004$) and in TCM-conditioned M1 macrophages compared to TCM-conditioned macrophages (Figure 3.7.C; $p < 0.0001$) under normoxia. Similarly, LPS/IFN-γ upregulated CD86 expression in M1 macrophages compared to MØ macrophages (Figure 3.7.D; $p < 0.0001$) and in TCM-conditioned M1 macrophages compared to TCM-conditioned macrophages (Figure 3.7.D; $p = 0.0003$) under hypoxia. Nonetheless, the increase in CD86 expression in hypoxic TCM-conditioned M1 macrophages was still significantly lower than that seen in M1 macrophages (Figure 3.7.E; $p = 0.003$). Figure 3.7.F shows that hypoxic TCM-conditioned M1 cells have lower CD86 expression than normoxic TCM-conditioned M1 ($p = 0.002$). These data indicate that hypoxic TCM confounds the ability of macrophages to upregulate CD86 in response to LPS/IFN-γ. Again, these data suggest that mesothelioma cells are significantly affected by oxygen levels and that this influences their crosstalk with macrophages. In this case, hypoxic TCM plus an environment of reduced oxygen, impair the ability of M1 macrophages to activate T cells because of reduced CD86.

3.3.1.1.8 How do normoxic and hypoxic tumour-conditioned macrophages respond to M2-inducing IL-4/IL-13?

Next, the role of IL-4/IL-13 in regulating expression of the same activation markers (HLA-DR, CD40, CD80 and CD86) by macrophages was determined. As expected, the data showed that IL-4/IL-13 did not change HLA-DR and CD40 expression levels in macrophages (data not shown). However, CD80 (Figure 3.8C) expression significantly increased whilst CD86 (Figure 3.8E) decreased under normoxic conditions but not under tumour-exposed or hypoxic conditions. The data again show the influence of oxygen levels on the functional capacity of macrophages.

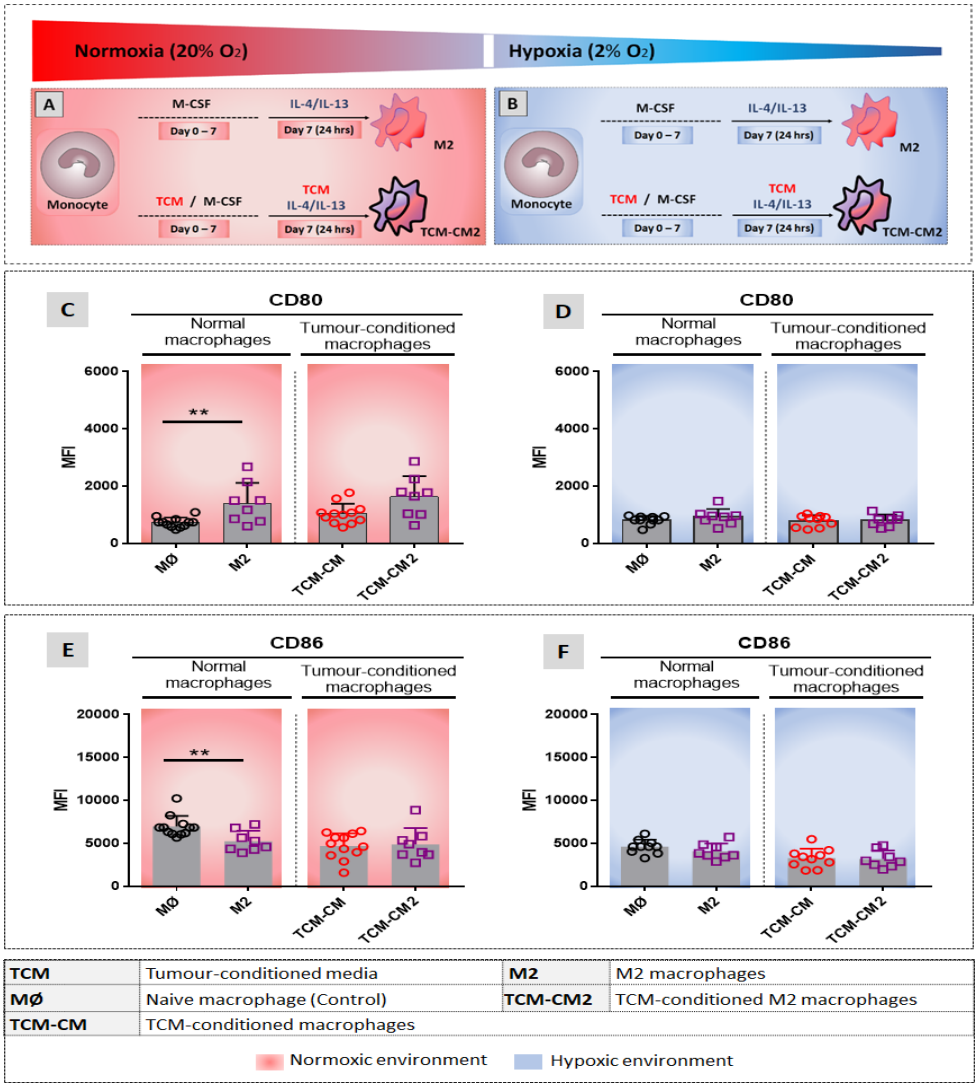

TCM	Tumour-conditioned media	**M2**	M2 macrophages
MØ	Naive macrophage (Control)	**TCM-CM2**	TCM-conditioned M2 macrophages
TCM-CM	TCM-conditioned macrophages		

Figure 3.8 The effect of IL-4/IL-13 on macrophage CD80 and CD86 expression under normoxic and hypoxic conditions

Normal and tumour-conditioned macrophages differentiated from monocytes were stimulated with IL-4/IL-13 to generate M2 macrophages and tumour-conditioned M2 macrophages (TCM-CM2) at day 7 for 24 h, under normoxic (A) and hypoxic (B) conditions and stained for CD80 and CD86. Pooled MFI data of CD80 (C and D) and CD86 (E and F) are expressed as mean ± SEM. P-values were determined using the Mann-Whitney test, * = $p < 0.05$, ** = $p < 0.005$, *** = $p < 0.0005$ **** = $p < 0.0001$, n = 8 replicates per normoxic and hypoxic (M2 and TCM-CM2) conditions.

3.3.1.1.8.1 Hypoxia and mesothelioma factors prevent macrophages from increasing CD80 in response to IL-4/IL-13

CD80 expression was upregulated in normoxic M2 macrophages compared to normoxic controls (Figure 3.8.C; $p = 0.0066$). However, no differences were seen between normoxic TCM-conditioned macrophages versus TCM-conditioned M2 macrophages (Figure 3.8.C; $p = 0.07$), or hypoxic controls versus M2 macrophages and hypoxic TCM-conditioned macrophages versus TCM-conditioned M2 macrophages (Figure 3.8.D). The data suggest that regardless of oxygen levels, mesothelioma derived factors hinder the ability of macrophages to respond to IL-4/IL-14 by upregulating CD80.

3.3.1.1.8.2 Hypoxia and mesothelioma factors prevent macrophages from decreasing CD86 expression in response to IL-4/IL-13

CD86 expression decreased under normoxia when macrophages were exposed to IL-4/IL-13 (Figure 3.8.E; $p = 0.007$). No differences were seen between normoxic TCM-conditioned macrophages versus TCM-conditioned M2 macrophages, hypoxic controls versus M2 macrophages, and hypoxic TCM-conditioned macrophages versus TCM-conditioned M2 macrophages (Figure 3.8.F).

3.3.1.2 Comparing the effect of normoxic versus hypoxic-induced mesothelioma factors on macrophage expression of regulatory markers

The aim of this study was to examine macrophage-mesothelioma interactions under normoxic and hypoxic conditions and evaluate macrophage expression of CD39, A2A-R, PD-L1 and Gal-9.

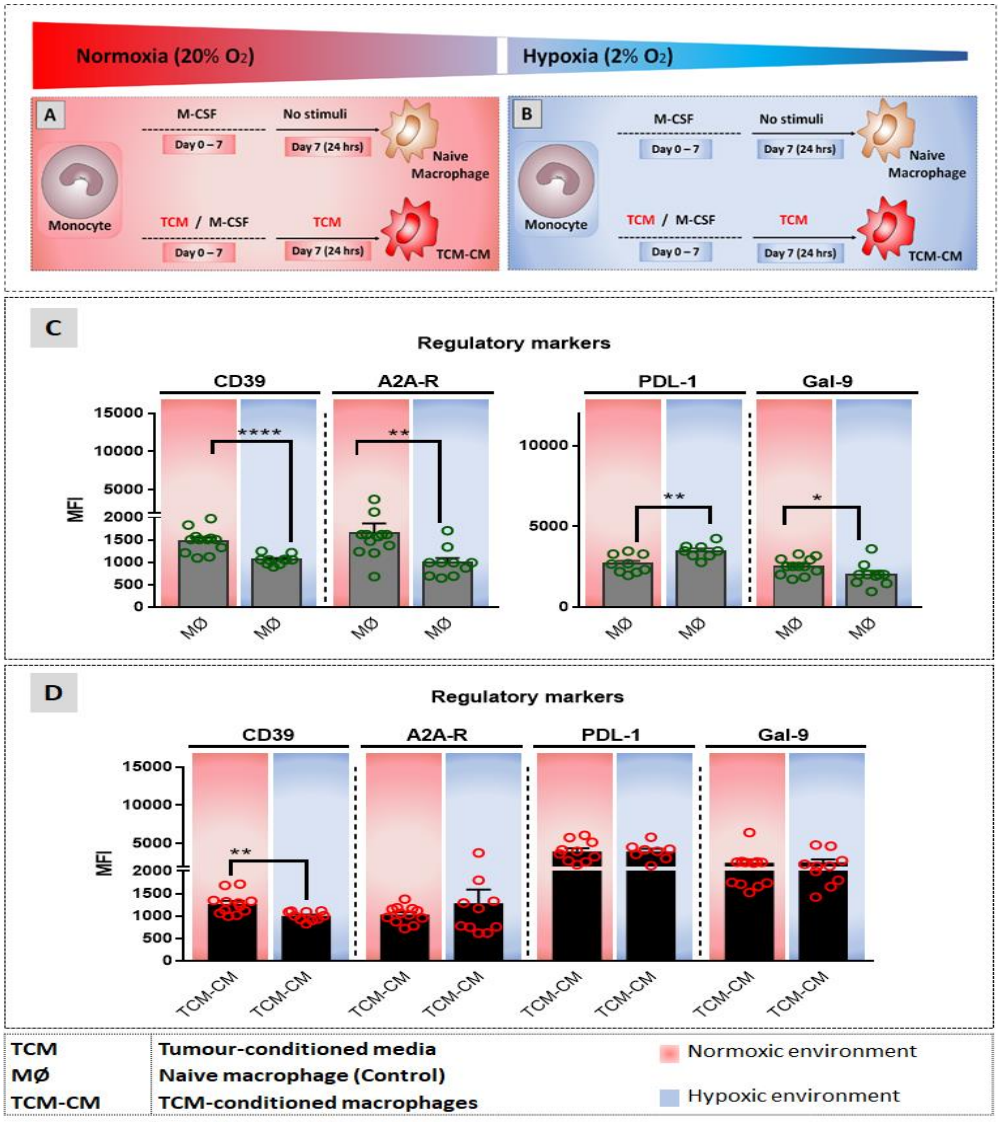

Figure 3.9 Role of normoxic and hypoxic tumour conditions on macrophage expression of regulatory markers (CD39, A2A-R, PDL-1 and Gal-9)

Normal and tumour-conditioned macrophages differentiated from monocytes under normoxic (A) and hypoxic (B) conditions were stained for regulatory markers CD39, A2A-R, PDL-1 and Gal-9 for flow cytometric analysis. Pooled data of surface expression levels (MFI) (C) and percentages of positive cells (D) are expressed as mean ± SEM. P-values were determined using the Mann-Whitney test, * = $p < 0.05$, ** = $p < 0.005$, *** = $p < 0.0005$ **** = $p < 0.0001$, n=12 replicates per normoxic condition, n=10 replicates per hypoxic condition.

3.3.1.2.1 Hypoxia downregulates CD39, A2A-R and Gal-9 and upregulates PDL-1 on macrophages

The data demonstrates significant downregulation of CD39, A2A-R and Gal-9 expression in hypoxic macrophage controls relative to their normoxic controls (Figure 3.9.C; $p < 0.0001$; $p = 0.007$; $p = 0.046$ respectively). However, there was a significant increase of PDL-1 in hypoxic macrophage controls compared to their normoxic controls (Figure 3.9.C; $p = 0.007$). Thus, the data show that hypoxia elevates PDL-1 on macrophages, which could exacerbate immune suppression in hypoxic tissues.

3.3.1.2.2 Hypoxia-induced mesothelioma factors reduce CD39 yet maintain A2A-R, PDL-1 and Gal-9

There were no significant differences between normoxic TCM-conditioned macrophages and hypoxic TCM-conditioned macrophages in A2A-R, PDL-1 and Gal-9 (Figure 3.9.D). However, a significant reduction was seen in CD39 expression (Figure 3.9.D; $p = 0.002$) under hypoxia. Thus, the data show that hypoxia maintains mesothelioma-associated immune suppression via A2AA-R, PDL-1 and Gal-9 expression by macrophages.

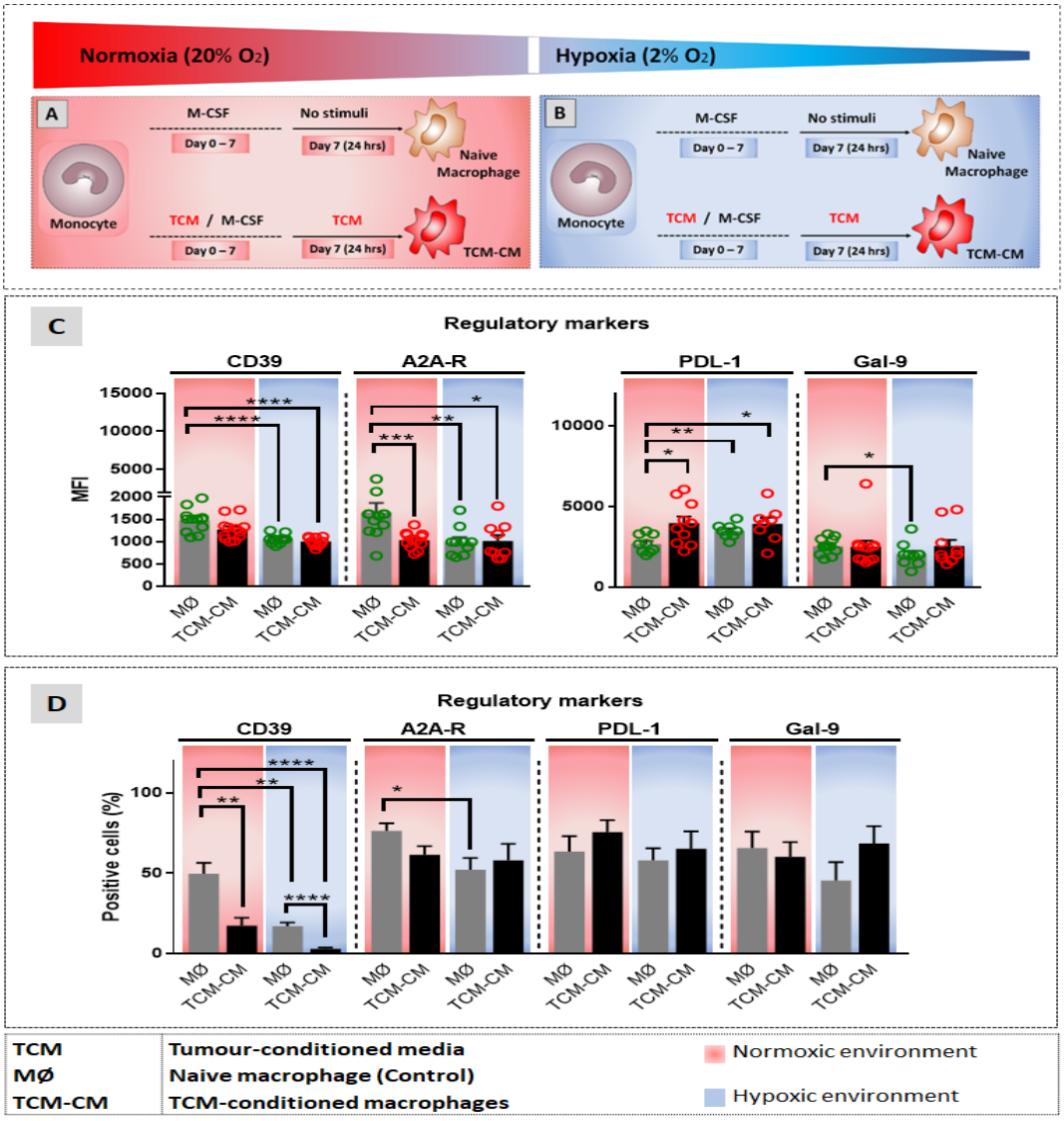

Figure 3. 10 Figure 3.10 The effect of normoxic and hypoxic-induced tumour conditioned media on macrophage expression of CD39, A2A-R, PDL-1 and Gal-9

Normal macrophages and tumour-conditioned macrophages differentiated from monocytes under normoxic (A) and hypoxic (B) conditions were stained for regulatory markers (CD39, A2A-R, PDL-1 and Gal-9) for flow cytometric analysis. Pooled data of surface expression levels (MFI) (C) and the percentages of positive cells (D) are expressed as mean ± SEM. P-values were determined using the Mann-

Whitney test, * = $p < 0.05$, ** = $p < 0.005$, *** = $p < 0.0005$ **** = $p < 0.0001$, n=12 replicates per normoxic condition, n=10 replicates per hypoxic condition.

3.3.1.2.3 Hypoxia plays an essential role in downregulating CD39 expression

There was significant downregulation in CD39 expression in hypoxia-exposed normal macrophages and hypoxic induced TCM-conditioned macrophages compared to normoxic controls (Figure 3.10C; $p < 0.0001$; $p = 0.007$ respectively). Similarly, the percentage of $CD39^+$ cells in hypoxic TCM-conditioned macrophages was significantly lower than hypoxic normal macrophages (Figure 3.10D; $p < 0.0001$). There were no other differences between hypoxic controls and hypoxic-induced TCM-conditioned macrophages or between hypoxic controls and hypoxic TCM-conditioned macrophages (Figure 3.10C). However, normoxic TCM-conditioned macrophages also significantly decreased the percentage of cells expressing $CD39^+$ relative to normoxic controls, hypoxic controls and hypoxic TCM-conditioned macrophages (Figure 3.10D; $p = 0.002$; $p = 0.02$; $p < 0.0001$ respectively). These data suggest that macrophage expression of CD39 is reduced by mesothelioma-derived factors and oxygen deprivation and that the adenosine pathway may not play a role in macrophage-mediated immune suppression in mesothelioma.

3.3.1.2.4 Hypoxia and normoxic/hypoxic-induced mesothelioma-derived factors downregulate A2A-R expression by macrophages

A2A-R expression levels were significantly downregulated in normoxic TCM-conditioned macrophages, hypoxic controls and hypoxic TCM-conditioned macrophages relative to normoxic controls (Figure 3.10.C; $p = 0.0005$; $p = 0.007$; $p = 0.01$ respectively). There were no differences between hypoxic controls and hypoxic TCM-conditioned macrophages (Figure 3.10.C). There was also a significant decrease in the percentage of $A2A\text{-}R^+$ macrophages in hypoxic controls compared to normoxic controls (Figure 3.10.D; $p = 0.02$). Thus, the data indicate that regardless of oxygen levels, TCM contains molecules that lead to downregulation of A2A-R expression in macrophages, again suggesting that the adenosine pathway may not play a role in immune suppression in mesothelioma.

3.3.1.2.5 Hypoxia and TCM increase PDL-1 expression

Expression of PDL-1 increased significantly in normoxic TCM-conditioned macrophages relative to hypoxic controls, hypoxic TCM-conditioned macrophages and normoxic controls (Figure 3.10.C; $p = 0.02$; $p = 0.007$; $p = 0.01$). However, there were no differences between hypoxic controls and hypoxic TCM-conditioned macrophages (Figure 3.10.C; $p = 0.3$). Note that the percentage of PDL-1^+ cells did not change in response to the different oxygen levels and TCM (data not shown). Thus, the data indicate that macrophages increase PDL-1 in response to hypoxia and mesothelioma-derived factors generated under normoxia and hypoxia, implying an important suppressive role in the PDL-1/PD-1 pathway in mesothelioma.

3.3.1.2.6 Hypoxia decreases Gal-9 expression

No differences were observed in Gal-9 expression when normoxic controls were compared to normoxic TCM-conditioned macrophages and hypoxic TCM-conditioned macrophages (Figure 3.10.C). However, there was a significant decrease of Gal-9 in hypoxic controls compared to normoxic controls (Figure 3.10.C; $p = 0.046$). There were no differences between hypoxic- and hypoxic TCM-conditioned macrophages (Figure 3.10.C). The data suggest that mesothelioma-derived factors may induce macrophages to maintain their ability to induce apoptosis in $CD8^+$ cells under hypoxia via Gal-9 (96, 97).

3.3.1.2.7 Do normoxic and hypoxic tumour-conditioned macrophages respond to proinflammatory stimuli LPS/IFN-γ?

Next, the ability of macrophages cultured with TCM under normoxic and hypoxic conditions to respond to the M1 stimulus, LPS/IFN-γ, was investigated.

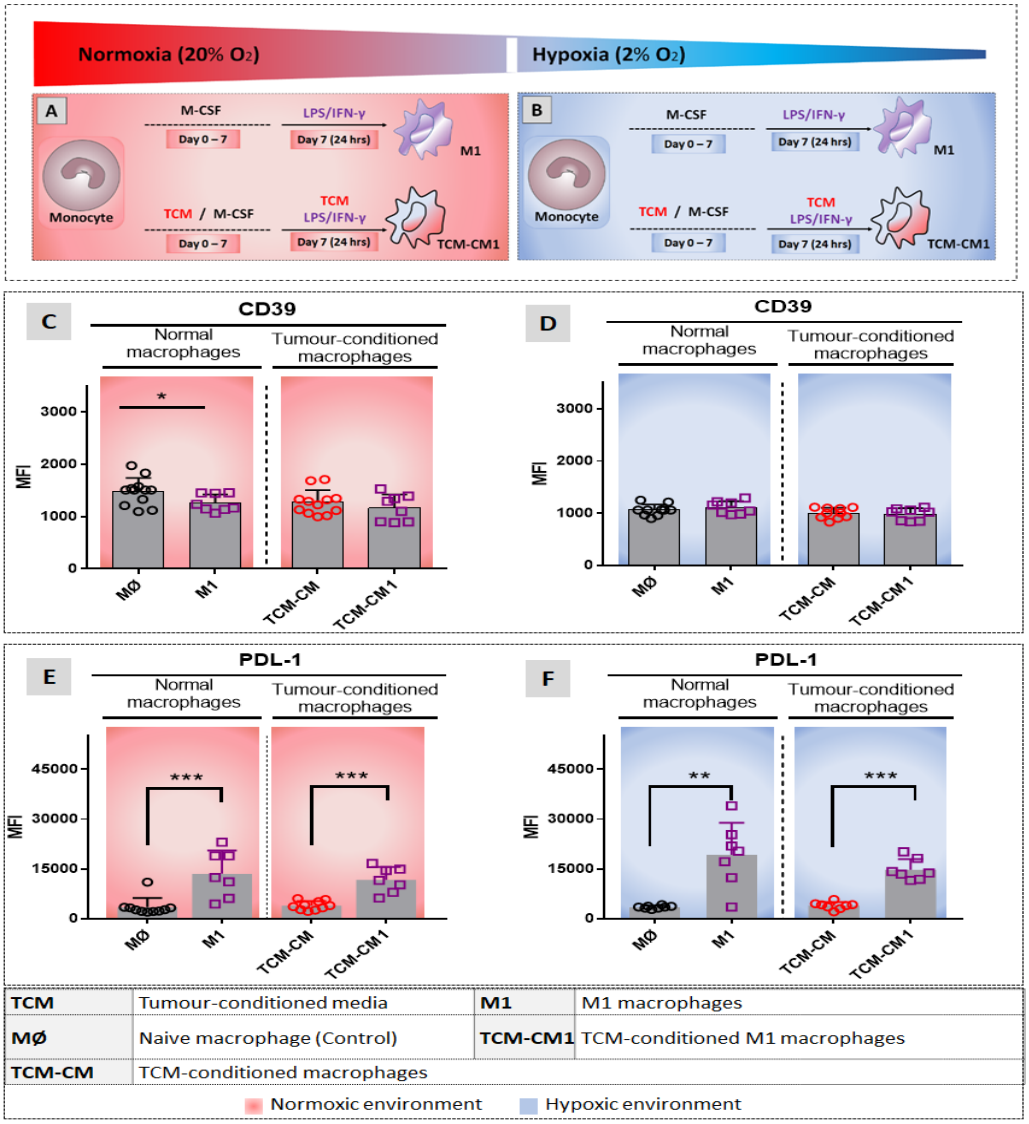

Figure 3. 11 The effect of LPS/IFN-γ on macrophage expression of CD39, PDL-1 and Gal-9 in normoxic and hypoxic conditions

Normal and tumour-conditioned macrophages differentiated from monocytes were stimulated with LPS/IFN-γ to generate M1 macrophages and tumour-conditioned M1 macrophages (TCM-CM1) under normoxic (A) and hypoxic (B) conditions and stained for CD39 and PDL-1 before flow cytometric analysis. Pooled data (MFI) (C, D, E and F) are expressed as mean ± SEM. P-values were determined using the Mann-Whitney test, * = $p < 0.05$, ** = $p < 0.005$, *** = $p < 0.0005$ **** = $p < 0.0001$, n=8 replicates per normoxic and hypoxic M1 and TCM-CM1 conditions.

3.3.1.2.7.1 Hypoxia and mesothelioma factors prevent macrophages from decreasing CD39 expression in response to LPS/IFN-γ

CD39 expression significantly lowered in normoxic macrophages compared to normoxic naïve controls in response to LPS/IFN-γ (Figure 3.11.C; $p = 0.04$). No differences in CD39 expression were observed in all other conditions, including hypoxia. The data suggest that regardless of oxygen levels, mesothelioma derived factors prevent LPS/IFN-γ from reducing suppressive adenosine generation by maintaining CD39 expression levels.

3.3.1.2.7.2 Hypoxia and normoxic/hypoxic-induced mesothelioma factors do not affect LPS/IFN-γ upregulation of PDL-1

PDL-1 surface expression was significantly upregulated by LPS/IFN-γ in M1 macrophages compared with MØ macrophages (Figure 3.11.E; $p = 0.0004$) and in TCM-conditioned M1 macrophages compared with TCM-conditioned macrophages (Figure 3.11.E; $p = 0.0001$) under normoxia. Further, LPS/IFN-γ upregulated PDL-1 expression in M1 macrophages compared with MØ macrophages (Figure 3.11.F; $p = 0.002$) and in TCM-conditioned M1 macrophages compared with TCM-conditioned macrophages (Figure 3.11.F; $p = 0.0003$) under hypoxia. The data suggest that regardless of oxygen level and therefore mesothelioma tumour size, LPS/IFN-γ could increase regulatory potential via increased PD-L1 expression on macrophages.

3.3.1.2.8 How do normoxic versus hypoxic tumour-conditioned macrophages respond to IL-4/IL-13?

Next, the ability of macrophages previously cultured with TCM under normoxic and hypoxic conditions to respond to IL-4/IL-13 was determined.

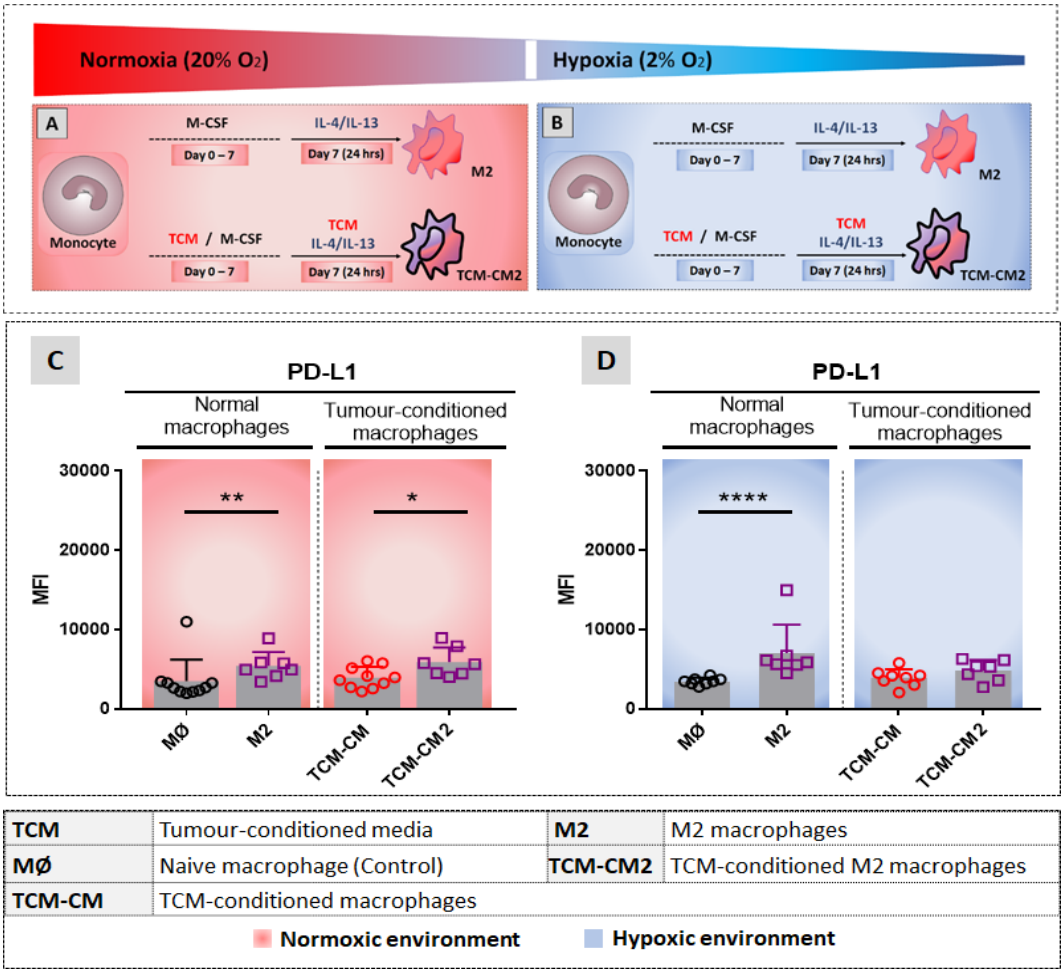

Figure 3. 12 The effect of IL-4/IL-13 on macrophage expression of PDL-1 under normoxic and hypoxic conditions

Normal macrophages and tumour-conditioned macrophages differentiated from monocytes were stimulated with IL-4/IL-13 to generate M2 macrophages and tumour-conditioned M2 macrophages (TCM-CM2) at day 7 for 24 h, under normoxic (A) and hypoxic (B) conditions and stained for PDL-1 flow cytometric analysis. Pooled data of surface expression levels (MFI) (C and D) are expressed as mean ± SEM. P-values were determined using the Mann-Whitney test, * = $p < 0.05$, ** = $p < 0.005$, *** = $p < 0.0005$ **** = $p < 0.0001$, n=8 replicates per normoxic and hypoxic (M2 and TCM-CM2) conditions.

3.3.1.2.8.1 Hypoxia-induced mesothelioma factors prevent IL-4/IL-13 from upregulating PDL-1 expression

Figure 3.12 shows that normoxic M2 macrophages express higher levels of PDL-1 than normoxic controls (Figure 3.12.C; $p = 0.006$). Furthermore, IL-4/IL-13 significantly upregulated PDL-1 on normoxic TCM-conditioned M2 macrophages compared to normoxic TCM-conditioned macrophages (Figure 3.12.C; $p = 0.03$). These data imply a suppressive role for M2 macrophages, as expected.

Under hypoxia, IL-4/IL-13-stimulated M2 macrophages significantly upregulated PDL-1 expression compared to hypoxic controls (Figure 3.12.D; $p = 0.0003$), again an expected suppressive response. However hypoxic TCM-conditioned macrophages did not respond similarly, as there were no differences between hypoxic TCM-conditioned macrophages and TCM-conditioned M2 macrophages (Figure 3.12.D). The data implies hypoxia affects mesothelioma cells in way that changes tumour cell-macrophage crosstalk when faced with IL-13 and IL-4. The result being reduced PDL-1 that may reduce the suppressive function of TAMs.

3.3.1.3 Comparing the effect of normoxic versus hypoxic-induced mesothelioma factors on macrophage expression of scavenger receptors

The aim of this study was to examine macrophage-mesothelioma interactions in the in-vitro normoxic and hypoxic mesothelioma models to evaluate macrophage expression of CD163 and CD206 and assess the effects when they are stimulated with INF-γ/LPS or with IL-4/IL-13.

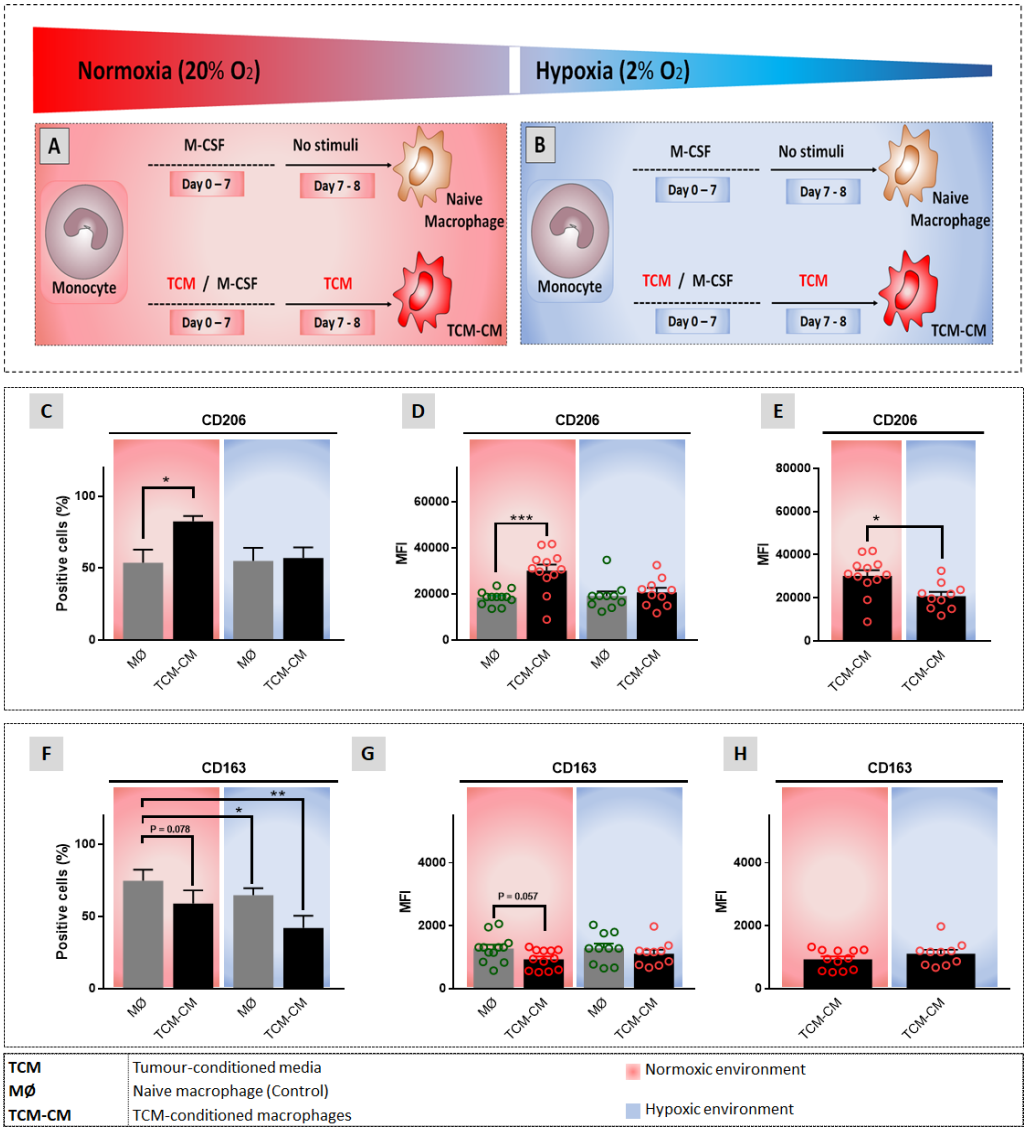

Figure 3. 13 Effect of normoxic and hypoxic tumours on scavenger receptors

Normal and tumour-conditioned macrophages differentiated under normoxic (A) and hypoxic (B) conditions were stained for CD163 and CD206. Pooled data of percentages of positive cells (C, F) and MFI (D, E, G, H) expressed as mean ± SEM. P-values determined using Mann-Whitney test, * = $p < 0.05$, ** = $p < 0.005$, *** = $p < 0.0005$ **** = $p < 0.0001$, n=12 replicates per normoxic condition, n=10 replicates per hypoxic condition.

3.3.1.3.1 Hypoxic-induced tumour factors further reduce CD206 expression relative to normoxic-induced factors

The percentage of $CD206^{+}$ normoxic TCM exposed macrophages increased (Figure 3.13.C; $p = 0.02$); this associated with significantly elevated CD206 expression levels relative to normoxic controls (Figure 3.13.D; $p = 0.0004$). No differences in the percentage of CD206+ cells and CD206 expression levels were observed under hypoxia compared to hypoxic controls (Figure 3.13.C and D). Moreover, hypoxic TCM-conditioned macrophages had significantly lower CD206 relative to normoxic TCM-conditioned macrophages (Figure 3.13.E; $p = 0.01$).

In contrast, a decreasing trend was seen for the percentage of CD163+ cells in normoxic TCM-conditioned macrophages compared to normoxic controls (Figure 3.13.F; $p = 0.08$). This effect was amplified under hypoxia, as the decrease in the percentage of CD163+ cells was significantly lower in hypoxic controls and hypoxic TCM-conditioned macrophages relative to normoxic controls (Figure 3.13.F; $p = 0.05$; $p = 0.0034$). No differences were observed in CD163 expression levels between normoxic and hypoxic TCM-conditioned macrophages (Figure 3.13).

The data suggest that mesothelioma-derived factors in the normoxic early stages of disease development mediate macrophage polarization toward M2-like cells through increasing CD206 expression. However, this M2-like phenotype is only partially maintained as mesothelioma progresses into a hypoxic state where TAM reduce CD206 and CD163 and may assume a mixed M1/M2 phenotype, as shown in our group's murine studies (246).

3.3.1.3.2 How do normoxic and hypoxic tumour-conditioned macrophages respond to proinflammatory stimuli LPS/IFN-γ?

Next, the ability of macrophages previously cultured with TCM under normoxic and hypoxic conditions to respond to LPS/IFN-γ was determined.

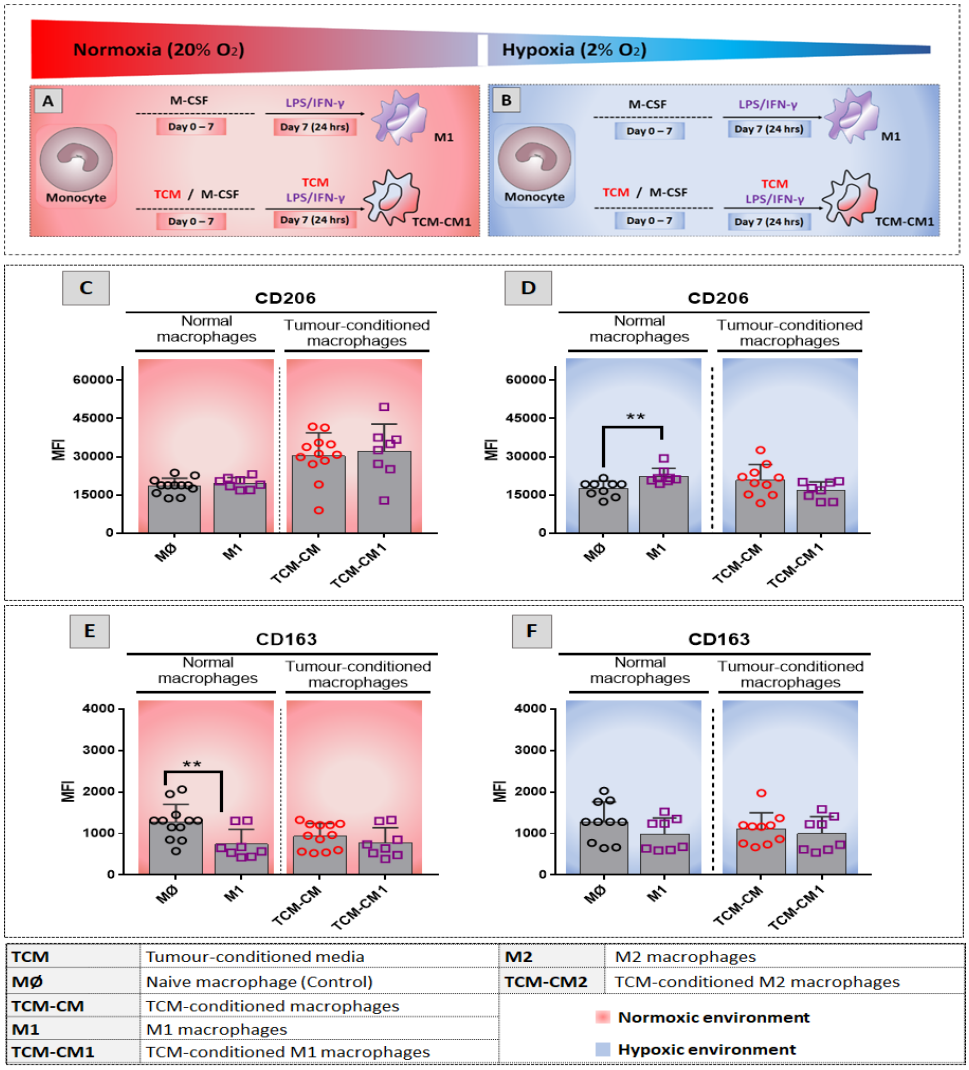

Figure 3. 14 Effect of LPS/IFN-γ on macrophage CD206 and CD163 expression under normoxic and hypoxic condition

Normal and tumour-conditioned macrophages differentiated from monocytes were stimulated with LPS/IFN-γ to generate M1 macrophages and tumour-conditioned M1 macrophages (TCM-CM1), under normoxic (A) and hypoxic (B) conditions and stained for CD206 and CD163 flow cytometric analysis. Pooled data of surface expression levels (MFI) (C, D, E and F) are expressed as mean ± SEM. P-values were determined using the Mann-Whitney test, * = $p < 0.05$, ** = $p < 0.005$, *** = $p < 0.0005$ **** = $p < 0.0001$, n=8 replicates per normoxic and hypoxic M1 and TCM-CM1 conditions.

3.3.1.3.2.1 Under hypoxia, LPS/IFN-γ increases CD206 in normal but not TCM-conditioned macrophages

CD206 expression significantly increased under hypoxia when naïve macrophages were stimulated with LPS/IFN-γ (Figure 3.14.D; $p = 0.002$). No changes were seen under normoxic conditions (Figure 3.14.C), normoxic tumour conditions (Figure 3.14.D) or hypoxic tumour conditions (Figure 3.14.D).

3.3.1.3.2.2 Hypoxia and normoxic and hypoxic-induced mesothelioma factors hamper LPS/IFN-γ in decreasing CD163 expression

CD163 expression was downregulated under normoxia when naive macrophages were stimulated with LPS/IFN-γ (Figure 3.14.E; $p = 0.007$). However, no differences were seen in hypoxic naïve macrophages (Figure 3.14.F), normoxic TCM-conditioned macrophages (Figure 3.14.E) and hypoxic TCM-conditioned macrophages (Figure 3.14.F) after stimulation with LPS/IFN-γ. This data suggests that hypoxia and mesothelioma factors may impair potential polarization toward the M1 phenotype after stimulation with LPS/IFN-γ.

3.3.1.3.3 How do normoxic and hypoxic tumour-conditioned macrophages respond to anti-inflammatory stimuli IL-4/IL-13?

The ability of macrophages previously cultured with TCM under normoxic and hypoxic conditions to respond to IL-4/IL-13 was also determined.

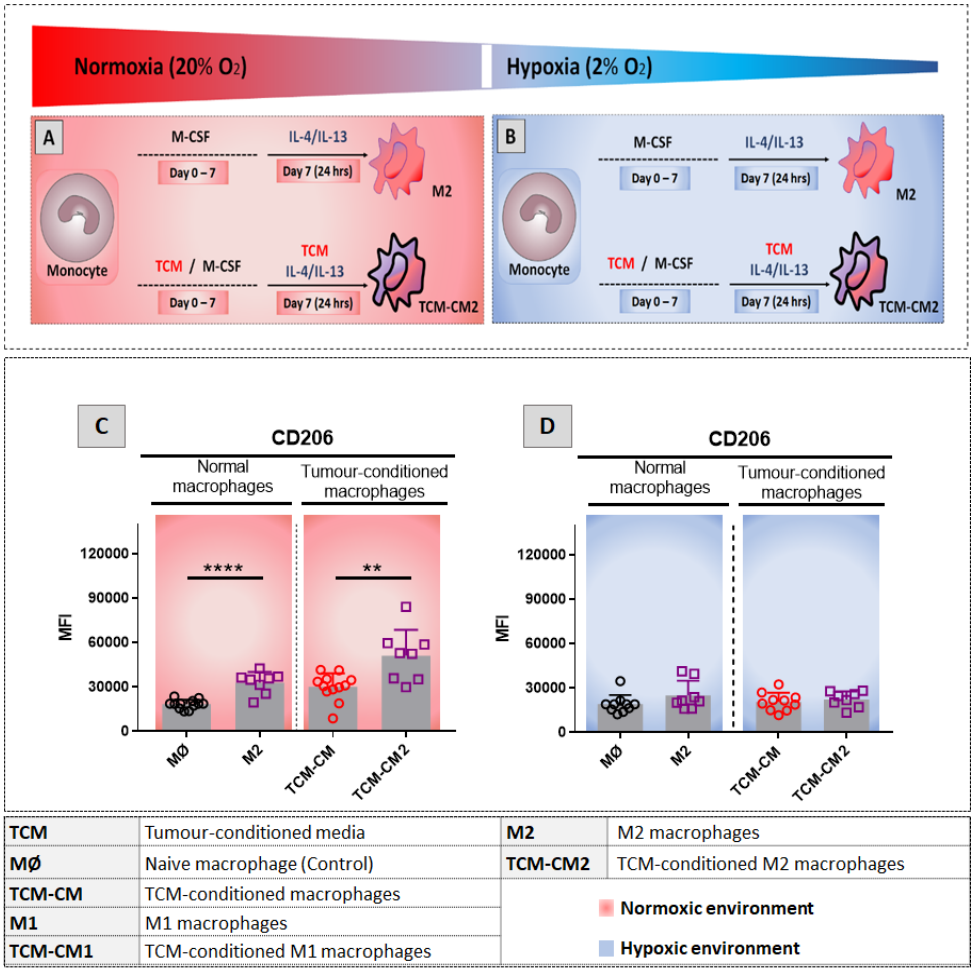

Figure 3. 15 Effect of IL-4/IL-13 on macrophage expression of CD206 and CD163 under normoxic and hypoxic conditions

Normal macrophages and tumour-conditioned macrophages differentiated from monocytes were stimulated with IL-4/IL-13 to generate M2 macrophages and tumour-conditioned M2 macrophages (TCM-CM2) at day 7 for 24 h, under normoxic (A) and hypoxic (B) conditions and stained for CD206 flow cytometric analysis. Pooled data of surface expression levels (MFI) (C and D) are expressed as mean ± SEM. P-values were determined using the Mann-Whitney test, * = $p < 0.05$, ** = $p < 0.005$, *** = $p < 0.0005$ **** = $p < 0.0001$, n=8 replicates per normoxic and hypoxic (M2 and TCM-CM2) conditions.

3.3.1.3.3.1 Hypoxia prevents elevated CD206 expression in macrophages responding to IL-4/IL-13

IL-4/IL-13 significantly increased CD206 expression under normoxic conditions compared to normoxic control (Figure 3.15.C; $p < 0.0001$), as expected. The same IL-4/IL-13 effect was seen on normoxic TCM-conditioned macrophages (TCM-CM2) compared to unstimulated normoxic TCM-conditioned macrophages (TCM-CM) (Figure 3.15.C; $p = 0.004$) but at lower levels.No changes in CD206 were seen in naïve macrophages and TCM-conditioned macrophages to IL-4/IL-13 under hypoxia (Figure 3.15.D). These data suggest that hypoxia may impair polarization toward the M2 phenotype after stimulation with IL-4/IL-13.

3.3.2 Assessing metabolic changes of macrophages in response to mesothelioma-derived factors induced under normoxic and hypoxic conditions

Immunometabolic studies emphasise the relationship between metabolic statues and immune cell phenotype (184). Macrophages can utilise energy from glycolysis or oxidative phosphorylation (OXPHOS) with the energy source determining their phenotype (184). Polarisation of macrophages also includes metabolic reprogramming; for example, M1 macrophages upregulate glycolysis that involves an increase in glucose uptake. M2 macrophages are characterised by decreased glycolysis, as they use OXPHOS as the main means to generate ATP (177-179). A metabolic switch that leads to enhanced aerobic glycolysis is considered a hallmark of most cancer and immune cells' ability to sustain their viability and promote inflammatory activity (178, 247). Inhibition of this metabolic shift results in blockage of the M1 phenotype and decreases pro-inflammatory cytokine/chemokine production (178, 247). The tumour microenvironment, often via hypoxia and factors secreted by tumour cells, reprogram the metabolic processes of other tumour-associated cells, such as proliferation, survival, cytokine production and phagocytosis (182). The metabolic features of TAMs have always been considered complicated, as they display complex forms of metabolic change. Although it has been suggested that TAMs are M2 like, many studies have demonstrated similarities to M1 macrophages as TAMs have a high glycolytic rate (181, 182). However, TAMs have shown increased OXPHOS, even with a broken TCA

cycle (182). Moreover, tumour microenvironmental factors can create different TAMs with different metabolic programs and phenotypes, such as hypoxia, depending on the area within the tumour they occupy (182). Therefore, understanding metabolic regulation of TAMs by tumour-derived factors may provide insights into how macrophages access their energy needs and how this may affect their function. This may also reveal novel therapeutic targets for the treatment of tumours.

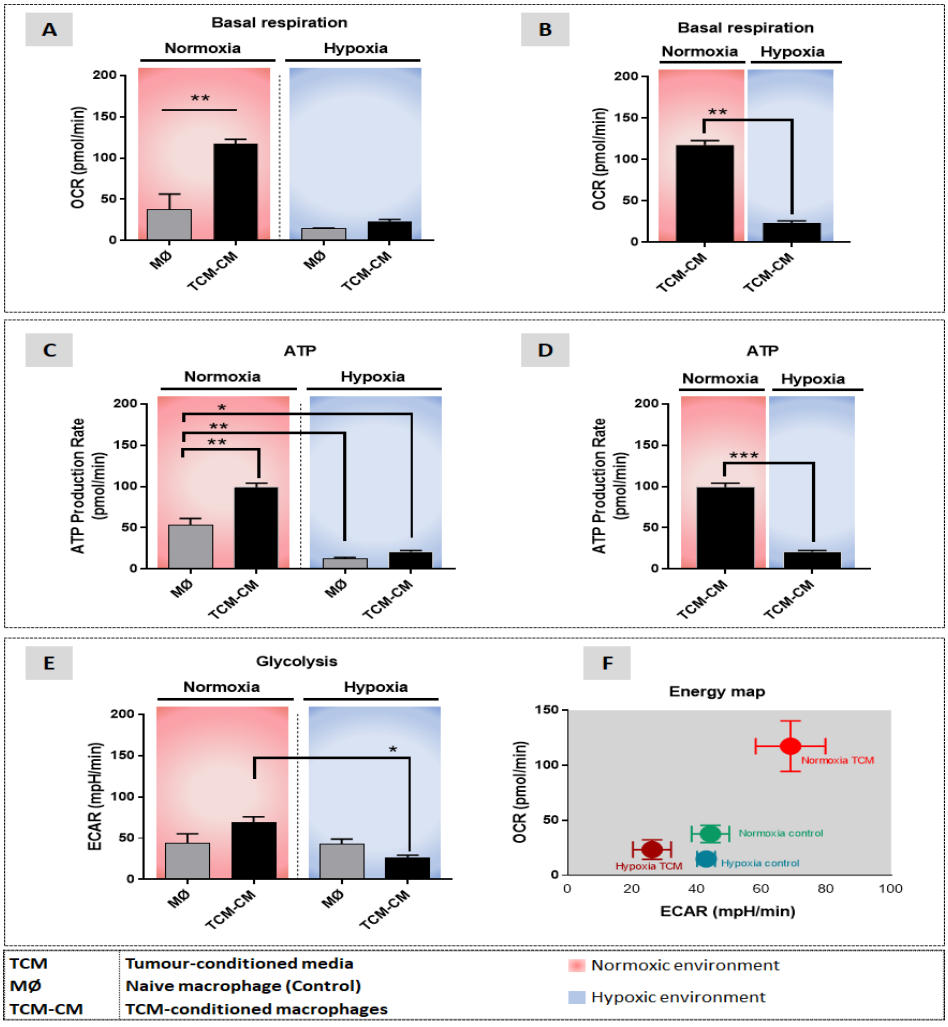

Figure 3. 16 Bioenergetic profiling of macrophages under normoxic and hypoxic tumour conditions

Normal and tumour-conditioned macrophages differentiated under normoxic (A) and hypoxic (B) conditions were investigated for oxygen consumption rates (OCR) and

extracellular acidification rates (ECAR) to quantify mitochondrial respiration and glycolysis respectively. Pooled data for basal respiration rate (A, B), ATP production rate (C, D) and glycolytic rate (E) are expressed as mean ± SEM. An energy map (F) of the 4 conditions was obtained by plotting ECAR and OCR values obtained from the data shown in (A) and (C). P-values were determined using two-way ANOVA. * = $p < 0.05$, ** = $p < 0.005$, *** = $p < 0.0005$, **** = $p < 0.0001$.

3.3.2.1 Mitochondrial OCR is upregulated by normoxic TCM and downregulated under hypoxic conditions

Compared to normoxic controls, normoxic TCM-conditioned macrophages increased their mitochondrial oxygen consumption rate (OCR; Figure 3.16.A; $p = 0.007$). Hypoxic controls and hypoxic TCM-conditioned macrophages (Figure 3.16.A) demonstrated a decreasing trend compared to normoxic controls. There were no differences between hypoxic controls and hypoxic TCM-conditioned macrophages (Figure 3.16.A) indicating a regulatory role by oxygen deprivation. Data suggest that mesothelioma-secreted molecules induce macrophages to upregulate mitochondrial OXPHOS under normoxia, whereas hypoxia abrogated this effect on macrophages.

3.3.2.2 Oxidative ATP production is upregulated by normoxic TCM and downregulated under hypoxia

Measuring the rate of oxidative ATP production showed a significant increase in ATP production in normoxic TCM-conditioned macrophages compared to normoxic controls (Figure 3.16.C; $p = 0.004$). Further, a significant decrease in ATP production was observed in hypoxic controls (Figure 3.16.C; $p = 0.0075$) and hypoxic TCM-conditioned macrophages (Figure 3.16.C; $p = 0.02$) relative to normoxic control. There were no significant differences between hypoxic controls and hypoxic TCM-conditioned macrophages (Figure 3.16.C). As expected, under normoxia, ATP production level increases as a result of OXPHOS upregulation, whereas hypoxia decreases it.

3.3.2.3 Glycolysis is upregulated by normoxic TCM and downregulated by hypoxic TCM

Normoxic TCM-conditioned macrophages demonstrated high glycolytic activity compared to hypoxic TCM-conditioned macrophages (Figure 3.16.E; $p = 0.01$). No other differences were seen including between normoxic TCM-conditioned macrophages and normoxic controls; hypoxic TCM-conditioned macrophages versus normoxic control; and hypoxic controls versus hypoxic TCM-conditioned macrophages (Figure 3.16.E). The data imply that when oxygen is sufficient, mesothelioma induces aerobic glycolysis in macrophages. However, when oxygen is lacking, mesothelioma reduces the glycolytic rate in macrophages.

3.3.2.4 Comparing normoxic and hypoxic tumour conditions on the macrophage bioenergetic profile

The data shows that hypoxic TCM-conditioned macrophages have significantly lower basal respiration (Figure 3.16.B; $p = 0.003$), ATP production (Figure 3.16.D; $p = 0.0003$) and glycolytic rate (Figure 3.16.E; $p = 0.01$). These data suggest that under normoxia, mesothelioma-derived factors drive macrophages into an M2 state, as M2 cell obtain energy mostly from oxidative metabolism, while, M1 cells increase their glycolytic rate and attenuate oxidative rates (69). However, under hypoxia, reduced mitochondrial respiration and maintenance of glycolysis may result in significantly less ATP production which may attenuate macrophage activity.

3.4 Discussion

Mesothelioma is an aggressive tumour that develops on surfaces of body cavities lined by mesothelial cells decades after exposure to asbestos. Hypoxia is a hallmark of locally advanced solid tumours and is recognised as a key determinant of tumour aggressiveness (1). It has been reported that as human malignant mesothelioma progresses, the tumour creates hypoxic regions (2, 248). Tumour hypoxia plays a fundamental role in the recruitment and accumulation of macrophages (5). The relationship between mesothelioma and macrophages has not been studied under the influence of hypoxia. Most tumour studies that include mesothelioma have

been conducted in an atmospheric environment (21% O_2), on the grounds that the results may not differ between the atmospheric environment and the hypoxic environment (2% O_2). However this might not simulate the tumour microenvironment (13). Burt et al., (2011) demonstrated that macrophages made up about 27% of malignant pleural mesothelioma cellularity and expressed high levels of HLA-DR, CD206 and CD206 and low or modest levels of CD80 and CD86. There are also data showing that macrophage infiltrates promote tumour growth and are associated with poor survival in mesothelioma patients (114). Another study assessed the relationship between several cancers (colorectal, prostate, ovarian and breast) with macrophages. Colorectal cancer enhanced expression of HLA-DR, CD40, CD80 and CD86, while the other cancers significantly lowered expression of these molecules. The authors concluded that macrophages in colorectal cancer were pro-inflammatory as enhanced antigen presentation and T-cell co-stimulation correlated with good prognoses, while the other cancers had a minimal capacity to present antigens, co-stimulate T-cells, and promoted tumour growth (249).

Note that this chapter initially aimed to understand the relationship between macrophages and mesothelioma cells using the 2D model shown in the results and then to compare/confirm this relationship with the 3D tumour model that better mimics the in vivo tumour microenvironment. However, attempts to develop a multicellular spheroid model had limited success.

The data showed that mesothelioma-derived factors decreased HLA-DRexpression regardless of oxygen levels, i.e. this response was mostly tumour dependent but hypoxic condition further reduced HLA-DRexpression. Decreased HLA-DR implies a reduction in mesothelioma tumour antigens presented by macrophages to local $CD4^+$ T-cells. Thus, the data suggest that mesotheliomas impair the ability of macrophage to present antigens to $CD4^+$ T-cells and that this capability was further impaired at hypoxic state. Decreased HLA-DR expression has been seen in pro-tumour macrophages in prostate, ovarian and breast cancer, yet remains high in macrophages in colorectal cancer (249) and human mesothelioma (114). The contradictory results of the present study and those of the study conducted by BM Burt et al. (2011) (114) in terms of HLA-DR

expression may be due to the fact that in the latter, macrophages were assessed in mesothelioma tumour tissue from patients who underwent cytoreductive surgery, in which many factors could influence macrophages compared to in vitro studies.

Furthermore, this study showed that CD40 expression was downregulated under hypoxic conditions, suggesting oxygenation influences CD40 expression. Macrophage expression of CD40 has been detected in mesothelioma (250); however, there is no data investigating the level of expression. CD40–CD40L engagement regulates T-cell functions and macrophage activation. High levels of ligation between CD40 and CD40L lead to macrophage activation and IL-12 production, resulting in the skewing of Th0 CD4+ T cells toward Th1 cells. In contrast, low levels of CD40–CD40L ligation induce T-cells to produce IL-10, TGF-b and IL-2, resulting in deactivated macrophages and generation of Th2 and Treg cells (251). In addition, upon CD40 ligation, macrophages up-regulate CD80 and CD86, which are required for $CD8^+$ T-cell co-stimulation via CD28 to generate anti-tumour responses (252) or for cytolytic T-lymphocyte–associated protein 4 (CTLA-4) to return T-cells to a quiescent state (72).

These data imply that when macrophages accumulate in hypoxic regions, theyare polarised towards an M2-like state resulting in an in ability to recruit and activate effector $CD4^+$ Th1 and $CD8^+$ T cells as well as NK cells. This, increase immune tolerance and supports mesothelioma tumour development. The data also suggest that, in a hypoxic state, low CD40–CD40L interactions due to reduced CD40 may induce the development of Tregs to further promote an immunosuppressive environment by producing IL-10 and TGF-B. Decreased CD40 expression has been seen in macrophages in prostate, ovarian and breast cancers (249).

	Hypoxia	Normoxia TCM	Hypoxia TCM
HLA-DR		↓***	↓****
CD40	↓*		↓**
CD80		↑*	
CD86	↓****	↓***	↓****
CD39	↓****		↓****
A2A-R	↓**	↓***	↓*
PDL-1	↑**	↑*	↑*
Gal-9	↓*		
CD206	↑***		
CD163			

Table 3. 1 Summary of the role of normoxic and hypoxic tumour conditions on macrophage expression relative to normoxic controls

Only statistically significant results are shown. P-values were determined using the Mann-Whitney test, * = $p < 0.05$, ** = $p < 0.005$, *** = $p < 0.0005$ **** = $p < 0.0001$.

The results showed that mesothelioma-derived factors, generated under normoxia, decrease CD86, which was is further decreased under hypoxia, in agreement with Burt et al. (2011), who mention CD86 decreases in macrophages in MPM without referring to the likely source of this effect. In this research, CD80 only increased when macrophages were conditioned with mesothelioma-derived factors generated under normoxia. This implies that the co-stimulation signal, CD86, required to activate T-cells by macrophages is weakened in the presence of mesothelioma-derived factors and worsens under hypoxia. The data also suggest that, under normoxia, macrophages may be able to activate T-cells by increased CD80 expression. In a normoxic model, increased CD80 expression agreed with that seen in the proinflammatory macrophages in colorectal cancer (249). In addition, in the hypoxic model, the data agreed with the macrophage phenotype described in human mesothelioma in which macrophages were able to maintain their level of CD80 (114).

Mesothelioma-derived molecules generated under normoxia and hypoxia decreased CD39 expression on macrophages which was further reduced under hypoxia. This was associated with decreased expression of A2A-R. These results suggest that regardless of oxygen level, mesothelioma-derived molecules do not significantly contribute in the CD39/adenosine pathway. In contrast, the PD-1/PD-L1 signalling pathway may

contribute to an immunosuppressive tumour microenvironment as mesothelioma-derived molecules generated under normoxia and hypoxia increased PD-L1 expression. In agreement with Burt et al. (2011), the data indicate that, in the presence of sufficient oxygen, mesothelioma cells secrete molecules that induce CD206 expression by macrophages, which is regarded as a marker of the M2 phenotype. Further, CD206 expression remains unchanged in macrophages generated under hypoxic conditions supporting the presence of M2-like macrophages in mesothelioma.

The ability of macrophage to respond to M1-inducing LPS and IFNγ was also examined. Following exposure to LPS/IFNγ, macrophages in normoxic conditions increased CD80 and CD86 expression, as expected. This also seen in macrophages exposed to normoxic-derived TCM, however a lower response was seen in response to hypoxic-derived TCM, implying a suppressive role for oxygen deprivation. Similarly, in response to normoxic-derived TCM, macrophages still increased CD40 expression following LPS/IFNγ stimulation; this was not seen in response to hypoxic-derived TCM. In addition, macrophages increased PD-L1 expression in response to LPS/IFNγ stimulation under all normoxic and hypoxic conditions. These data suggest that proinflammatory signals may improve macrophages tumour immunogenicity in the presence of sufficient oxygen, where mesothelioma-derived factors have no significant effect on CD80, CD86 and CD40 expression. However, with in vitro mesothelioma cells exposed to hypoxia, mesothelioma-derived factors diminish macrophages' responses to proinflammatory signals, such as LPS/IFNγ, in terms of CD80 and CD86 and make them disappear entirely in terms of CD40.

	Normoxia M1	Normoxia M1/TCM	Hypoxia M1	Hypoxia M1/TCM
HLA-DR				
CD40	↑ **	↑ ***	↑ ***	
CD80	↑ ****	↑ ****	↑ ****	↑ ****
CD86	↑ **	↑ ****	↑ ****	↑ ***
CD39	↑ *			
A2A-R				
PDL-1	↑ ***	↑ ***	↑ **	↑ ***
Gal-9				
CD163	↓ **			
CD206			↑ **	

Table 3. 2 Summary of macrophage responses to INF-γ/LPS when exposed to normoxic- and hypoxic-derived TCM

Only statistically significant results are shown. P-values were determined using the Mann-Whitney test, * = $p < 0.05$, ** = $p < 0.005$, *** = $p < 0.0005$ **** = $p < 0.0001$. Normoxic MØ macrophages are the controls for normoxic M1, whilst normoxic M1 are controlz for normoxic M1/TCM. Similarly, hypoxic MØ macrophages are the controls for hypoxic M1, and hypoxic M1 are the controls for hypoxic M1/TCM.

This research also examined macrophage responses to M2-inducing IL-4 and IL-13 when exposed to normoxic and hypoxic-derived TCM. CD206 expression remained unchanged under hypoxic conditions and partially elevated in response to normoxic-derived TCM. PD-L1 expression was slightly elevated under normoxia and further elevated under hypoxia but not in response to hypoxic-derived TCM. These data suggest it is possible that IL-4 and IL-13 only partially polarise macrophages into M2-like cells when in hypoxic regions in mesothelioma. This is supported by an in vivo study by our lab, which has shown that M1/M2 intermediates (M3 cells) are the dominant macrophage subset in large murine mesotheliomas (246).

	Normoxia M2	Normoxia M2/TCM	Hypoxia M2	Hypoxia M2/TCM
HLA-DR				
CD40				
CD80	↑ **			
CD86	↑ **			
CD39	↑ *			
A2A-R				
PDL-1	↑ **	↑ *	↑ ****	
Gal-9				
CD163	↓ **			
CD206	↑ ****	↑ **		

Table 3. 3 Summary of macrophage responses to IL-4/IL-13 when exposed to normoxic- and hypoxic-derived TCM

Only statistically significant results are shown. P-values were determined using the Mann-Whitney test, * = $p < 0.05$, ** = $p < 0.005$, *** = $p < 0.0005$ **** = $p < 0.0001$. Normoxic MØ macrophages are the controls for normoxic M2, normoxic M2 are the controls for normoxic M2/TCM. Similarly, hypoxic

MØ macrophages are the controls for hypoxic M1, and hypoxic M1s are the controls for hypoxic M1/TCM.

The effect of mesothelioma-derived factors on macrophage bioenergetics was also examined in this thesis. The results highlight that, in an atmospheric environment, mesothelioma modifies the metabolic profile of macrophages towards high OXPHOS, associated with high ATP production, yet simultaneously maintains glycolysis. This may be because the limited glucose in tumours due to poor vascularity stresses tumour cells and induces competition with immune cells for glucose (253). Tumour cells may dictate the polarisation of macrophages to an immunosuppressive M2-like phenotype by inducing a metabolic switch to oxidative metabolism (254). However, macrophages in hypoxic regions increase HIF-1α expression, which is responsible for elevating glycolysis and inducing M1 macrophage polarisation (255), again accounting for an M3 phenotype. These data suggest that malignant cells can harness metabolic by-products to hijack the functions of macrophages for their own benefit and that, in the presence of sufficient oxygen, macrophages possess M2 metabolic features (256). However, with inadequate oxygen availability, macrophages decrease mitochondrial ATP production through OXPHOS but maintain their glycolytic rate. This metabolic profile could contribute to macrophage dysfunction, as they lack the energy to respond to stimuli.

Altogether, this work demonstrates the importance of choosing the appropriate in vitro environment in which to study tumours, as hypoxia could directly affect macrophages and/or modulate factors secreted by mesothelioma cells, which then exact a number of effects on macrophages, including down-regulating activation markers such as CD40, CD80 and CD86 and interfering with the ability of macrophages to respond to stimuli, such as LPS/IFN-γ and IL-4/IL-13, compared to mesothelioma factors derived under a normoxic environment. Furthermore, hypoxia significantly down-regulated mitochondrial respiratory activity and ATP production in mesothelioma-exposed macrophages, likely contributing to macrophage dysfunction.

CHAPTER 4
ASSESSING THE RESPONSE OF ENDOTHELIAL CELLS TO NORMOXIC AND HYPOXIC MESOTHELIOMA TUMOURS

4.1 Study characteristics

This study was approved by Curtin University Human Research Ethics Committee (approval number HRE2017-0823). HUVECs were used as an in-vitro vascular model to assess endothelial responses to mesothelioma-derived factors or macrophage-derived factors. Passage 6 HUVECs were used for all experiments to ensure consistency.

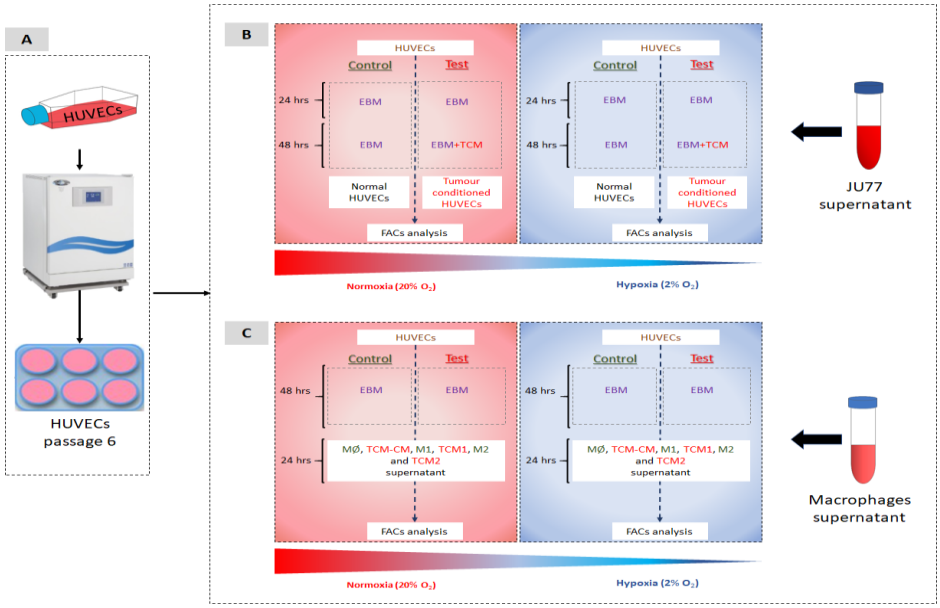

Figure 4. 1 Experimental design

HUVECs maintained in supplemented endothelial basal medium (EBM) at 37°C and 5% CO_2 and grown until passage 6 (A) were seeded in 2 ml of HUVEC media and incubated for 24 h to allow adherence. Media was replaced with 2 ml of 100% HUVEC media or a 50:50 mixture of 1 ml of HUVEC media and 1 ml TCM and cells incubated for 48 h to generate TCM-conditioned HUVECs (B), or stimulated with supernatant from naive MØ or TCM-exposed macrophages to study the crosstalk between macrophages and ECs (C).

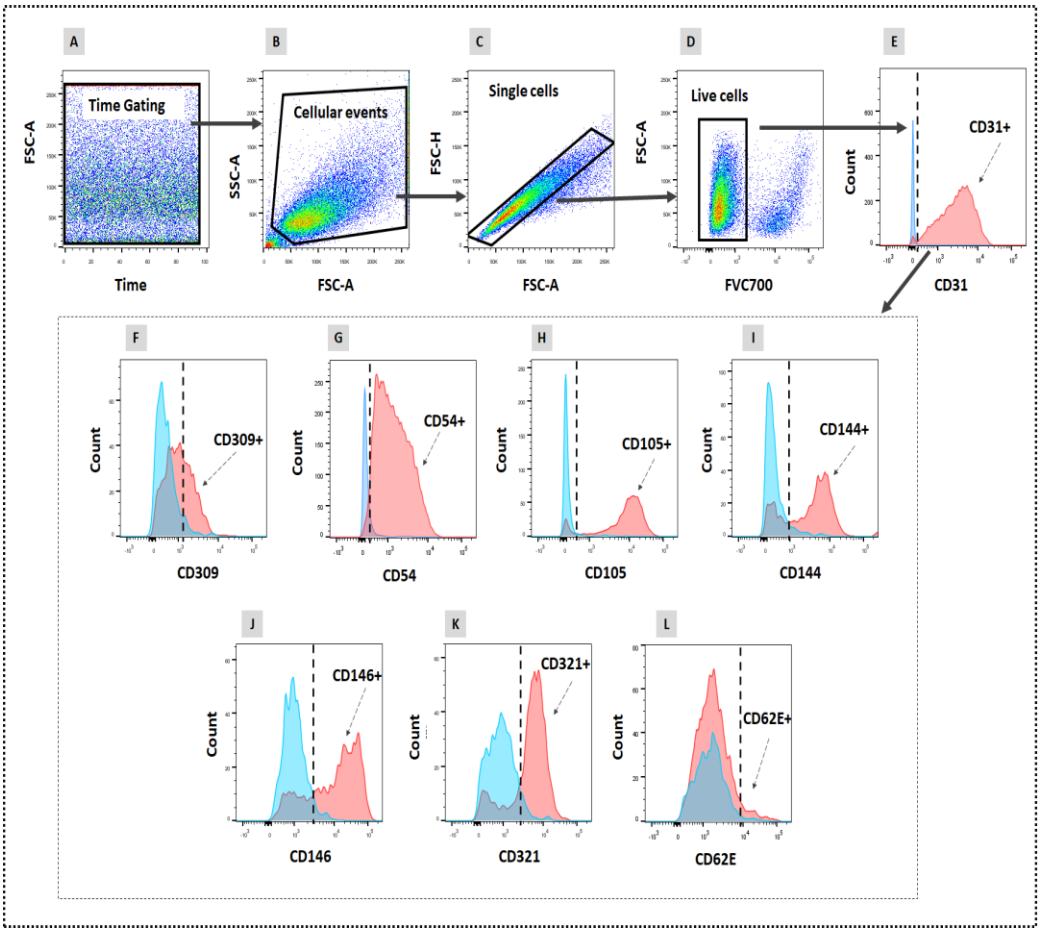

Figure 4. 2 Flow cytometric analysis of HUVECs

(A) FSC-A and time were used to exclude electronic noise. (B) FSC-A and SSC-A were used to gate cellular events based on size and granularity. (C) FSC-A and FSC-H were used to eliminate doublets by gating on single cells. (D) The viability gate was used to eliminate dead cells stained with Fixable Viability Stain 700 (FVS700). (E) Live cells were further analysed by gating on CD31+ cells. CD31+ HUVECs were analysed for CD309 (F), CD54 (G), CD105 (H), CD144 (I), CD146 (J), CD321 (K) and CD62E (L). Figures (F-L) show red coloured histograms (the stained positive dataset), overlaid onto blue histograms (unstained cell background), in order to accurately identify the positive dataset.

4.2 Results

4.3 Introduction

Tumours require a vascular system to satisfy their need for oxygen and nutrients and to remove waste in order to grow beyond a certain size (257). Rapidly proliferating tumour cells and poor vasculature development leads to hypoxia (258). Tumour cells and tumour-associated stromal cells, such as macrophages and endothelial cells, play an essential role in tumour angiogenesis (259). Tumour-associated macrophages (TAMs) are a key component of inflammation during tumorigenesis: they sense hypoxia in avascular areas of tumours and release proangiogenic factors, such as vascular endothelial growth factor (VEGF) (260). Hypoxia and chronic secretion of growth factors result in excessive proliferation and transformation of endothelial cells at the cellular and molecular level. Vascular endothelial cells (ECs) form the inner lining of blood vessels and serve as a barrier in extravasation and intravasation processes (261). Compared to blood vessels in surrounding normal tissues, tumour blood vessels are irregular and tortuous: they are more permeable and leakier, and blood flow is abnormal (262).

The aim of this chapter is two-fold: Firstly, to evaluate and compare interactions between ECs and mesothelioma tumour cells under normoxic (20% O_2) and hypoxic (2% O_2) environments. As macrophages and endothelial cells are often co-located in tumours, the second aim was to assess likely interactions between ECs and macrophages under the two conditions (Figure 4.1). To achieve these aims, human umbilical vein endothelial cells (HUVECs) were incubated with normoxic and hypoxic-induced conditioned medium from human mesothelioma JU77 cells to assess direct effects of mesothelioma on healthy ECs; HUVECs were also cultured under the same normoxic/hypoxic conditions. To address interactions between tumour-conditioned macrophages and ECs, HUVECS were incubated with normoxic/hypoxic TCM-exposed macrophage media collected as described in Chapter 3 (Figure 3.1). Changes to HUVECs were assessed using flow cytometry (Figure 4.2).

4.3.1 Evaluating the effect of normoxic- versus hypoxic-induced mesothelioma factors and mesothelioma-exposed macrophages on HUVECs

4.3.1.1 Vascular Endothelial Receptor, CD309

VEGF binds VEGF receptors (R), members of the receptor tyrosine kinases (RTK) family: VEGFR-1, CD309 and VEGFR-3.VEGFR-2 (or CD309) is a type III RTK, alternatively denoted as kinase insert domain protein receptor [KDR] or Flk1 (foetal liver kinase 1) (263-265). CD309 is expressed mostly on vascular ECs, and its expression is elevated in tumour vasculature (231), including malignant mesotheliomas (264). CD309 regulates endothelial migration and proliferation and plays a direct role in normal and pathological vascular permeability (266). Therefore, activation of CD309 by VEGF is a crucial step in signalling pathways that start tumour angiogenesis (267). Besides expanding vascular networks to support tumour growth, excessive activation of CD309 mediates tissue-damaging vascular changes (268). Similar to VEGF, hypoxia results in upregulation of VEGFR-1 and CD309 genes in ECs. Furthermore, heightened VEGFR gene expression is triggered by binding VEGF resulting in further amplification of VEGF signalling. In human colorectal cancer, elevated VEGF/CD309 level is associated with tumour microvessel density, progression, invasion and metastasis (269, 270). In non-small-cell lung cancer (NSCLC), high intratumoural microvessel density is seen as a predictor of poor prognosis for survival (271). Similarly, a study of 203 human colon cancer samples showed that poor prognosis, tumour metastasis and recurrence correlated with increased CD309 expression (231). In preclinical animal models, monoclonal antibodies against murine CD309 and administration of neutralizing VEGF antibodies curtails development of human tumour xenografts and leads to reduced microvessel density, reduced proliferation of tumour cells, tumour cell apoptosis and tumour necrosis (272, 273). This study examined potential interactions between HUVECs and mesothelioma cells and between HUVECs and MØ, TCM-CM, M1, TCM-CM1, M2 and TCM-CM2 macrophages in normoxic and hypoxic models.

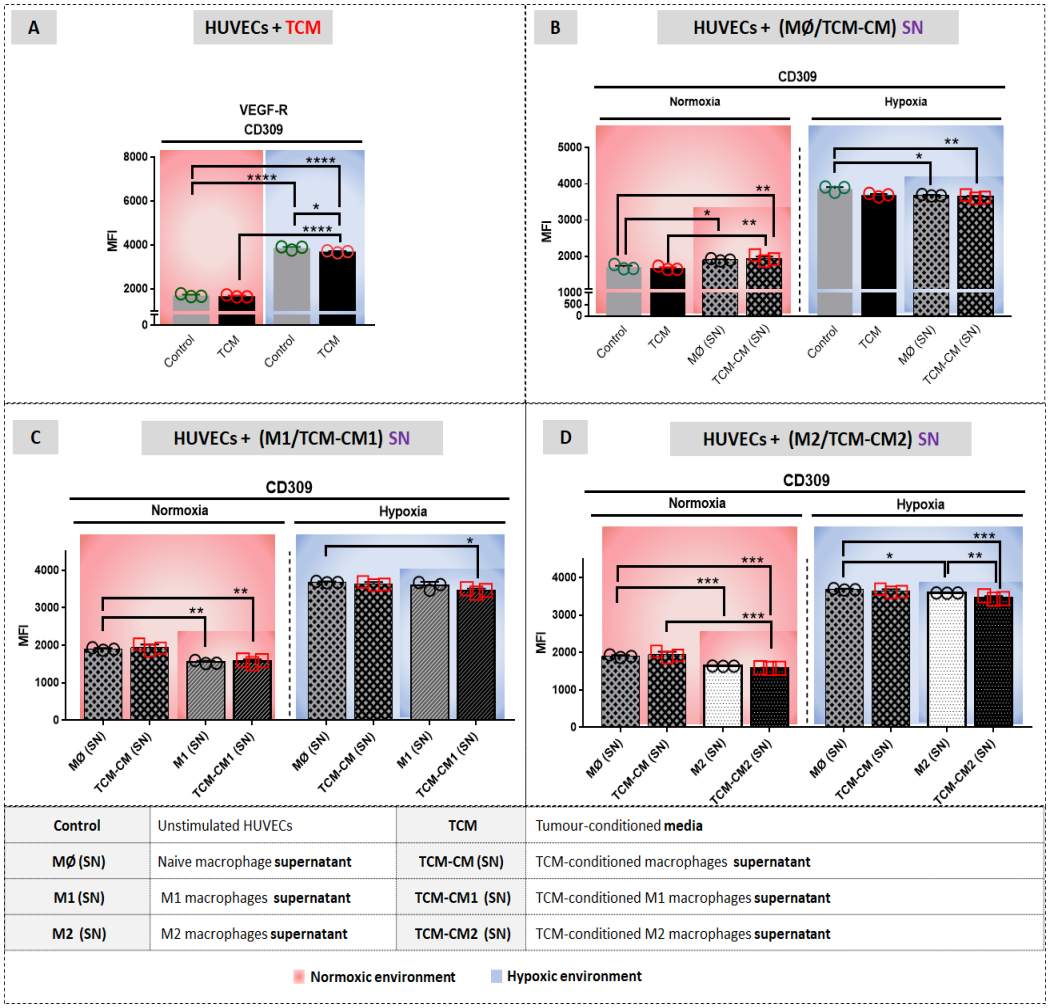

Control	Unstimulated HUVECs	**TCM**	Tumour-conditioned **media**
MØ (SN)	Naive macrophage **supernatant**	**TCM-CM (SN)**	TCM-conditioned macrophages **supernatant**
M1 (SN)	M1 macrophages **supernatant**	**TCM-CM1 (SN)**	TCM-conditioned M1 macrophages **supernatant**
M2 (SN)	M2 macrophages **supernatant**	**TCM-CM2 (SN)**	TCM-conditioned M2 macrophages **supernatant**

Normoxic environment **Hypoxic environment**

Figure 4. 3 Hypoxia increases expression of CD309 on HUVECs

Passage 6 HUVECs were incubated with HUVEC medium to generate controls or with media containing JU77 TCM to generate TCM-conditioned HUVECs under normoxic and hypoxic conditions, HUVECs were stained for CD309 and MFI measured (A). To assess the effect of tumour-exposed macrophages generated under normoxic and hypoxic conditions (B, C & D) HUVECs were also exposed to supernatant collected from MØ and TCM-CM (B), M1 and TCM-CM1 (C), and M2 and TCM-CM2 (C), see table above. Pooled data are expressed as mean ± SEM. P-values were determined using a two-way ANOVA test, * = $p < 0.05$, ** = $p < 0.005$, *** = $p < 0.0005$ **** = $p < 0.0001$, n = 3 replicates per condition.

4.3.1.1.1 Hypoxia directly increases CD309 expression on HUVECs

HUVECs increased CD309 expression under hypoxia relative to normoxic controls (Figure 4.3.A; $p < 0.0001$), showing that hypoxia alone modulates CD309 expression. However, exposure to hypoxic TCM significantly reduced CD309 expression relative to hypoxic controls (Figure 4.3.A; $p = 0.02$), showing that hypoxic TCM also modulates CD309 expression. In contrast, normoxic TCM did not affect CD309 expression compared with normoxic controls (Figure 4.3.A). Note that even thoughhypoxic TCM reduced CD309 expression relative to hypoxic controls, CD309 expression levels were higher than those seen in normoxic TCM (Figure 4.3.A; $p < 0.0001$). Taken together, the data suggest that hypoxia elevates CD309 expression.

4.3.1.1.2 TCM-conditioned macrophages increase CD309 under normoxia and decrease CD309 on HUVECs under hypoxia

HUVECs exposed to supernatant from normoxic MØ, slightly but significantly, upregulated CD309 relative to normoxic HUVEC controls (Figure 4.3.B; $p = 0.03$). Normoxic TCM-exposed macrophages also upregulated CD309 on HUVECs relative to normoxic TCM-exposed HUVECs (Figure 4.3.B; $p = 0.01$). These data suggest that with or without TCM, factors secreted by macrophages elevate CD309 expression on endothelial cells under normoxia.

In contrast, hypoxia-induced unpolarised macrophage-derived supernatants, with or without TCM, slightly but significantly down-regulated CD309 expression by HUVECs, which was already elevated due to the hypoxic conditions (Figure 4.3.B). These data suggest that oxygen levels modulate macrophages that then impact ECs.

4.3.1.1.3 M1 macrophages reduce CD309 expression on HUVECs under normoxic and hypoxic conditions

This study also asked if normoxia and/or hypoxia affect macrophage M1 polarisation and whether this then influences their crosstalk with ECs. Macrophages polarised to M1 cells and TCM-exposed M1 cells using LPS/IFN-γ reduced CD309 expression significantly in HUVECs under normoxia relative to naïve MØ (SN)-stimulated

HUVECs (Figure 4.3.C; p=0.002; p = 0.003, respectively). This M1-induced effect on ECs occurred with or without exposure to TCM, implying a dominant effect of normoxic M1 macrophages and not tumour-derived factors.

In contrast, hypoxic M1 macrophages did not affect CD309 expression on hypoxic HUVECs (relative to hypoxic MØ (SN)-stimulated HUVECs; Figure 4.3.C), while TCM-exposed M1 cells slightly but significantly reduced CD309 (relative to hypoxic MØ (SN)-stimulated HUVECs; Figure 4.3.C; p = 0.04). These data imply a dominant role by hypoxic tumour-derived factors that modulate the ability of macrophages to respond to LPS/IFN-γ which then influences endothelial cell function.

4.3.1.1.4 M2 macrophage-derived factors reduce CD309 expression on HUVECs under normoxic and hypoxic conditions

This study also asked if normoxia and/or hypoxia affect macrophage M2 polarisation and whether this then influences their crosstalk with ECs. Macrophages polarised to M2cells and TCM-exposed M2 cells using IL-4/IL-13 reduced CD309 expression significantly in HUVECs under normoxia relative to MØ (SN)-stimulated HUVECs (Figure 4.3.D; p = 0.001; p = 0.0004, respectively). This M2-induced effect on ECs occurred with or without exposure to TCM, implying a dominant effect by normoxic M2 macrophages and not tumour-derived factors.

Similarly, under hypoxia, hypoxic M2 and M2 exposed to tumour-derived factors reduced CD309 expression on hypoxic HUVECs relative to hypoxic MØ (SN)-stimulated HUVECs (Figure 4.3.D; p = 0.01; p = 0.0001, respectively), while the effect of TCM-exposed M2 cells on HUVECs in reducing CD309 expression was higher relative to M2 cells (Figure 4.3.D; p = 0.003). These data imply a dominant role by hypoxic tumour-derived factors that modulate the ability of macrophages to respond to IL-4/IL-13, which then influences EC function.

In summary, these data show that oxygen deprivation can directly affect HUVEC CD309 expression. Furthermore, the level of changes in CD309 expression as a result of exposure to mesothelioma/macrophage-derived factors remains significantly higher than normal HUVEC controls because of hypoxia.

4.3.1.2 Intercellular adhesion molecule-1 (ICAM-1), CD54

Intercellular adhesion molecule-1 (ICAM-1, CD54) is a membrane-bound glycoprotein of the immunoglobulin supergene family (274). CD54 is present in low levels on the surface of a variety of cell types, including fibroblasts, leukocytes, keratinocytes, ECs and epithelial cells. CD54 is upregulated in response to a number of inflammatory mediators, including virus infection, oxidant stresses such as H_2O_2, the pro-inflammatory cytokines IL-1β, tumour necrosis factor-alpha (TNF-α) and IFN-γ (160), hypoxia (275) and VEGF (276). Anti-inflammatory cytokines (TGF- β), IL-4, and IL-10 can temper the stimulatory impacts of these mediators (277). CD54 plays a central role in EC migration (278), cell–cell adhesive engagements, activation of lymphocytes, leukocyte trafficking plus numerous additional immune functions (225, 274). The abnormal function of tumour blood vessels is accompanied by CD54 overexpression and increased VEGF-A expression (199, 279). The role of CD54 overexpression and subsequent leukocyte transendothelial migration is controversial. High levels of CD54 expression have been shown to promote angiogenesis, tumour growth and progression in oral cancer (279, 280). In contrast, histologically examination of surgically excised glioblastoma (GB) tissues demonstrated that expression level of vascular CD54 did not affect survival (279). This study examined potential interactions between HUVECs and mesothelioma cells and between HUVECs and MØ, TCM-CM, M1, TCM-CM1, M2 and TCM-CM2 macrophages in normoxic and hypoxic models.

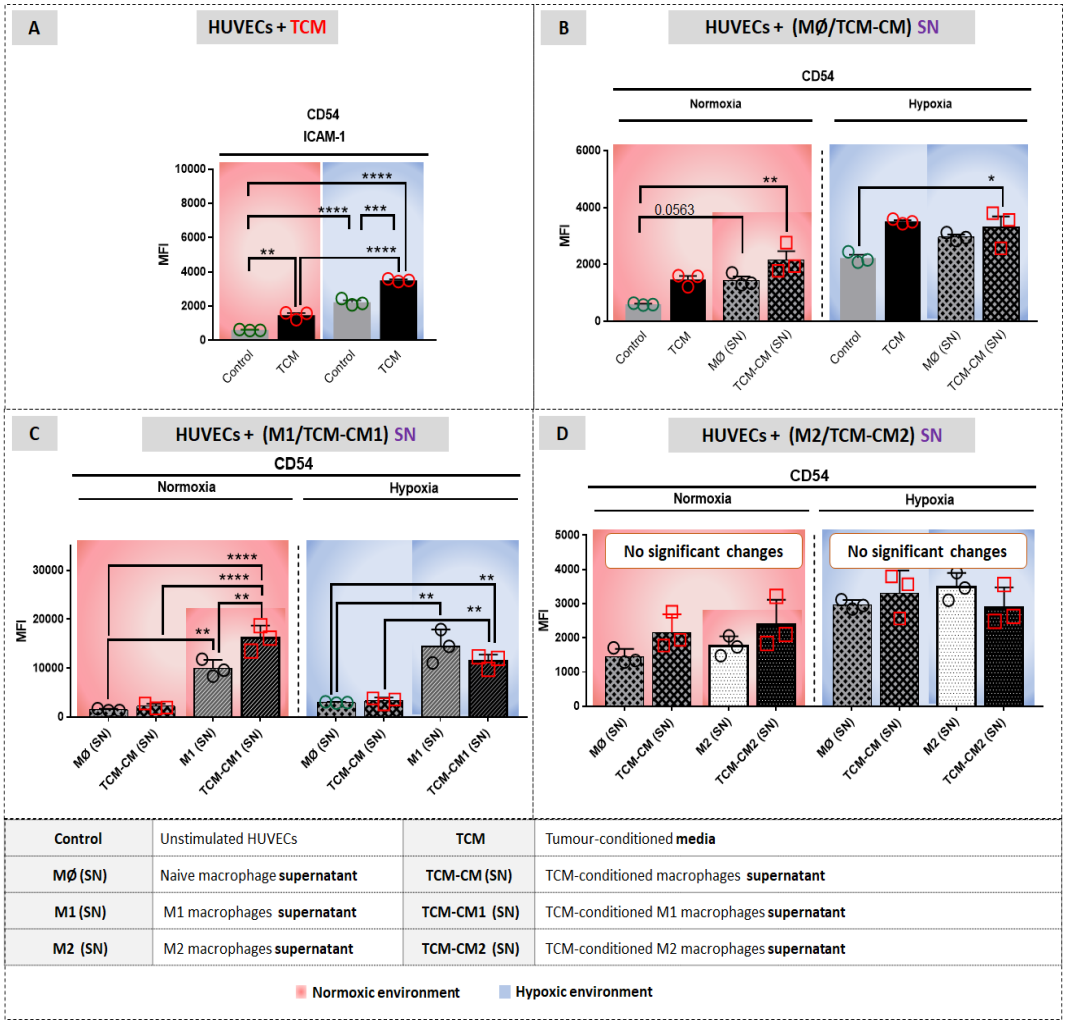

Control	Unstimulated HUVECs	**TCM**	Tumour-conditioned **media**
MØ (SN)	Naive macrophage **supernatant**	**TCM-CM (SN)**	TCM-conditioned macrophages **supernatant**
M1 (SN)	M1 macrophages **supernatant**	**TCM-CM1 (SN)**	TCM-conditioned M1 macrophages **supernatant**
M2 (SN)	M2 macrophages **supernatant**	**TCM-CM2 (SN)**	TCM-conditioned M2 macrophages **supernatant**

Normoxic environment **Hypoxic environment**

Figure 4. 4 Hypoxia and factors from mesothelioma and macrophages elevate expression of CD54 on HUVECs

Passage 6 HUVECs were incubated with HUVEC medium to generate controls or with media containing JU77 TCM to generate TCM-conditioned HUVECs under normoxic and hypoxic conditions and stained for CD54 (A). To assess the effect of macrophages generated under normoxic and hypoxic conditions (B, C & D) HUVECs were also exposed to supernatant collected from MØ and TCM-CM (B), M1 and TCM-CM1 (C), and M2 and TCM-CM2 (C). Pooled data are expressed as mean ± SEM in all conditions. P-values were determined using a two-way ANOVA test, * = $p < 0.05$, ** = $p < 0.005$, *** = $p < 0.0005$ **** = $p < 0.0001$, n = 3 replicates per condition.

4.3.1.2.1 Mesothelioma-derived factors and hypoxia increase CD54 expression on HUVECs

Normoxic TCM significantly increased CD54 expression by HUVECs relative to normoxic HUVECs controls (Figure 4.4.A; $p = 0.001$), showing that mesothelioma-derived factors alone modulate CD54 expression. Also, hypoxia alone increased CD54 expression in HUVECs relative to normal HUVECs (Figure 4.4.A; $p < 0.0001$). Furthermore, hypoxia-induced TCM increased CD54 expression relative to hypoxic HUVEC controls (Figure 4.4.A; $p < 0.0001$) and normoxic TCM-conditioned HUVECs (Figure 4.4.A; $p < 0.0001$), suggesting that the dual impact of hypoxia and TCM together on EC is much greater than the effect by either hypoxia or TCM.

4.3.1.2.2 Macrophage-derived factors do not change CD54 expression on HUVECs relative to mesothelioma-derived factors

HUVECs exposed to supernatant from normoxic MØ, slightly upregulated CD54 relative to normoxic HUVEC controls (Figure 4.4.B; $p = 0.06$). Normoxic TCM-exposed macrophages also upregulated CD54 on HUVECs relative to normoxic HUVEC controls (Figure 4.4.B; $p = 0.003$) but not to TCM-exposed HUVECs or to hypoxic control, suggesting that TCM plays a major role in upregulating CD54 under normoxia. Similarly, supernatant from hypoxic TCM-exposed macrophages significantly increased CD54 by HUVECs relative to hypoxic HUVEC controls (Figure 4.4.B; $p = 0.02$) but not to TCM-exposed HUVECs or to hypoxic MØ, showing that under hypoxia MØ macrophages do not modulate the function of ECs in terms of CD54 expression.

In contrast, hypoxia-induced unpolarised macrophage-derived supernatants, with or without TCM, slightly but significantly down-regulated CD54 expression by HUVECs, which was already elevated due to the hypoxic conditions (Figure 4.4.B). These data again suggest that oxygen levels modulate macrophages that then impact ECs.

4.3.1.2.3 M1 macrophage-derived factors increase CD54 expression on HUVECs under normoxic and hypoxic conditions

The effect of macrophages polarised to M1 cells using LPS/IFN-γ on HUVEC expression of CD54 was also investigated. M1 and TCM-exposed M1 significantly increased CD54 expression on HUVECs under normoxia relative to MØ (SN)-stimulated HUVECs (Figure 4.4.C; $p = 0.002$; $p < 0.0001$, respectively). This M1-induced effect on ECs occurred with or without exposure to TCM; however, TCM-exposed M1 cells have greater effects on HUVECs relative to M1 cells (Figure 4.4.C; $p = 0.002$), implying that the dominant effect by M1 cells on HUVECs is further increased when M1 cells are exposed to tumour-derived factors.

Similarly, under hypoxia, hypoxic M1 and TCM-exposed M1 increased CD54 expression on hypoxic HUVECs (relative to hypoxic MØ (SN)-stimulated HUVECs; Figure 4.4.C; $p = 0.001$ and Figure 4.4.C; $p = 0.006$). These data imply that neither hypoxia nor hypoxic tumour-derived factors affect the role of M1 in inducing HUVECs to increase CD54 expression.

4.3.1.2.4 M2 macrophage-derived factors do not change CD54 expression on HUVECs

M2 macrophages, with or without TCM, do not influence the expression of CD54 on HUVECs regardless of oxygen levels compared with controls (Figure 4.4.D).

In summary, these results show that mesothelioma-derived factors, M1-derived factors, and TCM-M1-derived factors generated under normoxic and hypoxic conditions upregulate CD54 expression on HUVECs. CD54 overexpression may increase immune cell trafficking into mesothelioma and may also induce vascular leakage in mesothelioma tumours leading to tumour metastasis and a poor prognosis (281-283).

4.3.1.3 Endoglin, CD105

CD105, also referred to as Endoglin, is an important accessory receptor to transforming growth factor beta (TGF-β). In addition to ECs, CD105 is expressed on bone marrow

stromal fibroblasts, hematopoietic progenitor cells, melanocytes, activated monocytes, syncytiotrophoblasts in placenta and differentiated macrophages (284). CD105 is abundantly expressed in tissues undergoing angiogenesis such as tumours and is recognised as an indicator of EC proliferation(285, 286). Endoglin is seen an appropriate marker for tumour neovascularization and angiogenesis (228). Different environmental factors and cytokines impact expression of endoglin. TGF-β, together with hypoxia, are potent stimuli that induce CD105 gene expression (285, 287). Compared to normal tissueneoplastic ECs are more prolific and overexpress endoglin, which may be evidence of its role in angiogenesis (284, 287, 288). In hypoxic ECs, CD105 induces an anti-apoptotic pathway which prevents apoptosis and promotes angiogenesis (285). In solid tumours, expression of endoglin is nearly exclusively on ECs of peri- and intra-tumoural blood vessels and on components of tumour stroma (289). Endoglin upregulation in many tumours correlates with reduced survival rates of patients and metastatic disease (290-292). In-vitro studies showed Endoglin suppression in HUVECs induced apoptosis and inhibited angiogenesis (228). In CD105-depressed human dermal microvascular endothelial cells HDMECs), hypoxia and TGFβ1 synergistically enhance cell apoptosis (285). This study examined potential interactions between HUVECs and mesothelioma cells and between HUVECs and MØ, TCM-CM, M1, TCM-CM1, M2 and TCM-CM2 macrophages in normoxic and hypoxic models.

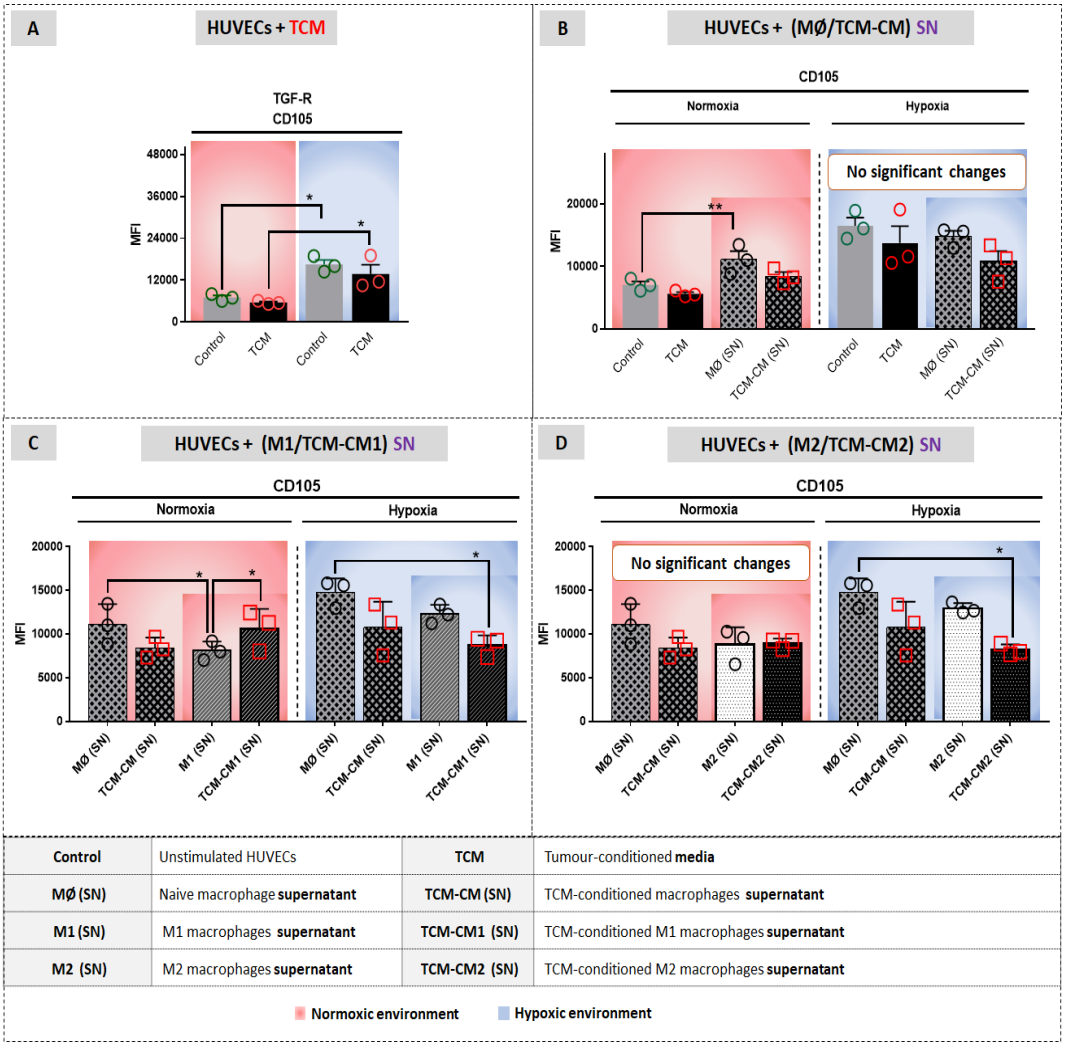

Control	Unstimulated HUVECs	**TCM**	Tumour-conditioned **media**
MØ (SN)	Naive macrophage **supernatant**	**TCM-CM (SN)**	TCM-conditioned macrophages **supernatant**
M1 (SN)	M1 macrophages **supernatant**	**TCM-CM1 (SN)**	TCM-conditioned M1 macrophages **supernatant**
M2 (SN)	M2 macrophages **supernatant**	**TCM-CM2 (SN)**	TCM-conditioned M2 macrophages **supernatant**

Normoxic environment **Hypoxic environment**

Figure 4. 5 Hypoxia elevates CD105 expression on HUVECs

Passage 6 HUVECs incubated with HUVEC medium to generate controls or with media containing JU77 TCM to generate TCM-conditioned HUVECs under normoxic and hypoxic conditions were stained for CD105 and MFI measured (A). To assess the effect of macrophages generated under normoxic and hypoxic conditions (B, C & D) HUVECs were exposed to supernatant collected from MØ and TCM-CM (B), M1 and TCM-CM1 (C), and M2 and TCM-CM2 (C). Pooled data are expressed as mean ± SEM in all conditions. P-values were determined using a two-way ANOVA test, * = $p < 0.05$, ** = $p < 0.005$, *** = $p < 0.0005$ **** = $p < 0.0001$, n = 3 replicates per condition.

4.3.1.3.1 Hypoxia increases CD105 on HUVECs

Hypoxia increased CD105 expression on HUVECs relative to normoxic controls (Figure 4.5.A; p = 0.02). However, no differences were observed in normoxic TCM-induced HUVECs or hypoxic TCM-induced HUVECs relative to normoxic HUVEC controls (Figure 4.5.A), while hypoxic TCM-induced HUVECs had a higher expression of CD105 relative to normoxic TCM-induced HUVECs (Figure 4.5.A; p = 0.04). Taken together, the data suggest that hypoxia elevates CD105 expression.

4.3.1.3.2 TCM macrophage-derived factors do not change CD105 expression on HUVECs under normoxia and hypoxia

HUVECs exposed to supernatant from normoxic MØ significantly upregulated CD105 relative to normoxic HUVEC controls (Figure 4.5.B; p = 0.008), while supernatant from normoxic TCM-exposed MØ macrophages did not change CD105 expression by HUVECs under normoxia (Figure 4.5.B). On the other hand, under hypoxia, no differences were observed between conditions (Figure 4.5.B).

4.3.1.3.3 M1-derived factors decreased CD105 expression on HUVECs under hypoxia

Assessing the effect of M1 cells and TCM-exposed M1 cells on HUVECs expression also showed that M1 macrophages significantly reduced CD105 expression on HUVECs relative to MØ (SN)-stimulated HUVECs (Figure 4.5.C; p=0.01) but not TCM-exposed M2, implying that tumour-derived factors can abrogate the effect of M1 cells on ECs.

Under hypoxia, hypoxic M1 macrophages did not affect CD105 expression on hypoxic HUVECs (relative to hypoxic MØ (SN)-stimulated HUVECs; Figure 4.5.C), while TCM-exposed M1 cells significantly reduced CD105 (relative to hypoxic MØ (SN)-stimulated HUVECs; Figure 4.5.C; p = 0.04). Suggesting that hypoxia, tumour-derived factors and IL-4/IL-13 together alter the function of macrophages, which in turn affects the function of ECs.

4.3.1.3.4 M2-derived factors decreased CD105 expression on HUVECs under hypoxia

Under normoxia, neither M2 cells nor TCM-exposed M2 cells changed the expression of CD105 relative to the normoxic HUVEC control (Figure 4.5.D). In contrast, under hypoxia, hypoxic TCM-exposed M2 cells significantly decreased CD105 expression (Figure 4.5.D; $p = 0.03$), suggesting that hypoxia, tumour-derived factors and IL-4/IL-13 together induce alteration in the macrophages that lead to changes in the endothelial cell expression of CD105.

In summary, these results suggest that CD105 upregulation on HUVECs in mesothelioma tumours may be due to hypoxia although factors derived from TCM-CM1 and TCM-CM2 can reduce CD105 expression. It has been reported that TGF-β levels are up-regulated in macrophages during hypoxia (293). Thus, the decrease in CD105 detection by flow cytometry may be due to CD105-TGF-β blocking interactions, which may prevent hypoxic ECs from undergoing apoptosis and thus promote mesothelioma tumourigenesis.

4.3.1.4 Vascular endothelial cadherin (VE-cadherin) CD144

Vascular endothelial cadherin (VE-cadherin), also known as CD144, is a transmembrane protein belonging to the cadherin superfamily of cell–cell adhesion molecules, which are specifically expressed by ECs (229). Notably, the importance of VE-cadherin was demonstrated by an experiment using mouse models deficient in VE-cadherin, which found that mice died at mid-gestation due to malformations (294). Furthermore, in adult mice, the significance of VE-cadherin in maintaining vascular integrity was evidenced after anti-VE-cadherin antibody administration resulted in a drastic rise in haemorrhage, permeability and vascular fragility (295). The endothelium creates a barrier that is selectively semi-permeable and regulates bidirectional transfer between irrigated tissues and blood vessels (296). Importantly, VE-cadherin is a master regulator of the dynamic architecture of endothelial cell–cell junctions, which coordinate opening and closing of the endothelial barrier, thus controlling permeability changes (296). Tumour vessel hyperpermeability correlates with reduced levels of VE-cadherin (297, 298). However, high VE-cadherin expression in melanoma and breast

cancer patients is associated with poor prognosis (299). Furthermore, VE-cadherin triggers appropriate activities of receptors across several types of ECs, including TGFβ-R2, Tie2 and FGF signalling (300). VE-cadherin can team up with VEGFR2 to lower proliferation. Finally, its association with VEGFR2 could induce the AJ components' phosphorylation by SRC, thus potentially impairing the function of the endothelial barrier (301). This study examined potential interactions between HUVECs and mesothelioma cells and between HUVECs and MØ, TCM-CM, M1, TCM-CM1, M2 and TCM-CM2 macrophages in normoxic and hypoxic models.

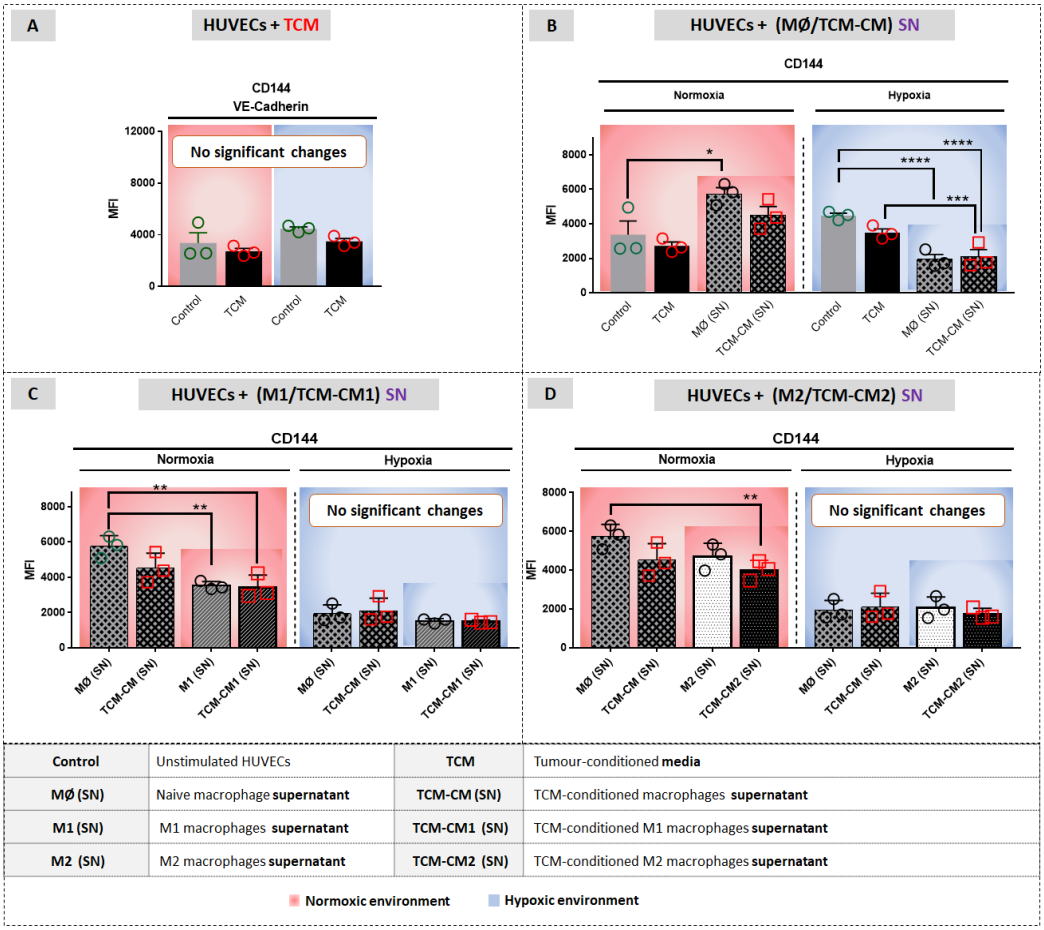

Control	Unstimulated HUVECs	**TCM**	Tumour-conditioned **media**
MØ (SN)	Naive macrophage **supernatant**	**TCM-CM (SN)**	TCM-conditioned macrophages **supernatant**
M1 (SN)	M1 macrophages **supernatant**	**TCM-CM1 (SN)**	TCM-conditioned M1 macrophages **supernatant**
M2 (SN)	M2 macrophages **supernatant**	**TCM-CM2 (SN)**	TCM-conditioned M2 macrophages **supernatant**

Normoxic environment **Hypoxic environment**

Figure 4. 6 Macrophage-derived factor generated under hypoxia decrease expression CD144 on HUVECs

Passage 6 HUVECs incubated with HUVEC medium to generate controls or with media containing JU77 TCM to generate TCM-conditioned HUVECs under

normoxic and hypoxic conditions were stained for CD144 (VE-cadherin) and MFI measured (A). To assess the effect of macrophages generated under normoxic and hypoxic conditions (B, C & D) HUVECs were also exposed to supernatant collected from MØ and TCM-CM (B), M1 and TCM-CM1 (C), and M2 and TCM-CM2 (C). Pooled data are expressed as mean ± SEM in all conditions. P-values were determined using a two-way ANOVA test, * = $p < 0.05$, ** = $p < 0.005$, *** = $p < 0.0005$ **** = $p < 0.0001$, n = 3 replicates per condition.

4.3.1.4.1 Mesothelioma does not influence CD144 expression on HUVECs regardless of oxygen levels

Mesothelioma-derived factors under normoxia and hypoxia did not change the expression level of CD144 on HUVECs under normoxic and hypoxic conditions (Figure 4.6.A).

4.3.1.4.2 Hypoxic macrophage-derived factors reduce CD144 expression by HUVECs under hypoxic conditions

HUVECs exposed to supernatant from normoxic MØ, slightly but significantly, upregulated CD144 relative to normoxic HUVEC controls (Figure 4.6.B; $p = 0.06$). However, normoxic TCM-exposed MØ did not change CD144 expression on HUVECs relative to normoxic MØ and TCM-exposed HUVECs (Figure 4.6.B), suggesting that mesothelioma-derived factors modulate the function of macrophages which then impact EC function.

In contrast, hypoxia-induced unpolarised macrophage-derived supernatants, with or without TCM significantly down-regulated CD144 expression by HUVECs relative to hypoxic HUVECs controls (Figure 4.6.B; $p < 0.0001$), suggesting an indirect effect of hypoxia on ECs through modulation of macrophage function that then impacts EC function.

4.3.1.4.3 M1 macrophage-derived factors reduce CD144 expression on HUVECs under normoxia

Macrophages polarised to M1 cells and TCM-exposed M1 cells using LPS/IFN-γ significantly reduced CD144 expression on HUVECs under normoxia relative to MØ (SN)-stimulated HUVECs (Figure 4.6.C; p = 0.006 and Figure 4.6.C; p = 0.004, respectively). This M1-induced effect on ECs occurred with or without exposure to TCM, implying a dominant effect by normoxic M1 macrophages and not tumour-derived factors, which suggests that M1 and TCM-exposed M1 modulate ECs relative to unpolarised macrophages.

In contrast, under hypoxia the level of CD144 did not change when HUVECs were exposed to supernatant from M1 or TCM-exposed M1 relative to hypoxic MØ (SN)-stimulated HUVECs (Figure 4.6.C). That suggests that hypoxia interferes with M1 cells, TCM-exposed M1 cells and unpolarised macrophages in a way that prevents their ability to affect EC function.

4.3.1.4.4 M2 macrophage-derived factors reduce CD144 expression on HUVECs under normoxia

Under normoxia, only supernatant from TCM-exposed M2 decreased HUVEC CD144 expression (Figure 4.6.D; p = 0.007). No differences were observed between MØ (SN)-stimulated HUVECs and M2 (SN)-stimulated HUVECs (Figure 4.6.D). The level of CD144 did not change when HUVECs were stimulated with M2 (SN) and TCM-CM2 (SN) under hypoxia compared to their relative control (Figure 4.6.D). **In summary,** these results suggest that CD144 downregulation on HUVECs in mesothelioma may be due to macrophage-derived factors generated under hypoxia.

4.3.1.5 Melanoma cell adhesion molecule (MCAM), CD146

CD146, also known as melanoma cell adhesion molecule (MCAM), S-endo-1, P1H12, and MUC18, is an integral membrane glycoprotein within the immunoglobulin superfamily (302-304). CD146 is expressed at cell–cell junctions in all ECs on all blood vessels regardless of vessel size (305, 306). CD146 can be expressed on smooth muscle

cells, pericytes, immune cells and some tumours, such as melanoma (307, 308). CD146 is involved in control of EC adhesion, cohesion, vessel permeability and integrity (304). Furthermore, CD146 is widely known asa novel endothelial biomarker associated with angiogenesis and participates in tumour progression (309). A number of factors regulate expression of CD146, including TNFα (310), IL-13 (311) and TGF-β1 (312). High expression of CD146 on ECs, as well as endothelial progenitors, is indicative of its role in physiological and pathological angiogenesis, such as tumour angiogenesis. For example, targeting membrane CD146 with the AA98-blocking antibody decreases the number of vessels in an animal model of xenografted tumour cells (313). CD146 plays a pivotal role in transendothelial migration (310). Removal of CD146 function through interfering RNA in pulmonary ECs has been linked to heightened monocyte infiltration and endothelial permeability in a chronic obstructive pulmonary disease model (314). This study examined potential interactions between HUVECs and mesothelioma cells and between HUVECs and MØ, TCM-CM, M1, TCM-CM1, M2 and TCM-CM2 macrophages in normoxic and hypoxic models.

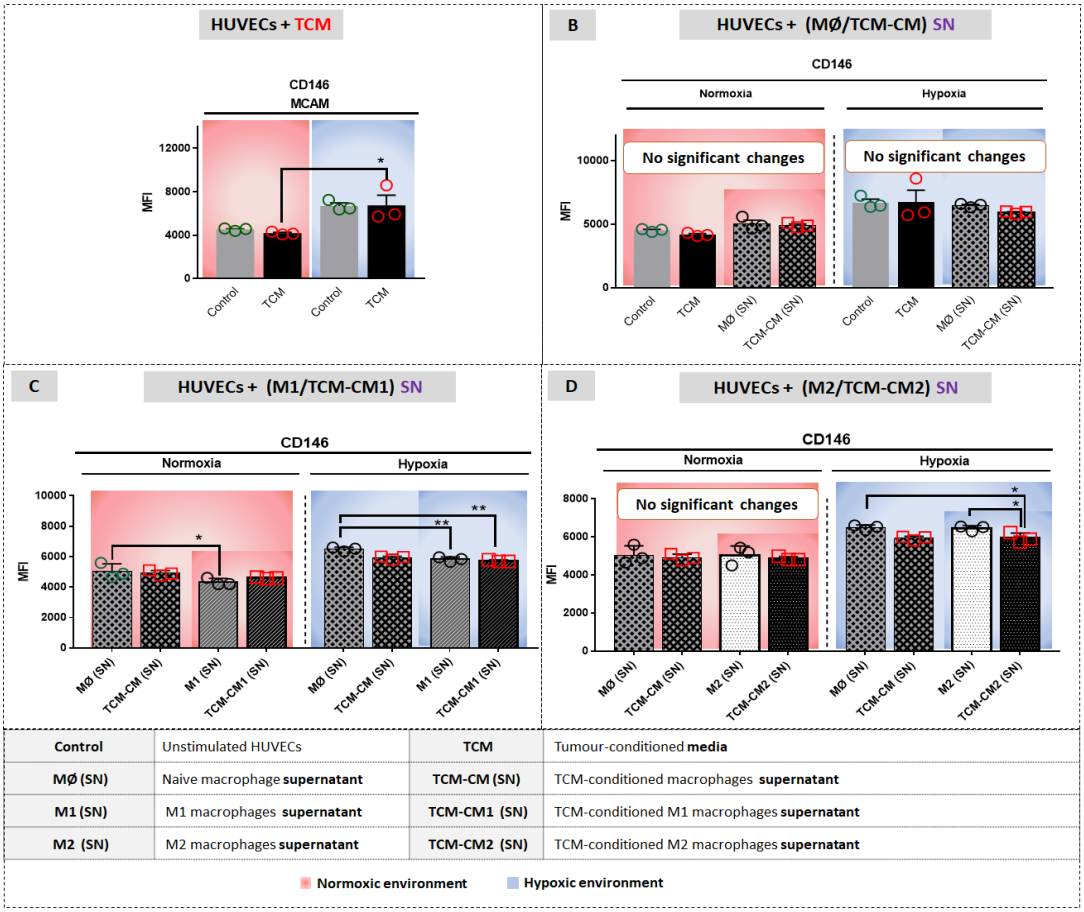

Figure 4. 7 Hypoxic mesothelioma tumours induce higher levels of CD146 compared to normoxic tumours

Passage 6 HUVECs incubated with HUVEC medium to generate controls or with media containing JU77 TCM to generate TCM-conditioned HUVECs under normoxic and hypoxic conditions were stained for CD146 and MFI measured (A). To assess the effect of macrophages generated under normoxic and hypoxic conditions (B, C & D) HUVECs were also exposed to supernatant collected from MØ and TCM-CM (B), M1 and TCM-CM1 (C), and M2 and TCM-CM2 (C). Pooled data are expressed as mean ± SEM in all conditions. P-values were determined using a two-way ANOVA test, * = $p < 0.05$, ** = $p < 0.005$, *** = $p < 0.0005$ **** = $p < 0.0001$, n = 3 replicates per condition.

4.3.1.5.1 Hypoxic-induced mesothelioma factors elevate CD146 expression on endothelial cells

TCM generated under hypoxic conditions elevated CD146 relative to normoxic TCM conditions (Figure 4.7.A; $p = 0.04$). No other differences were seen (Figure 4.7.A).

4.3.1.5.2 Mesothelioma-conditioned macrophage-derived factors did not change CD146 expression on HUVECs under normoxia and hypoxia

The level of CD146 did not change when HUVECs were stimulated with MØ (SN) and TCM-exposed MØ under normoxia and hypoxia compared to their relative controls (Figure 4.7.B).

4.3.1.5.3 M1-derived factors decreased CD146 expression on HUVECs under hypoxia

M1 normoxic macrophages significantly reduced CD146 expression on HUVECs relative to MØ (SN)-stimulated HUVECs (Figure 4.7.C; $p = 0.05$). Under hypoxia, M1 cells and TCM-exposed M1 significantly reduced CD146 expression on HUVECs relative to MØ (SN)-stimulated HUVECs (Figure 4.7.C; p 0.006 and Figure 4.7.C; $p = 0.001$, respectively). This M1-induced effect on endothelial cells occurred with or without exposure to TCM, implying a dominant effect by M1 macrophages and not tumour-derived factors.

4.3.1.5.4 M2-derived factors decreased CD146 expression on HUVECs under hypoxia

The level of CD146 did not change when HUVECs were exposed to supernatant from M2 cells or TCM-induced M2 cells relative to MØ (SN)-stimulated HUVECs under normoxia (Figure 4.7.D).

Under hypoxia, TCM-induced M2 decreased CD146 expression in HUVECs relative to MØ (SN)-stimulated HUVECs (Figure 4.7.D; $p = 0.02$). However, there were no differences observed when HUVECs were stimulated with M2 cells (SN) (Figure 4.7.D), suggesting that, hypoxia and tumour-derived factors together alter M2 cell function, which in turn changes EC function.

In summary, these results show that hypoxia-induced mesothelioma factors, lead to a higher level of CD146 expression on HUVECs than mesothelioma factors generated under normoxia. Whilst, hypoxic TCM-exposed M1/M2 cells decrease CD146 expression on endothelial cells. High expression of CD146 may increase mesothelioma cell metastasis by inducing mesothelioma-endothelial adhesion.

4.4 Discussion

Solid tumours, including mesothelioma, initiate new vessel formation to support their growth and metastasis (6). The newly formed blood vessels result in poorly functioning vasculature, which enforces a hypoxic environment within tumours (7). It has been shown that significant regions of hypoxia are found in mesothelioma (3) and that hypoxia augments aggressive phenotypes of human malignant mesothelioma (4). Also, data in chapter 3 showed that hypoxia and hypoxic tumour conditions regulate macrophage functions. There are no published studies investigating the crosstalk between mesothelioma tumour cells or macrophages with ECs that consider hypoxia.

The aim of this chapter was to understand the potential effects of hypoxia, directly or indirectly (by modulating mesothelioma cell and macrophage secretory products) on ECs in 2D cell culture monolayers and 3D co-culture systems. However, ECs failed to remain viable in the multicellular spheroid model therefore, only 2D cell culture monolayers could be used. In the 2D cell models, the effect of mesothelioma-derived factors on ECs was investigated by incubating HUVECs in normoxic/hypoxic conditions and exposing them to normoxic/hypoxic-derived mesothelioma factors.

The findings reveal that hypoxia is a major player in upregulation of CD309 on normal healthy HUVECs. However, CD309 expression significantly reduced upon HUVEC exposure to mesothelioma-derived factors or factors derived from mesothelioma-conditioned macrophage subsets; nonetheless, the level of CD309 remained relatively high in HUVECs under hypoxia. Macrophages are a major source of VEGF, and hypoxia has been shown to increase VEGF expression in macrophages (315-317). Thus, one possibility is that the decrease in CD309 detected by flow cytometry may in

fact be due to blocking via VEGF engagement. VEGF/CD309 interactions may increase, as well as tumour progression, invasion, and metastasis. This finding agrees with data showing that hypoxia upregulates CD309 in ECs (318). These data imply that regulation of endothelial cells CD309 expression in mesothelioma tumours could be mainly controlled by hypoxia. High levels of CD309 expression in ECs may result in their proliferation and induction of permeability.

Furthermore, the data showed that mesothelioma-derived factors generated under normoxia and hypoxia increased CD54 expression. Additionally, the results found that oxygen deficiency is a key contributor leading to elevated CD54 expression in HUVECs. The data also revealed that supernatants from LPS-INF-γ-stimulated mesothelioma-conditioned macrophages increased CD54 expression. In terms of the effect of hypoxia, the results are consistent with data showing that hypoxia upregulates CD54 expression by HUVECs (319). Increased CD54 expression can lead to increased vascular permeability and leukocyte transmigration (282, 283, 320). CD54 is expressed by many cancers, including mesothelioma and its overexpression on blood vessels might favour killing mesothelioma cells by promoting adhesion of infiltrating leukocytes in mesothelioma (321). However, Podgrabinska et al. reported that interaction between Mac-1 on DCs and CD54 on lymphatic ECs suppresses dendritic cell maturation and activates T cells function (322). Therefore, although CD54 plays an important role in facilitating invasion of tumour by immune cells, endothelial CD54 can also be involved in tumour-EC adhesion, which may promote progression and metastases (323-326). For example, Laurent et al. showed that CD54 expressed on ECs is involved in adhesion of invasive bladder cancer cells (327). Additionally, blocking CD54 in the endothelium of lungs (323) or brain (328) abrogates metastasis.

This study demonstrates that hypoxic environments elevate CD105. However, CD105 was not affected by molecules derived from mesothelioma tumour cells or macrophages under normoxia or hypoxia. Hypoxia induces cell cycle arrest in the G1 phase of many cells, including ECs (288, 329). High expression of CD105 may protect hypoxic ECs from apoptosis and promote tumorigenesis via CD105 signalling.

These data revealed that hypoxia indirectly affects VE-cadherin (CD144) expressionby HUVECs by modulating soluble molecules derived from macrophages. There are no publications investigating the effects of macrophages on VE-cadherin in ECs. However, our results are consistent with a study showing that hypoxia has no direct effect on VE-cadherin expression in ECs (330). These data imply that macrophage functions are regulated by hypoxia, which induce macrophages to secrete molecules that may lead to mesothelioma tumour vessel leakiness via decreased VE-cadherin expression.

The data also demonstrate that CD146 expression was directly affected by hypoxia, however it was not affected by mesothelioma tumour cell and macrophage-derived factors generated under normoxia and hypoxia. In a previous study, CD146 expression was seen in mesothelioma cells and tumour-associated blood vessels although, expression levels were not determined (331). The finding of overexpressed CD146 in ECs agrees with data showing that blood vessels in colorectal and renal malignancies express high levels of CD146 (332). CD146 is involved in control of EC adhesion and cohesion, as well as vessel permeability and integrity (304) and is associated with angiogenesis and participates in tumour progression (309). This finding implies that high expression of CD146 may result in endothelial adhesion to mesothelioma cells, which may lead to mesothelioma metastasis.

Altogether, this work demonstrates the importance of choosing appropriate in vitro culture conditions to study the tumour microenvironment, as hypoxia can directly induce changes to ECs, specifically to expression of CD309, CD54, CD105 and CD146. Hypoxia may also indirectly modulate ECs by affecting soluble factors secreted by macrophages to change VE-cadherinexpression, which alters blood vessels to be more permissive and leaky.

CHAPTER 5

ASSESSING THE EFFECT OF OXYGENATION ON IL-2, ANTI-CD40 ANTIBODY AND/OR VTX-2337 TREATED, MESOTHELIOMA-EXPOSED MACROPHAGES AND ENDOTHELIAL CELLS

5.1 Introduction

Strategies to improve cancer immunotherapy include identifying and targeting key immune cell types in the tumour microenvironment that contribute to tumour progression, such as tumour-associated macrophages (TAMs), myeloid-derived suppressor cells (MDSCs) and T cells. This is because they can suppress anti-tumour effector cells, such as cytotoxic T cells (333). TAMs represent a major cellular population in many tumours, and are increasingly being examined as therapeutic targets on account of their influence on adaptive immune cells, their involvement in tumour progression and their correlation with poor prognosis (334). There is evidence that M1-dominance decreases with tumour progression with M2-cells taking over (335, 336). Re-polarising M2 macrophages to M1 macrophages has been shown to reduce tumour growth (337). Furthermore, once M2 TAMs are deliberately converted to M1 cells, and the ratio of M2/M1 macrophages is modulated, antitumor activity is enhanced. For example, Ren, Fan and Mei found that IFN-γ-induced M1 cells play a role in inhibiting the growth of lung tumours (338). The pro-tumoral phenotype of TAM and their plasticity, referred to as reprogramming, enables this phenotypic change, making them appropriate targets for anticancer therapy (339).

The concept of reprogramming involves polarization of M2-like TAMs towards M1 cells with antitumoral activities that promote tumour regression (62). Our group has shown this is possible using a combination of IL-2 with an agonist anti-CD40 monoclonal antibody (30). Our group has also shown that intra-tumoural injection of IL-2 or anti-CD40 alone can shrink small, but not large, mesothelioma tumours (8, 9). However, our group also found that intra-tumoural injection of IL-2 combined with

anti-CD40 induced curative regression of large tumours (8, 9, 340). M2 cells are involved in the formation of defective tumour blood vessels, while M1 cells tend to normalize irregular tumour vascular networks (147, 341-343). Normalizing tumour vessels is hypothesized to alleviate hypoxia in the tumour microenvironment in order to restore perfusion, thus reducing metastatic potential and improving drug delivery (344, 345).

As mentioned above, immunotherapeutic approaches that have shown positive results in murine mesothelioma models include IL-2 and an agonist anti-CD40 antibody (α-CD40) (9, 10, 346). Furthermore, VTX-2337, a synthetic small-molecule based on a 2-aminobenzazepine core structure, has been shown to activate immune cells via TLR7/8, and has been assessed in a phase I oncology trial (12). All three reagents/therapeutics were tested in this chapter.

This chapter has three aims.

The first is to assess the effect of IL-2, α-CD40, or VTX-2337 as monotherapies, as well as the combination of IL-2/α-CD40 on mesothelioma-exposed macrophages under normoxic and hypoxic conditions.

The second aim is to assess the effect of IL-2, α-CD40, IL-2/α-CD40 and VTX-2337 on mesothelioma-exposed human umbilical vein endothelial cells (HUVECs) under normoxic and hypoxic conditions.

The third aim is to assess the effect of mesothelioma-exposed macrophages given these therapies on endothelial cells by exposing HUVECs to supernatant from IL-2, α-CD40, IL-2/α-CD40 and VTX-2337-stimulated macrophages (Figure 5.1). In this scenario, the hypothesis is that macrophages activated by any of these reagents might then secrete factors that further modulate tumour vessels.

Figure 5. 1 Experimental design

(A) Normal macrophages and mesothelioma-conditioned macrophages differentiated from monocytes were stimulated with IL-2, α-CD40, IL-2 plus α-CD40, VTX-2337 or DMSO (diluent control) at day 7 for 24hrs, under normoxic (A) and hypoxic (B) conditions. **(B)** Passage 6 normal HUVECs and tumour-conditioned HUVECs were stimulated with IL-2 or α-CD40 or IL-2/α-CD40 or VTX-2337 or DMSO for 24hrs, (C) and hypoxic (D) conditions.

5.2 Results

5.2.1 Evaluating the effect of IL-2 on mesothelioma-exposed macrophages and endothelial cells under normoxic and hypoxic conditions

Our group has shown that administration of IL-2 when used as single drugs into tumours can cure small murine mesothelioma tumours (9). However, for larger tumours, the rate of survival did not increase (9). One aim of this study was to assess the direct effect of IL-2 on mesothelioma-exposed macrophages and HUVECs under normoxic and hypoxic conditions. The second aim was to evaluate the effect of mesothelioma-exposed/IL-2-activated macrophages on endothelial cells by exposing HUVECs to factors derived from IL-2-stimulated macrophages.

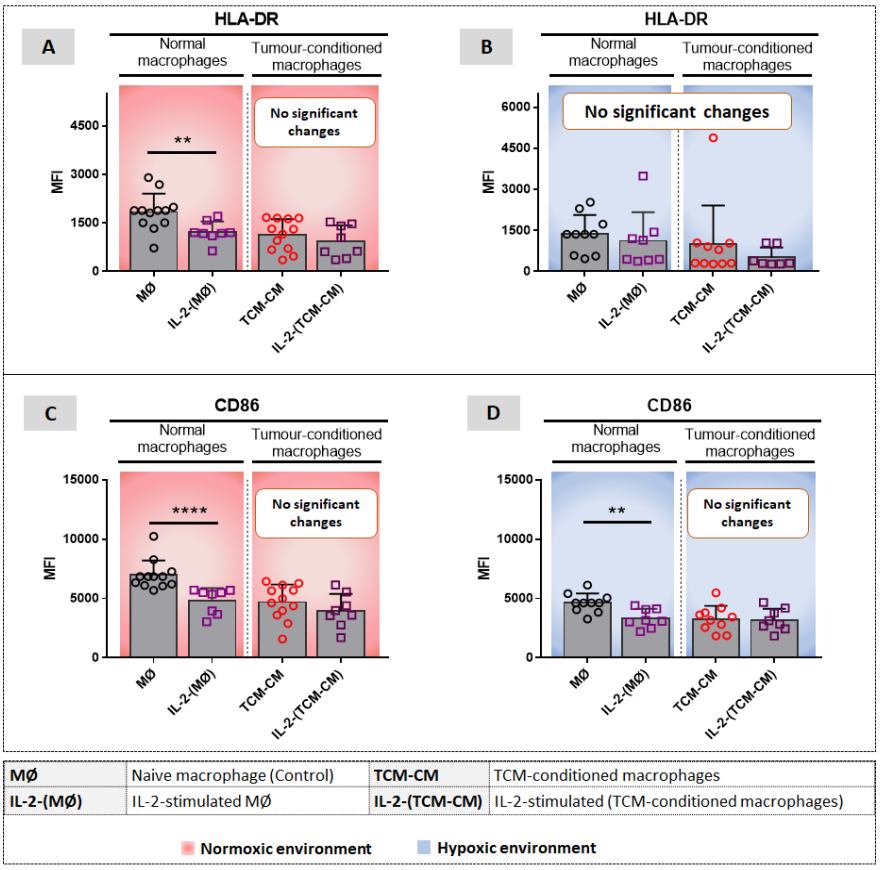

Figure 5. 2 The effect of IL-2 on macrophage HLA-DR and CD86 under normoxic and hypoxic conditions

Normal and tumour-conditioned macrophages differentiated from monocytes were stimulated with IL-2 at day 7 for 24hrs, under normoxic and hypoxic conditions and stained for HLA-DR and CD86. Pooled data of HLA-DR (A, B) and CD86 (C, D) are expressed as mean ± SEM in normoxic naive macrophages (MØ) (control) versus normoxic IL-2-(MØ); normoxic TCM-CM versus normoxic IL-2-(TCM-CM); hypoxic MØ controls versus hypoxic IL-2-(MØ); and hypoxic TCM-CM versus hypoxic IL-2-(TCM-CM). The p-values were determined using the Mann-Whitney test, * = $p < 0.05$, ** = $p < 0.005$, *** = $p < 0.0005$ **** = $p < 0.0001$, n = 12 replicates per normoxic MØ, n = 10 replicates per hypoxic MØ, n = 8 replicates per normoxic and hypoxic IL-2-(MØ) and IL-2-(TCM-CM) conditions.

5.2.1.1 Hypoxia and mesothelioma prevent macrophages from decreasing HLA-DR in response to IL-2

Under normoxic conditions, IL-2 reduced HLA-DR expression in naïve macrophages (Figure 5.2.A; $p = 0.005$). However, no differences in HLA-DR expression were observed in all other experimental conditions, including normoxia (Figure 5.2.A.B). The data imply that IL-2 reduced antigen presentation potential to $CD4^+$ T cells due to decreased HLA-DR expression by macrophages. This effect was lost under hypoxia and when macrophages were exposed to mesothelioma-derived factors regardless of oxygenation levels. These data suggest that macrophages in mesothelioma tumours and/or under hypoxia maintain their ability to present antigen to $CD4^+$ T cells in the presence of IL-2. However, this response could be pro-tumourigenic as the $CD4^+$ T cells might be regulatory T cells that use IL-2 to proliferate and disable effector $CD8^+$ T cells. This could account for the observation that only small and not large tumours respond to intratumoural IL-2, as the latter have a higher total number of regulatory T cells (9).

5.2.1.2 Regardless of oxygenation levels mesothelioma prevents IL-2 from downregulating CD86

Relative to normoxic controls, IL-2 significantly decreased CD86 expression in MØ macrophages under normoxia (Figure 5.2.C; $p < 0.0001$). Similarly, IL-2 also

downregulated CD86 in hypoxic MØ macrophages relative to hypoxic controls (Figure 5.2.D; p = 0.004). However, IL-2 did not change CD86 expression in mesothelioma-conditioned macrophages under normoxic and hypoxic conditions. The data indicate that regardless of oxygen levels, mesothelioma-derived factors prevent IL-2 from decreasing CD86 on macrophages. One possibility is that maintenance of CD86 expression by mesothelioma-derived factors might enable macrophages to inhibit effector T cells via CD86-CTLA-4 interactions. Again, this may help explain why small and not large tumoursrespond to intratumoural IL-2, as the latter have a high number of macrophages (9).

5.2.2 Evaluating the effect of α-CD40 on mesothelioma-exposed macrophages and HUVECs under normoxic and hypoxic conditions

Our group has shown that administration of an agonist anti-CD40 antibody when used as single drugs into tumours can cure small murine mesothelioma tumours (346). Agonist anti-CD40 antibody generates a number of changes when targeted into the tumour bed (347). For example, CD40-activated tumour blood vessels become permissive to T cell migration and DC emigration (347). However, anti-CD40 antibody activated endothelial cells have also been shown to promote tumour neoangiogenesis in a murine model of mammary carcinoma (44, 347). The aim of this study was to assess the effect of α-CD40 on mesothelioma-exposed macrophages and HUVECs, and to evaluate the effect of α-CD40-activated/mesothelioma-exposed macrophages on HUVECs under normoxic and hypoxic conditions. The results showed that α-CD40 reduced the expression of CD163, CD206, HLA-DR and CD86 (Figure 5.4, Figure 5.5 and Figure 5.6) on normal and mesothelioma-exposed macrophages under normoxia but not hypoxia. The effect of anti-CD40 treatment on macrophage CD40 expression is shown in Figure 5.3. These data show that hypoxia interferes with macrophage responses to CD40 signalling. On the other hand, no effects on CD309, CD54, CD105, CD144, CD146, CD321 and CD62E expression were observed on HUVECs, regardless of oxygenation levels and the source of soluble factors.

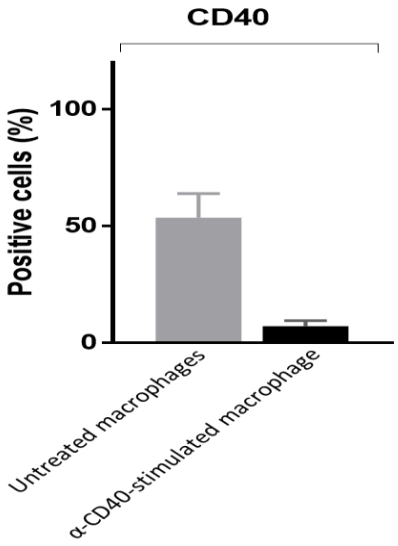

Figure 5. 3 This figure aimed to show the effect of anti-CD40 treatment on macrophage CD40 expression

It appears that CD40 expression is reduced. There are two possibilities. One is that CD40 expression was indeed reduced. The other is suggested by the reviewer, in which the staining anti-CD40 antibody could not attach to CD40 on macrophages as it was ‘covered’ by the treating antibody.

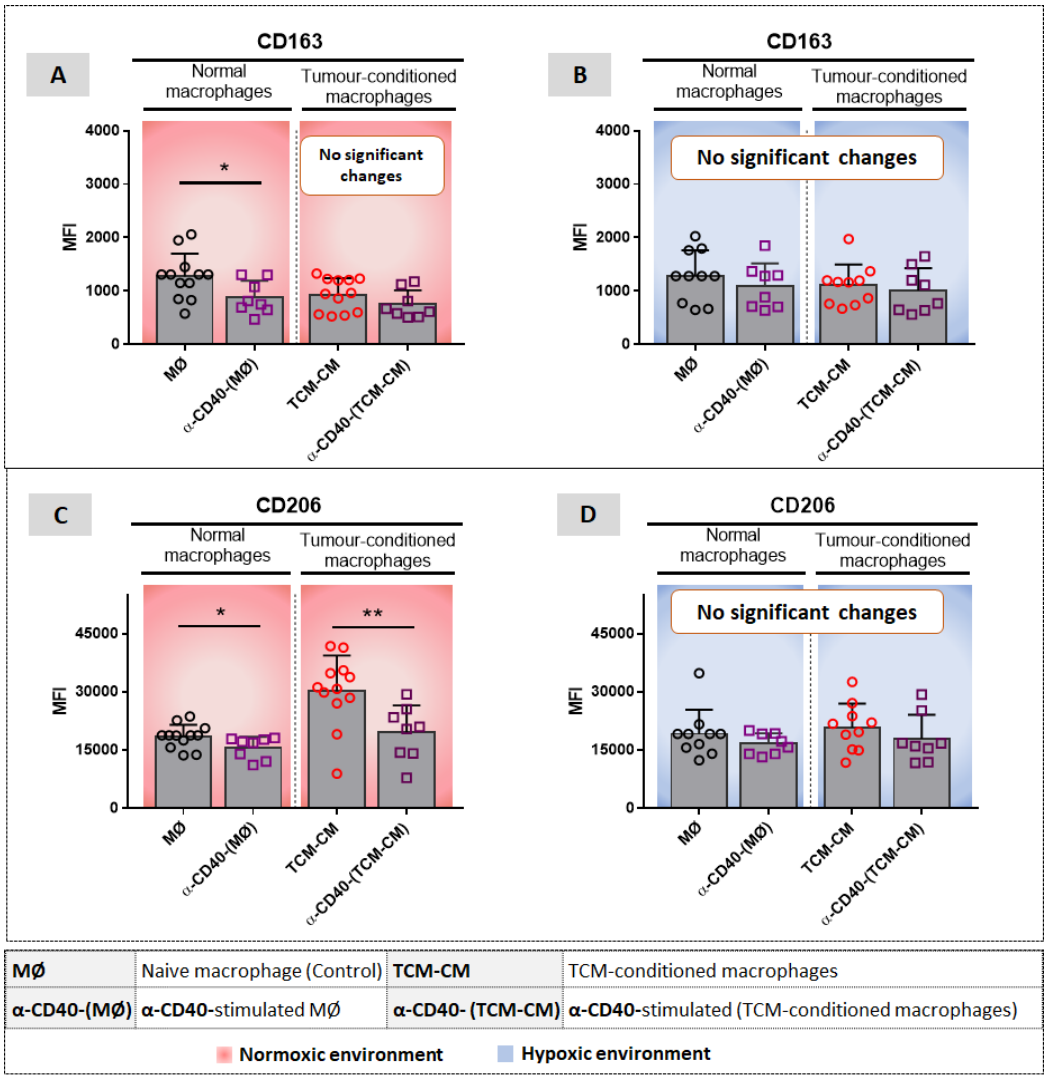

Figure 5. 4 The effect of α-CD40 on macrophage CD163 and CD206 under normoxia and hypoxia

Normal and TCM-conditioned macrophages differentiated from monocytes were stimulated with α-CD40 at day 7 for 24hrs, under normoxic and hypoxic conditions and stained for CD163 and CD206. Pooled data for CD163 (A, B) and CD206 (C, D) are expressed as mean ± SEM. The p-values were determined using the Mann-Whitney test, * = $p < 0.05$, ** = $p < 0.005$, *** = $p < 0.0005$ **** = $p < 0.0001$, n = 12 replicates per normoxic MØ, n = 10 replicates per hypoxic MØ, n=8 replicates per normoxic and hypoxic α-CD40-(MØ) and α-CD40-(TCM-CM) conditions.

5.2.2.1 Hypoxia and mesothelioma prevent α-CD40 from decreasing CD163

Under normoxic conditions, α-CD40 reduced expression of the M2 phenotype marker CD163 in normal macrophages (Figure 5.4.A; $p = 0.02$). No differences in CD163 expression were observed in all other conditions, including exposure to TCM. Decreased CD163 expression may indicate polarising away from an M2 phenotype and towards a proinflammatory M1 phenotype. However, mesothelioma-derived factors and hypoxia prevented this α-CD40-induced decrease in CD163 expression in macrophages (Figure 5.4.A.B). These data suggest that a hypoxic mesothelioma environment could maintain suppressive M2 macrophages when faced with CD40 stimulation. This could help account for the failure of α-CD40 antibody to mediate regression of large tumours (346).

5.2.2.2 Hypoxia prevents macrophages from downregulating CD206 in response to α-CD40

Under normoxic conditions, α-CD40 significantly downregulated expression of another M2 marker, CD206, in MØ macrophages relative to unstimulated MØ macrophage controls (Figure 5.4.C; $p = 0.03$) and in mesothelioma-conditioned macrophages relative to normoxic unstimulated mesothelioma-conditioned macrophages (Figure 5.4.C; $p = 0.007$). These data suggest normoxia, or high oxygenation levels, play a key role in regulating macrophage responses to α-CD40. Decreased CD206 expression may again indicate polarisation away from M2 and towards the proinflammatory M1 phenotype that could help mediate regression of small tumours in response to local CD40 stimulation (346).

However, under hypoxic conditions, α-CD40 stimulation of MØ macrophages and mesothelioma-conditioned macrophages did not change CD206 expression (Figure 5.4.D). The data indicate that hypoxia prevents CD206 reduction in macrophages in response to α-CD40 stimulation. Preventing polarisation away from an M2 phenotype in a hypoxic tumour environment could maintain local immune suppression.

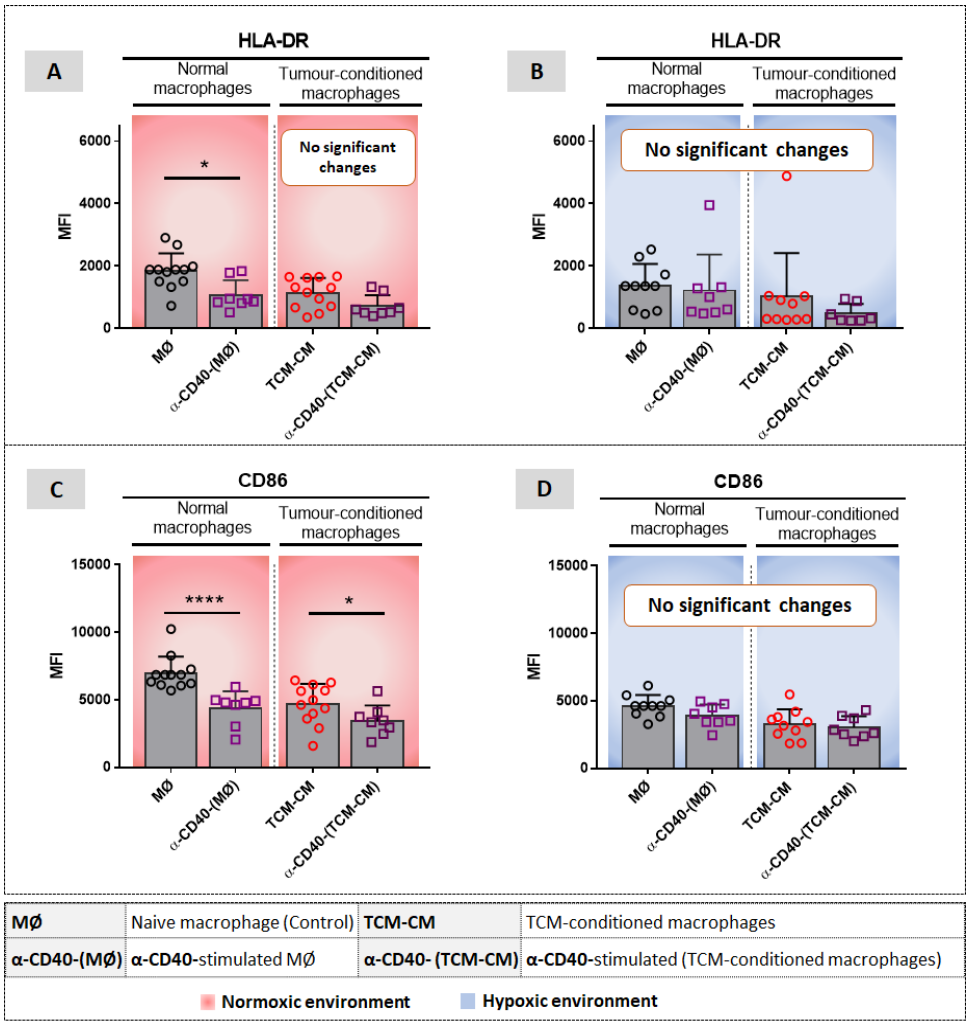

Figure 5. 5 The effect of α-CD40 on macrophage HLA-DR and CD163 under normoxic and hypoxic conditions

Normal macrophages and tumour-conditioned macrophages differentiated from monocytes were stimulated with α-CD40 at day 7 for 24hrs, under normoxic and hypoxic conditions and stained for HLA-DR and CD86. Pooled MFI data of HLA-DR (A, B) and CD86 (C, D) are expressed as mean ± SEM. The p-values were determined using the Mann-Whitney test, * = $p < 0.05$, ** = $p < 0.005$, *** = $p < 0.0005$ **** = $p < 0.0001$, n = 12 replicates per normoxic MØ, n = 10 replicates per hypoxic MØ, n=8 replicates per normoxic and hypoxic α-CD40-(MØ) and α-CD40-(TCM-CM) conditions.

5.2.2.3 Hypoxia and mesothelioma prevent macrophages from decreasing HLA-DR expression in response to α-CD40

Under normoxic conditions, α-CD40 stimulation unexpectedly reduced HLA-DR expression in MØ macrophages (Figure 5.5.A; p = 0.007). No other conditions modulated HLA-DR expression including exposure to TCM and hypoxia (Figure 5.5.A.B). The data imply that intratumoural α-CD40 may reduce the capacity of local macrophage to present antigens to CD4+ T-cells due to decreased HLA-DR, this could be beneficial in avoiding activating regulatory T cells in tumours.

5.2.2.4 Hypoxia prevents macrophages from downregulating CD86 in response to α-CD40

Under normoxic conditions, α-CD40 significantly downregulated CD86 expression in MØ macrophages relative to unstimulated normoxic controls (Figure 5.4.C; p <0.0001) and in mesothelioma-conditioned macrophages relative to normoxic unstimulated mesothelioma-conditioned macrophages (Figure 5.5.C; p = 0.05). CD86 expression was not changed under hypoxic conditions (Figure 5.5.D) suggesting a key role for oxygen deprivation in regulating CD86 expression. As mentioned above, this might inhibit T cell function via CD86-CTLA-4 interactions and explain why large tumoursfail to respond to intratumoural α-CD40 (346), as the latter have a high number of macrophages (9).

5.2.3 Evaluating the effect of IL-2/α-CD40 on mesothelioma-exposed macrophages and HUVECs under normoxic and hypoxic conditions

Preclinical mouse studies have shown remarkable curative responses to intra-tumoural IL-2 combined with α-CD40 in mesothelioma (348, 349). Therefore, the aim of this study was to assess the direct effect of IL-2/α-CD40 on mesothelioma-exposed macrophages and HUVECs and to evaluate the effect of IL-2/α-CD40-activated/mesothelioma-exposed macrophages on HUVECs under normoxic and hypoxic conditions.

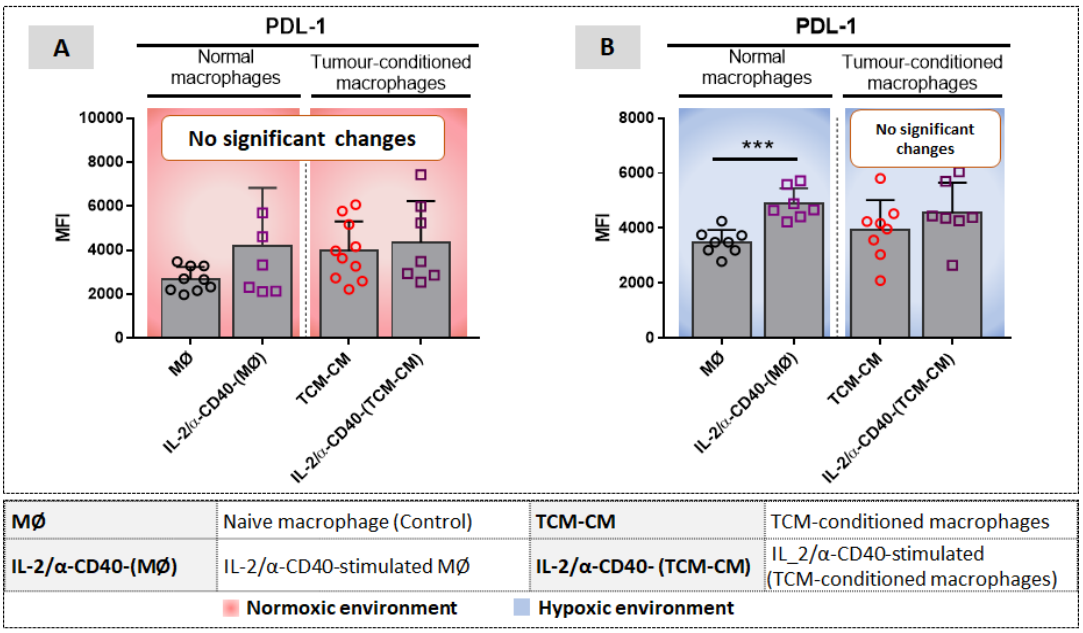

Figure 5. 6 The effect of IL-2/α-CD40 on PDL-1 under normoxia and hypoxia

Normal and tumour-conditioned macrophages were stimulated with IL-2/α-CD40 at day 7 for 24hrs, under normoxic and hypoxic conditions and stained for PDL-1. Pooled data are expressed as mean ± SEM, p-values were determined using the Mann-Whitney test, * = $p < 0.05$, ** = $p < 0.005$, *** = $p < 0.0005$ **** = $p < 0.0001$, n = 12 replicates per normoxic MØ, n = 10 replicates per hypoxic MØ, n=8 replicates per normoxic and hypoxic IL-2/α-CD40-(MØ) and IL-2/α-CD40-(TCM-CM) conditions.

5.2.3.1 IL-2/α-CD40 and hypoxia increase PDL-1 expression in MØ macrophages

Under hypoxic conditions, IL-2/α-CD40 upregulated PDL-1 expression in MØ macrophages (Figure 5.6.B; $p = 0.0006$). No changes in PDL-1 expression were observed in all other conditions, including normoxia (Figure 5.6.A.B). The data imply that hypoxia promotes a more suppressive environment, as PDL-1/PD-1 interactions inhibit effector T cell function.

5.2.4 Evaluating the response of mesothelioma-conditioned macrophages to VTX-2337 under normoxic and hypoxic conditions

VTX-2337, a synthetic small-molecule based on a 2-aminobenzazepine core structure, has been shown to activate innate immune cells via TLR7 and 8, and has been assessed in a phase I oncology trial (12). VTX-2337 may help shift the TAM phenotype from M2 towards M1. Therefore, the aim of this study was to assess the direct effect of VTX-2337 on mesothelioma-exposed macrophages and HUVECs and to evaluate the effect of VTX-2337-activated/mesothelioma-exposed macrophages on HUVECs under normoxic and hypoxic conditions.

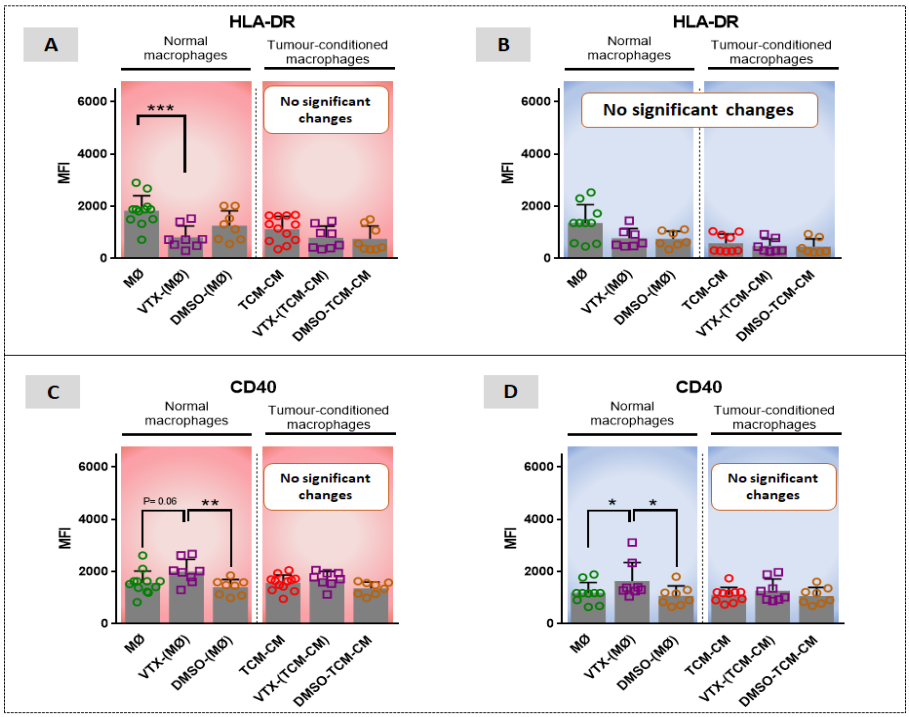

Figure 5. 7 The effect of VTX-2337 on macrophage HLA-DR and CD40 under normoxic and hypoxic conditions

Normal and tumour-conditioned macrophages were stimulated with VTX or DMSO (diluent control) at day 7 for 24hrs under normoxia and hypoxia and stained for HLA-

DR and CD40. Pooled data for HLA-DR (A, B) and CD40 (C, D) expressed as mean ± SEM, p-values determined using Mann-Whitney test, * = $p < 0.05$, ** = $p < 0.005$, *** = $p < 0.0005$ **** = $p < 0.0001$, n = 12 replicates per normoxic MØ, n = 10 replicates per hypoxic MØ, n=8 replicates per normoxic and hypoxic VTX-(MØ) and VTX-(TCM-CM), DMSO-(MØ) and DMSO-(TCM-CM) conditions.

5.2.4.1 Hypoxia and mesothelioma prevent macrophages from decreasing HLA-DR in response to VTX-2337

Under normoxia, a significant decrease in HLA-DR was seen in MØ macrophages following VTX-2337 stimulation relative to unstimulated MØ (Figure 5.7.A; p = 0.0008). HLA-DR was reduced by TCM and VTX-2337 did not change its expression (Figure 5.7.A). Similar results were seen under hypoxia (Figure 5.7.B). The data imply that, VTX-2337-stimulated macrophages lose their capacity to present antigens to CD4+ T cells under normoxia but not hypoxia.

5.2.4.2 Mesothelioma prevents VTX-2337 from upregulating CD40 expression

Under normoxia, VTX-2337 increased CD40 expression relative to unstimulated MØ (Figure 5.7.C; p = 0.06). Similarly, under hypoxic conditions, CD40 expression significantly increased after stimulation with VTX-2337 relative to unstimulated MØ (Figure 5.7.D; p = 0.04) or DMSO controls (Figure 5.7.D; p = 0.03). Yet VTX-2337 had no effect on mesothelioma-conditioned macrophages under normoxic or hypoxic conditions (Figure 5.7.C, D). These results suggest that mesothelioma-derived factors contain molecules that prevent CD40 upregulation and therefore prevent CD40/CD40L-mediated inflammatory responses, a response that is likely to be anti-tumourigenic.

5.2.4.3 Hypoxia and mesothelioma do not affect the role of VTX-2337 in upregulating CD80

CD80 expression increased following stimulation with VTX-2337 in normoxic MØ macrophages (Figure 5.8.A; p <0.0001), normoxic mesothelioma-conditioned macrophages (Figure 5.8.A; p = 0.005), hypoxic MØ macrophages (Figure 5.8.B; p

<0.0001) and hypoxic mesothelioma-conditioned macrophages (Figure 5.8.B; p = 0.02), relative to their unstimulated controls. Similar to CD86, CD80 is a powerful co-stimulation signal required to activate T-cells if they interact with CD28. However, binding CTLA-4 negatively regulates T-cell activation. The data imply that in response to VTX-2337, macrophages in mesothelioma could increase stimulatory or regulatory activity depending on their engagement with CD28 or CTLA-4 on T-cells.

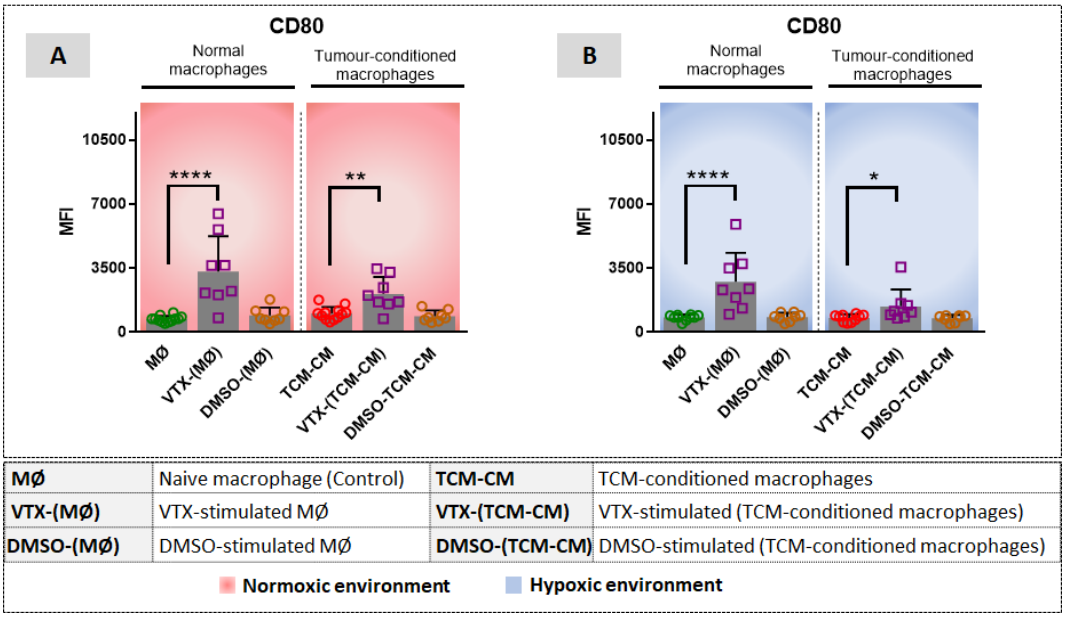

MØ	Naive macrophage (Control)	**TCM-CM**	TCM-conditioned macrophages
VTX-(MØ)	VTX-stimulated MØ	**VTX-(TCM-CM)**	VTX-stimulated (TCM-conditioned macrophages)
DMSO-(MØ)	DMSO-stimulated MØ	**DMSO-(TCM-CM)**	DMSO-stimulated (TCM-conditioned macrophages)

Normoxic environment **Hypoxic environment**

Figure 5. 8 The effect of VTX on macrophage CD80 expressions under normoxic and hypoxic conditions

Normal and tumour-conditioned macrophages were stimulated with VTX or DMSO (diluent control) at day 7 for 24hr under normoxic and hypoxic conditions and stained for CD80. Pooled data (A and B) are expressed as mean ± SEM. The p-values were determined using the Mann-Whitney test, * = $p < 0.05$, ** = $p < 0.005$, *** = $p < 0.0005$ **** = $p < 0.0001$, n = 12 replicates per normoxic MØ, n = 10 replicates per hypoxic MØ, n=8 replicates per normoxic and hypoxic VTX-(MØ) and VTX-(TCM-CM), DMSO-(MØ) and DMSO-(TCM-CM), conditions.

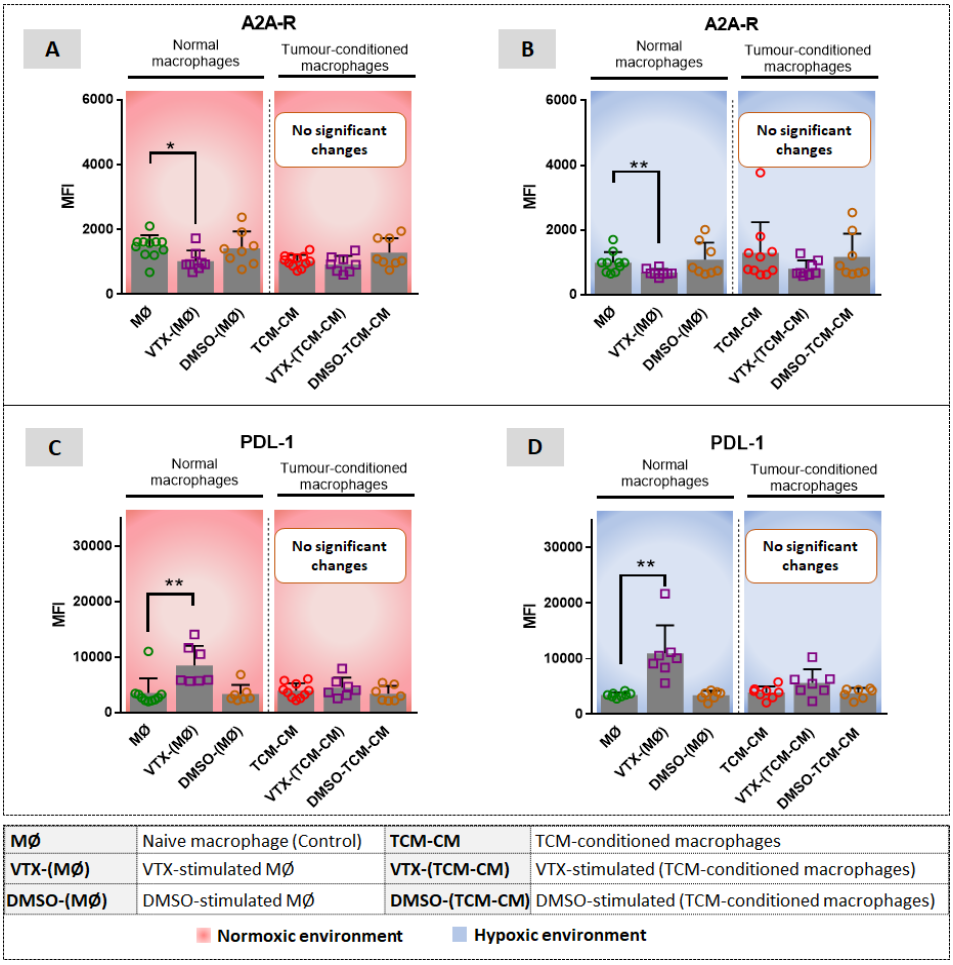

MØ	Naive macrophage (Control)	**TCM-CM**	TCM-conditioned macrophages
VTX-(MØ)	VTX-stimulated MØ	**VTX-(TCM-CM)**	VTX-stimulated (TCM-conditioned macrophages)
DMSO-(MØ)	DMSO-stimulated MØ	**DMSO-(TCM-CM)**	DMSO-stimulated (TCM-conditioned macrophages)

Normoxic environment **Hypoxic environment**

Figure 5. 9 The effect of VTX on macrophage A2A-R and PDL-1 expression under normoxic and hypoxic conditions

Normal and tumour-conditioned macrophages were stimulated with VTX or DMSO (diluent control) at day 7 for 24hr under normoxia and hypoxia and stained for A2A-R and PDL-1. Pooled data of A2A-R (A, B) and PDL-1 (C, D) are expressed as mean ± SEM. P-values were determined using the Mann-Whitney test, * = $p < 0.05$, ** = $p < 0.005$, *** = $p < 0.0005$ **** = $p < 0.0001$, n = 12 replicates per normoxic MØ, n = 10 replicates per hypoxic MØ, n=8 replicates per normoxic and hypoxic VTX-(MØ) and VTX-(TCM-CM), DMSO-(MØ) and DMSO-(TCM-CM) conditions.

5.2.4.4 Regardless of oxygenation levels mesothelioma-derived factors prevent VTX-2337 from downregulating A2A-R expression

Under normoxic (Figure 5.9.A; $p = 0.02$) and hypoxic conditions (Figure 5.9.B; $p = 0.0003$), A2A-R expression reduced on MØ macrophages after VTX-2337 stimulation relative to their unstimulated MØ controls, implying removal of a suppressive checkpoint that could enable macrophages to function as pro-inflammatory cells. However, regardless of oxygen levels, mesothelioma-prevented A2AR reduction, meaning tumour-exposed macrophages become resistant to VTX-2337-stimulation and maintain suppressive function (Figure 5.9.A, B).

5.2.4.5 Regardless of oxygenation levels mesothelioma-derived factors prevent VTX-2337 from upregulating PDL-1 expression

Expression of PDL-1 increased in normoxic MØ (Figure 5.9.C; $p = 0.002$) and hypoxic MØ (Figure 5.9.D; $p = 0.0003$) relative to their unstimulated MØ controls after stimulation with VTX-2337. No differences in PDL-1 expression were observed in all other conditions including exposure to mesothelioma-derived factors (Figure 5.9.C, D). These data imply that regardless of oxygen levels, TCM-exposed macrophages prevent VTX-2337 from upregulating PDL-1 expression.

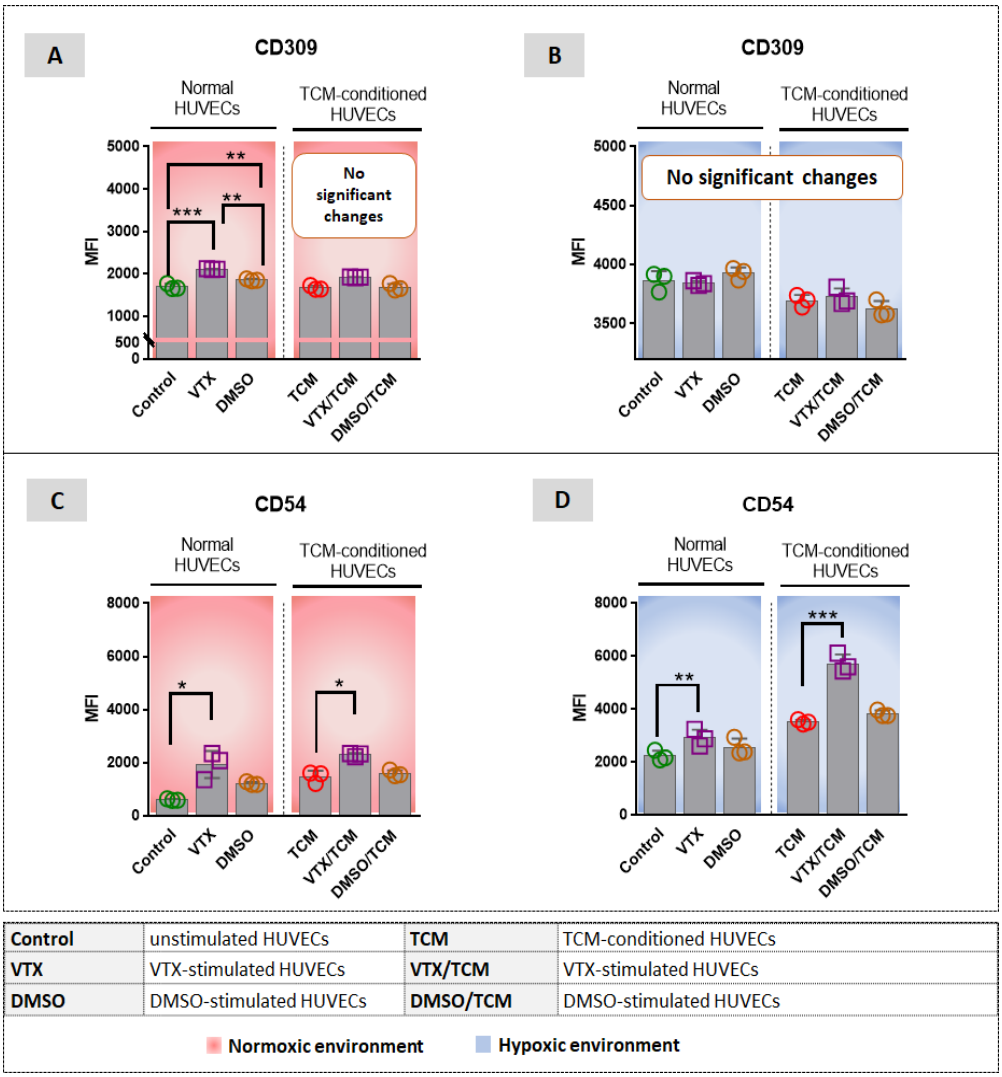

Control	unstimulated HUVECs	**TCM**	TCM-conditioned HUVECs
VTX	VTX-stimulated HUVECs	**VTX/TCM**	VTX-stimulated HUVECs
DMSO	DMSO-stimulated HUVECs	**DMSO/TCM**	DMSO-stimulated HUVECs

Figure 5. 10 The effect of VTX on CD309 and CD54 on HUVECs under normoxia and hypoxia

Passage 6 normal HUVECs and tumour-conditioned HUVECs were stimulated with VTX-2337 or DMSO (diluent control) for 24hrs, under normoxia and hypoxia and stained for CD309 and CD54. Pooled data of CD309 (A, B) and CD54 (C, D) are expressed as mean ± SEM. The p-values were determined using a two-way ANOVA test, * = $p < 0.05$, ** = $p < 0.005$, *** = $p < 0.0005$, **** = $p < 0.0001$, n = 3 replicates per condition.

5.2.4.6 Hypoxia and mesothelioma prevent VTX-2337 from upregulating CD309 on normoxic normal HUVECs

Under normoxic conditions, VTX-2337 increased CD309 expression in HUVECs relative to unstimulated controls (Figure 5.10.A; $p = 0.001$; $p = 0.0002$). VTX-2337 had no effect on mesothelioma-conditioned HUVECs and hypoxic HUVECs (Figure 5.10.A.B). The data suggest that VTX-2337 could promote VEGF-induced proliferation and possibly vessel permeability in normal, healthy endothelial cells. However, this response was negated by hypoxia and mesothelioma-derived factors, regardless of oxygen levels.

5.2.4.7 Hypoxia and mesothelioma do not affect the role of VTX-2337 in upregulating CD54 on HUVECS

CD54 expression increased following VTX-2337 stimulation in normoxic HUVECs (Figure 5.10.C; $p = 0.02$), normoxic mesothelioma-conditioned HUVECs (Figure 5.10.C; $p = 0.01$), hypoxic HUVECs (Figure 5.10.D; $p = 0.005$) and hypoxic mesothelioma-conditioned HUVECs (Figure 5.10.D; $p = 0.0006$) relative to their unstimulated controls. The data indicate that hypoxia and mesothelioma-derived factors generated under hypoxic conditions further increase CD54 in response to VTX-2337. These data imply that VTX-2337 may increase the potential of leukocyte extravasation to and from hypoxic mesothelioma tumours. This could be a promising therapeutic strategy for mesothelioma patients, if combined with other strategies that overcome local immune suppression.

5.2.5 Assessing the bioenergetic profiles of macrophages in response to IL-2/α-CD40 or VTx-2337 under normoxic and hypoxic conditions

Several studies have shown that macrophage polarisation also involves metabolic reprogramming (350, 351). Alterations in the metabolic profile of macrophages depend on the stimuli received by the microenvironment (351). The aim of this study was to assess the metabolic alterations in IL-2/α-CD40-activated macrophages.

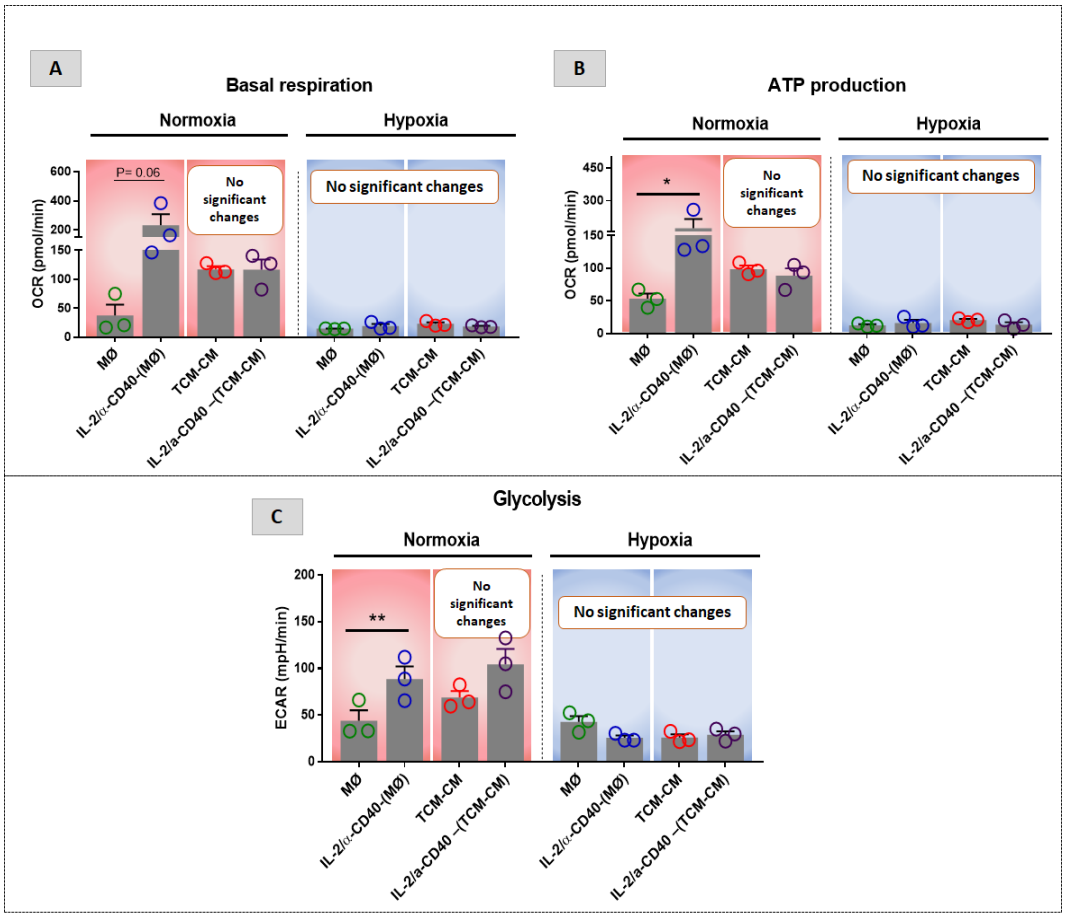

Figure 5. 11 The bioenergetic profile of macrophages is modulated in response to IL-2/α-CD40 under normoxic tumour conditions

Normal and tumour-conditioned macrophages differentiated from monocytes under normoxic and hypoxic conditions were stimulated with IL-2/α-CD40 and investigated for oxygen consumption rates (OCR) and extracellular acidification rates (ECAR) to quantify mitochondrial respiration and glycolysis. Pooled data for the basal respiration rate (A and D), ATP production rate (B) and glycolytic rate (C) are expressed as mean ± SEM. The p-values were determined using two-way ANOVA. * = $p < 0.05$, ** = $p < 0.005$, *** = $p < 0.0005$, **** = $p < 0.0001$.

5.2.5.1 Regardless of oxygen levels, mesothelioma prevents IL-2/α-CD40 from affecting macrophage bioenergetic profiles

Stimulating MØ macrophages with IL-2/α-CD40 showed a trend (that did not reach statistical significance) towards increased oxygen consumption rate (OCR) (Figure 5.11.A; $p = 0.06$) in association with a significant increase in ATP production (Figure 5.11.B; $p = 0.004$) and glycolysis (Figure 5.11.C; $p = 0.004$) under normoxic conditions. This response was completely ablated under hypoxic conditions (Figures 5.10.A, B and C).

Mesothelioma-exposed macrophages also significantly upregulated OCR and ATP production under normoxia relative to naïve macrophages (Figures 3.10.A, B and C). However, IL-2/α-CD40-stimulation did not significantly modulate these metabolic parameters. These data suggest that whilst mesothelioma-derived factors modulate macrophage metabolism, these cells lose their ability to alter their bioenergetic profile in response to IL-2/α-CD40. The data imply profound metabolic paralysis induction by mesothelioma. Hypoxic conditions completely disabled metabolic responses. These data clearly demonstrate that oxygenation is crucial for metabolic function in macrophages. The data also show that mesothelioma prevents metabolic changes in response to IL-2/α-CD40 stimulation. VTX-2337 did not affect on the bioenergetic profiles of macrophages (data not shown).

Stimulation by pro-inflammatory stimuli is known to switch macrophage metabolism towards glycolysis and away from oxidative phosphorylation (OXPHOS) (350). Therefore, these data imply that IL-2/α-CD40 is a pro-inflammatory signal in normal, naïve macrophages given the augmented glycolytic rate in association with a slight increase in mitochondrial oxygen consumption or OXPHOS. The data also imply that the likelihood of driving macrophages towards a pro-inflammatory state is diminished in mesothelioma. Moreover, the findings also indicate that a hypoxic environment induces profound metabolic dysfunction in macrophages.

5.3 Discussion

Patients with malignant mesothelioma have a median overall survival of seven to 27 months after diagnosis (23). To date, current treatment regimens aim to reduce patient symptoms, extend life expectancy and improve quality of life, however life extension tends to be only by a few months. Data from our lab has shown promising results when using IL-2/α-CD40 to treat mesothelioma-bearing mice, inducing curative regression of large tumours (348, 349). Furthermore, the TLR8 agonist, VTX-2337, has shown promise in Phase I clinical trials. However, there are no published in vitro studies investigating the effects of IL-2, α-CD40, IL-2/α-CD40 and VTX-2337 on mesothelioma-exposed macrophages and ECs under varying oxygenation conditions.

In this study, interest was directed towards evaluating the effect of these treatments in 2D monolayer cultures and a 3D cell culture system. 3D cell cultures are reported to show drug responses similar to those seen in humans (352, 353). However, because attempts to develop a 3D multicellular mesothelioma spheroid model had limited success, only the in vitro results between normoxic and hypoxic 2D cell culture monolayers are presented. It is hoped that the results aid translational studies in assessing treatment effects for humans with mesothelioma.

Table 5. 1 Summary of IL-2 effects on macrophages

	Normoxia		Hypoxia	
	MØ	TCM-CM	MØ	TCM-CM
CD206				
CD163				
HLA-DR	↓ **			
CD40				
CD80				
CD86	↓ ****		↓ **	
A2A-R				
PDL-1				

TCM	Tumour-conditioned media
MØ	Naive macrophage (Control)
TCM-CM	TCM-conditioned macrophages

Normoxic environment

Hypoxic environment

The data (summarised in Table 5.1) show that using IL-2 to treat macrophages as a monotherapy decreases HLA-DR expression in normal, naïve, unpolarised MØ macrophages under normoxia; this implies that antigen presentation to $CD4^+$ T-cells may be impaired. However, macrophages under hypoxia, as well as mesothelioma-conditioned macrophages regardless of oxygenation levels, which were treated with IL-2, did not reduce HLA-DR expression, suggesting that macrophages in mesothelioma tumours maintain their capacity to present antigen to $CD4^+$ T-cells in the presence of IL-2. However, as mentioned previously, this response could be driving regulatory $CD4^+$ T-cells and could why large tumours do not respond to intratumoural IL-2, as there latter are more regulatory T-cells (9).

The data also demonstrate that targeting naïve, unpolarised MØ macrophages under normoxia and hypoxia with IL-2 reduces CD86 expression. However, mesothelioma-conditioned macrophages did not respond to IL-2 in terms of CD86 expression. CD86 expression by macrophages mediates antitumor immunity if it binds to CD28 on $CD8^+$ T effector cells, or it induces immune tolerance if it binds to CTLA-4 in $CD8^+$ T effector cells, the latter could be more likely to occur in large tumours.

Table 5. 2 Summary of α-CD40 effects on macrophages

	Normoxia		Hypoxia	
	MØ	TCM-CM	MØ	TCM-CM
CD206	↓ *	↓ **		
CD163	↓ *			
HLA-DR	↓ *			
CD40				
CD80				
CD86	↓ ****	↓ *		
A2A-R				
PDL-1				

TCM	Tumour-conditioned media
MØ	Naive macrophage (Control)
TCM-CM	TCM-conditioned macrophages

Normoxic environment

Hypoxic environment

Administration of anti-CD40 antibody as a monotherapy led to downregulation of CD206, CD163, HLA-DR and CD86 on MØ macrophages under normoxic conditions (data summarised in Table 5.2). However, under normoxia, mesothelioma slightly modified these responses as only CD206 and CD86 were downregulated. In contrast, no changes to macrophageswere seen to the same molecules under hypoxic conditions. It is worth noting that high CD86 is considered a marker of the M1 phenotype (354), whilst the M2 phenotype is characterised by high CD163 and CD206 expression (353). The data imply that unpolarised MØ macrophages, activated with anti-CD40 under normoxia, share features of M1 and M2 macrophages through the reduction of CD206, CD163, HLA-DR and CD86. One possibility is that anti-CD40 only reduces M2 markers in early stage, smaller tumours in vivo, due to higher oxygenation levels and lower concentrations of suppressive factors secreted by mesothelioma tumour cells. Thus, the effect of anti-CD40 on macrophages is diminished when administered in hypoxic mesotheliomas. The results from Chapter 3 showed that hypoxia directly and/or indirectly affects macrophages though hypoxic-induced, mesothelioma-derived factors by decreasing CD40 expression. Overall, the data suggest that mesothelioma exerts a profound, negative effect on macrophage responses to CD40 signalling, particularly under hypoxic conditions.

Table 5. 3 Summary of IL-2/α-CD40 efects on macrophage bioenergy

	Normoxia		Hypoxia	
	MØ	TCM-CM	MØ	TCM-CM
Basal respiration	↑P= 0.06			
ATP production	↑ *			
Glycolysis	↑ **			

TCM	Tumour-conditioned media
MØ	Naive macrophage (Control)
TCM-CM	TCM-conditioned macrophages

Normoxic environment

Hypoxic environment

The combination of IL-2 and anti-CD40 (Table 5.3) showed a similar effect as that of IL-2 and anti-CD40 as single agents by downregulating macrophage expression of CD206, CD163, HLA-DR and CD86 under normoxia and hypoxia.

These data suggest that combining IL-2 and α-CD40 may induce polarisation away from an M2 phenotype via downregulation of CD163 and CD206. Furthermore, using IL-2/α-CD40 reduce the potential of CD86 binding CTLA-4, as well as the capacity of to present antigens to CD4+ T-cells because of decreased HLA-DR. As a result, this could lead to enhanced anti-tumour immunity via effector T-cells.

Interestingly, macrophage bioenergetics changed in response to the IL-2 and anti-CD40 combination, as an increase in OCR, ATP production and glycolysis was seen in MØ macrophages under normoxia. However, hypoxia and normoxic/hypoxic-induced mesothelioma-derived factors confounded these effects by ablating the ability of IL-2/anti-CD40 to upregulate glycolysis and mitochondrial respiration in macrophages. These data imply that the inability of normoxic/hypoxic, mesothelioma-conditioned macrophages to respond similarly to normal, naïve, unpolarised MØ macrophages stimulated with IL-2/anti-CD40 may be due to profound bioenergetic dysfunction.

Table 5. 4 Summary of VTX-2337 effects on macrophages

	Normoxia		Hypoxia	
	MØ	TCM-CM	MØ	TCM-CM
CD206				
CD163				
HLA-DR	↓ ***			
CD40	↑ P= 0.06		↑ *	
CD80	↑ ****	↑ **	↑ ****	↑ *
CD86	↓ ****			
A2A-R	↓ *		↓ **	
PDL-1	↑ **		↑ **	

TCM	Tumour-conditioned media	Normoxic environment
MØ	Naive macrophage (Control)	Hypoxic environment
TCM-CM	TCM-conditioned macrophages	

This study also examined macrophage responses to VTX-2337, a TLR 7/8 agonist (summarised in Table 5.4). Following exposure to VTX-2337 under normoxia and hypoxia, normal MØ macrophages increased expression of CD40, CD80 and PDL-1 and decreased HLA-DR, CD86 and A2A-R. However, regardless of oxygen levels, mesothelioma-exposed macrophages only increased CD80 expression relative to the MØ controls. These results imply that regardless of where macrophages are located in tumours, their response to VTX-2337 is likely to be limited to increased CD80. Nonetheless, this limited effect of VTX-2337 could mediate pro-inflammatory actions.

Neither normal HUVECs nor mesothelioma-conditioned HUVECs responded to IL-2, α-CD40, IL-2/α-CD40 or supernatants derived from IL-2-stimulated macrophages, α-CD40-stimulated macrophages, IL-2/α-CD40-stimulated macrophages or VTX-2337-stimulated macrophages under normoxia and hypoxia. These data suggest that there is limited crosstalk between macrophages and endothelial cells under these conditions.

Table 5. 5 Summary of VTX-2337 effects on HUVECs

	Normoxia		Hypoxia	
	HUVECs	TCM-HUVECs	HUVECs	TCM-HUVECs
CD309	↑ ***			
CD54	↑ *	↑ *	↑ **	↑ ***

TCM	Tumour-conditioned media		Normoxic environment
HUVECs	Normal HUVECs		Hypoxic environment
TCM-HUVECs	TCM-conditioned HUVECs		

However, although CD54 plays an important role in facilitating the invasion of tumour tissue by immune cells, endothelial CD54 has been shown to be involved in tumour–endothelial cell adhesion, which may promote progression and metastases in cancer (323-326). Laurent et al. showed that CD54 on endothelial cells is involved in adhesion of invasive bladder cancer cells to ECs (327). Additionally, blocking CD54 expression in lung (323) and brain (328) endothelia abrogates metastasis to these organs. The data imply that VTX-2337 may mediate anti-tumour immunity via increased leukocyte

extravasation into mesothelioma and/or may facilitate mesothelioma cell intravasation and metastasis originating from hypoxic tumours.

Conclusion

A previous study by our group showed that as murine mesothelioma progressed, the number of macrophages and regulatory T-cells increased. Moreover, using IL-2 or α-CD40 as monotherapies cured small mesothelioma, whereas a large mesothelioma tumour can be cured when IL-2/α-CD40 is used in combination. Macrophage responses to these immunotherapies and their role in this effect are not well understood. The present study demonstrates that signals from IL-2, α-CD40 or IL-2/α-CD40 reduces expression of CD206 and CD163, which is an indication of partial polarisation towards the M1 phenotype, although reduced HLA-DR and CD86 was also seen; this may imply a decrease in activation of regulatory T cells and enhanced CD8+ T-cell cytotoxic activity by avoiding CTLA-4 ligation.

CHAPTER 6

DEVELOPING 3D-MULTICELLULAR TUMOUR SPHEROIDS TO STUDY THE EFFECTS OF IL-2, ANTI-CD40 AND VTX-2337 IMMUNOTHERAPIES

6.1 Introduction

Translating findings from an animal model to successful clinical practice is often challenging. In fact, successful translation from animal models to human clinical trials of cancer is under 8% (355). Animal models are constrained in their capacity to imitate the intricate process of human carcinogenesis, physiology and development. Thus, the safety and viability of an immunotherapy identified in animal trials does not necessarily transfer to human trials (205). It is therefore imperative to develop improved in vitro models that better mimic the behaviours of human cells in vivo to help predict drug efficacy and toxicity (352, 356), although it must be acknowledged that in vivo testing remains the gold standard.

There has been increasing enthusiasm for utilizing 3D-spheroid models, or organoids, to test malignant growth and tissue biology in response to specific therapeutics to assist with their translation into clinical practice. Multicellular tumour spheroid (MCTS) models are gaining interest for assessing anti-tumour activity and drug efficacy in vitro due to their advantage of providing a more physiological context than standard 2D in vitro testing (352, 356-360). The 3D microenvironment can impersonate various cell heterogeneities of in vivo settings (205). MCTSs are capable, not only of reproducing the harsh conditions seen in poorly vascularised tumours, but also of assessing compound (drug) infiltration properties (210-212).

This study attempts to mimic key features of the tumour microenvironment, such as cell–cell interactions and metabolic gradients, by developing 3D tumour spheroid models that incorporate the three types of cells of interest in this project - mesothelioma cells, macrophages and endothelial cells - which may help validate the 2D in vitro findings. This study also aimed to examine the effect of IL-2, anti-CD40 antibody and

VTX-2337 immunotherapies on 3D tumour spheroids. Optimization of MCTSincluded determining the appropriate cell-seeding density, seeding time, media formulation, time needed to form spheroids and time for spheroid disaggregation.

6.2 Materials and Methods

Optimizing the spheroid models used the following cells and cell lines, media and plates:

6.2.1 Cells

- **AE17 cell line**: A murine mesothelioma cell line (C57BL/6J strain, female).
- **JU77 cell line**: A human malignant mesothelioma cell line.
- **THP-1 cell line**: A human monocytic cell line derived from an acute monocytic leukemia patient. (Note: THP-1 cells were differentiated into a macrophage-like phenotype using 20nM phorbol-12-myristate-13-acetate (PMA) for 8–12 hrs.)
- **PBMC-Mac**: Human peripheral blood mononuclear cell (PBMC)-derived macrophages.
- **HUVECs**: Human umbilical vein endothelial cells.

6.2.2 Media formulation

To maintain the growth of AE17, JU77, THP-1 cells and PBMCs-MACs, the following media was used:

- cRPMI media containing 10% FCS, 1% glutamax, 50 μM 2-mercaptoethanol (2-ME), 100 U/ml penicillin and 50 mg/ml streptomycin (Life Technologies, USA) (see page 29).

To culture HUVECs, the following media were used:

- **LVES-supplemented Medium 200:** Large Vessel Endothelial Supplement (LVES, contains fetal bovine serum, hydrocortisone, human epidermal growth factor, basic fibroblast growth factor, heparin and ascorbic acid) used in conjunction with Medium 200 (M200, a basal culture media containing

essential and non-essential amino acids, vitamins, other organic compounds, trace minerals and inorganic salts) to grow HUVECs. Both from Gibco, Invitrogen

- **Endothelial Basal Medium (EBM):** EBM is supplemented with ascorbic acid, hydrocortisone, bovine brain extract, foetal bovine serum, gentamicin/amphotericin-b and human epidermal growth factor (Lonza, Walkersville, MD USA).

6.2.3 Ultra-low attachment plates

- After several attempts to use in-house low attachment plates coated with agarose, the decision was made to use 96-well round-bottom ultra-low attachment plates that effectively inhibit cellular attachment (Corning Costar, Corning, NY, USA).

6.3 Generation and assessment of monocellular and multicellular spheroid models

6.3.1 Generating monocellular spheroids

6.3.1.1 Mesothelioma cells

Murine AE17 or human JU77 mesothelioma cells were maintained as a monolayer culture in cRPMI medium. In the ultra-low attachment plates, both cell lines formed a spheroid in 100% cRPMI medium; however, only AE17 proliferated, and JU77 did not develop over time, suggesting that both human and mice mesothelioma cell lines can form spheroids in ultra-low attachment plates. However, the JU77 cell line did form spheroids that did expand in a 50:50 mixture of (M200:cRPMI) or (EBM:cRPMI) (Figure 6.1).

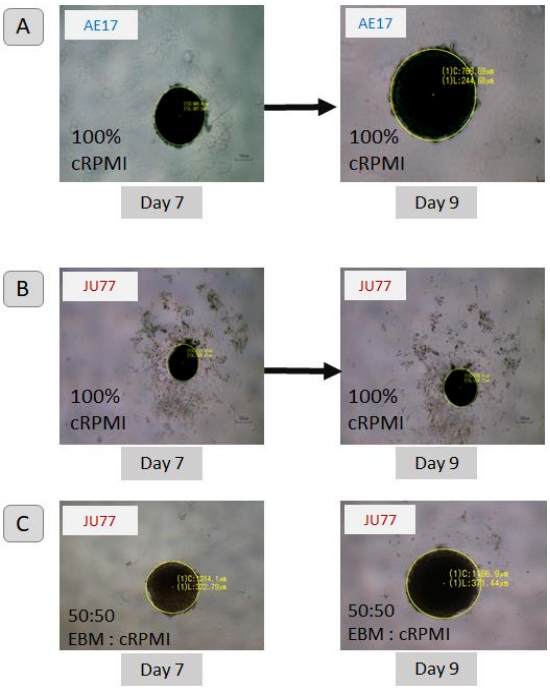

Figure 6. 1 Formation of monocellular spheroids

To generate monocellular spheroids from AE17 cells, 2 x10^4 cells/well were seeded in cRPMI (A); the medium was replaced at the beginning of day 3 to avoid aggregation disruption and then every two days. To generate monocellular spheroids from JU77, 2 x10^4 cells/well were seeded in cRPMI (B) or in 50:50 (EBM:cRPMI) (C); media was replaced at the beginning of day 3 and then every two days.

6.3.1.2 Macrophages

THP-1-derived macrophages or PBMC-derived macrophages grew in 100% cRPMI or a 50:50 mixture of (M200:cRPMI) or (EBM:cRPMI) but did not form spheroids in ultra-low attachment plates (Figure 6.2).

Figure 6. 2 Attempts to generate monocellular spheroids from macrophages

To generate monocellular spheroids from macrophages, 2 x 10^4 cells/well were seeded in a 50:50 mixture of (EBM:cRPMI). The medium was replaced at the beginning of day 3 to avoid aggregation disruption and then every 2 days.

6.3.1.3 HUVECs

Although HUVECs were maintained in M200 medium as a monolayer and showed a normal proliferative rate in ultra-low attachment plates, they did not form spheroids and did not proliferate in 100% M200 and in a 50:50 mixture of (M200:cRPMI). In contrast, HUVECs did form a spheroid in 100% EBM (Figure 6.3) and in a 50:50 mixture of (EBM:cRPMI), but did not proliferate (Figure 6.4). HUVEC viability in a 50:50 mixture of (EBM:cRPMI) was assessed at days 3 and 5 (Figure 6.3). The data showed low viability with detection of 42 viable cells and 348 dead cells on day 3 and 3 viable cells and 131 dead cells on day 5. These results suggest that a high number of seeded cell (5 x 10^3 cells/well) deteriorated (361).

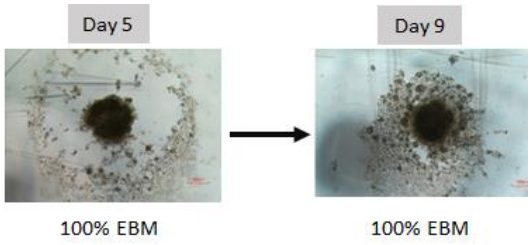

Figure 6. 3 Formation of monocellular spheroids from HUVECs

To generate monocellular spheroids from HUVECs, 2x10^4 cells/well were seeded in 100% EBM as shown above or (EBM:cRPMI). The medium was replaced at the beginning of day 3 to avoid aggregation disruption and then every 2 days.

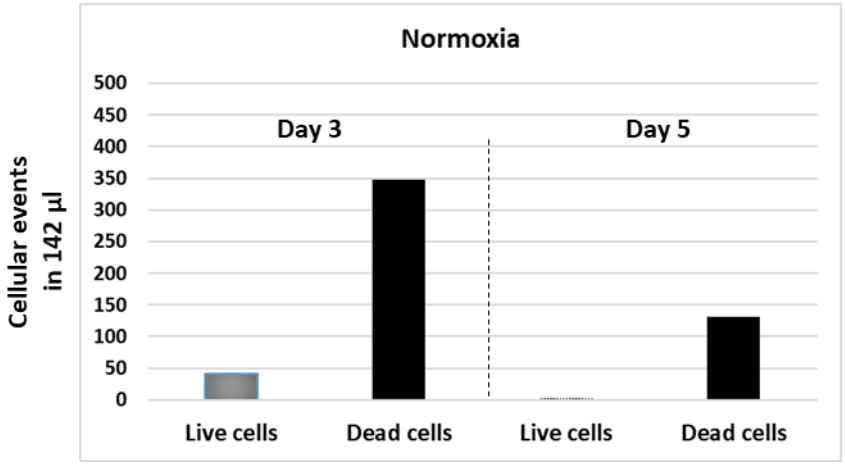

Figure 6. 4 Quantifying live and dead cells in HUVEC spheroids

HUVEC spheroids (5 x 10^3 cells/well) were generated under normoxic conditions. On days 3 and 5 of culture, the spheroids were isolated with a pipette, transferred to uncoated 96-well plates, washed with PBS twice, and then disaggregated with Type 4 collagenase/DNase. To minimize cell clumps, cell suspensions were filtered using a 40 µm cell strainer. The cells were stained with Zombie NIR and an attune flow cytometer used for analysis.

6.3.2 Generating multicellular spheroids

To generate multicellular mesothelioma tumour spheroids that could mimic the tumour microenvironment, cell-to-cell ratios were considered. The above experiments suggested that using 2 x 10^4JU77cells/well generated a useful spheroid that could expand without significant cell death, and therefore provide useful growth data in response to immunotherapeutic intervention. Previous data from our lab has shown that 50% of the cellular makeup of murine AE17 mesothelioma tumours consists of macrophages (362), similar data has been reported for human mesothelioma (363). Therefore 2 x 10^4JU77cells/well plus 2 x10^4macrophages cells/well (representing a 50:50 ratio) were used as a starting point to develop the spheroids. Determining a useful ratio, and therefore cell number, for HUVECs to incorporate into spheroids was more problematic and it was assumed that starting with a lower number would be appropriate,

therefore 5 x10^3HUVECs /well were used. The intention was to identify cell ratio/cell seeding numbers that might support HUVEC viability and generate a useful mesothelioma MCTS model. It was expected that several different seeding densities were going to be tested.

6.3.2.1 Examples of the generation of multi-cellular spheroids under normoxic conditions

Co-culturing JU77 cells, HUVECs and THP-1-derived macrophages or PBMC-derived macrophages on day 0 generated dispersed small spheroids. This was resolved by centrifuging the plate to aggregate the dispersed spheroids to form one spheroid. As shown in Figure 6.5, spheroids were more easily generated by seeding only JU77 tumour cells (2x10^4 cells/well) on day 0, adding macrophages (2x10^4 cells/well) on day 3 and HUVECs (5x10^3 cells/well) on day 5, or alternatively by centrifuging the ultra-low attachment plates instantly after seeding all cells (4.5x10^4 cells/well) together on day 0 in a 50:50 mixture of (EBM:cRPMI) under normoxic (20% O_2, 5% CO_2, 37^{o}C) conditions (Figure 6.6). However, a majorissue that was not resolved was that the HUVECs did not expand as hoped as the results revealed the seeded cells (5 x 10^3 cells/well) deteriorated. Measuring cell yields and viabilityof multicellular spheroids incorporating JU77 cells, THP-1-derived macrophages and HUVECs on Day 3, when intact spheroids had formed, showed the highest yield consisted of JU77 cells with very low yields for HUVECs (Figure 6.7).

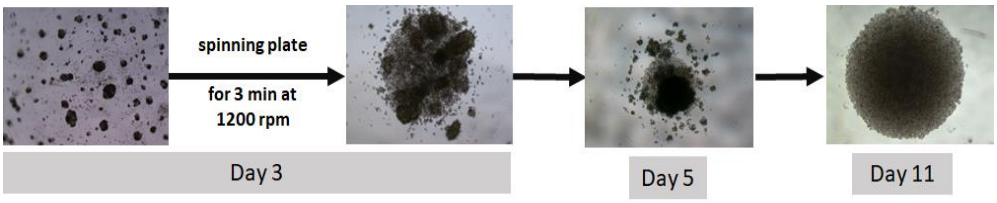

Figure 6. 5 Formation of mesothelioma-based multicellular spheroids from JU77 cells, PBMC-derived macrophages and HUVECs

JU77 (2x10^4 cells/well), macrophages (2x10^4 cells/well)and HUVECs (5x10^3 cells/well) were seeded on day 0. At day 3, the cells formed small spheroids. After changing the medium, the plate was centrifuged at 1200 rpm for 3 minutes to promote spheroid aggregation. On day 11, the cells formed an intact spheroid.

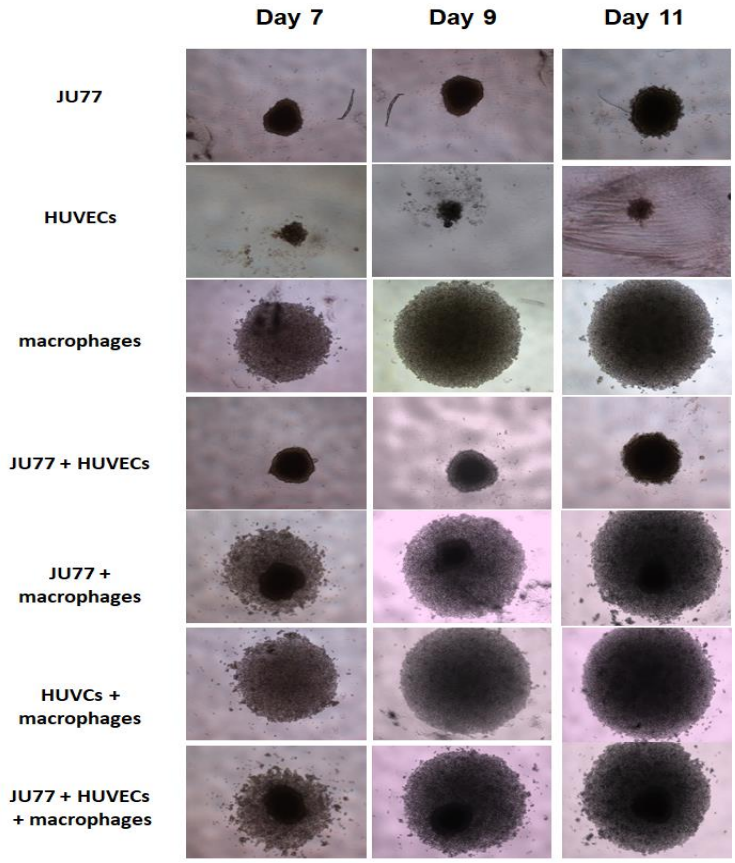

Figure 6. 6 Generating multi-cellular spheroids under normoxic conditions

JU77 (2 x10^4 cells/well), THP-1 macrophages (2 x 10^4 cells/well) and HUVECs (5 x10^3 cells/well) were seeded on day 0 in a 50:50 mixture of (EBM:cRPMI) in 96-well round-bottom ultra-low attachment plates and incubated at 20% O_2, 5% CO_2, 37^{o}C. The medium was replaced at the beginning of day 3 and every 2 days thereafter. Under normoxic conditions, JU77 cells only formed spheroids which then expanded suggesting proliferation; HUVECs only appeared to form spheroids but did not expand; macrophages expanded likely due to rapid proliferation but they had aggregated in the middle of the well without adhesion (confirmed by gentle pipetting). Strong adhesive interactions and spheroid development was seen in co-cultures of JU77 cells with HUVECs or macrophages; co-cultures of HUVECs with macrophages; or co-cultures of JU77 with HUVECs and macrophages.

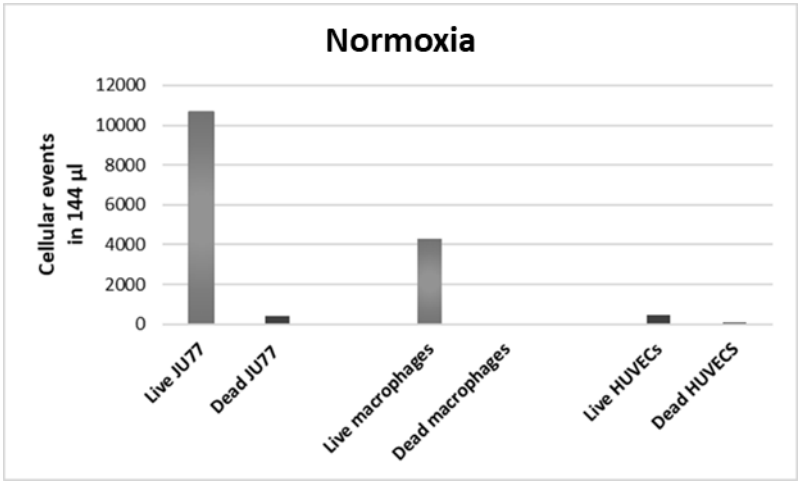

Figure 6. 7 Quantifying live and dead cells in multicellular spheroids using JU77 cells, THP-1-derived macrophages and HUVECs

MCTS cultures from JU77 mesothelioma cells, HUVECs and macrophages were generated under normoxic conditions using a single spheroid/well. At day 5 the spheroids were isolated with a pipette, transferred to uncoated 96-well plates, washed with PBS twice and then disaggregated with Type 4 collagenase/DNase. To minimize cell clumps, cell suspensions were filtered using a 40 µm cell strainer. The cells were stained with Zombie NIR and an attune flow cytometer used for analysis.

6.3.2.2 Examples of the generation of multi-cellular spheroids under hypoxic condition

JU77 ($2x10^4$ cells/well), THP-1 macrophages ($2 x10^4$ cells/well) and HUVECs ($5 x10^3$ cells/well) were seeded on day 0 in a 50:50 mixture of (EBM:cRPMI) in 96-well round-bottom ultra-low attachment plates. The plate was centrifuged at 1200 rpm for 3 minutes to accelerate cell aggregation and incubated under hypoxic conditions (2% O_2, 5% CO_2, 37^{o}C) (Figure 6.8).

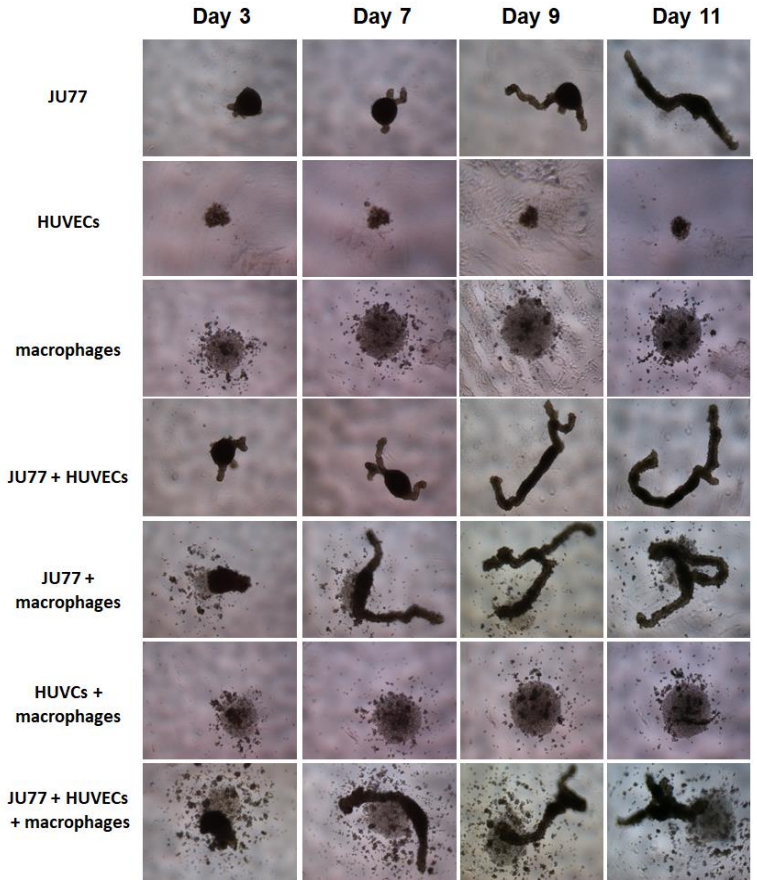

Figure 6. 8 Generating multi-cellular spheroids under hypoxic conditions

JU77 (2 x10^4 cells/well), THP-1 macrophages (2 x10^4 cells/well) and HUVECs (5 x10^4 cells/well) were seeded on day 0 in a 50:50 mixture of (EBM:cRPMI) in 96-well round-bottom ultra-low attachment plates and incubated at 2% O_2, 5% CO_2, 37^{o}C. The medium was replaced on day 3 and every 2 days thereafter. Under hypoxia, the JU77 only spheroid showed irregular longitudinal growth. HUVECs formed intact spheroids but did not expand. The macrophage only spheroid expanded at a slower rate relative to the normoxic model and again aggregated in the middle of the well without adhering to each other. Co-culture of JU77 cells with HUVECs or macrophages; HUVECs with macrophages; and JU77 cells with HUVECs and macrophages showed some level of adherence tested by gentle pipetting, but spheroids did not develop.

6.4 Disaggregating the spheroid

Different attempts were made to disaggregate the spheroids into single-cell populations aiming to assess the impact of the disaggregation process on cell yield and viability data. Trypsin, trypsin-EDTA (0.25%), PBS and type 4 collagenase (1 mg/mL; Sigma-Aldrich, Missouri, USA) and bovine pancreatic DNase (0.1 mg/mL, Sigma-Aldrich) were tested. Trypsin, trypsin-EDTA (0.25%) and PBS were tested under normoxic and hypoxic conditions, while type 4 collagenase/DNase was tested only under normoxia.

6.4.1 Assessing trypsin, trypsin-EDTA (0.25%) and PBS under normoxic conditions

Under normoxia, the number of single cells recovered after disaggregation using trypsin, trypsin-EDTA (0.25%) and PBS were similar, although trypsin-EDTA (0.25%) may be slightly better (Figure 6.9).

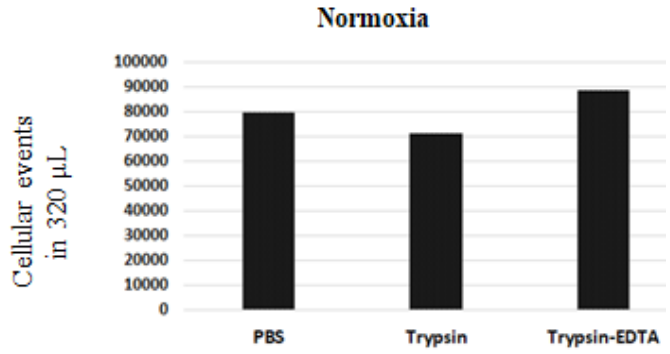

Figure 6. 9 Comparing cell yields of three disaggregation methods for the MCTS cultured under normoxic conditions

MCTS cultures from JU77 mesothelioma cells, HUVECs and macrophages were generated under normoxic conditions with a single spheroid per well (Figure 6.5). The spheroid was isolated with a pipette, transferred to an uncoated 96-well plate, washed twice with PBS and then disaggregated with PBS, trypsin or trypsin-EDTA (0.25%). The disaggregation process took 4 to 5 minutes using trypsin or trypsin-EDTA (0.25%). The process using PBS took 8 to10 minutes. To minimize cell

clumps, cell suspensions were filtered using a 40 µm cell strainer. An attune flow cytometer was used for cell counting.

6.4.2 Assessing trypsin, trypsin-EDTA (0.25%) and PBS under hypoxic conditions

Under hypoxia, trypsin proved to be superior over trypsin-EDTA (0.25%) and PBS (Figure 6.10), although the number of single-cell events was low compared to normoxic conditions for two reasons. First, the expansion/proliferation rate under hypoxia was lower than under nomoxia thus, the number of cells was low. Second, unlike normoxic conditions, cells remained firmly attached and trypsin, trypsin-EDTA (0.25%) and PBS could not fully dissociate them, even after using manual pipetting.

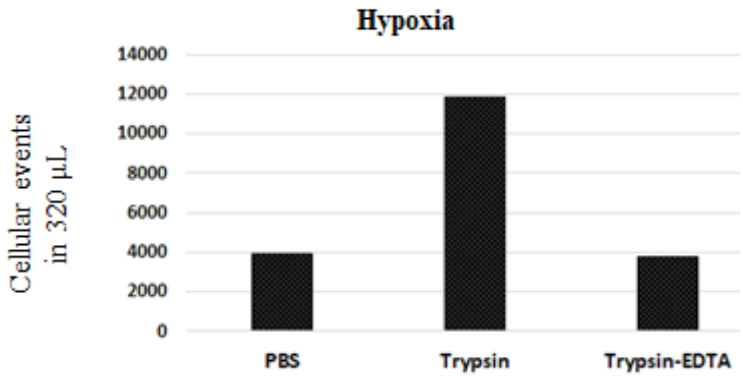

Figure 6. 10 Comparing cell yields from three disaggregation methods for MCTS cultured under hypoxic conditions

Aggregated and adhered multicellular (non-spheroid) cultures from JU77 mesothelioma, HUVECs and macrophages were generated under hypoxic conditions (Figure 6.6). Adherent (non-spheroid) cells were isolated with a pipette and transferred to uncoated 96-well plates. Cells were washed with PBS twice, and spheroids disaggregated with PBS, trypsin or trypsin-EDTA (0.25%). The disaggregation process was stopped after 9 minutes, with the cells still firmly attached (more than in normoxic spheroids) and barely disaggregated. To minimize

cell clumps, cell suspensions were filtered using a 40 µm cell strainer. An attune flow cytometer was used to determine cell yields.

6.4.3 Does longer incubation with trypsin, trypsin-EDTA (0.25%) and PBS affect HUVECs?

The time taken (4 to 5 minutes) to disaggregate MCTS using trypsin, trypsin-EDTA (0.25%) and PBS (8 to 10 minutes) was longer than the time taken to detach JU77, macrophages and HUVECs (2 minutes for trypsin or trypsin-EDTA (0.25%) and 6 minutes for PBS) from the T25 flask or 6-well plates when grown as a monolayer.

However, incubating HUVECs with trypsin for 5 minutes, with trypsin-EDTA (0.25%) for 5 minutes and with PBS for 10 minutes as a monolayer indicated normal viability and proliferation. Thus, prolonged incubation of MCTS with trypsin or trypsin/EDTA does not damage HUVECs.

6.4.4 Assessing Type 4 collagenase/DNase under normoxic conditions

Type 4 collagenase/DNase was used to disaggregate the MCTS spheroids consisting of JU77 mesothelioma cells, HUVECs and macrophages; disaggregation was rapid and occurred in less than 3 minutes. The PBS controls were stopped in parallel with Type 4 collagenase/DNase (i.e. after 2 minutes) and cell suspensions were filtered using a 40 µm cell strainer. The Type 4 collagenase/DNase gave a much higher yield of cells than the PBS controls and the trypsin or trypsin/EDTA tested above and shown in Figure 6.11.

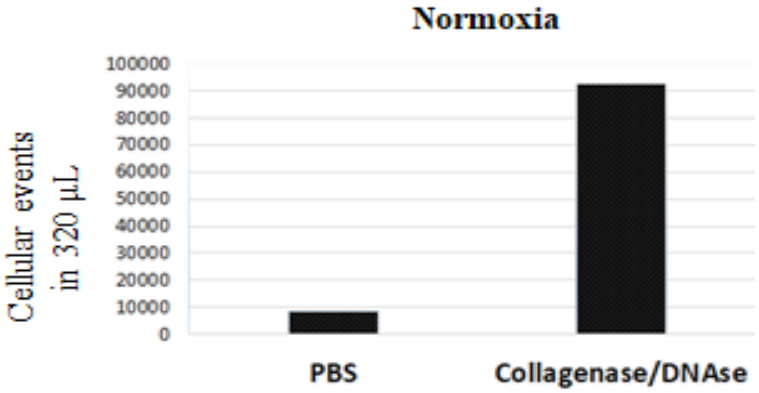

Figure 6. 11 Comparing cell yields from Type 4 collagenase/DNase to PBS disaggregated spheroids s

MCTS cultures consisting of JU77 mesothelioma cells, HUVECs and macrophages were generated under normoxic conditions using a single spheroid per well. The spheroids were isolated with a pipette, transferred to uncoated 96-well plates, washed with PBS twice and then disaggregated with Type 4 collagenase/DNase or PBS. The disaggregation process using Type 4 collagenase/DNase took 2 to 3 minutes. To minimize cell clumps, cell suspensions were filtered using a 40 µm cell strainer. An attune flow cytometer was used for cell counting.

6.5 Conclusion

This chapter describes attempts to develop multicellular spheroid models from human JU77 mesothelioma cells, macrophages and endothelial cells (HUVECs), as well as testing monocellular spheroids using murine AE17 mesothelioma cells. Optimisation attempts included choosing an appropriate round bottom ultra-low attachment surface plate to keep cells in suspension and help cell aggregation, testing different media, different seeding densities and disaggregation processes. Human JU77 mesothelioma cells formed spheroids when incubated in cRPMI but failed to expand/proliferate. In contrast, murine AE17 mesothelioma cells formed spheroids and rapidly expand likely due to rapid proliferation. Further testing showed that culturing JU77 cells in a 50:50 mixture of (M200:cRPMI) induced spheroid formation but they

did not expand, yet JU77 cells formed spheroids and grew in EBM:cRPMI. It is possible that other media options and/or combinations may have improved spheroid development. Under hypoxia, the JU77 only spheroid showed irregular longitudinal growth. There are no published data explaining why JU77 mesothelioma cells grow differently under hypoxic conditions however, the longitudinal shape that mesothelioma tumours adopted under 2% O_2 may be an adaptive response to their environment that allows cells maximal access to the O_2 that is available. This may explain why at the early stages from days 0 to 3, a smallspheroid is formed which then elongates.

As expected, HUVECs showed a high rate of viability and proliferation when cultured in a M200 medium supplemented with LVES on a flat surface as a monolayer, however growing HUVECs in the same medium on an ultra-low attachment surface demonstrated a significant reduction in cell yield and loss of viability. Using EBM media induced HUVECs to form monocellular spheroids (i.e. HUVECs only) as well as multicellular spheroids with JU77 cells, or macrophages, or JU77 and macrophages. However, under all conditions, although they appeared to integrate into spheroids, HUVECs failed to expand indicating a failure to proliferate and likely cell death.

Different cell densities and seeding times were also tested and failed to improve HUVEC proliferation. Moreover, different methods to dissociate spheroids, including trypsin, trypsin-EDTA (0.25%), PBS and type 4 collagenase /DNase were tested and the data showed none of these approaches negatively affected HUVECs. Nonetheless, collagenase was quicker and produced greater single cell yields.Unfortunately, attempts to further develop/optimise MCTS from JU77 mesothelioma cells, macrophages and HUVECs had to stop due to time and budget constraints. As a result comparing in vitro normoxic and hypoxic 2D tumour models continued as an important part of the study.

CHAPTER 7

CHARACTERIZING THE IN VIVO POTENTIAL OF MESOTHELIOMA-EXPOSED MACROPHAGES AND ENDOTHELIAL CELLS TO RESPOND TO HYPOXIA USING HYPOXIA-RESPONSE ELEMENT (HRE) PREDICTION

7.1 Introduction

Significant regions of hypoxia are found in the human mesothelioma microenvironment (364) which can lead to more aggressive disease (365). As macrophages and endothelial cells (ECs) are components of the tumour microenvironment and the overall aim of this PhD was to better understand the potential cross talk between mesothelioma cells, macrophages and ECs. The *in vitro*data from the previous chapters showed differential molecular responses by mesothelioma-exposed macrophages and ECs under normoxic versus hypoxic conditions. Table 7.1 summarises the effect of normoxia and hypoxia on molecules expressed by mesothelioma-exposed macrophages.

Table 7. 1 Summary of the effect of normoxic and hypoxic conditions on TCM-exposed macrophage expression of the molecules below, relative to normoxic non-TCM exposed macrophage controls

	Normoxia TCM	Hypoxia TCM
HLA-DR	↓***	↓****
CD40	--	↓**
CD80	↑*	--
CD86	↓***	↓****
CD39		↓****
A2A-R	↓***	↓*
PDL-1	↑*	↑*
Gal-9	--	--
CD206	--	--
CD163	--	--

The results of these *in vitro* studies warrant *in vivo* investigations however, performing *in vivo* studies was not possible, as the PhD candidate returned to their home country.

Therefore, an alternative strategy to investigate an *in vivo* association between the target genes (i.e. the molecules in Table 7.1) and mesothelioma was employed using public databases such as FireBrowse (http://firebrowse.org/). The first approach involved confirming expression of genes coding for the molecules of interest (HLA-DR, CD206, CD309, CD54, CD40, CD144, A2A-R, CD105, CD163, CD80, Gal-9, CD39, CD86, PDL-1, and CD146) in human mesothelioma (MESO) and comparing their expression levels to different cancer types including: breast invasive carcinoma (BRCA); colon adenocarcinoma (COAD); colorectal adenocarcinoma (COADREAD); lung adenocarcinoma (LUAD); and lung squamous cell carcinoma (LUSC) using FireBrowse. This approach validates expression of the target genes in vivo in human mesothelioma.

Cells can respond to and tolerate hypoxia through transcriptional regulation of gene expressionvia hypoxia response elements (HREs) located within the promoter/enhancer region of specific genes. Therefore, the second aim of this study was to use an *in silico* approach to determine whether HREs or other hypoxia-related transcription factor binding sites (TFBSs) are present in the promoter regions of the four molecules found to be upregulated under hypoxic conditions in macrophages (PD-L1) and HUVECS (CD309, CD54, CD105) (Table 7.2).

This study also investigated the interplay between TLR-7/8, IL-2R and CD40 signalling (via VTX-2337, IL-2 and anti-CD40 antibody respectively) and hypoxia, for the target genes. This is because the data in chapter 5 showed that when macrophages were stimulated with IL-2 combined with anti-CD40 antibody under hypoxia, PD-L1 was further upregulated relative to untreated hypoxic macrophage controls. Similarly, when ECs were stimulated with VTX-2337 CD54 was further upregulated relative to hypoxic EC controls. Therefore, signalling pathways for TLR-7/8 activation via VTX2337, as well as for IL-2/IL-2R, CD40 activation, were explored to understand potential mechanisms of action for activating hypoxia related transcription factors (TFs) relating to these specific signalling pathways.

Gene promoter regions were identified using bioinformatic tools and databases. HREs and other TFBSs related to hypoxia in the promoter region were examined by

employing PROMO (Version 3.0.2) software (366). An absence of HREs in a promoter region prompted an investigation of binding sites of TFs related to hypoxia such as: Hypoxia inducible factors (HIF) nuclear factor-kappaB (NF-kB), cAMP response element-binding protein (CREB), Myc, nuclear factor erythroid 2–related factor 2 (Nrf2) and signal transducer and activator of transcription (STATs). The data generated could show if there is a direct relationship between the molecules of interest and hypoxia, thereby providing a potential mechanistic explanation of the results seen in the preceding chapters.

Table 7. 2 Level of changes in upregulated molecules expressed by macrophages and endothelial cell under hypoxia relative to normoxia

Cell	Molecule	Responses to Hypoxia
ECs	CD309	↑↑↑↑
	CD54	↑↑↑↑
	CD105	↑
Macrophages	PDL-1	↑↑

7.2 Hypoxia Responsible Elements (HREs)

Hypoxia inducible factors (HIF) are a family of TFs regulating expression of genes that play a role in hypoxia tolerance. HIF is a heterodimeric transcription factor consisting of two major subunits, HIF-α (with three isoforms HIF-1α, HIF-2α and HIF-3α) and HIF-β, also known as Aryl Hydrocarbon Receptor Nuclear Translocator (ARNT; 1β, 2β and 3β) (367). Under normoxia, the α subunit is inactive and is present in the proteasome degradation pathway. Conversely, under hypoxia, the α-subunit is stabilised and accumulates in the cell, forming a dimer with the β-subunit when transferred to the nucleus (365, 368). The active complex of α-β subunit binds to the HRE motif in the target genes, as shown in Figure 1.

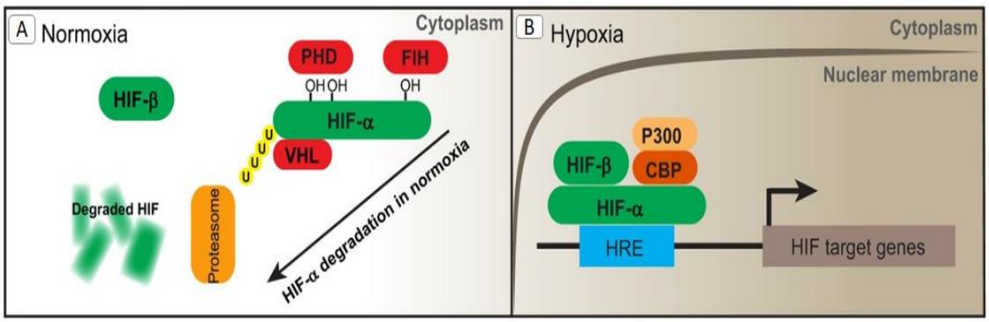

Figure 7. 1 Representation of HIF-signalling. Under normoxia, HIF-1α is hydroxylated by prolyl hydroxylase (PHD), ubiquitinated and degraded by the proteasome. Under hypoxia, HIF-1α binds with HIF-1β to form a heterodimer that locates to the nucleus and binds to HRE. Adapted from (365).

The process of converting DNA to RNA involves a specific DNA region, or promoter, that initiates the process of transcription. A promoter region is comprised of protein binding sites and transcription start sites (TSS) (364). Promoter regions in many genes possess TFBSs including HREs, which are recognized by HIF under hypoxic conditions and enhance expression of genes that prevent/minimize hypoxia effects. Studies reveal the importance of HIFs during hypoxia in regulating expression of genes involved in apoptosis, differentiation, glucose homeostasis, cell proliferation, vascular permeability, angiogenesis and inflammation (369-374). HREs are frequently present in the enhancer or promoter region and the 3' untranslated regions of a gene (375). Several hypoxia-inducible genes have been reported to contain an HRE motif (5'-RCGTG-3') in conjunction with a hypoxia ancillary sequence (HAS) motif. The latter is described as C and A conserved in the first and second places, G or C in the third place, any purine base in the fourth place and T or G or C in the fifth place (i.e. 5'-CA(G|C)(A|G)(T|G|C)-3') (376). Functionally active HREs typically contain a HAS motif within 7–15 nucleotides downstream of the HRE motif (376).

Eukaryotes hold the basal transcriptional machinery of genes in their upstream promoter regions. A promoter is typically characterized as having core, proximal and distal elements (376, 377). The core promoter is located immediately upstream from the TSS. Further upstream is the proximal promoter region containing CpG islands and several motifs that bind a specific transcription factor (TF) to regulate gene expression

(378, 379). The distal promoter region is several kilobases from the TSS and comprises regulatory elements such as enhancers (upregulation), silencers (downregulation) and insulators (protective regulation). These regions include protein binding sites or TF binding sites (TFB) for TFs (380). The HRE element, when preceded by a C on 5′, like 5′-CRCGTG-3′, forms enhancer box (E-box) binding sites, where TFs of the basic helix-loop-helix (bHLH) protein families bind (365, 376).

7.2.1 HRE identification protocol in promoter regions

The identification of promoters provides deep insight into genome organization. Promoters are usually identified through experimental techniques such as binding assays, ChiP-chip and ChiP-seq. Due to issues related to cost, time and labour in experimental methods, an alternative *in silico* approach can be adopted for the fast and reliable prediction of promoters in gene sequences. The core promoter region is usually 30–100 nucleotides in length, characterized by the presence of sequence motifs such as the TATA box and the Inr element, where the basal transcription machinery assembles. The proximal promoter regions are characterized by the presence of the GC box, the CAAT box and cis-regulatory modules (CRM) within 500 base pairs relative to the TSS. Distal promoter regions are characterized by the presence of enhancers, insulators and silencers, which can extend up to 10 kb from the TSS in upstream and downstream regions. The mammalian promoter region is marked by the presence of TF binding elements and CpG islands (369).

7.3 Transcription Factor Binding Sites

Certain TFs are activated under hypoxia to regulate hypoxic responses. The TFs activated under hypoxia are:

Nuclear factor kappa B: NF-κB is associated with inflammatory responses and is activated in macrophages during the early phase of hypoxia (381). NF-kB is reported to bind in the promoter region of HIF-1α in monocytes to induce its expression (382) and NF-kB and HIF-1α form a positive regulatory loop (383).

cAMP-response element binding protein: CREB was first identified to mediate gene expression downstream of cAMP signaling (384). Under prolonged hypoxia, CREB regulates the migration and invasion of cancer cells. Phosphorylation of CREB is induced by prolonged hypoxia to increase expression of genes involved in cell migration (385).

Nuclear factor erythroid 2-related factor 2: Nrf2 regulates expression of antioxidant genes. Hypoxic conditions also induce expression and activity of Nrf2 when reactive oxygen species are produced. Under hypoxia, HIF-1α stabilization and expression of its target genes are reduced in Nrf2-knockdown (KD) cells, which indicates the critical role of Nrf2 in regulation of HIF-1α expression (386). Nrf2 signalling plays an essential role in activation of the HIF-1 response. Studies have revealed that the knockdown of Nrf2 is required for a reduction in HIF-1α at the post-translational level (387).

Signal transducers and activators of transcription: TFs from the STAT family are activated by cytokine signaling (388). Under hypoxia, expression of STAT1, STAT3, and STAT5 is induced (389). Activation of STAT3 promotes cell survival and growth, while its inhibition leads to reductions in STAT3 and expression of target genes (390).

Myc: The Myc transcription factor was discovered based on the homology between an avian virus oncogene (Myelocytomatosis) and cellular Myc which was observed to be over-expressed in human cancers (391). Myc induces expression of genes related to the regulation of cell growth, differentiation, death, angiogenesis and metabolism. HIF-1α is a negative regulator of Myc. Under hypoxia, overexpression of Myc promotes the cell cycle. Simultaneously, it increases expression of the proapoptotic genes, Noxa and Puma, that lead to cell death (386). Myc overexpression also promotes tumor metastasis and invasion (392, 393).

7.4 Approach: Tools used to compare gene expression and identify promoter regions, HREs and HAS

To demonstrate expression of the target genes across selected cancer types, an online automated robust database, FireBrowse, was used for graphical representation of the data set. FireBrowse is a publicly available platform for exploring cancer data through

a Representational State Transfer (REST) Application Programmable Interface (API). The database consists of more than 80K sample aliquots from 11,000+ cancer patients, spanning 38 unique disease cohorts.

Target gene sequences were retrieved from the National Center for Biotechnology Information's (NCBI) gene database (www.ncbi.nlm.nih.gov/gene) that consolidates gene-related information from several authentic resources into discrete records. Various gene-specific data are connected, encompassing optimal information of sequence accessions, nomenclature, genomic location and organization, gene products and their attributes, gene expression, interactions with other genes, pathways involved, homology, variation and phenotypic consequences, publications and useful links to databases internal and external to NCBI (394). The gene sequences were further annotated based on information retrieved through the NCBI Reference Sequence (RefSeq) database. The gene sequences were submitted to the Eukaryotic Promoter Database (EPD), an annotated non-redundant collection of experimentally characterized eukaryotic RNA polymerase II**(**POL II) promoters, to obtain promoter region sequences based on the TSS for further evaluation (395).

Gene sequences with promoter sequences were further analyzed using the University of California at Santa Cruz (UCSC) Genome Browser (https://genome.ucsc.edu), a graphical viewer for exploring genome annotations primarily from human and mouse genomes. The Genome Browser includes regularly updated software, including new formats for chromosome interactions, a ChIP-Seq peak display for track hubs and improved support for HGVS. For annotation, gnomAD, TCGA expression, RefSeq Functional elements, GTEx eQTLs, CRISPR Guides and SNPpedia are also available for deep insight into a genome (394).

The predicted promoter sequences were analyzed for TFBSs using PROMO Version 3.0.2 software. PROMO is a virtual laboratory for the identification of putative TFBSs in DNA sequences from a species or groups of species of interest. PROMO constructs positional weight matrices from known TF binding sites in a species to search for matches in a DNA sequence (396). For each target gene, identified promoter sequences were loaded as the query sequence to search for potential binding sites. TFBS prediction

was carried out considering only human factors and only human sites. The methodology for identifying promoter regions and the presence of HREs in target gene sequences is shown in Figure 2.

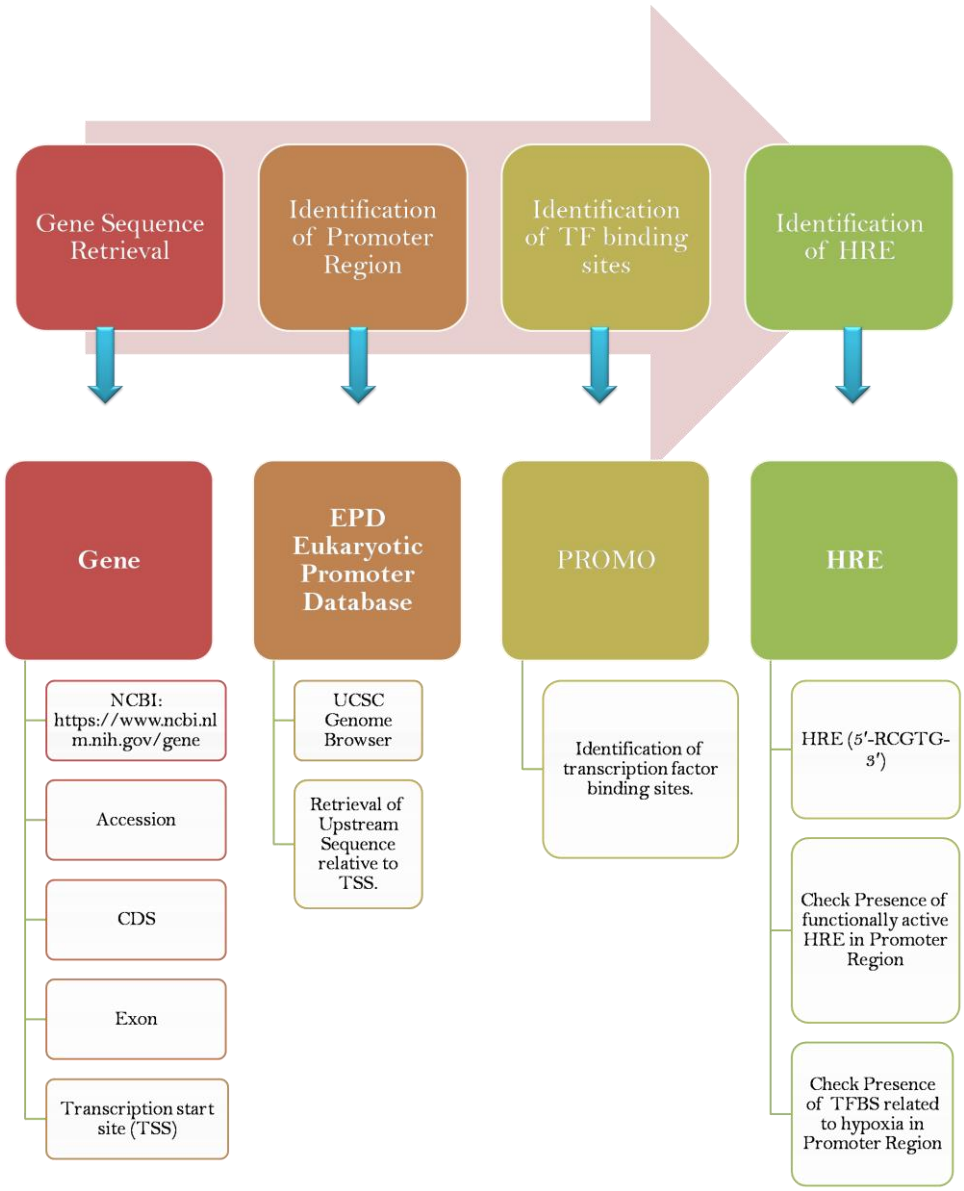

Figure 7. 2 Methodology adopted to identify promoter regions, TFBSs and HREs in promoter regions of the upregulated genes of interest

7.5 Results

7.5.1 Gene Expression Analysis

To better examine target gene expression status in various cancers (BRCA, COAD, COADREAD, LUAD, LUSC and MESO), the FireBrowse gene expression viewer was used to analyse expression data in the form of a boxplot graph, collected from various whole genome RNA-Seq studies. This approach detected expression of the target genes in the selected cancer types corresponding to tumour tissue, as shown in Figures 3-17. Therefore, the data show that human mesothelioma has the potential to express the molecules of interest at similar levels to the other cancers examined.

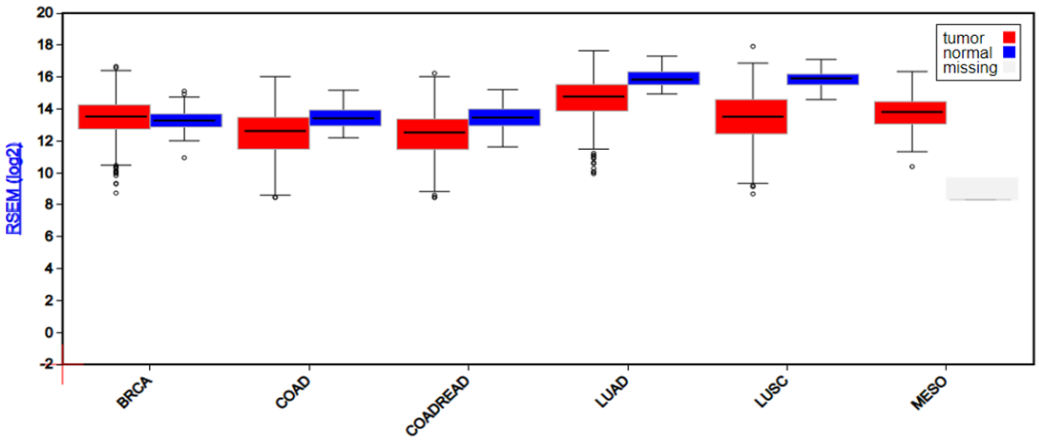

Figure 7. 3 HLA-DR gene expression status in BRCA, COAD, COADREAD, LUAD, LUSC and MESO

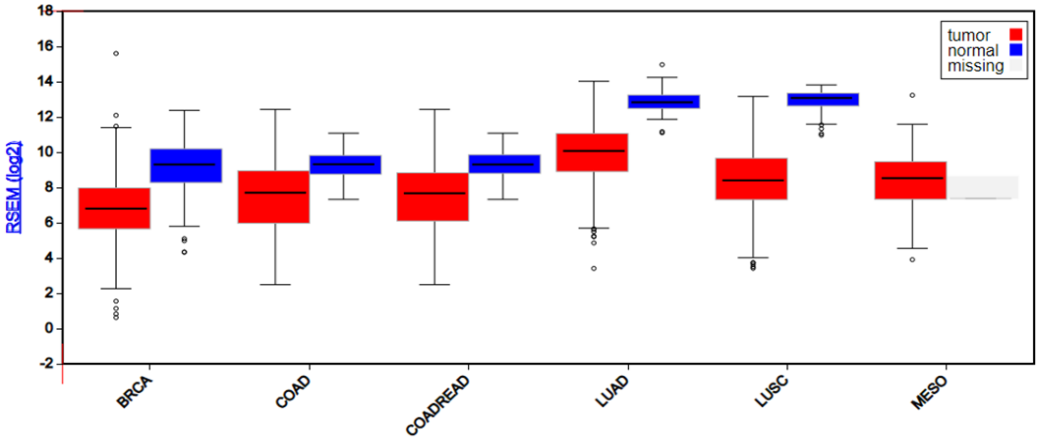

Figure 7. 4 CD206 gene expression status in BRCA, COAD, COADREAD, LUAD, LUSC and MESO

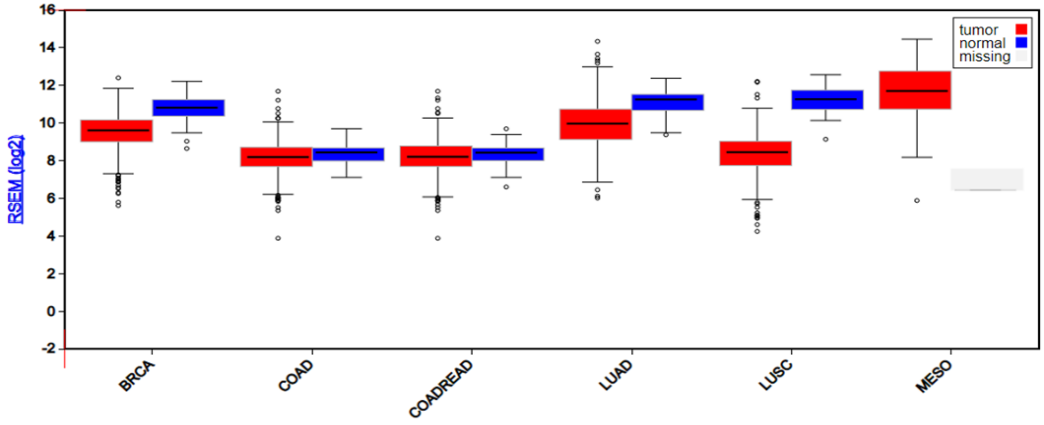

Figure 7. 5 CD309 gene expression status in BRCA, COAD, COADREAD, LUAD, LUSC and MESO

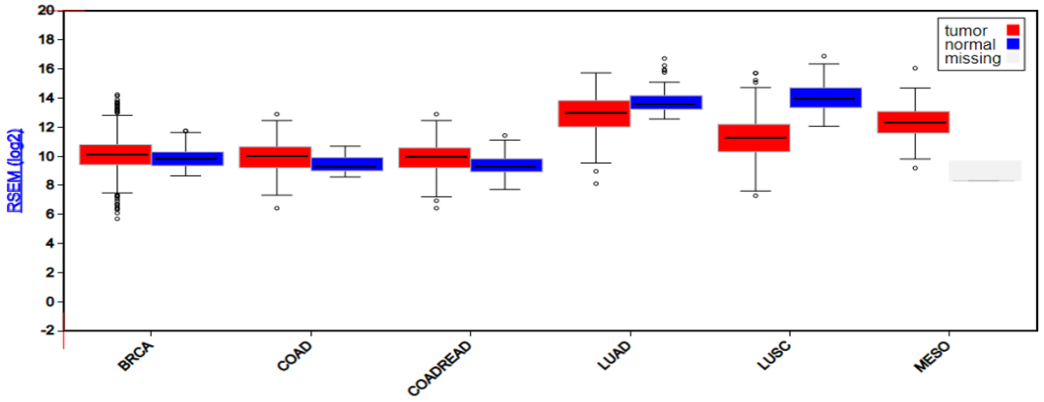

Figure 7. 6CD54 gene expression status in BRCA, COAD, COADREAD, LUAD, LUSC and MESO

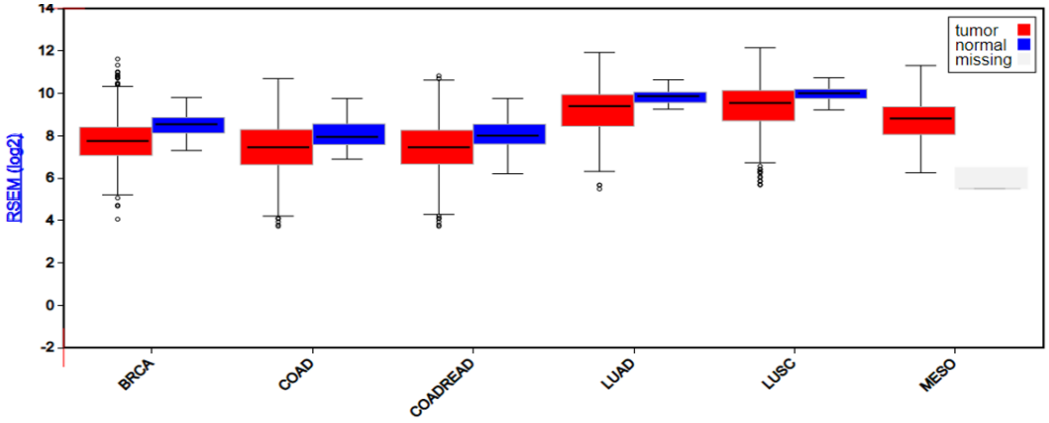

Figure 7. 7CD40 gene expression status in BRCA, COAD, COADREAD, LUAD, LUSC and MESO

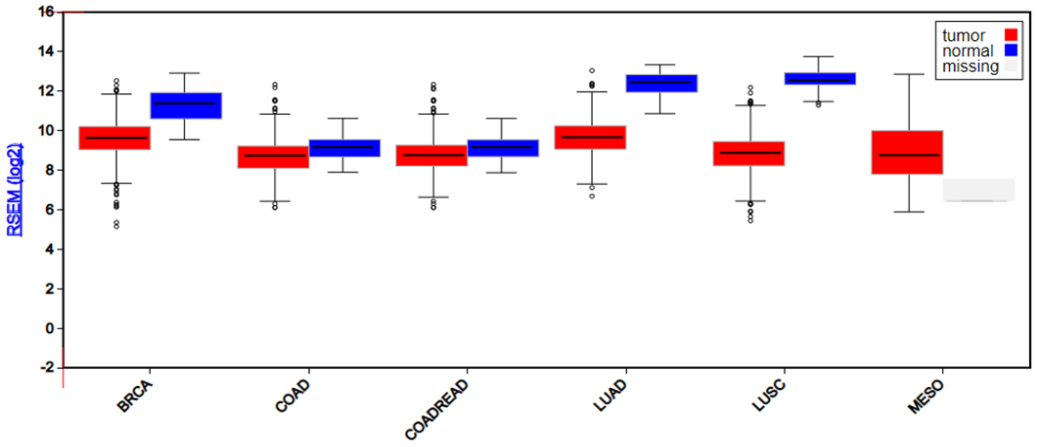

Figure 7. 8CD144 gene expression status in BRCA, COAD, COADREAD, LUAD, LUSC and MESO

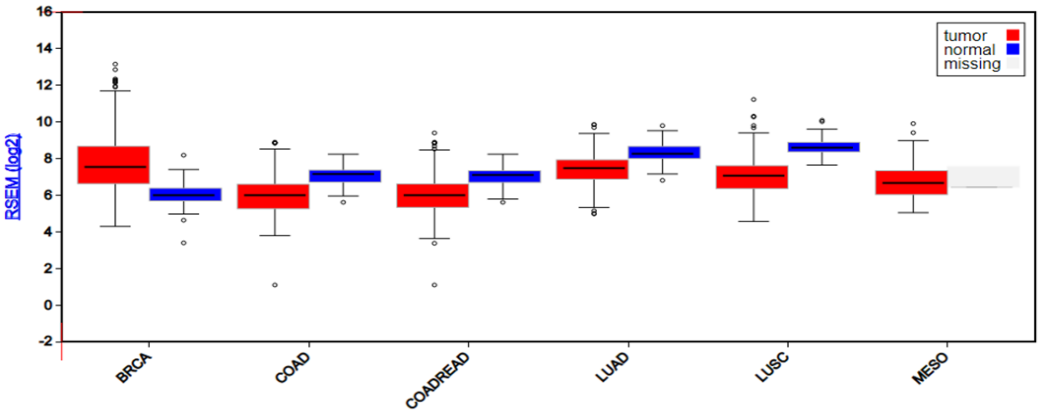

Figure 7. 9A2A-R gene expression status in BRCA, COAD, COADREAD, LUAD, LUSC and MESO

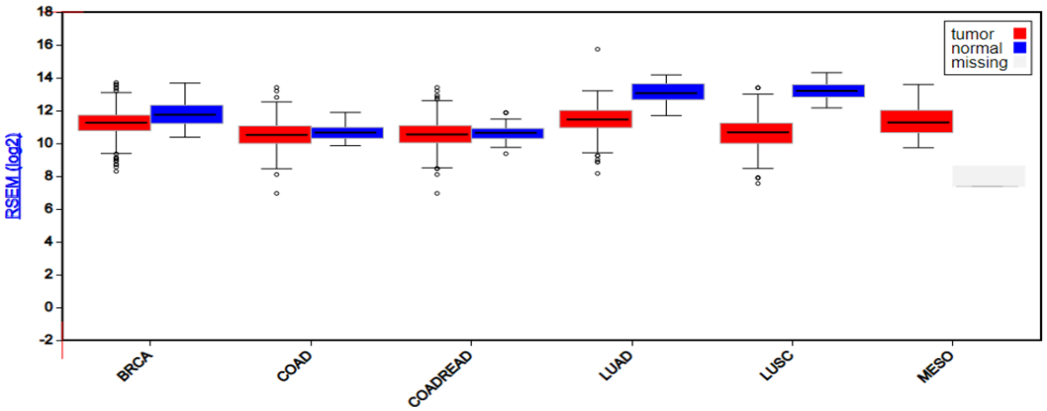

Figure 7. 10CD105 gene expression status in BRCA, COAD, COADREAD, LUAD, LUSC and MESO

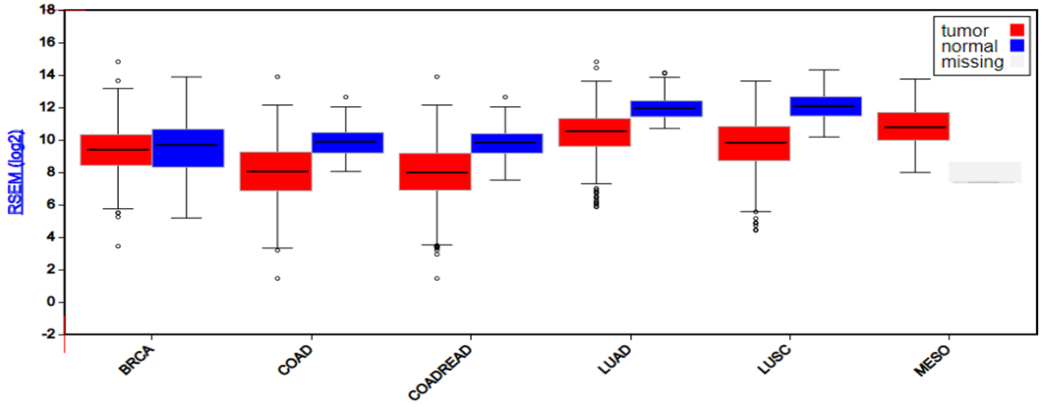

Figure 7. 11 CD163 gene expression status in BRCA, COAD, COADREAD, LUAD, LUSC and MESO

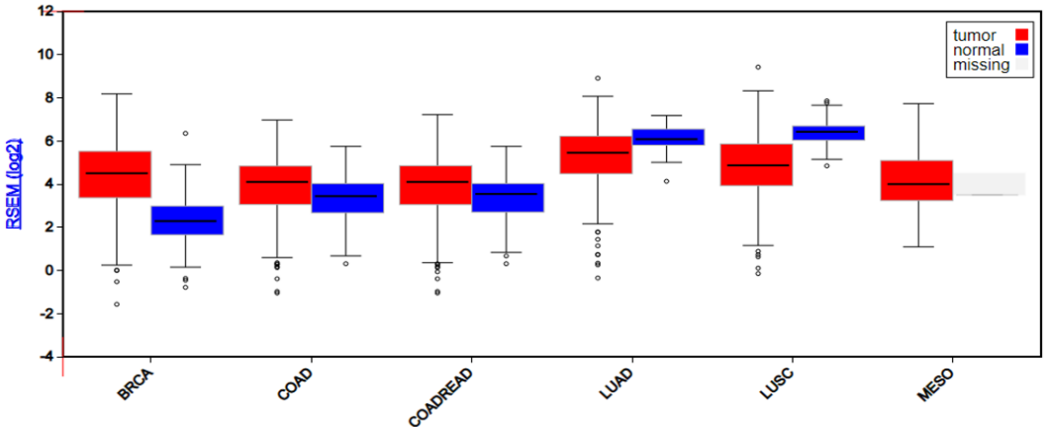

Figure 7. 12 CD80 gene expression status in BRCA, COAD, COADREAD, LUAD, LUSC and MESO

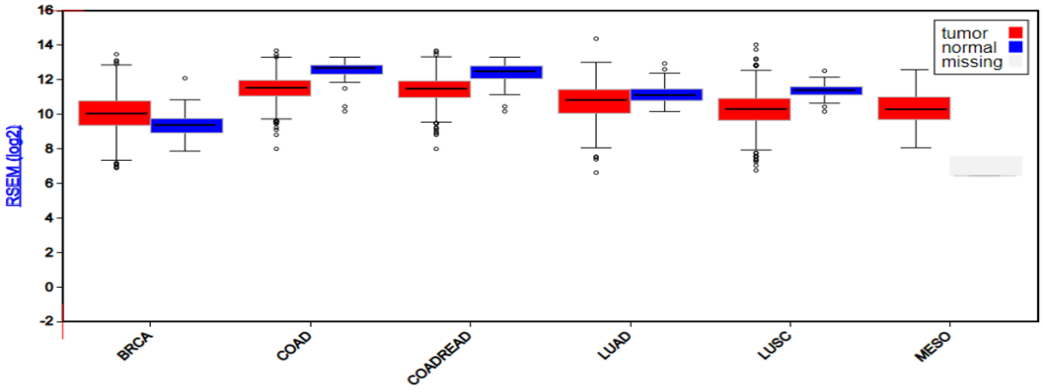

Figure 7. 13 Gal-9 gene expression status in BRCA, COAD, COADREAD, LUAD, LUSC and MESO

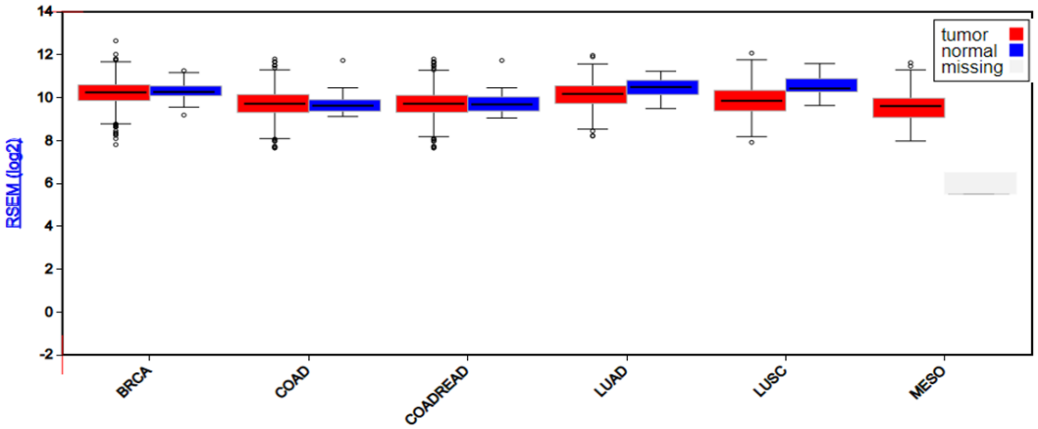

Figure 7. 14CD39 gene expression status in BRCA, COAD, COADREAD, LUAD, LUSC and MESO

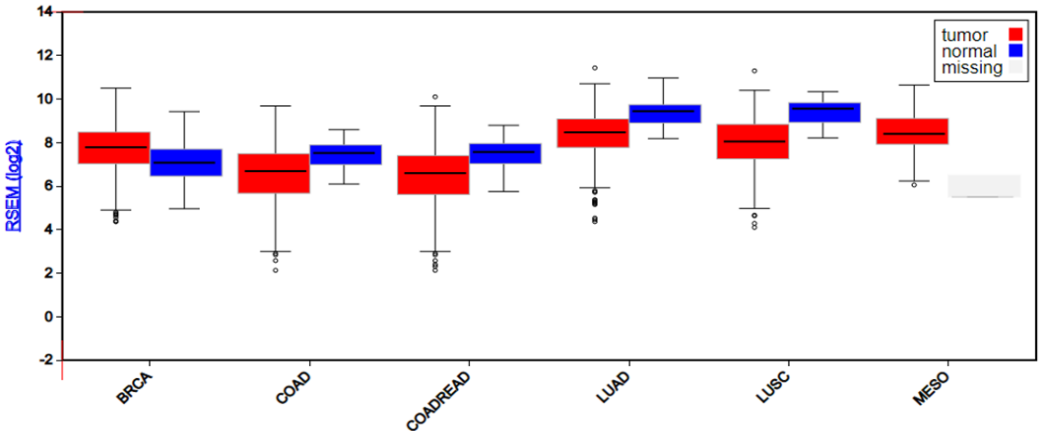

Figure 7. 15 CD86 gene expression status in BRCA, COAD, COADREAD, LUAD, LUSC and MESO

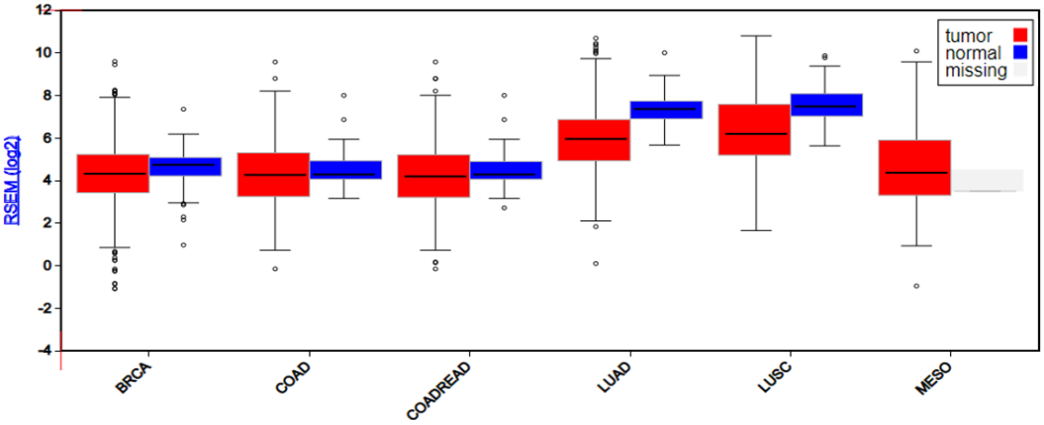

Figure 7. 16 PDL1 gene expression status in BRCA, COAD, COADREAD, LUAD, LUSC and MESO

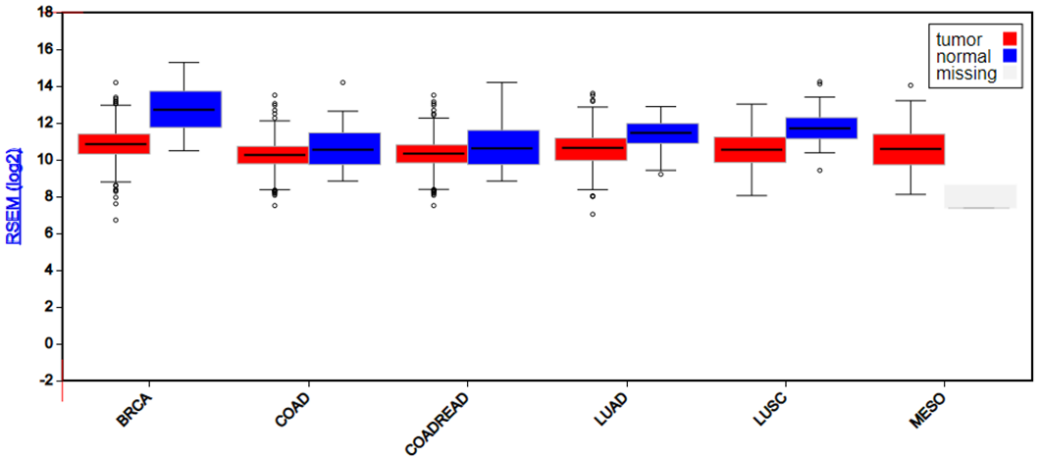

Figure 7. 17 CD146 gene expression status in BRCA, COAD, COADREAD, LUAD, LUSC and MESO

7.5.2 HRE & Hypoxia related TFBSs

7.5.2.1 HRE

The preceding chapters showed that CD309, CD54, CD105 in ECs, and PD-L1 in macrophages were up-regulated under hypoxia. Therefore, human genes for these molecules were investigated for the presence of functionally active HRE in their promoter regions. Promoter regions upstream of TSS were examined for the presence of HRE motifs (5`-RCGTG-3`) and HASs motifs (5`-CA(G|C)(A|G)(T|G|C)-3`). Putative HREs were identified based on a match to the consensus HRE motif 5'-RCGTG-3' and then the region immediately downstream was scanned for the presence of a HAS motif: 5'-CA(G|C)(A|G)(T|G|C)-3'in order to identify functionally active HRE.

VEGFR2/CD309, regulates endothelial cell migration and proliferation and plays a direct role in normal and pathological vascular permeability (266). Therefore, activation of CD309 by VEGF is a crucial step in signaling pathways that initiate tumour angiogenesis (267).

As shown in Figure 18, the CD309 gene is Homo sapiens kinase insert domain receptor (KDR), which corresponds to NCBI reference sequence NM_002253.3. The RefSeq gene transcript is 5849 nt in length and consists of 30 exons. The coding sequence, (highlighted in grey) starts from position 303 with the start codon "ATG" (highlighted in green) and ends at position 4373 with the stop codon "TAA" (highlighted in red). The signal peptide is encoded by nucleotides 303 to 359 (light grey). The first exon runs from nucleotides 1 to 369 and the first exon junction is highlighted in blue. The 5` UTR and 3' UTR are underlined and the TSS site at position 1 is shown in bold. The predicted promoter sequence of 2000 nucleotides is placed before the TSS, where HREs are highlighted in turquoise and the adjacent HAS in pink.

Examination of the promoter region of CD309 through *in silico* techniques revealed the presence of HREs 5` upstream from TSS at -1195 with an adjacent HAS within 21 nucleotides. However, the identified HREs are considered functionally inactive since HAS is not located within the range of 7–15 nt from HREs. The other HRE located 5` upstream from TSS at -867 is preceded by "C" and has an adjacent HAS within 21 nucleotides turning it into E-box, as shown in Figure 18.

Gene: CD309
Definition Homo sapiens kinase insert domain receptor (KDR), mRNA
Accession No.: NM_002253.3
Length: 5849 bp
Exons: 30
First Exon: 1 to 369 ntd
Coding region: 303 to 4373 ntd
Signal Peptide: 303 to 359

AGAGGAAGTGTCATGAACTGTAAATAAGGCTGATAGGGAATTGTTTGGTGATGGGGATGGA
GAAAAACTGCCCTCTCCAAACCAGGTTCCATCTCCCACCCCTTTATCCAACTTTGCCAGAGTC
CATCCTATTTTATTTGCTGAGTTTACTAGCAGGAAGAGAGGAGTTTCTTTAAAGATTCTCTCC
CCTCCCCAAATAAATACCTCCCAGATAAATATGAGTACATCTATATAGTAGAGCACTATGCC
AACATTGAAAAGATGGAAGGATGGAGCTTTGTTCGCAGCCAGCTTAGGCAACATAGTGAGA
CCCTGCCTCTATATAAAAATAAATAAATAAATAAATAAATAAATAAATAAATAAAAGATGG
AGCTTTAAAGGTTGATGTAGAACGAATCTCCAGTGTATATTATAAAGTGAAGGCTGGGCAGG
GTGGCTCGTGCTTGTAATCCCAGCACTTTGGGAGACTGAGGCAGGAGGATGGACTGAGTCCA
GGCATTGGAGACCAGCCTGGGCAACATAGTGAGACCTTGTCTCAAATAAATAAATCAAATTT
AAAGGGAAAAAAGCCAAGGCTCAAATAGCATTTATACCAAGCAATTGTGGGAAGAGAAGG
GTGACATGTCTACATACTTGTGTTTAAGAATCTGCTTGGAAAAAAAAGGAAACATAAAAATG
CCTCTGCCAAAAGAAAAGTCTTTTCACTCTAAGCCTTTTTGTGTTTTTCCAAAATTTTTTTTTG
CCATATACATTCATTATATTTCAGCATTAAAATATTTCACCTGTCAACTTGGAAAAGTAAAA
GCGTGAATACAGTAAATATTTAAAAACAGATGAAGATAAGTAACAGGTTACATTAATTGTA
TACAATCAATCTAGTTTGAATTAGGTGTAGATATAATAATTCTGTGTGTTTATCTTGGTGAAG
AATGGTCCTTTAGGTTGTCATTAAAAAGCACCTCTGGGAGGTAAAAGACATAGGCATCTGGA
AGATTCATATTTAATGAAGTTAGGGGACATTTGATGTCACTCCCCAGGTGTGGGGAGATATG
GACAGAAAACCAGAAGGAACGAATGTGGTCAGGAAGGAATTGGAGTTCCCCTCCAAACAGC
TGCCACAAGAAGTCCACACACGTGGAGACAGTTGTGCAATTTGGTCACAGAGTGTCCTAGG
TGCTTTTGCTTCATTGCTCCTCCACTGAAGCACGCTGGCAGCTGGCCTCCTTCCCCTGGGACT
AAGGATATCTTGGCTGGAAGCTCTGCTCTGAAAAGGGGCATGGCCAAACTTTCACTAGGGCT
CTTCGTTGGGGAGCACGATGGACAAAAGCCTTCTTGGGGCTAGGCAGGTCACTTCAAACTTG
GAGCCGCCAAATATTTTGGGAAATAGCGGGAATGTTGGCGAACTGGGCAAGTGCGTTTTCTG
ATTAAGAGCAACCAGATTCAGCTTTTTAAACTACAATTATACTGGCCAAACAAAATACCCTT
ATACAAAAACCAAAACTACTGGCAGGAGTCGCTGCCAGCTTGCGACCCGGCATACTTGGCT
GAGTATCCGCTTCTCCCTTGTGGCTCCAAACTGCTGCAGATTCTCGGCCACTTCAGACGCGCG
CGATGGCGAAGAGGGTCCTGCACTTTGACGCGCCTGGTGAGGGAGCGCTGCTCTTCGCAGCG
CTCCTGGTGATGCTCCCCAAATTTCGGGGACCGGCAAGCGATTAAATCTTGGAGTTGCTCAG
CGCCCGTTACCGAGTACTTTTTATTTACACCAGAAACAAAGTTGTTGCTCTGGGATGTTCTCT
CCTGGGCGACTTGGGGCCCAGCGCAGTCCAGTTGTGTGGGGAAATGGGGAGATGTAAATGG
GCTTGGGGAGCTGGAGATCGCCGCCGGGTACCCGGGTGAGGGGCGGGGCTGGCCGCACGGG
AGAGCCCCTCCTCCGCTCCGGCCCCGCCCCGCATGGCCCCGCCTCCGCGCTCTAGAGTTTCG
GCACCAGCTCCCACCCTGCAACTGAGTCCCGGGACCCCGGGAGAGCGGTCAATGTGTGGTC
GCTGCGTTTCCTCTGCCTGCGCCGGGCATCACTTGCGCGCCGCAGAAAGTCCGTCTGGCAGC
CTGGATATCCTCTCCTACCGGCACCCGCAGACGCCCCTGCAGCCGCGGTCGGCGCCCGGGCT
CCCTAGCCCTGTGCGCTCAACTGTCCTGCGCTGCGGGGTGCCGCGAGTTCCACCTCCGCGCC
TCCTTCTCTAGACAGGCGCTGGGAGAAAGAACCGGCTCCCGAGTTCTGGGCATTTCGCCCGG
CTCGAGGTGCAGGATGCAGAGCAAGGTGCTGCTGGCCGTCGCCCTGTGGCTCTGCGTGGAG

ACCCGGGCCGCCTCTGTGGGTTTGCCTAGTGTTTCTCTTGATCTGCCCAGGCTCAGCATACAA
AAAGACATACTTACAATTAAGGCTAATACAACTCTTCAAATTACTTGCAGGGGACAGAGGG
ACTTGGACTGGCTTTGGCCCAATAATCAGAGTGGCAGTGAGCAAAGGGTGGAGGTGACTGA
GTGCAGCGATGGCCTCTTCTGTAAGACACTCACAATTCCAAAAGTGATCGGAAATGACACTG
GAGCCTACAAGTGCTTCTACCGGGAAACTGACTTGGCCTCGGTCATTTATGTCTATGTTCAA
GATTACAGATCTCCATTTATTGCTTCTGTTAGTGACCAACATGGAGTCGTGTACATTACTGAG
AACAAAAACAAAACTGTGGTGATTCCATGTCTCGGGTCCATTTCAAATCTCAACGTGTCACT
TTGTGCAAGATACCCAGAAAAGAGATTTGTTCCTGATGGTAACAGAATTTCCTGGGACAGCA
AGAAGGGCTTTACTATTCCCAGCTACATGATCAGCTATGCTGGCATGGTCTTCTGTGAAGCA
AAAATTAATGATGAAAGTTACCAGTCTATTATGTACATAGTTGTCGTTGTAGGGTATAGGAT
TTATGATGTGGTTCTGAGTCCGTCTCATGGAATTGAACTATCTGTTGGAGAAAAGCTTGTCTT
AAATTGTACAGCAAGAACTGAACTAAATGTGGGGATTGACTTCAACTGGGAATACCCTTCTT
CGAAGCATCAGCATAAGAAACTTGTAAACCGAGACCTAAAAACCCAGTCTGGGAGTGAGAT
GAAGAAATTTTTGAGCACCTTAACTATAGATGGTGTAACCCGGAGTGACCAAGGATTGTACA
CCTGTGCAGCATCCAGTGGGCTGATGACCAAGAAGAACAGCACATTTGTCAGGGTCCATGA
AAAACCTTTTGTTGCTTTTGGAAGTGGCATGGAATCTCTGGTGGAAGCCACGGTGGGGGAGC
GTGTCAGAATCCCTGCGAAGTACCTTGGTTACCCACCCCCAGAAATAAAATGGTATAAAAAT
GGAATACCCCTTGAGTCCAATCACACAATTAAAGCGGGGCATGTACTGACGATTATGGAAGT
GAGTGAAAGAGACACAGGAAATTACACTGTCATCCTTACCAATCCCATTTCAAAGGAGAAG
CAGAGCCATGTGGTCTCTCTGGTTGTGTATGTCCCACCCCAGATTGGTGAGAAATCTCTAATC
TCTCCTGTGGATTCCTACCAGTACGGCACCACTCAAACGCTGACATGTACGGTCTATGCCATT
CCTCCCCCGCATCACATCCACTGGTATTGGCAGTTGGAGGAAGAGTGCGCCAACGAGCCCAG
CCAAGCTGTCTCAGTGACAAACCCATACCCTTGTGAAGAATGGAGAAGTGTGGAGGACTTCC
AGGGAGGAAATAAAATTGAAGTTAATAAAAATCAATTTGCTCTAATTGAAGGAAAAAACAA
AACTGTAAGTACCCTTGTTATCCAAGCGGCAAATGTGTCAGCTTTGTACAAATGTGAAGCGG
TCAACAAAGTCGGGAGAGGAGAGAGGGTGATCTCCTTCCACGTGACCAGGGGTCCTGAAAT
TACTTTGCAACCTGACATGCAGCCCACTGAGCAGGAGAGCGTGTCTTTGTGGTGCACTGCAG
ACAGATCTACGTTTGAGAACCTCACATGGTACAAGCTTGGCCCACAGCCTCTGCCAATCCAT
GTGGGAGAGTTGCCCACACCTGTTTGCAAGAACTTGGATACTCTTTGGAAATTGAATGCCAC
CATGTTCTCTAATAGCACAAATGACATTTTGATCATGGAGCTTAAGAATGCATCCTTGCAGG
ACCAAGGAGACTATGTCTGCCTTGCTCAAGACAGGAAGACCAAGAAAAGACATTGCGTGGT
CAGGCAGCTCACAGTCCTAGAGCGTGTGGCACCCACGATCACAGGAAACCTGGAGAATCAG
ACGACAAGTATTGGGGAAAGCATCGAAGTCTCATGCACGGCATCTGGGAATCCCCCTCCAC
AGATCATGTGGTTTAAAGATAATGAGACCCTTGTAGAAGACTCAGGCATTGTATTGAAGGAT
GGGAACCGGAACCTCACTATCCGCAGAGTGAGGAAGGAGGACGAAGGCCTCTACACCTGCC
AGGCATGCAGTGTTCTTGGCTGTGCAAAAGTGGAGGCATTTTTCATAATAGAAGGTGCCCAG
GAAAAGACGAACTTGGAAATCATTATTCTAGTAGGCACGGCGGTGATTGCCATGTTCTTCTG
GCTACTTCTTGTCATCATCCTACGGACCGTTAAGCGGGCCAATGGAGGGGAACTGAAGACAG
GCTACTTGTCCATCGTCATGGATCCAGATGAACTCCCATTGGATGAACATTGTGAACGACTG
CCTTATGATGCCAGCAAATGGGAATTCCCCAGAGACCGGCTGAAGCTAGGTAAGCCTCTTGG
CCGTGGTGCCTTTGGCCAAGTGATTGAAGCAGATGCCTTTGGAATTGACAAGACAGCAACTT
GCAGGACAGTAGCAGTCAAAATGTTGAAAGAAGGAGCAACACACAGTGAGCATCGAGCTCT
CATGTCTGAACTCAAGATCCTCATTCATATTGGTCACCATCTCAATGTGGTCAACCTTCTAGG
TGCCTGTACCAAGCCAGGAGGGCCACTCATGGTGATTGTGGAATTCTGCAAATTTGGAAACC
TGTCCACTTACCTGAGGAGCAAGAGAAATGAATTTGTCCCCTACAAGACCAAAGGGGCACG
ATTCCGTCAAGGGAAAGACTACGTTGGAGCAATCCCTGTGGATCTGAAACGGCGCTTGGAC
AGCATCACCAGTAGCCAGAGCTCAGCCAGCTCTGGATTTGTGGAGGAGAAGTCCCTCAGTG
ATGTAGAAGAAGAGGAAGCTCCTGAAGATCTGTATAAGGACTTCCTGACCTTGGAGCATCTC
ATCTGTTACAGCTTCCAAGTGGCTAAGGGCATGGAGTTCTTGGCATCGCGAAAGTGTATCCA
CAGGGACCTGGCGGCACGAAATATCCTCTTATCGGAGAAGAACGTGGTTAAAATCTGTGACT
TTGGCTTGGCCCGGGATATTTATAAAGATCCAGATTATGTCAGAAAAGGAGATGCTCGCCTC
CCTTTGAAATGGATGGCCCCAGAAACAATTTTTGACAGAGTGTACACAATCCAGAGTGACGT

Figure 7. 18 The CD309 gene and its annotation indicating the promoter region, HRE, HAS, TSS and the coding region

CD54: CD54 plays a central role in EC migration (224), cell–cell adhesive engagements, activation of lymphocytes, leukocyte trafficking, and numerous additional immune functions (225, 226). As shown in Figure 19, the CD54 gene is Homo sapiens intercellular adhesion molecule 1 (ICAM1), which corresponds to NCBI reference sequence NM_000201.3. The RefSeq gene transcript is 2967 nt in length and consists of 7 exons. The coding sequence (highlighted in grey) starts from position 41 with the start codon “ATG” (highlighted in green) and ends at position 1639 with the

stop codon “TGA” (highlighted in red). The signal peptide is encoded by nucleotides 42 to 121 (light grey). The first exon runs from nucleotides 1 to 107 and the first exon junction is highlighted in blue. The 5` UTR and 3’ UTR are underlined and the TSS site at position 1 is shown in bold. The predicted promoter sequence of 2000 nucleotides is placed before the TSS, where HREs are highlighted in turquoise and adjacent HASs in pink.

Analysis of the data shows two HREs with HASs in proximity in the promoter region of CD54 gene. One HRE is 5` upstream from TSS at -651 and has an adjacent HAS within 23 nucleotides. The other HRE is 5` upstream from TSS at -1073, with an overlapping HAS within 21 nucleotides (Figure 19). However, similar to CD309, the HREs in CD54 are also not functionally active because the HASs are located beyond 8 nt and 6 nt respectively from the functionally active HRE position.

Gene: CD54
Definition: Homo sapiens intercellular adhesion molecule 1 (ICAM1), mRNA
Accession No.: NM_000201.3
Length: 2967 bp
Exons: 7
First Exon: 1 to 107 ntd
Coding region: 41 to 1639 ntd
Signal Peptide: 42 to 121

TCGAATCTCTCCTTTGCTAAGCCTGCTCCAGCCACACTGTTCTCCTGGCTGTTCCTTTTTTTTT
TTTTTTTTTTTTTTTTTTGAGTCTCACTCTCACCCAGGCTGGAGTGCAGTGCCTCTATCTTGGC
TCACTGCAACCTCCGCCTGCCGGGTTCAAGAGATTCTCCTGCATCAGCCTCCCAAGTAGGTG
GAATTACAGGTGTGCACCACCACACCCGGCTAATTTTTGTATTTTGCATAGAGATGGGGGTC
TCCCTATGTTGCCCAGGCTGGTCTTGAACTCCTGGGCTCAAGTGATCCTCCCATCTCGGCCTC
CCAAAATGCTGGGATTACAGGTGGGAGCCGCGCCCAGGTGGATTTTTGTCTGACTCTGTTCA
TTCCTGTGTCCCCAGTACCTGGAAGGACGCCAAGCACACAGTAGGCGCTTAAAAAACATTGA
GCCACATGTTGAGAAAAGAACGGCACCATTGTGGCTGCAAGTGGGACTTGGGCCGCGCGGG
GGAGCTCGCGCACCTCGGGCCGGGGCAAGAGCTCAGTGGAACCCGCCCGAGGAAGAACCCG
TGGCGCAGGATTTTCCCAGGCCTTCTGAGGACCAGGGGCGTCCCCCGTCCCACCCTGTGACT
TTGCTCAGGCCGTTCCGGGGCGGGAATTCAGAACTCCTCAGCCCCCCAAGAAAAAAATATCC
CCGTGGAAATTCCTTGGGAATGACCGAGGCGGGGGAAATATGCGTCTCTGGATGGCCAGTG
ACTCGCAGCCCCCTTCCCCGATAGGAAGGGCCTGCGCGTCCGGGGACCCTTCGCTTCCCCTT
CTGCTGCGCGACCTCCCTGGCCCCTCGGAGATCTCCATGGCGACGCCGCGCGCGCCCCACAA
CAGGAAAGCCTTAGGCGGCGCGGCTTGGTGCTCGGAGACTTAAGAGTACCCAGCCTCGACG
TGGTGGATGTCGAGTCTTGGGGTCACACGCACAGGCGGTGGCCAAGCAAACACCCGCTCAT
ATTTAGTGCATGAGCCTGGGTTCGAGTTGCCGGAGCCTCGCGCGTAGGGCAGGGGTTCGAGC
GCCCCTTCTCCCTGCCTCGCCTCTGCGCCTGGGGGCTGCTGCCTCAGTTTCCCAGCGACAGGC
AGGGATTTCGAGCGTCCCCCTCCCCTCCCTCGTCAAGATCCAAGCTAGCTGCCTCAGTTTCCC
CGCGGAGCCTGGGACGCCAGCGGAGGGGCTCGGCGCGTAGGGATCACGCAGCTTCCTTCCT
TTTTCTGGGAGCTGTAAAGACGCCTCCGCGGCCAAGGCCGAAAGGGGAAGCGAGGAGGCCG
CCGGGGTGAGTGCCCTCGGGTGTAGAGAGAGGACGCCGATTTCCCCGGACGTGGTGAGACC
GCGCTTCGTCACTCCCACGGTTAGCGGTCGCCGGGAGGTGCCTGGCTCTGCTCTGGCCGCTT
CTCGAGAAATGCCCGTGTCAGCTAGGTGTGGACGTGACCTAGGGGGAGGGGCATCCCTCAG
TGGAGGGAGCCCGGGGAGGATTCCTGGGCCCCCACCCAGGCAGGGGGCTCATCCACTCGAT
TAAAGAGGCCTGCGTAAGCTGGAGAGGGAGGACTTGAGTTCGGACCCCCTCGCAGCCTGGA
GTCTCAGTTTACCGCTTTGTGAAATGGACACAATAACAGTCTCCACTCTCCGGGGAAGTTGG
CAGTATTTAAAAGTACTTAATAAACCGCTTAGCGCGGTGTAGACCGTGATTCAAGCTTAGCC
TGGCCGGGAAACGGGAGGCGTGGAGGCCGGGAGCAGCCCCCGGGGTCATCGCCCTGCCACC
GCCGCCCGATTGCTTTAGCTTGGAAATTCCGGAGCTGAAGCGGCCAGCGAGGGAGGATGAC
CCTCTCGGCCCGGGCACCCTGTCAGTCCGGAAATAACTGCAGCATTTGTTCCGGAGGGGAAG
GCGCGAGGTTTCCGGGAAAGCAGCACCGCCCCTTGGCCCCCAGGTGGCTAGCGCTATAAAG
GATCACGCGCCCCAGTCGACGCTGGAGCTCCTCTGCTACTCAGAGTTGCAACCTCAGCCTCG
CTATGGCTCCCAGCAGCCCCCGGCCCGCGCTGCCCGCACTCCTGGTCCTGCTCGGGGCTCTG
TTCCCAGGACCTGGCAATGCCCAGACATCTGTGTCCCCCTCAAAAGTCATCCTGCCCCGGGG
AGGCTCCGTGCTGGTGACATGCAGCACCTCCTGTGACCAGCCCAAGTTGTTGGGCATAGAGA
CCCCGTTGCCTAAAAAGGAGTTGCTCCTGCCTGGGAACAACCGGAAGGTGTATGAACTGAG

CAATGTGCAAGAAGATAGCCAACCAATGTGCTATTCAAACTGCCCTGATGGGCAGTCAACA
GCTAAAACCTTCCTCACCGTGTACTGGACTCCAGAACGGGTGGAACTGGCACCCCTCCCCTC
TTGGCAGCCAGTGGGCAAGAACCTTACCCTACGCTGCCAGGTGGAGGGTGGGGCACCCCGG
GCCAACCTCACCGTGGTGCTGCTCCGTGGGGAGAAGGAGCTGAAACGGGAGCCAGCTGTGG
GGGAGCCCGCTGAGGTCACGACCACGGTGCTGGTGAGGAGAGATCACCATGGAGCCAATTT
CTCGTGCCGCACTGAACTGGACCTGCGGCCCCAAGGGCTGGAGCTGTTTGAGAACACCTCGG
CCCCCTACCAGCTCCAGACCTTTGTCCTGCCAGCGACTCCCCCACAACTTGTCAGCCCCCGG
GTCCTAGAGGTGGACACGCAGGGGACCGTGGTCTGTTCCCTGGACGGGCTGTTCCCAGTCTC
GGAGGCCCAGGTCCACCTGGCACTGGGGGACCAGAGGTTGAACCCCACAGTCACCTATGGC
AACGACTCCTTCTCGGCCAAGGCCTCAGTCAGTGTGACCGCAGAGGACGAGGGCACCCAGC
GGCTGACGTGTGCAGTAATACTGGGGAACCAGAGCCAGGAGACACTGCAGACAGTGACCAT
CTACAGCTTTCCGGCGCCCAACGTGATTCTGACGAAGCCAGAGGTCTCAGAAGGGACCGAG
GTGACAGTGAAGTGTGAGGCCCACCCTAGAGCCAAGGTGACGCTGAATGGGGTTCCAGCCC
AGCCACTGGGCCCGAGGGCCCAGCTCCTGCTGAAGGCCACCCCAGAGGACAACGGGCGCAG
CTTCTCCTGCTCTGCAACCCTGGAGGTGGCCGGCCAGCTTATACACAAGAACCAGACCCGGG
AGCTTCGTGTCCTGTATGGCCCCCGACTGGACGAGAGGGATTGTCCGGGAAACTGGACGTGG
CCAGAAAATTCCCAGCAGACTCCAATGTGCCAGGCTTGGGGGAACCCATTGCCCGAGCTCA
AGTGTCTAAAGGATGGCACTTTCCCACTGCCCATCGGGGAATCAGTGACTGTCACTCGAGAT
CTTGAGGGCACCTACCTCTGTCGGGCCAGGAGCACTCAAGGGGAGGTCACCCGCAAGGTGA
CCGTGAATGTGCTCTCCCCCCGGTATGAGATTGTCATCATCACTGTGGTAGCAGCCGCAGTC
ATAATGGGCACTGCAGGCCTCAGCACGTACCTCTATAACCGCCAGCGGAAGATCAAGAAAT
ACAGACTACAACAGGCCCAAAAAGGGACCCCCATGAAACCGAACACACAAGCCACGCCTCC
CTGAACCTATCCCGGGACAGGGCCTCTTCCTCGGCCTTCCCATATTGGTGGCAGTGGTGCCA
CACTGAACAGAGTGGAAGACATATGCCATGCAGCTACACCTACCGGCCCTGGGACGCCGGA
GGACAGGGCATTGTCCTCAGTCAGATACAACAGCATTTGGGGCCATGGTACCTGCACACCTA
AAACACTAGGCCACGCATCTGATCTGTAGTCACATGACTAAGCCAAGAGGAAGGAGCAAGA
CTCAAGACATGATTGATGGATGTTAAAGTCTAGCCTGATGAGAGGGGAAGTGGTGGGGGAG
ACATAGCCCCACCATGAGGACATACAACTGGGAAATACTGAAACTTGCTGCCTATTGGGTAT
GCTGAGGCCCCACAGACTTACAGAAGAAGTGGCCCTCCATAGACATGTGTAGCATCAAAAC
ACAAAGGCCCACACTTCCTGACGGATGCCAGCTTGGGCACTGCTGTCTACTGACCCCAACCC
TTGATGATATGTATTTATTCATTTGTTATTTTACCAGCTATTTATTGAGTGTCTTTTATGTAGG
CTAAATGAACATAGGTCTCTGGCCTCACGGAGCTCCCAGTCCTAATCACATTCAAGGTCACC
AGGTACAGTTGTACAGGTTGTACACTGCAGGAGAGTGCCTGGCAAAAAGATCAAATGGGGC
TGGGACTTCTCATTGGCCAACCTGCCTTTCCCCAGAAGGAGTGATTTTTCTATCGGCACAAA
AGCACTATATGGACTGGTAATGGTTACAGGTTCAGAGATTACCCAGTGAGGCCTTATTCCTC
CCTTCCCCCCAAAACTGACACCTTTGTTAGCCACCTCCCCACCCACATACATTTCTGCCAGTG
TTCACAATGACACTCAGCGGTCATGTCTGGACATGAGTGCCCAGGGAATATGCCCAAGCTAT
GCCTTGTCCTCTTGTCCTGTTTGCATTTCACTGGGAGCTTGCACTATGCAGCTCCAGTTTCCTG
CAGTGATCAGGGTCCTGCAAGCAGTGGGGAAGGGGGCCAAGGTATTGGAGGACTCCCTCCC
AGCTTTGGAAGCCTCATCCGCGTGTGTGTGTGTGTGTATGTGTAGACAAGCTCTCGCTCTGTC
ACCCAGGCTGGAGTGCAGTGGTGCAATCATGGTTCACTGCAGTCTTGACCTTTTGGGCTCAA
GTGATCCTCCCACCTCAGCCTCCTGAGTAGCTGGGACCATAGGCTCACAACACCACACCTGG
CAAATTTGATTTTTTTTTTTTTTCCAGAGACGGGGTCTCGCAACATTGCCCAGACTTCCTTTGT
GTTAGTTAATAAAGCTTTCTCAACTGCC

Figure 7. 19 CD54 gene and its annotation indicating the promoter region, HRE, HAS, TSS, and coding region

CD105: In hypoxic ECs, CD105 induces an anti-apoptotic pathway which prevents apoptosis and promotes angiogenesis (285). As shown in Figure 20, the CD105 gene is Homo sapiens endoglin (ENG), which corresponds to NCBI reference sequence NM_001114753.3. The RefSeq gene transcript is 2946 nt in length and consists of 15 exons. The coding sequence (highlighted in grey) starts from position 304 with the start

codon “ATG” (highlighted in green) and ends at position 2280 with the stop codon “TAG” (highlighted in red). The signal peptide is encoded by nucleotides 304 to 378 (light grey). The first exon runs from nucleotides 1 to 37 and the first exon junction is highlighted in blue. The 5` UTR and 3’ UTR are underlined and the TSS site at position 1 is shown in bold. The predicted promoter sequence of 2000 nucleotides is placed before the TSS, where HREs are highlighted in turquoise and adjacent HASs in pink.

The promoter region in the CD105 gene, contains two HREs. One HRE is 5` upstream from TSS at -472 and another at -642. A third HRE was present 5` upstream from TSS at -1049 and is preceded by “C”, forming an E-box to allow binding of bHLH proteins, as shown in Figure 20. There are no functionally active HRE in CD105 due to absence of HASs near HREs.

Gene: CD105
Definition: Homo sapiens endoglin (ENG), transcript variant 1, mRNA
Accession No.: NM_001114753.3
Length: 2946 bp
Exons: 15
First Exon: 1 to 370 ntd
Coding region: 304 to 2280 ntd
Signal Peptide: 304 to 378 ntd

CAAGGCTGGGCAAGCAAAACTATCCCTAATCCCCACCCAAAGAGCCACACCGACCCTCCCA
GCCGCTGTGACAGCTCCTGCAGAGACAAACACACGGCCTACTCTTGTCACCCGGGCCGGCCA
ATAAGCACGGAGAGGCAAGGCCTCAGACCCTGGACAGACATCCTCCCTCCAGAGGCACCCA
GGGCCTCAGCCTTCTCCTCCCTCCCTGGGCCTCAATTTCTCCACCTGTGACCCAGGGCAGGTG
GATCCAGGGAGAAGAACCTTCTGGCTCCATCTCACCGTGGGTCCTGCCAGCACACACAAAG
ATTTGGCCTCTCAAAGCCTAGCTCTGCCAGCGTCCTTCTGCTCAAGAACTCTCCATGACTCCC
AGTGGCCCTAAGGACAAAGTCCTGGCATTTGAGGCCCTCCCAATGCAGGGCCAGACTCTGCC
TCTCCAGCTTCCTGTCCCCACCACACCCCTGCTGGTCTCACGGTGGTCCGACTGTTTCCTGCT
TCTGTGCCTTTGCTTAGTCTGGCACCCCTGCCTGGCATGCTTTCCTCACCCCTTCTTCTCCCCA
ATCCCAACTCACCCAGTCTTTCAAAGGGCAGGCCTAAATACCAGGCCCTCCAGGTGGCCCAG
GATTCCTTCTCTGAGCTTTCATGGGCCTGGCCCTGGGTGCTACCTGTGAGTAGTCCCACGGTG
GGTACATAGTAGGTGCGCTTACTGTTTGCAGAATGAACATGGGACAGTTTGGGGACTGTCAC
CCAGCTCAGGGAGCACTGATGGGGAAGCATCTCCTGTATGTCCCAGGGCTCAGTGCTGTAGT
GTCCTGACCCTCAGAAATCTCATAATGGCTTGGTCAGGAAGGCATCGTGCCCCACTTTGCAA
ACAGGGGGTGCTGAGAATTGAGGGGCCTTGTCCAAGGTCTCATGGCTAGGAGCAAGCAGAA
TCGGATTTGAACCCAGGGCCACGTGACTTCAGAAGTGCCATTAAAGTCCCCATAATTTGGAG
CTGTCTTCTTTTTTTTTTTCTTTTCTTTTTTTTGAGACCGAGCCTCACTCTGTCACCTAGGCCAG
GAGTGCAGTGGTCTGATCTCAGCTCACTGCAACCTCCGCCTCCTAGGTTCAAGTGATTCTCTA
GCCTCAGCCTCCCAAGTAGCTGGGACTACAGGCGCACGTCATCATGCCCAGCTAACTTTTGT
ATTTTTAGTAGAGATGGGTTTTCACCATGTTGGTCAGGCTGGTCTCGAACTCCTGACCTCAAG
TGATCCGTCTGCCTCGGCCTCTCAAAGTGCTGGGATTATAGGCTTGAGCCACTACACTCGGC
CTGGAGCTGTGTTTTGTCGGTGAAGGATTTTCCACCCATGAAGGGGTCAGACGTGAAGTGTG
TGGCCCTGGGCAGCTCCTCTGAGCCCAGAGACGCCAGCCCTAGCCGCCTTGCTGTGCCACTT
TGGGACTTCCCTCCCTAGCCTGAGCTTCAGTTTTCCTGCCTGTTAGGCAGCCCCATGTCAACT
GCACTTAGTAGGCCGGGTTTGATGCCCGACAAGACGTGAAGTGGTGGAGGTGGGCAGGATC
CCAGCGCTACCATCTTCTTGAACCAGTGATCTCAACACATCGGATTTCTGTTTCCTCATCTGC
AAAATGGGATCAGTGAGCTCAGGTGGGTCACAAATTCTACAGGAACTACTTTAGCCAAGAC
CGGCCCCCTGAAAGTTCCCCTCGGTGGGCTGTTAGGGTGATTGTTTTCATCTGTGGGGCTCCC
TGATGCGTCCCACCCACCAGCCTTGGAGAGGGTGGGATGGGAGGGTGGGGTGCTTGGGGAG
ACAAGCCTAGAGCCTGGGCCCTCCCACCCCACTGCCTCCCCCCATCCCAGGGCCCCCCACCC
AGTGACAAAGCCCGTGGCACTTCCTCTACCCGGTTGGCAGGCGGCCTGGCCCAGCCCCTTCT
CTAAGGAAGCGCATTTCCTGCCTCCCTGGGCCGGCCGGGCTGGATGAGCCAGGAGCTCCCTG
CTGCCGGTCAATACCACAGCCTTCATCTGCGCCCTGGGGCCAGGACTGCTGCTGTCACTGCC
ATCCATTGGAGCCCAGCACCCCCTCCCCGCCCATCCTTCGGACAGCAACTCCAGCCCAGCCC
CGCGTCCCTGTGTCCACTTCTCCTGACCCCTCGGCCGCCACCCCAGAAGGCTGGAGCAGGGA
CGCCGTCGCTCCGGCCGCCTGCTCCCCTCGGGTCCCCGTGCGAGCCCACGCCGGCCCCGGTG
CCCGCCCGCAGCCCTGCCACTGGACACAGGATAAGGCCCAGCGCACAGGCCCCCACGTGGA
CAGCATGGACCGCGGCACGCTCCCTCTGGCTGTTGCCCTGCTGCTGGCCAGCTGCAGCCTCA
GCCCCACAAGTCTTGCAGAAACAGTCCATTGTGACCTTCAGCCTGTGGGCCCCGAGAGGGGC

GAGGTGACATATACCACTAGCCAGGTCTCGAAGGGCTGCGTGGCTCAGGCCCCCAATGCCAT
CCTTGAAGTCCATGTCCTCTTCCTGGAGTTCCCAACGGGCCCGTCACAGCTGGAGCTGACTCT
CCAGGCATCCAAGCAAAATGGCACCTGGCCCCGAGAGGTGCTTCTGGTCCTCAGTGTAAACA
GCAGTGTCTTCCTGCATCTCCAGGCCCTGGGAATCCCACTGCACTTGGCCTACAATTCCAGCC
TGGTCACCTTCCAAGAGCCCCCGGGGGTCAACACCACAGAGCTGCCATCCTTCCCCAAGACC
CAGATCCTTGAGTGGGCAGCTGAGAGGGGCCCCATCACCTCTGCTGCTGAGCTGAATGACCC
CCAGAGCATCCTCCTCCGACTGGGCCAAGCCCAGGGGTCACTGTCCTTCTGCATGCTGGAAG
CCAGCCAGGACATGGGCCGCACGCTCGAGTGGCGGCCGCGTACTCCAGCCTTGGTCCGGGG
CTGCCACTTGGAAGGCGTGGCCGGCCACAAGGAGGCGCACATCCTGAGGGTCCTGCCGGGC
CACTCGGCCGGGCCCCGGACGGTGACGGTGAAGGTGGAACTGAGCTGCGCACCCGGGGATC
TCGATGCCGTCCTCATCCTGCAGGGTCCCCCCTACGTGTCCTGGCTCATCGACGCCAACCAC
AACATGCAGATCTGGACCACTGGAGAATACTCCTTCAAGATCTTTCCAGAGAAAAACATTCG
TGGCTTCAAGCTCCCAGACACACCTCAAGGCCTCCTGGGGGAGGCCCGGATGCTCAATGCCA
GCATTGTGGCATCCTTCGTGGAGCTACCGCTGGCCAGCATTGTCTCACTTCATGCCTCCAGCT
GCGGTGGTAGGCTGCAGACCTCACCCGCACCGATCCAGACCACTCCTCCCAAGGACACTTGT
AGCCCGGAGCTGCTCATGTCCTTGATCCAGACAAAGTGTGCCGACGACGCCATGACCCTGGT
ACTAAAGAAAGAGCTTGTTGCGCATTTGAAGTGCACCATCACGGGCCTGACCTTCTGGGACC
CCAGCTGTGAGGCAGAGGACAGGGGTGACAAGTTTGTCTTGCGCAGTGCTTACTCCAGCTGT
GGCATGCAGGTGTCAGCAAGTATGATCAGCAATGAGGCGGTGGTCAATATCCTGTCGAGCTC
ATCACCACAGCGGAAAAAGGTGCACTGCCTCAACATGGACAGCCTCTCTTTCCAGCTGGGCC
TCTACCTCAGCCCACACTTCCTCCAGGCCTCCAACACCATCGAGCCGGGGCAGCAGAGCTTT
GTGCAGGTCAGAGTGTCCCCATCCGTCTCCGAGTTCCTGCTCCAGTTAGACAGCTGCCACCT
GGACTTGGGGCCTGAGGGAGGCACCGTGGAACTCATCCAGGGCCGGGCGGCCAAGGGCAAC
TGTGTGAGCCTGCTGTCCCCAAGCCCCGAGGGTGACCCGCGCTTCAGCTTCCTCCTCCACTTC
TACACAGTACCCATACCCAAAACCGGCACCCTCAGCTGCACGGTAGCCCTGCGTCCCAAGAC
CGGGTCTCAAGACCAGGAAGTCCATAGGACTGTCTTCATGCGCTTGAACATCATCAGCCCTG
ACCTGTCTGGTTGCACAAGCAAAGGCCTCGTCCTGCCCGCCGTGCTGGGCATCACCTTTGGT
GCCTTCCTCATCGGGGCCCTGCTCACTGCTGCACTCTGGTACATCTACTCGCACACGCGTTCC
CCCAGCAAGCGGGAGCCCGTGGTGGCGGTGGCTGCCCCGGCCTCCTCGGAGAGCAGCAGCA
CCAACCACAGCATCGGGAGCACCCAGAGCACCCCCTGCTCCACCAGCAGCATGGCATAGCC
CCGGCCCCCCGCGCTCGCCCAGCAGGAGAGACTGAGCAGCCGCCAGCTGGGAGCACTGGTG
TGAACTCACCCTGGGAGCCAGTCCTCCACTCGACCCAGAATGGAGCCTGCTCTCCGCGCCTA
CCCTTCCCGCCTCCCTCTCAGAGGCCTGCTGCCAGTGCAGCCACTGGCTTGGAACACCTTGG
GGTCCCTCCACCCCACAGAACCTTCAACCCAGTGGGTCTGGGATATGGCTGCCCAGGAGACA
GACCACTTGCCACGCTGTTGTAAAAACCCAAGTCCCTGTCATTTGAACCTGGATCCAGCACT
GGTGAACTGAGCTGGGCAGGAAGGGAGAACTTGAAACAGATTCAGGCCAGCCCAGCCAGGC
CAACAGCACCTCCCCGCTGGGAAGAGAAGAGGGCCCAGCCCAGAGCCACCTGGATCTATCC
CTGCGGCCTCCACACCTGAACTTGCCTAACTAACTGGCAGGGGAGACAGGAGCCTAGCGGA
GCCCAGCCTGGGAGCCCAGAGGGTGGCAAGAACAGTGGGCGTTGGGAGCCTAGCTCCTGCC
ACATGGAGCCCCCTCTGCCGGTCGGGCAGCCAGCAGAGGGGGAGTAGCCAAGCTGCTTGTC
CTGGGCCTGCCCCTGTGTATTCACCACCAATAAATCAGACCATGAAACCA

Figure 7. 20 CD105 gene and its annotation indicating the promoter region, HRE, HAS, TSS and coding region.

PD-1 and PD-L1: As shown in Figure 21, the PD-L1 gene is Homo sapiens CD274, which corresponds to NCBI reference sequence NM_014143.4. The RefSeq gene transcript is 3634 nt in length and consists of 7 exons. The coding sequence (highlighted in grey) starts from position 70 with the start codon “ATG” (highlighted in green) and

ends at position 940 with the stop codon “TAA” (highlighted in red). The signal peptide is encoded by nucleotides 70 to 123 (light grey). The first exon runs from nucleotides 1 to 155 and the first exon junction is highlighted in blue. The 5` UTR and 3’ UTR are underlined and the TSS site at position 1 is shown in bold. The predicted promoter sequence of 2000 nucleotides is placed before the TSS. Increased hypoxia enhances interactions between PD-1 and PD-L1 and inhibits CTLs (91). Although expression of PD-L1 increased on macrophages under hypoxia, the presence of HREs was not detected, therefore, other TFBSs associated with hypoxia were examined, as shown in Figure 21.

Gene: PDL1
Definition: Homo sapiens CD274 molecule (CD274), transcript variant 1, mRNA
Accession No.: NM_014143.4
Length: 3634 bp
Exons: 7
First Exon: 1 to 155 ntd
Coding region: 70 to 942 ntd
Signal Peptide: 70 to 123 ntd

TTTCTCTTTTTCTAAACACAGCCTGTTTTTCAATCTCCGGGTAGTTGATCAATTGTATGGGAA
AATGAATGGCTGAAGGGTAGAAACAGGTGGGAAAGATGAACAAAAACACGAATCCTCACA
TTACTAATACGCAAATCACTGAGCAGCAAGCTGAGCAAATACCCTCAATTCCCATCAGCAAC
TTTAGAGAAAGGCAAATTCCGTTTGCCTCATTGATCATTTAGGTAGACCCTGAACACTGCTTT
CATAAAACAAAAACAAAATACCCATCCCCAGTTTAAAAAATTATTCATAGATCATCCAGGCC
ATCTAGGAGGATATGATTTAATCCTGGCTACTTGGTAAATTATTTGCCCAAGTTAACTCAGCT
AGTTAGTGGTAGATGGCTCTGAAGCCAGTTGTTTTTTTTTGTTTTGTTTTTTGCAGACCTCAA
GAGTCATGATGAACTAGCAGATCATAAAGTTTATGCCCTGGGTCTTGACCATTTTTAGAAAA
ATAAAACATTAAATGAAAATATCAGAGGGCATTGCAGATAGTAGATCTAAGTATTTTTTCAT
GAAACTTGTTGTACATGTGTGTGTCATACACAGACTATATATATGCAGTACCTGTAAACTGT
ATTGCCACATAATGTCTATATTTTCCTAGAGGTCACAGTCACCAAAGTTGGGAAGTCACCCA
ACTTCGGGAACTTTGGGAAGTCACCCAAACTTACAGTCACCAAAATTGCTCTATTCTACTAT
GTGACCTCAAAAGTGATTTGAAAGAAGGAACATCTGAGCTGGGCCCAAACCCTATTGCAATT
TTATTGGGGCCAAAGAGAACTCCATGCTCCTGCCAAATCAAGGCAGTGTCAGCCTCAATAAT
TTCCCAGATAAAAATAAAAATCTGTGATACAATCAGAATGTGAAAATTCTTATTTTGGAAGC
AAATGTCATAACCAATGCAAGGGCTATCTCAATATTCATTCATTATGCAGTATTTTGAACTGC
AGTTGAAATGAATAAGAAGGAAAGGCAAACAACGAAGAGTCCAATTTCTCAATTTAGAAAA
AGAGAAAAAAAAGAAAAGGGAGCACACAGGCACGGTGGCTCAAGCCTGTAATATCAGCAC
TTTGGCGGATCACTTGAGGTCAAGGAGTTCGAGAAAAGAGAGCACCTAGAAGTTCAGCGCG
GGATAATACTTAAGTAAATTATGACACCATCGTCTGTCATCTTGGGCCCATTCACTAACCCA
AAGCTTTCAAAAGGGCTTTCTTAACCCTCACCTAGAATAGGCTTCCGCAGCCTTAATCCTTAG
GGTGGCAGAATATCAGGGACCCTGAGCATTCTTAAAAGATGTAGCTCGGGATGGGAAGTTC
TTTTAATGACAAAGCAAATGAAGTTTCATTATGTCGAGGAACTTTGAGGAAGTCACAGAATC
CACGATTTAAAAATATATTTCCTATTATACACCCATACACACACACACACACCTACTTTCTAG
AATAAAAACCAAAGCCATATGGGTCTGCTGCTGACTTTTTATATGTTGTAGAGTTATATCAA
GTTATGTCAAGATGTTCAGTCACCTTGAAGAGGCTTTTATCAGAAAGGGGGACGCCTTTCTG
ATAAAGGTTAAGGGGTAACCTTAAGCTCTTACCCCTCTGAAGGTAAAATCAAGGTGCGTTCA
GATGTTGGCTTGTTGTAAATTTCTTTTTTTATTAATAACATACTAAATGTGGATTTGCTTTAAT
CTTCGAAACTCTTCCCGGTGAAAATCTCATTTACAAGAAAACTGGACTGACATGTTTCACTTT
CTGTTTCATTTCTATACACAGCTTTATTCCTAGGACACCAACACTAGATACCTAAACTGAAAG
CTTCCGCCGATTTCACCGAAGGTCAGGAAAGTCCAACGCCCGGCAAACTGGATTTGCTGCCT
TGGGCAGAGGTGGGCGGGACCCCGCCTCCGGGCCTGGCGCAACGCTGAGCAGCTGGCGCGT
CCCGCGCGGCCCCA**A**GTTCTGCGCAGCTTCCCGAGGCTCCGCACCAGCCGCGCTTCTGTCCG
CCTGCAGGGCATTCCAGAAAGATGAGGATATTTGCTGTCTTTATATTCATGACCTACTGGCA
TTTGCTGAACGCATTTACTGTCACGGTTCCCAAGGACCTATATGTGGTAGAGTATGGTAGCA
ATATGACAATTGAATGCAAATTCCCAGTAGAAAAACAATTAGACCTGGCTGCACTAATTGTC
TATTGGGAAATGGAGGATAAGAACATTATTCAATTTGTGCATGGAGAGGAAGACCTGAAGG
TTCAGCATAGTAGCTACAGACAGAGGGCCCGGCTGTTGAAGGACCAGCTCTCCCTGGGAAA
TGCTGCACTTCAGATCACAGATGTGAAATTGCAGGATGCAGGGGTGTACCGCTGCATGATCA
GCTATGGTGGTGCCGACTACAAGCGAATTACTGTGAAAGTCAATGCCCCATACAACAAAATC

AACCAAAGAATTTTGGTTGTGGATCCAGTCACCTCTGAACATGAACTGACATGTCAGGCTGA
GGGCTACCCCAAGGCCGAAGTCATCTGGACAAGCAGTGACCATCAAGTCCTGAGTGGTAAG
ACCACCACCACCAATTCCAAGAGAGAGGAGAAGCTTTTCAATGTGACCAGCACACTGAGAA
TCAACACAACAACTAATGAGATTTTCTACTGCACTTTTAGGAGATTAGATCCTGAGGAAAAC
CATACAGCTGAATTGGTCATCCCAGAACTACCTCTGGCACATCCTCCAAATGAAAGGACTCA
CTTGGTAATTCTGGGAGCCATCTTATTATGCCTTGGTGTAGCACTGACATTCATCTTCCGTTT
AAGAAAAGGGAGAATGATGGATGTGAAAAAATGTGGCATCCAAGATACAAACTCAAAGAA
GCAAAGTGATACACATTTGGAGGAGACGTAATCCAGCATTGGAACTTCTGATCTTCAAGCAG
GGATTCTCAACCTGTGGTTTAGGGGTTCATCGGGGCTGAGCGTGACAAGAGGAAGGAATGG
GCCCGTGGGATGCAGGCAATGTGGGACTTAAAAGGCCCAAGCACTGAAAATGGAACCTGGC
GAAAGCAGAGGAGGAGAATGAAGAAAGATGGAGTCAAACAGGGAGCCTGGAGGGAGACCT
TGATACTTTCAAATGCCTGAGGGGCTCATCGACGCCTGTGACAGGGAGAAAGGATACTTCTG
AACAAGGAGCCTCCAAGCAAATCATCCATTGCTCATCCTAGGAAGACGGGTTGAGAATCCCT
AATTTGAGGGTCAGTTCCTGCAGAAGTGCCCTTTGCCTCCACTCAATGCCTCAATTTGTTTTC
TGCATGACTGAGAGTCTCAGTGTTGGAACGGGACAGTATTTATGTATGAGTTTTTCCTATTTA
TTTTGAGTCTGTGAGGTCTTCTTGTCATGTGAGTGTGGTTGTGAATGATTTCTTTTGAAGATA
TATTGTAGTAGATGTTACAATTTTGTCGCCAAACTAAACTTGCTGCTTAATGATTTGCTCACA
TCTAGTAAAACATGGAGTATTTGTAAGGTGCTTGGTCTCCTCTATAACTACAAGTATACATTG
GAAGCATAAAGATCAAACCGTTGGTTGCATAGGATGTCACCTTTATTTAACCCATTAATACT
CTGGTTGACCTAATCTTATTCTCAGACCTCAAGTGTCTGTGCAGTATCTGTTCCATTTAAATA
TCAGCTTTACAATTATGTGGTAGCCTACACACATAATCTCATTTCATCGCTGTAACCACCCTG
TTGTGATAACCACTATTATTTTACCCATCGTACAGCTGAGGAAGCAAACAGATTAAGTAACT
TGCCCAAACCAGTAAATAGCAGACCTCAGACTGCCACCCACTGTCCTTTTATAATACAATTT
ACAGCTATATTTTACTTTAAGCAATTCTTTTATTCAAAAACCATTTATTAAGTGCCCTTGCAA
TATCAATCGCTGTGCCAGGCATTGAATCTACAGATGTGAGCAAGACAAAGTACCTGTCCTCA
AGGAGCTCATAGTATAATGAGGAGATTAACAAGAAAATGTATTATTACAATTTAGTCCAGTG
TCATAGCATAAGGATGATGCGAGGGGAAAACCCGAGCAGTGTTGCCAAGAGGAGGAAATA
GGCCAATGTGGTCTGGGACGGTTGGATATACTTAAACATCTTAATAATCAGAGTAATTTTCA
TTTACAAAGAGAGGTCGGTACTTAAAATAACCCTGAAAAATAACACTGGAATTCCTTTTCTA
GCATTATATTTATTCCTGATTTGCCTTTGCCATATAATCTAATGCTTGTTTATATAGTGTCTGG
TATTGTTTAACAGTTCTGTCTTTTCTATTTAAATGCCACTAAATTTTAAATTCATACCTTTCCA
TGATTCAAAATTCAAAAGATCCCATGGGAGATGGTTGGAAAATCTCCACTTCATCCTCCAAG
CCATTCAAGTTTCCTTTCCAGAAGCAACTGCTACTGCCTTTCATTCATATGTTCTTCTAAAGA
TAGTCTACATTTGGAAATGTATGTTAAAAGCACGTATTTTTAAAATTTTTTTCCTAAATAGTA
ACACATTGTATGTCTGCTGTGTACTTTGCTATTTTTATTTATTTTAGTGTTTCTTATATAGCAG
ATGGAATGAATTTGAAGTTCCCAGGGCTGAGGATCCATGCCTTCTTTGTTTCTAAGTTATCTT
TCCCATAGCTTTTCATTATCTTTCATATGATCCAGTATATGTTAAATATGTCCTACATATACAT
TTAGACAACCACCATTTGTTAAGTATTTGCTCTAGGACAGAGTTTGGATTTGTTTATGTTTGC
TCAAAAGGAGACCCATGGGCTCTCCAGGGTGCACTGAGTCAATCTAGTCCTAAAAAGCAAT
CTTATTATTAACTCTGTATGACAGAATCATGTCTGGAACTTTTGTTTTCTGCTTTCTGTCAAGT
ATAAACTTCACTTTGATGCTGTACTTGCAAAATCACATTTTCTTTCTGGAAATTCCGGCAGTG
TACCTTGACTGCTAGCTACCCTGTGCCAGAAAAGCCTCATTCGTTGTGCTTGAACCCTTGAAT
GCCACCAGCTGTCATCACTACACAGCCCTCCTAAGAGGCTTCCTGGAGGTTTCGAGATTCAG
ATGCCCTGGGAGATCCCAGAGTTTCCTTTCCCTCTTGGCCATATTCTGGTGTCAATGACAAGG
AGTACCTTGGCTTTGCCACATGTCAAGGCTGAAGAAACAGTGTCTCCAACAGAGCTCCTTGT
GTTATCTGTTTGTACATGTGCATTTGTACAGTAATTGGTGTGACAGTGTTCTTTGTGTGAATT
ACAGGCAAGAATTGTGGCTGAGCAAGGCACATAGTCTACTCAGTCTATTCCTAAGTCCTAAC
TCCTCCTTGTGGTGTTGGATTTGTAAGGCACTTTATCCCTTTTGTCTCATGTTTCATCGTAAAT
GGCATAGGCAGAGATGATACCTAATTCTGCATTTGATTGTCACTTTTTGTACCTGCATTAATT
TAATAAAATATTCTTATTTATTTTGTTACTTGGTACACCAGCATGTCCATTTTCTTGTTTATTT
TGTGTTTAATAAAATGTTCAGTTTAACATCCCA

Figure 7. 21 PD-L1 gene and its annotation indicating the promoter region, HRE, HAS, TSS, and coding region

As no active HREs were found in any of the genes of interest, they were further investigated for presence of binding sites for other TF related to hypoxia in order to identify a potential mechanism that could account for their upregulation on ECs and macrophages when under hypoxia.

7.5.2.2 Identifying NF-kB, STAT, Myc, cMyb, HIF1, CREB and Nrf2 binding sites

Essential TFs associated with hypoxia were investigated in the promoter regions of the target genes, CD309, CD54, CD105 and PD-L1, for specific binding sites using bioinformatic tools. PROMO tool analyses revealed TFs binding in the promoter region of target genes. The output from PROMO describes each TF binding site in detail and includes information such as: TF name and TRANSFAC database accession number, the start and end positions of the putative binding sequences, dissimilarity in percent (which indicates the rate of dissimilarity between the putative and consensus sequences for a given TF), nucleotide sequence of the potential binding site and, based on the dissimilarity index, the Random Expectation (RE) value, which shows the expected occurrences of the match in a random sequence of the same length as the query sequence. RE equally assumes equiprobability for the four nucleotides and RE query assumes nucleotide frequencies as in the query sequence. Following the annotations in the TRANSFAC gene entries, the regulatory regions of the genes also show a graphical representation of different sites to provide users the best predicted TFBSs (397, 398).

At first, transcription regulators in the promoter region of the CD309 gene within a dissimilarity margin less or equal than 15 % using PROMO (V. 3.0.2) software were identified, as shown in Figure 22. The TANSFAC database accession number shown in brackets with each of the predicted TF in the promoter region of CD309 provides the nucleotide sequence for TF binding sites (Figure 23). Then all hypoxia related TFs were studied to determine their number of binding sites and their sequences (listed in Table 7.3) in the CD309 promoter region, Hypoxia related TFBSs for HIF1, CREB, and Nrf2 were not detected in CD309. However, four NF-kappaB1, fourteen STAT4, five

STAT1B, one STAT5A, one cMyc, and seventeen cMyb binding sites were detected in the CD309 promoter region, indicating their potential role in CD309 upregulation under hypoxia, as found in the previous chapter of *in vitro* studies.

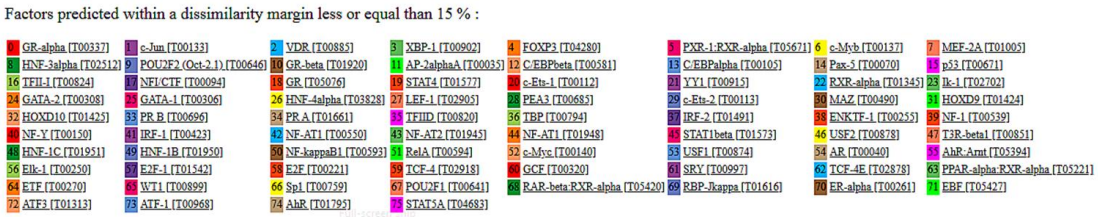

Figure 7. 22 Transcription regulators identified in the promoter region of the CD309 gene using PROMO (V. 3.0.2) software

Each TF is provided with a TRANSFAC database accession number for obtaining binding site sequences. 76 TFs were identified to have binding sites in the CD309 promoter region, including hypoxia related TFs such as NF-kappaB1, STAT4, STAT1beta, STAT5A, c-Myc, and c-Myb .however, binding sites related to hypoxia were focussed upon, therefore, only hypoxia related TFs and their binding sequences were extracted and are shown in Figure 23. Table 7.3 highlights nucleotide sequences of the identified hypoxia related TFs in the promoter sequences of the target genes.

Figure 7. 23 Nucleotide sequences for hypoxia related TFBS in the CD309 promoter region

Nucleotide sequences for STAT1B binding sites are highlighted in a grey box with a grey border, nucleotide sequences for STAT4 binding sites are in blue text, nucleotide sequences for STAT5 binding site are highlighted in green, nucleotide sequences for NF-kB1 are highlighted in yellow, nucleotide sequence for c-Myb are highlighted in light-purple with a purple border, and nucleotide sequences for c-Myc are highlighted in cyan. Note: Certain TFBS overlap as highlighted in the promoter sequence.

Table 7. 3 Prediction of hypoxia related transcription regulators and their binding sites in CD309 using Promo software					
CD309					
NF-kappaB1	**STAT4**	**STAT1beta**	**STAT5A**	**c-Myc**	**c-Myb**
TGTCACTCCCC	GGAAGT	GCTTGGAAAA	GAGTTTCTTTAAA	CACGTG	GAACTGTA
TGGAGTTCCCC	GGAATT	TTTTCCAAAA			AAACTGCC
TGATGCTCCCC	GGTTCC	ACTTGGAAAA			CAACTTTG
GGGGACCGGCA	GGAAGA	TTTGGGAAAT			AGGAGTTT
	GGAAGG	GTGGGGAAAT			CAACTTGG
	GGAAAA				TGAAGTTA
	GGAAAC				TGGAGTTC
	TTTTCC				GACAGTTG
	GGAACG				AAACTTTC
	AGTTCC				AAACTTGG
	CCTTCC				GAACTGGG
	GGAAGC				AAACTACA
	GGAAAT				AAACTACT
	GGAATG				AAACTGCT
					TGGAGTTG
					CAAAGTTG
					TCCAGTTG

Similarly, PROMO (V. 3.0.2) software was used to detect TFs in the promoter region of CD54 gene, as shown in Figure 24. A number of binding sites for hypoxia related TFs along with their sequences were identified (Figure 25), as listed in Table 4. Hypoxia related TFBSs for HIF1, CREB, and Nrf2 were not detected in CD309. However, two NF-kappaB,three NF-kappaB1, twenty STAT4, twelve STAT1B, one STAT5A and five c-Myb binding sites were detected in the CD54 promoter region.

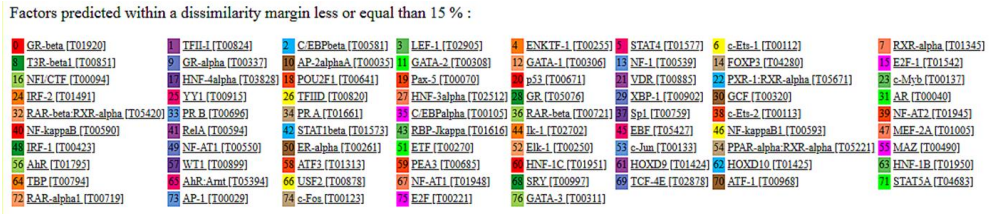

Figure 7. 24 Transcription regulators identified in the promoter region of the CD54 gene using PROMO (V. 3.0.2) software

Each TF is provided with a TRANSFAC database accession number for obtaining binding site sequences. 77 TFs were identified to have binding sites in the CD54 promoter region, including hypoxia related TFs such as NF-kappaB, NF-kappaB1, STAT4, STAT1beta, STAT5A, and c-Myb. However, binding sites related to hypoxia were focussed upon, therefore, only hypoxia related TFs and their binding sequences were extracted and are shown in Figure 25. Table 7.4 highlights nucleotide sequences of the identified hypoxia related TFs in the promoter sequences of the target genes.

Figure 7. 25 Nucleotide sequences for hypoxia related TFBS in the CD54 promoter region

Nucleotide sequences for STAT1B binding sites are highlighted in a grey box with a grey border, nucleotide sequences for STAT4 binding sites are in blue text, nucleotide sequences for STAT5 binding site are highlighted in green, nucleotide sequences for NF-kB are highlighted in light-orange, nucleotide sequences for NF-kB1 are highlighted in yellow, and nucleotide sequences for c-Myb are highlighted in light-purple with a purple border. Note: Certain TFBS overlap as highlighted in the promoter sequence.

Table 7. 4 Prediction of hypoxia related transcription regulators and their binding sites in CD54 using Promo software

CD54					
NF-kappaB	NF-kappaB1	STAT4	STAT1beta	STAT5A	c-Myb
AGGATTTTCCCA	GGGGCGTCCCC	TGTTCC	TTTTCCCAGG	CTTTTTCTGGGAG	GAACTCCT
TGGGAATGACCG	CGAGCGTCCCC	GGAATT	CCGTGGAAAT		TCGAGTTG
	GGGGAGGGGCA	CATTCC	CGGGGGAAAT		CTCAGTTT
		GGAAGG	AACAGGAAAG		GGAAGTTG
		GGAACC	GTTTCCCAGC		TAACTGCA
		GGAAGA	GTTTCCCCGC		
		TTTTCC	ATTTCCCCGG		
		CGTTCC	GCCGGGAAAC		
		GGAAAT	GCTTGGAAAT		
		AATTCC	GTCCGGAAAT		
		GGAATG	GTTTCCGGGA		
		CCTTCC	TCCGGGAAAG		
		GCTTCC			
		GGAAAG			
		GTTTCC			
		GGAAGC			
		ATTTCC			
		GATTCC			
		GGAAGT			
		GGAAAC			

TFs were also discovered in the promoter region of the CD105 gene, as shown in Figure 25. Nucleotide sequences for binding sites for the TFs retrieved through the TRANSFAC database accession number provided each identified TF in the CD105 promoter region as shown in Figure 27. Binding sites for hypoxia related TFs were also identified, as listed in Table 7.5. TFBSs for two NF-kappaB,one NF-kappaB1, eleven

STAT4, six STAT1B, one c-Myc, ten c-Myb, and one CREB were present in the CD105 promoter region.

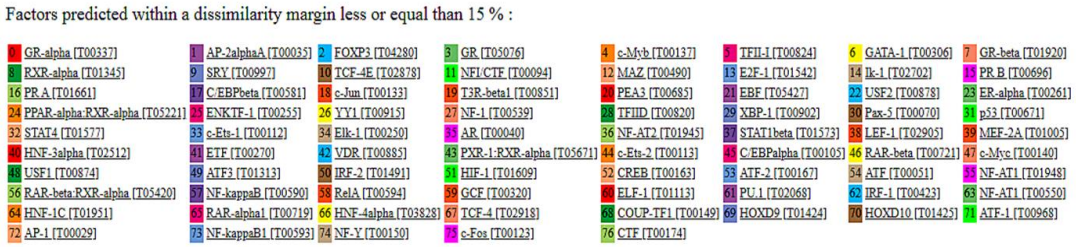

Figure 7. 26 Transcription regulators identified in the promoter region of the CD105 gene using PROMO (V. 3.0.2) software.

Each TF is provided with a TRANSFAC database accession number for obtaining binding site sequences. 77 TFs were identified to have binding sites in the CD105 promoter region, including hypoxia related TFs such as NF-kappaB, NF-kappaB1, STAT4, STAT1beta, c-Myc, c-Myb, and CREB. However, binding sites related to hypoxia were focussed upon, therefore, only hypoxia related TFs and their binding sequences were extracted and are shown in Figure 27. Table 7.5 highlights nucleotide sequences of the identified hypoxia related TFs in the promoter sequences of the target genes.

Figure 7. 27 Nucleotide sequences for hypoxia related TFBS in the CD105 promoter region

Nucleotide sequences for STAT1B binding sites are highlighted in a grey box with a grey border, nucleotide sequences for STAT4 binding sites are in blue text, nucleotide sequences for NF-kB are highlighted in light-orange, nucleotide sequences for NF-kB1 are highlighted in yellow, nucleotide sequences for c-Myb are highlighted in light-purple with a purple border, nucleotide sequences for c-Myc are highlighted in cyan, and nucleotide sequences for CREB is highlighted in dark purple with a white text. Note: Certain TFBS overlap as highlighted in the promoter sequence

Table 7. 5 Prediction of hypoxia related transcription regulators and their binding sites in CD105 using Promo software						
CD105						
NF-kappaB	**NF-kappaB1**	**STAT4**	**STAT1beta**	**c-Myc**	**c-Myb**	**CREB**
TGGGACTTCCCT	GGGGACTGTCA	GCTTCC	GTTTCCTGCT	CACGTG	AAACTATC	CGCACGTCA
TGAAAGTTCCCC		GTTTCC	CTTTCCTCAC		GAACTCTC	
		CTTTCC	TTTTCCACCC		CAACTCAC	
		GATTCC	TTTTCCTGCC		GACAGTTT	
		GGAAGC	GTTTCCTCAT		TAACTTTT	
		GGAAGG	ATTTCCTGCC		GAACTCCT	
		TTTTCC			TTCAGTTT	
		ACTTCC			CAACTGCA	
		GGAACT			GAACTACT	
		AGTTCC			GAAAGTTC	
		ATTTCC				

Various TFs were discovered in the promoter region of the PD-L1 gene, as shown in Figure 28. Details of binding sites including number and sequence for hypoxia related TFs are listed in Table 7.6 and Figure 29. PD-L1 showed one NF-kappaB, twelve STAT4, seven STAT1B, three STAT5A, and twenty-five c-Myb binding sites in the promoter region.

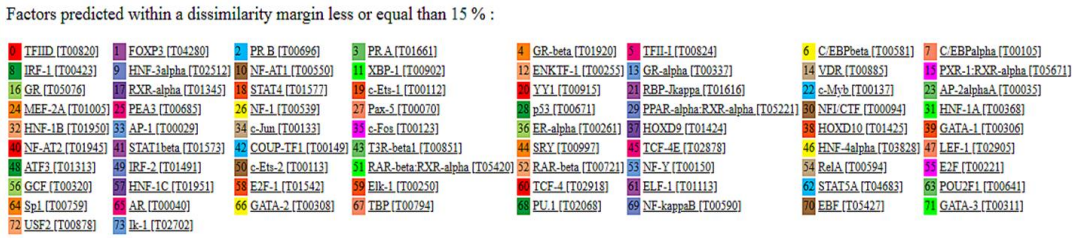

Figure 7. 28 TFBSs identified in the promoter region of the PD-L1 using PROMO (V. 3.0.2) software.

Each TF is provided with a TRANSFAC database accession number for obtaining binding site sequences. 77 TFs were identified to have binding sites in the PD-L1 promoter region, including hypoxia related TFs such as NF-kappaB, STAT4, STAT1beta, STAT5A, and c-Myb. However, binding sites related to hypoxia were focussed upon, therefore, only hypoxia related TFs and their binding sequences were extracted and are shown in Figure 29. Table 7.6 highlights nucleotide sequences of the identified hypoxia related TFs in the promoter sequences of the target genes.

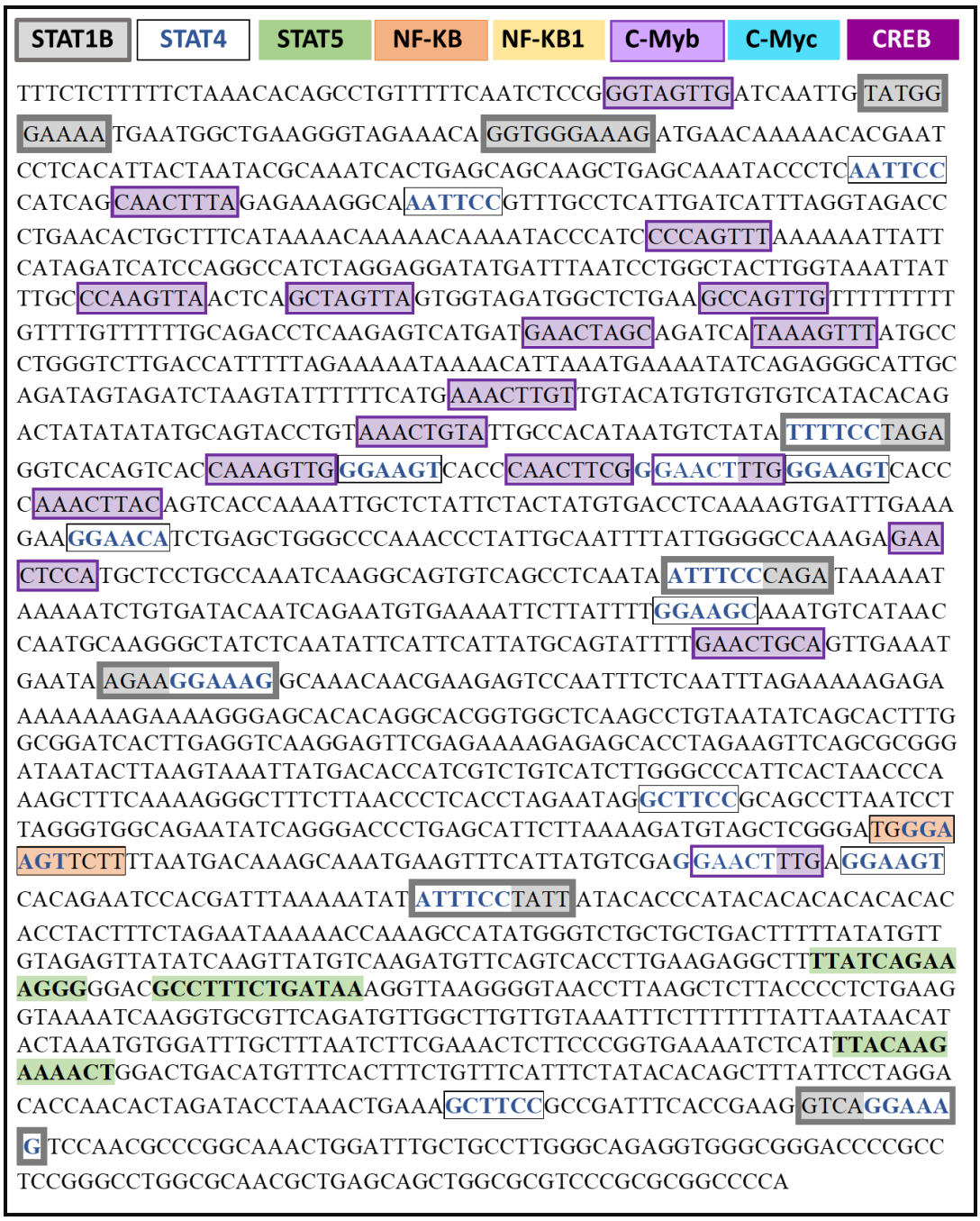

Figure 7. 29 Presentation of the nucleotide sequences for the hypoxia related TFBS in the promoter region of PD-L1.

Nucleotide sequences for STAT1B binding sites are highlighted in a grey box with a grey border, nucleotide sequences for STAT4 binding sites are in blue text, nucleotide sequences for STAT5 binding sites are highlighted in green, nucleotide sequences for NF-kB are highlighted in light-orange, and nucleotide sequences for c-Myb are highlighted in light-purple with a purple border.

Table 7. 6 List of hypoxia related TFBSs in the promoter region of PD-L1 using PROMO software

PD-L1				
NF-kappaB	**STAT4**	**STAT1beta**	**STAT5A**	**c-Myb**
TGGGAAGTTCTT	GGAAAA	TATGGGAAAA	TTATCAGAAAGGG	GGTAGTTG
	GGAAAG	GGTGGGAAAG	GCCTTTCTGATAA	CAACTTTA
	AATTCC	TTTTCCTAGA	TTACAAGAAAACT	CCCAGTTT
	TTTTCC	ATTTCCCAGA		CCAAGTTA
	GGAAGT	AGAAGGAAAG		TAACTCAG
	GGAACT	ATTTCCTATT		GCTAGTTA
	GGAACA	GTCAGGAAAG		GCCAGTTG
	ATTTCC			GAACTAGC
	GGAAGC			TAAAGTTT
	GCTTCC			AAACTTGT
	TCTTCC			AAACTGTA
	TATTCC			CAAAGTTG
				CAACTTCG
				GAACTTTG
				AAACTTAC
				GAACTCCA
				GAACTGCA
				TGCAGTTG
				AGGAGTTC
				AGAAGTTC
				GGAAGTTC
				TGAAGTTT
				TCAAGTTA
				AAACTGGA
				AAACTGAA

7.6 Discussion

Most tumours, including mesothelioma, are associated with decreased oxygen supply, resulting in regions of hypoxia (399, 400). To survive tumour cells respond to hypoxia by secreting soluble factors that interact (cross talk) with ECs to form new blood vessels and increase local oxygen supply. To regulate a hypoxic response, specific transcription and splicing factors are activated that assist cell survival. Several studies have revealed that mesothelioma aggressiveness is determined by hypoxia (400), and the *in vitro*studies in this thesis show that ECs and macrophages associated with the mesothelioma microenvironment (via exposure to TCM) respond to hypoxia by modulating surface expression of certain molecules. This *in silico* study confirms expression of the target genes among human cancers related to mesothelioma, such as colon adenocarcinoma (COADREAD), colorectal adenocarcinoma (COAD), lung adenocarcinoma (LUAD), lung squamous cell carcinoma (LUSC) and breast invasive carcinoma (BRCA).

The *in silico* studies aimed to identify mechanisms that could account for upregulation of the molecules seen in mesothelioma-exposed ECs and macrophages under hypoxia. A study of HREs and HASs was conducted to identify functionally active HREs in promoter regions of genes observed to be upregulated in the *in vitro* studies. As TFs such as HIF, STAT, NF-kB, CREB, Myc and Nrf2 play a crucial role in hypoxic responses (386) an additional *in silico* study was conducted to identify TF binding sites in promoter regions of the target genes.

Two HREs with adjacent HASs were identified in CD309 however, neither HRE was functionally active. In contrast, another HRE was found that contained an adjacent HAS within 21 nucleotides at -867 position 5' upstream from TSS, and is preceded by 'C', turning it into an E-box allowing binding of TFs from the bHLH protein family. Hence, these *in silico* techniques show that the promoter region of CD309 presents TF binding sites for NF-kB1, STAT4, STAT1B, STAT5A c-Myb and c-Myc to enable cellular responses to hypoxia. These observations provide a mechanism for results seen in the *in vitro* data from Chapter 4, which show upregulation of CD309 in tumour-exposed ECs due to hypoxia. Furthermore, HIF and VEGF pathway analyses revealed that the

HIF-1□ subunit is stabilised to interact with coactivators that modulate its transcriptional activity to regulate hypoxia-inducible genes under hypoxia. Thus, higher VEGF levels, secreted by hypoxic mesothelioma cells, bind CD309 on hypoxic ECs to mediate EC proliferation and angiogenesis. CD309 stimulates NF-kB1 under hypoxia (401, 402), as shown in Figure 30. This implies that the upregulation of CD309 seen in Chapter 4 on mesothelioma-exposed ECs under hypoxia is mainly controlled by NF-kB, STAT4, STAT1B, STAT5A c-Myb and c-Myc TFs because their binding sites are predicted in the CD309 promoter region. Furthermore, indirect activation of NF-kB through the VEGF signalling pathway via activation of HIF may also upregulate CD309 expression (403-407). High levels of CD309 expression by ECs under hypoxia may result in their proliferation and induction of vascular permeability, a feature of tumour blood vessels (408).

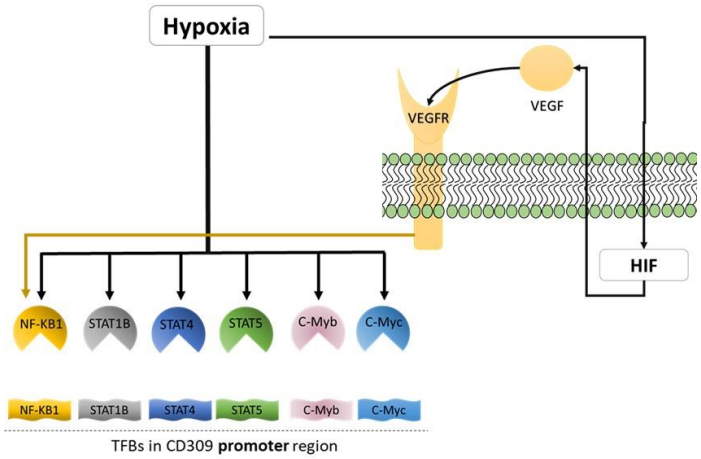

Figure 7. 30 Schematic representation of in silico analyses of TFs and the VEGF signalling pathway: NF-kB, STAT1B, STAT4, STAT5, c-Myb and c-Myc are hypoxia-related TFs that have a corresponding binding site in the promoter region of CD309. VEGFR shows activation of NF-kB1 under hypoxia.

The *in vitro* results showed an increase in CD54/ICAM expression by mesothelioma-exposed ECs under hypoxia, which was further elevated when these ECs were stimulated by the TLR7/8 agonist, VTX-2337. The *in silico* analyses detected four non-functionally active HREs, as well as binding sites for the hypoxia-related TFs, NF-kB, NF-kB1, STAT4, STAT1B, STAT5A and c-Myb, in the CD54 promoter region (Figure 31C). The results correspond with previous findings of CD54 upregulation under

hypoxia (409). The response to VTX-2337 under hypoxia may be because VTX-2337 activates the myeloid differentiation primary response gene 88 (MyD88) via TLR7 and 8 (410-412) which activates NF-kB and c-Jun. Activation of NF-kB involves MyD88 binding to interleukin-1 receptor-associated kinases (IRAK), which in turn binds TNF receptor-associated factor 6 (TRAF6) which directly binds TAK1 (MAP3K7) or TAB1/TAB2 to phosphorylate IKK-beta, leading to NF-kBactivation (11; shown in Figure 31B). The NF-kB binding site is present in the CD54 promoter region suggesting that under hypoxia, mesothelioma-exposed ECs upregulate CD54 expression leading to their survival under hypoxic conditions, VTX-2337 further promotes this response.

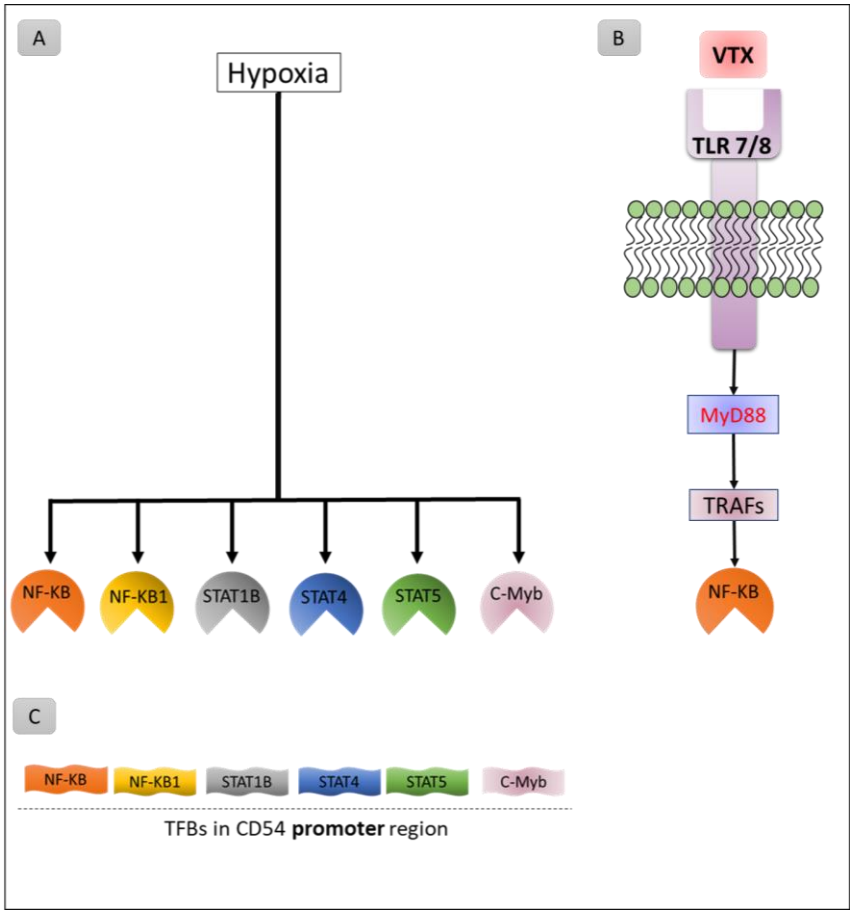

Figure 7. 31 Schematic representation of the *in silico* analysis of TLR7/8-VTX-2337 signalling pathway: NF-kB, NF-kB 1, STAT1B, STAT4, STAT5 and c-Myb are hypoxia-related TFs with corresponding binding sites in the CD54 promoter region. NF-kB activation is mediated by VTX-2337 under hypoxia.

Previous studies have demonstrated that VEGF is responsible for the upregulation of CD54 (413, 414). The *in silico* study and pathway analysis illustrate that, under hypoxia, HIF stimulates VEGF binding to VEGFR to promote activation of NF-kB1 in the same manner as described in Figure 30 for CD309. Another mechanism by which hypoxia upregulates CD54 is through HIF1α-Arg-II-mitochondrial reactive oxygen species (ROS). Hypoxia inhibits the interaction of HIF-PHD and leads to the accumulation and stabilisation of an HIF-α subunit to initiate transcription of hypoxia-driven target genes (415). Hypoxia stimulates Arg-II protein levels in ECs. HIF-1α regulates Arg-II, which induces upregulation of ICAM-1 under hypoxia in ECs (409), as shown in Figure 32.

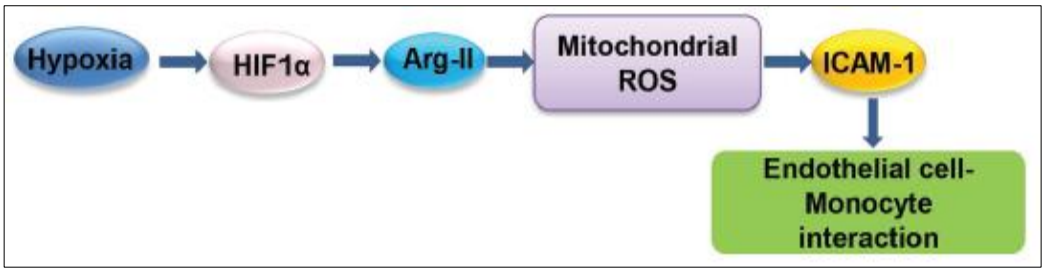

Figure 7. 32 Schematic description of the role of HIF 1α, Arg-II and mitochondrial ROS in the upregulation of ICAM-1 (CD54). Adapted from(409).

The *in silico* study and signalling pathways analyses suggest that CD54 upregulation under hypoxia is mainly due to NF-kB, NF-kB1, STAT4, STAT1B, STAT5A and c-Myb activation on account of the presence of their binding sites in the CD54 promoter region. Additionally, upregulation of CD54 was observed by activation of HIF-1α under hypoxia through the HIF-1α-Arg-II mitochondrial ROS pathway. CD54 upregulation in blood vessels represents a double-edged sword, as it could promote adhesion of infiltrating leukocytes in mesothelioma to mediate tumour regression (321), however it could also suppress dendritic cell maturation (322) and/or promote tumour-endothelial cell adhesion and metastases (323, 324).

The *in vitro* findings also showed increased CD105 (Endoglin) expression by mesothelioma-exposed ECs under hypoxia; this is in agreement with Li et al. who reported an increase in CD105 expression induced by hypoxia (285). The *in silico* study revealed three non-functionally active HREs in the CD105 promoter region. One HRE

was 5’ upstream from TSS at -472, and another was at -642. A third HRE was present 5’ upstream from TSS at -1049 and preceded by a ‘C’, forming an E-box to allow binding of bHLH proteins, as shown in Figure 20. Moreover, the *in silico* study demonstrated binding sites for NF-kB, NF-kB1, STAT4, STAT1B, c-Myc and CREB in the CD105 promoter region.

CD105or Endoglin is particularly interesting as it is a type I transmembrane protein reported to induce activation and proliferation of ECs (416). It has been reported that VEGF overexpression is associated with increased CD105 expression (417, 418). The *in silico* study and VEGF signalling pathway analyses describe how the interaction of VEGF–VEGFR activates NF-kB1 (Figure 30), whose binding sites are located in the promoter regions of CD105 and CD309. The analysis postulates upregulation of CD105 under hypoxia due to activation of NF-kB, NF-kB1, STAT4, STAT1B, c-Myc and CREB TFs and their binding sites in the CD105 promoter region (Figure 33). High expression of CD105 protects hypoxic ECs from apoptosis because hypoxia can induce cell-cycle arrest in the G1 phase of many cells, including ECs (288, 329).

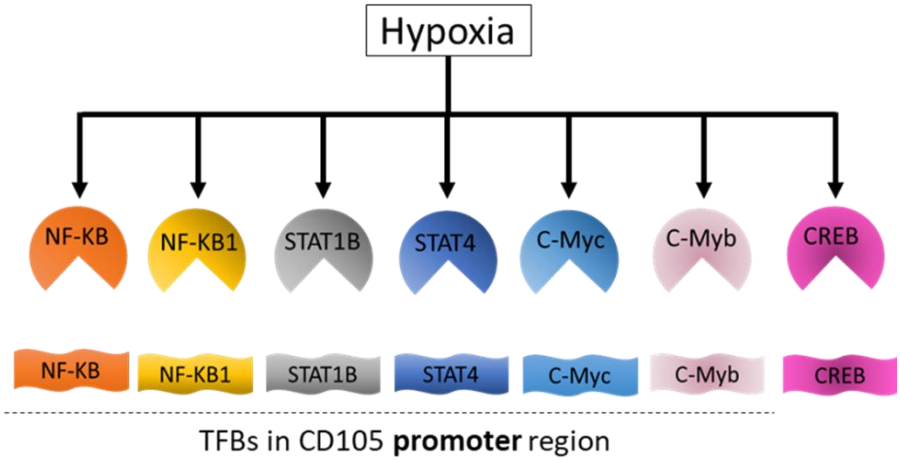

Figure 7. 33 NF-kB, NF-kB 1, STAT1B, STAT4, c-Myc, c-Myb and CREB are hypoxia-related TFs that have a corresponding binding site in the promoter region of CD105.

The *in vitro* study revealed increased expression of PD-L1 on mesothelioma-exposed macrophages under hypoxia. Moreover, PD-L1expression was further elevated upon stimulation by the combination of IL-2 with an agonist α-CD40 antibody under

hypoxia. In contrast, under normoxia, PD-L1 expression remained unaffected by IL-2/α-CD40 stimulation. No HREs were detected in the PDL-1 promoter region. However, *in silico* analyses revealed the presence of binding sites for hypoxia-related TFs (NF-kB, STAT1B, STAT4, STAT5 and c-Myb) in the PD-L1 promoter region, shown in Figure 34C.

Pathway analyses provide a possible explanation of the role of IL-2 and α-CD40 in activation of the hypoxia-related TFs, NF-kB, STAT1B and STAT5 (Figure 30 B).

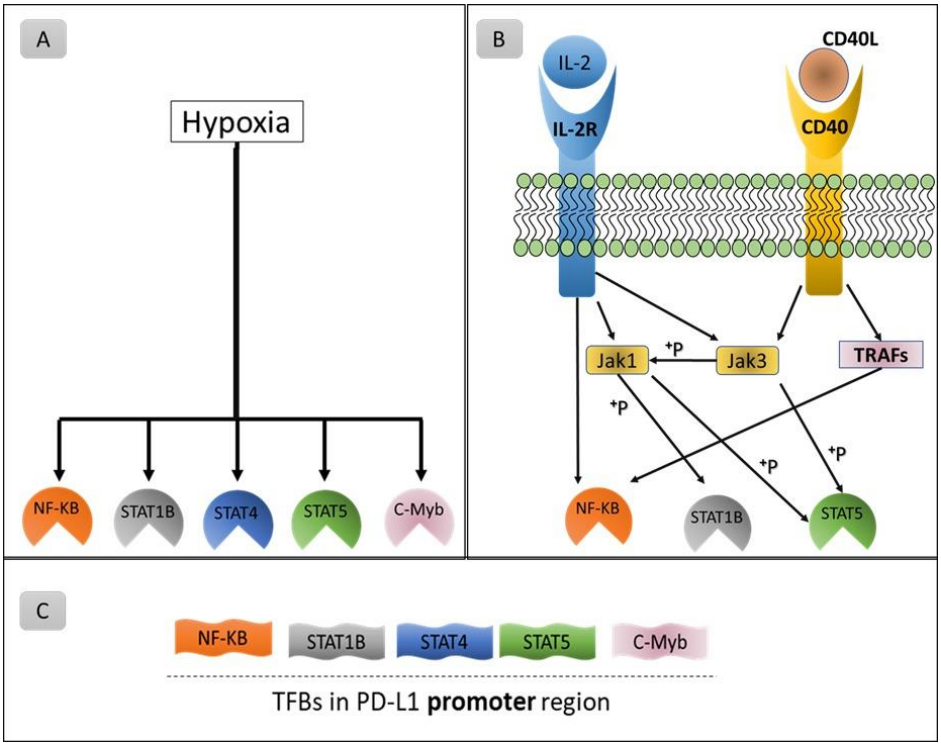

Figure 7. 34 Schematic representation of (A) hypoxia-induced activation of hypoxia-related TFs. (B) IL-2 activates NF-kB and stimulates JAK1 to phosphorylate STAT1B and STAT5. IL-2 stimulates JAK3 to phosphorylate STAT5. CD40L binds to CD40 to stimulate TRAFs to activate NF-kB, which also activates JAK3 to phosphorylate STAT5. (C) Hypoxia-related TFBSs in the promoter region of PD-L1.

CD40L binds to CD40 to engage TNFR-associated factors (TRAFs) to the cytoplasmic domain of CD40 (419). TRAFs activate various signalling pathways, including NF-kB,

mitogen-activated protein kinases (MAPKs), phosphoinositide 3-kinase (PI3K) and the phospholipase Cγ (PLCγ) (419). The cytoplasmic domain of CD40 may also directly bind the Janus family kinase 3 (Jak3) to phosphorylate STAT5 (420, 421). These complex pathways are shown to induce signals that initiate diverse cellular processes through CD40 whilst phosphorylation of STAT induces expression of PD-L1 (27).

IL-2 signalling is mediated by a multichain IL-2 receptor complex (IL-2Rα, IL-2Rβ, IL-2Rγ) (422). IL-2 binds IL-2R to activate Janus kinases-1 and -3 (JAK1 and JAK3). The cytoplasmic domain of the IL-2R is phosphorylated to provide docking sites for JAK1 and JAK3 (423). JAK3 autophosphorylates and provides docking sites for TF-STAT5. Phosphorylation instigates dimerisation and nuclear translocation of STAT5 complexes to foster transcription of specific target genes (424, 425). Downstream of JAK1, the IL-2 receptor complex binds spleen tyrosine kinase (Syk) (426). Activated Syk induces expression of the c-Myc gene (427). Lymphocyte-specific protein tyrosine kinases (Lck) are activated downstream of JAK3, which are required for induction of c-Myc genes (428). IL-2 receptor signalling also activates phosphatidylinositol 3-kinase (PI3K reg class IA (p85)/ PI3K cat class IA), which catalyses phosphorylation of phosphatidylinositol-3,4,5-trisphosphate (PtdIns(3,4,5)P3), which in turn recruits AKT to the cell membrane. AKT signalling upregulates I-kappaB (I-kB) degradation via phosphorylation of I-kB kinase alpha (IKK-alpha) to stimulate NF-kB activity, which allows transcription of NF-kB target genes (429-431).

Thus, the IL-2 and CD40 signalling pathway analyses revealed activation of the hypoxia-related TFs NF-kB, STAT1B and STAT5, whose binding sites are located in the PD-L1 promoter region, suggesting their role in further upregulation of PD-L1 expression under hypoxia.

Conclusion

This study showed that genes expressed by macrophages and ECs could be modulated by a human hypoxic mesothelioma microenvironment. In vivo expression of the target genes in human mesothelioma and other cancer types suggests an important relationship between the target genes, tumour development and responses to

immunotherapy. The presence of binding sites for essential TFs related to hypoxia in the CD309, CD54, CD105 and PD-L1 genes on ECs and/or macrophages provides a plausible underlying mechanism for their upregulation in the hypoxic mesothelioma microenvironment, as depicted in the pathway analyses. These *in silico* analyses provide deeper insight into the presence of hypoxia-related TF binding sites in the promoter regions of molecules that were elevated under hypoxic conditions on mesothelioma-exposed macrophages and ECs. The *in vitro* studies confirmed that upregulation of the target genes on ECs and/or macrophages is due to the influence of mesothelioma-derived factors (whose key function is cellular cross talk) together with hypoxia. The activation of hypoxia-related TFs via presence of their binding sites in promoter regions of the target genes. may help identify novel targets and possible combination treatments for mesothelioma.

CHAPTER 8
FINAL DISCUSSION

Our laboratory has promising preclinical data showing that IL-2/CD40-based immunotherapy can induce the regression of large mesothelioma tumours in mice. VTX-2337 has also produced promising results in preclinical models. Our research group (246) and others (114) have shown that a large proportion of the mesothelioma tumour microenvironment consists of macrophages, and this thesis considered the possibility that oxygenation levels can modify the functional status of macrophages. Similarly, ECs play a key role in tumour development, and they may also be influenced by different levels of oxygen. Therefore, the ultimate goal of this study was to understand the effect of these drugs on two key components of tumour development – macrophages and ECs – due to the major roles they play in tumour growth and drug resistance. It is also possible that oxygenation levels influence the soluble factors secreted by tumour cells, macrophages and/or ECs and therefore alter the in situ cross talk between the three cell types during tumour growth and in response to therapy.

It is known that the results of animal models may not translate into successful human research. Therefore, this project was designed: (1) to examine the crosstalk between mesothelioma tumour cells, macrophages and ECs in 2D cell culture monolayers and in a 3D co-culture system under normoxic (20% O_2) and hypoxic (2% O_2) conditions; and (2) to investigate cellular responses to immunotherapies (IL-2, α-CD40, IL-2/α-CD40 and VTX-2337). However, because attempts to develop a 3D multicellular spheroid model had limited success, only results between the normoxic and hypoxic 2D cell culture monolayers are discussed.

The results of this study confirm that normoxia and hypoxia significantly affect macrophages and ECs. However, it is still necessary to validate that the molecular differences seen in response to immunotherapies are biologically relevant by using in vivo models and developing 3D multicellular spheroid models that closely mimic the in vivo tumour microenvironment.

The effects of normoxic and hypoxic induced mesothelioma-derived factors on macrophages

Hypoxic environments are formed in tumours as they advance and macrophages are recruited and accumulate in hypoxic regions of tumours (7). Burt et al. showed that macrophages comprise approximately 27% of human malignant pleural mesothelioma cellularity and express high levels of HLA-DR, CD163 and CD206 and low or modest levels of CD80 and CD86 (114).

This study demonstrated that HLA-DR is downregulated in human macrophages regardless of oxygenation levels in response to mesothelioma-derived factors. This indicates that mesothelioma-derived factors impair the ability of tumour-associated macrophages to present antigen to $CD4^+$ T cells regardless of disease stage. However, this defect is further pronounced under hypoxic conditions. Hegmans, et al. reported that human MM tumours contain effector $CD4^+$ T cells, as well as a significant number of regulatory T cells (432). Additionally, our group (Jackaman et al.) showed that small numbers of tumour-infiltrating $CD4^+$ T cells were activated in tumour-bearing mice (433). Taken together, these data suggest that macrophages in mesothelioma might be crucial for activating $CD4^+$ T cells enabling them to exert their effector function locally in mesotheliomas.

The results also reveal that mesothelioma compromises the ability of macrophages to provide costimulatory signals for T cell activation through reduced CD40 and CD86. However, CD80 was increased under normoxia and remained unchanged under hypoxia. The further reduction of CD86 under hypoxia suggests that mesothelioma tumours may confound the ability of macrophages to stimulate tumour-specific T cells that have penetrated the tumour microenvironment. These findings partly agreed with the results reported by Burt et al. in which macrophages in mesothelioma patients were shown to express low or modest levels of CD80 and CD86, but higher levels of HLA-DR (249). In terms of HLA-DR, the conflict between the present study's findings and Burt et al's findings may be because in vivo mesothelioma tumour tissue contains factors other than those found in in vitro models. The significant decrease in CD86 and modest changes to CD80 shown in the present study better aligns with the in vivo

situation described by Burt et al., and suggests that the 'hypoxic mesothelioma model' more closely mimics real life.

No studies have reported the effect of mesothelioma on macrophage expression of CD40. However, one study examined colorectal, prostate, ovarian and breast cancers on macrophage and demonstrated that macrophages in these cancers exhibit low CD40 expression and are associated with poor prognosis, likely due to an inability to activate T cells in situ (114). This study found that mesothelioma reduces CD40 expression by macrophages under hypoxia, again implying a poor prognosis.

The data here show that, regardless of oxygen levels, mesothelioma induces upregulation of PDL-1 in macrophages, which may decrease antigen-stimulated T cell proliferation, cytokine production and effector function via PDL-1/PD-1 interactions with effector T cells. This is supported by studies showing that macrophages restrict $CD8^+$ T cell activities upon binding PD-L1 (199, 279). Moreover, PD-L1 has been found to be upregulated in macrophages in gastric cancer, which is consistent with the findings in this thesis (277). Unexpectedly, mesothelioma-exposed macrophages in normoxic and hypoxic conditions were also associated with decreased expression of several inhibitory markers, particularly A2A-R and CD39. These data suggest that the CD39/CD73/A2AR pathway does not play a role in preventing tumour-specific T cell responses in mesothelioma. This is not always the case, as d'Almeida et al. showed that macrophages isolated from ovarian cancer express the same levels of CD39 as in vitro M-CSF monocyte-derived macrophages (434), suggesting different types of cancer induce different immune evasion mechanisms. Furthermore, A2AR expression by macrophages has been proven to occur in many solid tumours confounding the issue (435, 436).

The effect of normoxic and hypoxic induced mesothelioma-derived factors on macrophage subsets

Following classical M1 LPS/IFNγ stimulation, mesothelioma-exposed macrophages increased CD40, CD80 and CD86 expression under normoxia; this represents a normal response to LPS/IFNγ-driven inflammatory signals. However, under hypoxia, CD40

expression did not change, and less upregulation of CD80 and CD86 expression was observed. The results also showed that in both normoxic and hypoxic conditions, macrophages increased PD-L1 expression in response to LPS/IFNγ stimulation. These data suggest that pro-inflammatory signals under normoxic conditions may improve anti-tumour immunogenicity, but under hypoxia, macrophage responses to proinflammatory signals, such as LPS/IFNγ, weaken in terms of CD80 and CD86 and disappear in terms of CD40. The influence of proinflammatory signals over macrophages is indirectly affected by hypoxia, which modulates secretion of soluble factors by tumours. LPS and IFNγ may boost the anti-tumour response but, because of hypoxia, responses to LPS and IFNγ decline. These data suggest that, when macrophages accumulate in hypoxic regions of mesothelioma tumours, LPS and IFNγ may be able to only partially polarise macrophages toward the M1 phenotype.

Following stimulation to induce classical M2 macrophages using IL-4 and IL-13, macrophages acquired the features of anti-inflammatory M2 cells through increased CD206 and PD-L1 expression under normoxic conditions; this was not seen under hypoxic conditions. This finding implies that IL-4/IL-13 polarisation of macrophages to anti-inflammatory, pro-tumourigenic M2-like cells increases in the presence of sufficient oxygen via elevated CD206 and PD-L1 expression. It is possible that this susceptibility to induction of an M2-like phenotype under normoxia represents an immune evasion mechanism adopted by mesothelioma. It is worth noting that incomplete polarisation toward an M2 phenotype was also seen by our group (246) as these ‘M3’ macrophages were the dominant macrophages subset in large murine mesotheliomas (246, 437).

The effect of normoxia and hypoxia on metabolic oxidative phosphorylation and glycolysis

The macrophage phenotype is largely determined based on its energy state. Macrophages produce their energy needs through oxidative phosphorylation (OXPHOS) or glycolysis (181). Glycolysis occurs within a cell’s cytosol where glycolytic enzymes are found and by which glucose is converted into pyruvate to give a small net energy (167). The OXPHOS system is located in the mitochondria and

produces large amounts of ATP (181). Proinflammatory M1 macrophages rely on glycolysis for ATP production and reduce the rate of OXPHOS upon activation (438). In contrast, M2 macrophages primarily use OXPHOS to obtain energy (351).

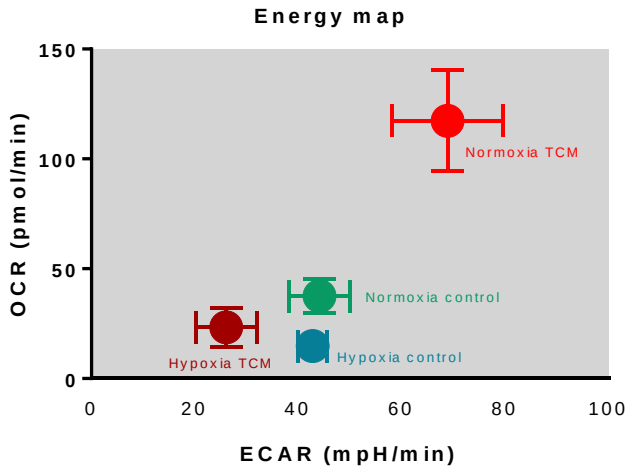

Figure 8. 1 Energy map based on OCR and ECAR macrophage responses

An energy map was obtained by plotting the ECAR and OCR values of unpolarised MØ macrophages under normoxia (normoxia control), unpolarised MØ macrophages under normoxia (hypoxia control), TCM-conditioned macrophages under normoxia (normoxia TCM) and TCM-conditioned macrophages under normoxia (hypoxia TCM).

Limited glucose availability stresses tumour cells and leads to competition for glucose with immune cells, including macrophages (253). Tumour cells dictate polarisation of macrophages to an immunosuppressive M2 phenotype via regulation of metabolic switches to rely on OXPHOS (254). In hypoxic regions, macrophages increase HIF-1α expression, which elevates glycolysis and induces polarisation towards M1 macrophages (255). In this context, malignant cells can harness metabolic by-products to hijack the function of macrophages to their own benefit. For example, macrophages

exposed to lactate secreted by glycolytic tumour cells stabilise HIF-1α that skews polarisation toward the M2 phenotype (254).

The present study's findings demonstrate that access to oxygen affects the metabolic profile of macrophages (Figure 6.1). Under normoxia, mesothelioma-exposed macrophages upregulate mitochondrial OXPHOS with high ATP production yet maintain their glycolysis rate. Under hypoxic conditions, the amount of ATP produced by OXPHOS in macrophages is reduced, but they still maintain their glycolysis rate. It is possible that mesothelioma-derived factors contain a high concentration of lactate since supernatants were collected at cell confluency. In this case, the metabolic switch under normoxia in macrophages towards OXPHOS may be due to lactate exposure. Similarly, under hypoxia, the inability of unpolarised macrophages and tumour-conditioned macrophages to increase glycolysis may also be due to lactate, which, as mentioned above, stabilises HIF-1α, thus preventing polarisation towards the M1 phenotype.

The effects of normoxic and hypoxic induced mesothelioma-derived factors on endothelial cells

Tumours require a vascular system to satisfy their need for oxygen and nutrients (236). Rapidly proliferating tumour cells and poor vasculature development lead to hypoxia. Hypoxia and the chronic secretion of growth factors result in excessive proliferation and transformation of ECs at cellular and molecular levels. However, the effect of hypoxia on ECs in mesothelioma has not yet been studied. The present study explored potential alterations in a mesothelioma tumour's newly formed blood vessels by assessing EC sensitivity to possible changes in the tumour microenvironment, including hypoxia. This study demonstrated that normoxic and hypoxic tumour derived factors can modify the functional status of ECs. Under normoxia, only CD54 increased with CD309, CD146, CD144 and CD105 remaining unchanged; however, hypoxia led to upregulation of CD309, CD146, CD105 and CD54.

Mesothelioma-derived factors induce increased CD54 expression under normoxia and hypoxia; however, CD54 was further upregulated under hypoxia. This result is

consistent with the findings that reported increased CD54 expression under hypoxia in HUVECs (319). Increased CD54 expression can lead to increased vascular permeability and leukocyte transmigration (282, 283, 320). Additionally, it has been reported that CD54 is expressed by many types of cancers, including mesothelioma (321). Overexpression of ICAM-I on mesothelioma blood vessels might favour killing mesothelioma cells by promoting adhesion of infiltrating leukocytes in (321). However, Podgrabinska et al. reported that interactions between Mac-1 on DCs and CD54 on lymphatic ECs suppress dendritic cell maturation and activate T cell function (322). However, although CD54 plays an important role in facilitating the invasion of tumour tissue by immune cells, endothelial CD54 has been shown to be involved in tumour-EC adhesion, which may facilitate disease progression and metastases in numerous types of cancer (323-326). For example, Laurent et al. showed that CD54 expressed on the surface of ECs is involved in the adhesion of different invasive bladder cancer cells to ECs (327). Additionally, a reduction in CD54 by blocking expression of CD54 in the endothelium of either the lung (301) or brain (306) abrogates metastasis to these organs. This suggests that CD54 overexpression may play a dual role in mesothelioma, which could be antitumorigenic by facilitating trafficking of anti-tumour cells, or protumourigenic by mediating mesothelioma metastasis, affecting DC maturation and facilitating monocyte infiltration that then adopt an M2-like phenotype.

Previously, CD309 overexpression has been shown under hypoxic conditions (318). This suggests that regulation of EC by VEGFR-2 expression in mesothelioma tumours is controlled by hypoxia. High levels of VEGFR-2 expression in ECs may result in their proliferation and induce permeability in mesothelioma vascularity, which may facilitate tumour metastasis, leading to a more aggressive tumour. CD105, which was upregulated under hypoxia, could protect hypoxic ECs from apoptosis, thus promoting mesothelioma angiogenesis via activated CD105 signalling (288, 439). CD146 is involved in controlling EC adhesion and cohesion, as well as vessel permeability and integrity (304). It is also associated with angiogenesis. CD146 participates in tumour progression with homophilic binding properties (309). CD146 only increased under

hypoxic conditions, implying that high CD146 expression may result in interactions with mesothelioma cells, which may lead to disease progression and metastasis.

Determining possible crosstalk between tumour-associated macrophages and endothelial cells

Tumour-associated cells, such as macrophages and ECs, play an essential role in tumour angiogenesis (259). Macrophages are a key component of inflammation during tumourigenesis; they sense hypoxia in avascular areas of tumours and release proangiogenic factors, such as VEGF (260). Thus, this study also examined the effect of macrophage-derived conditioned media under normoxic and hypoxic conditions on ECs.The data revealed that hypoxia indirectly affects VE-cadherin (CD144) expression by HUVECs by modulating soluble molecules derived from macrophages. To the best of our knowledge, no previous studies have investigated the effects of macrophages on VE-cadherin in ECs. However, our results are consistent with a study showing that hypoxia has no direct effect on VE-cadherin expression in ECs (330). These data imply that macrophage functions are regulated by hypoxia, which induces macrophages to secrete molecules that decrease VE-cadherin expression in ECs and may lead to tumour vessel leakiness in mesotheliomas. Furthermore, factors derived from LPS/INF-γ-stimulated macrophages increased CD54 expression. This suggests that the M1 phenotype may provoke leaky vasculature in mesothelioma tumours, leading to metastasis and poor prognosis.

An investigation of the possible effect of IL-2 when used as a local immunotherapy revealed that IL-2 induces unpolarised non-tumour exposed MØ macrophages to downregulate HLA-DR under normoxia, and to downregulate CD86 under normoxia and hypoxia. In contrast, regardless of oxygen level, mesothelioma-derived factors inhibited the effect of IL-2 and enabled macrophages to maintain antigen presentation via HLA-DR. The findings suggest that IL-2, in the presence of sufficient oxygen, may activate mesothelioma-associated effector $CD4^+$ T-cells by maintaining HLA-DR expression. However, under low oxygenation levels, the inability of IL-2 to elicit anti-tumour effects could result from regulatory T-cells being preferentially activated.

No effect on ECs was observed following their exposure to IL-2 or to factors derived from IL-2-stimulated macrophages.

The effect of anti-CD40 antibody on macrophages and endothelial cells under normoxia and hypoxia

Under normoxia, CD40-activated unpolarised non-tumour exposed MØ macrophages decreased CD206, CD163, HLA-DR and CD86 expression. These data contrast to findings that LPS/IFN-γ-stimulated M1 cells express high levels of CD86 and HLA-DR, and that IL-13/IL-4 stimulated M2 cells are characterised by high CD163 and CD206 expression levels. Accordingly, the data imply that naïve, unpolarised MØ macrophages activated with anti-CD40 under normoxia share features of both M1 and M2 polarised macrophages through reduction of CD206, CD163, HLA-DR and CD86. However, the impact on tumour-exposed macrophages was limited to reduced CD206 and CD86 under normoxic conditions. Under hypoxic conditions, CD40-stimulation of unpolarised MØ macrophages did not induce significant changes in the same molecules, implying hypoxia-mediated loss of function in macrophages. The data imply that α-CD40 may induce polarisation of local macrophages away from an M2 phenotype and reduce interactions between CD86 and CTLA-4 on $CD8^+$ T effector cells. No effect on ECs was found following exposure to anti-CD40 or to factors derived from anti-CD40-stimulated macrophages.

The effect of IL-2 and anti-CD40 on macrophages and endothelial cells under normoxic and hypoxic conditions

The possible effect of combining IL-2 and anti-CD40 on macrophages was investigated. The effect was found to be similar to that seen in IL-2 and anti-CD40 when used as single agents, i.e. decreased expression of CD206, CD163, HLA-DR and CD86 in macrophages under normoxia/hypoxia. These data suggest that combining IL-2 and α-CD40 may induce polarisation away from an M2 phenotype via downregulation of CD163 and CD206 likely due to α-CD40. Using IL-2/α-CD40 may reduce interactions between CD86 and CTLA-4, and reduce the capacity of local macrophages to present antigens to $CD4^+$ T cells, including regulatory $CD4^+$ T cells, due to decreased

HLA-DR via a dual effect from both IL-2 and α-CD40, which may lead to enhanced anti-tumour immunity via effector $CD8^+$ T cells.

Assessing the effect of IL-2/α-CD40 administration on macrophage bioenergetic profiles (Table 6.1) showed that, under normoxia, IL-2/anti-CD40 beneficially modulated the bioenergetics of control macrophages through upregulation of mitochondrial OXPHOS, ATP production and glycolysis, all of which are important for cell proliferation, survival and cytokine production. However, IL-2/α-CD40-induced alterations of cellular bioenergetics in macrophages were frustrated under hypoxia and upon exposure to mesothelioma derived factors, both of which perturb macrophage metabolism and likely impair macrophage function.

Table 7.1 Summary of IL-2/α-CD40 administration in macrophage bioenergetic profiles

	Normoxia		Hypoxia	
	MØ	TCM-CM	MØ	TCM-CM
Basal respiration	↑ P= 0.06			
ATP production	↑ *			
Glycolysis	↑ **			

TCM	Tumour-conditioned media
MØ	Naive macrophage (Control)
TCM-CM	TCM-conditioned macrophages

Normoxic environment

Hypoxic environment

The effect of VTX-2337 on macrophages under normoxic and hypoxic conditions

The possible effect of TLR 7/8 agonist, VTX-2337, was investigated. It was found that, under normoxia, VTX-2337 increased expression of CD40, CD80 and PDL-1 while simultaneously decreasing HLA-DR, CD86 and A2A-R in unpolarised (non-tumour exposed) MØ macrophages. VTX-2337 had a similar effect under hypoxia with increased expression of CD80 and CD40, however, no effect on HLA-DR and CD86 expression was observed. Under normoxic and hypoxic conditions, the effect of

mesothelioma-derived factors on responses to VTX-2337 was limited to upregulation of CD80 expression. These data suggest that mesothelioma modifies macrophage responses to VTX-2337 regardless of oxygenation levels, and the response is likely to be limited to increased CD80. Considering that mesothelioma contains a large number of macrophages (114), these data suggest that VTX-2337 may enhance immunogenicity by reducing macrophage expression of A2A-R and HLA-DR (thereby reducing the chance of driving $CD4^+$ regulatory T cells) as well as by slight upregulation of CD80 and CD40.

Effect of VTX-2337 on endothelial cells under normoxic and hypoxic conditions

The possible effect of VTX-2337on ECs was investigated. It was found that CD309 expression increased under normal normoxic, but not hypoxic, conditions in response to VTX-2337. However, under both normoxia and hypoxia VTX-2337 led to increased expression of CD54 under normal conditions, as well as upon exposure to tumour-conditioned media. Therefore, VTX-2337 might mediate anti-tumour immunity via increased leukocytes extravasation into mesothelioma and/or it might facilitate mesothelioma cell intravasation and implantation at a secondary site to form distant metastasis, specifically in hypoxic tumours. Furthermore, VTX-2337 increased CD309 expression in normoxic normal HUVECs. CD309 overexpression induces angiogenesis via increased EC proliferation and migration, as well as by increasing vascular permeability (440). However, the effect of VTX-2337 on EC expression of CD309 was hindered under hypoxia and in both mesothelioma tumour models. This suggests that potential vascular hyperpermeability, resulting from VTX-2337 stimulation, may be hindered in mesothelioma. No effect was observed on ECs following exposure to factors derived from VTX-2337-stimulated macrophages.

In silico techniques validated gene expression of key target molecules in human mesothelioma

The *in silico* study confirmed expression of target genes (CD309, CD54, CD54, and PD-L1) in human mesothelioma and other similar cancers such as colon adenocarcinoma (COADREAD), colorectal adenocarcinoma (COAD), lung

adenocarcinoma (LUAD), lung squamous cell carcinoma (LUSC) and breast invasive carcinoma (BRCA) providing more confidence in the *in vitro* findings described in this thesis.

HREs and hypoxia related TFBSs in promoter regions of genes upregulated under hypoxia

This part of the *in silico* study was performed to identify plausible mechanisms that could account for the elevated expression of molecules seen on mesothelioma-exposed macrophages and ECs under hypoxic conditions. CD309 was elevated on ECs and results from the study demonstrated that promoter regions of the CD309 gene contain two HREs with HASs in proximity of 21 and 23 nucleotides, respectively. However, while none of the HRE were considered functionally active in CD309 specific hypoxia related TFBSs including NF-kB1, STAT4, STAT1B, STAT5A c-Myb, and c-Myc were discovered in the CD309 promoter region providing a possible mechanism underlying elevated CD309 gene expression by ECs in mesothelioma tumours. Another possible mechanism is activation of NF-kB1 through VEGF/VEGFR interactions via the HIF signaling pathway (403-407). These findings suggest presence of the hypoxia related TFBSs, NF-kB1, STAT4, STAT1B, STAT5A c-Myb, and c-Myc, in CD309 promoter regions induce cellular response to hypoxia resulting in CD309 upregulation in mesothelioma-associated ECs (408).

Mesothelioma-exposed ECs also upregulated CD54 and CD105 under hypoxia. The *in silico* investigation identified 4 non-functionally HREs in the CD54 promoter region. However, hypoxia related TFBSs, NF-kB, NF-kB1, STAT4, STAT1B, STAT5A and c-Myb, were found in the CD54 promoter region which could account for the upregulation of CD54 on ECs observed under hypoxia. Another mechanism related to hypoxia that upregulates CD54 is HIF1α-Arg-II-mitochondrial reactive oxygen species (ROS) (409). TLR7/8 signaling further elevated CD54 on ECs under hypoxia. NF-kB is activated by agonist VTX-2337 through MyD88 and TRAFs (410-412). Taken together, multiple hypoxia related transcription factors, and TLR7/8 play a major role in upregulation of CD54 expression by ECs in mesothelioma under hypoxia.

The *in silico* analysis results for regulation of CD105 expression suggest the presence of three non-functionally active HREs in the promoter region. However, the *in silico* study located binding sites for NF-kB, NF-kB1, STAT4, STAT1B, c-Myc and CREB in the CD105 promoter region. VEGF signaling pathway analyses demonstrated activation of NF-kB1 through VEGF–VEGFR interactions and VEGF overexpression is reported to increase CD105 expression (417, 418). The analysis postulates upregulation of CD105 in mesothelioma-associated ECs under hypoxia due to activation of NF-kB, NF-kB1, STAT4, STAT1B, c-Myc and CREB TFs and their binding sites in the CD105 promoter region.

Mesothelioma-exposed macrophages upregulated PD-L1 under hypoxia; PD-L1 was further elevated when these macrophages were treated with IL-2/CD40. No HREs were detected in PD-L1 promoter regions through the *in silico* approach. However, its promoter region contained binding sites for the hypoxia related TFBS, NF-kB, STAT1B, STAT4, STAT5 and c-Myb, indicating their role in PD-L1 upregulation on mesothelioma-associated macrophages. Signaling pathway analyses for IL-2 and CD40 revealed activation of NF-kB, STAT1B, and STAT5 through Jak1, Jak3, and TRAFs (420, 421, 423-425) suggesting possible mechanism for further upregulation of PD-L1 under hypoxia. It is unclear if this is a helpful or unhelpful response. It is tempting to speculate that macrophage upregulation of PD-L1 would confound local effector $CD8^+$ T cell function, yet murine studies show that at least 80% of IL-2/CD40 treated AE17 mesothelioma are permanently cured (340).

Conclusions

The results of this study showed that oxygen levels affect mesothelioma tumour cells, macrophages and ECs. The data highlighted the complexity of the potential crosstalk between mesothelioma cells, macrophages and ECs under two different oxygenation levels, especially when considering that a single tumour microenvironment can contain both hypoxic and normoxic regions. This becomes more complicated when attempting to dissect the effect of responses to stimuli, such as LPS/IFN-γ, IL-4/IL-13, IL-2+/-anti-CD40 and VTX-2337. The impact on macrophages includes modulating their capacity for T cell stimulation via decreased HLA-DR antigen presentation, decreased or

increased co-stimulatory and co-inhibitory pathway activity, and modification of their bioenergetic profiles. The hypoxic environment proved to be harsh on macrophages, as their responses to LPS/IFN-γ were compromised in comparison to those seen under normoxia, which may contribute to their poor immunogenicity, poor responses to stimuli, downregulated mitochondrial respiratory activity and ATP production. Hypoxia plays a major role directly and indirectly on ECs by modifying molecules secreted by macrophages, thereby affecting ECs. This study demonstrates that normoxic and hypoxic mesothelioma-derived factors modify the functional status of ECs. Under normoxia, only CD54 increased, with CD309, CD146, CD144 and CD105 remaining unchanged; however, hypoxia led to upregulation of CD309, CD146, CD105 and CD54. Thus, the data suggest that mesothelioma effects on ECs include increased vascular permeability, leukocyte extravasation and potential metastatic activity. The *in silico* study confirmed genetic expression of these molecules in different cancers, including mesothelioma.

The *in silico* study also revealed an absence of functionally active HREs in genes for molecules that were upregulated on mesothelioma-associated ECs and macrophages under hypoxia, namely CD309, CD54, CD105 and PD-L1. However, hypoxia related TFBSs were identified in promoter regions of these upregulated genes. The presence of binding sites for essential TFs related to hypoxia in the VEGFR2, CD54, CD105 and PD-L1 genes on ECs and/or macrophages provides a plausible underlying mechanism for their upregulation in hypoxic regions of the mesothelioma microenvironment.

Limitations and Future Study

Firstly, the process of developing 3D multicellular mesothelioma spheroid models to validate that the differences seen in the surface-expressed molecules are biologically relevant, should continue to be optimised. Secondly, preclinical in vivo studies should be conducted using tumour samples collected at different time points during disease progression. RNASeq analyses focussing on changes to markers of hypoxia, angiogenesis and macrophage subpopulations would be very informative. Our findings may help identify novel targets and possible combination treatments for mesothelioma.

Bibliography

1. Vaupel P. Hypoxia and aggressive tumor phenotype: implications for therapy and prognosis. Oncologist. 2008;13 Suppl 3:21-6.
2. Klabatsa A, Sheaff MT, Steele JP, Evans MT, Rudd RM, Fennell DA. Expression and prognostic significance of hypoxia-inducible factor 1alpha (HIF-1alpha) in malignant pleural mesothelioma (MPM). Lung Cancer. 2006;51(1):53-9.
3. Francis RJ, Segard T, Morandeau L, Lee YC, Millward MJ, Segal A, et al. Characterization of hypoxia in malignant pleural mesothelioma with FMISO PET-CT. Lung Cancer. 2015;90(1):55-60.
4. Kim MC, Hwang SH, Kim NY, Lee HS, Ji S, Yang Y, et al. Hypoxia promotes acquisition of aggressive phenotypes in human malignant mesothelioma. BMC Cancer. 2018;18(1):819.
5. Lewis C, Murdoch C. Macrophage responses to hypoxia: implications for tumor progression and anti-cancer therapies. Am J Pathol. 2005;167(3):627-35.
6. Yancopoulos GD, Davis S, Gale NW, Rudge JS, Wiegand SJ, Holash J. Vascular-specific growth factors and blood vessel formation. Nature. 2000;407(6801):242-8.
7. Jain RK. Normalization of tumor vasculature: an emerging concept in antiangiogenic therapy. Science. 2005;307(5706):58-62.
8. Jackaman C, Cornwall S, Graham PT, Nelson DJ. CD40-activated B cells contribute to mesothelioma tumor regression. Immunol Cell Biol. 2011;89(2):255-67.
9. Jackaman C, Bundell CS, Kinnear BF, Smith AM, Filion P, van Hagen D, et al. IL-2 intratumoral immunotherapy enhances CD8+ T cells that mediate destruction of tumor cells and tumor-associated vasculature: a novel mechanism for IL-2. J Immunol. 2003;171(10):5051-63.
10. Jackaman C, Lew AM, Zhan Y, Allan JE, Koloska B, Graham PT, et al. Deliberately provoking local inflammation drives tumors to become their own protective vaccine site. Int Immunol. 2008;20(11):1467-79.
11. Augments A. VTX-2337 Is a Novel TLR8 Agonist That Activates NK Cells and. 2012.
12. Lu H, Dietsch GN, Matthews M-AH, Yang Y, Ghanekar S, Inokuma M, et al. VTX-2337 is a novel TLR8 agonist that activates NK cells and augments ADCC. Clinical cancer research. 2012;18(2):499-509.
13. Sun W, Chen Y, Wang Y, Luo P, Zhang M, Zhang H, et al. Interaction study of cancer cells and fibroblasts on a spatially confined oxygen gradient microfluidic chip to investigate the tumor microenvironment. Analyst. 2018;143(22):5431-7.
14. Shavelle R, Vavra-Musser K, Lee J, Brooks J. Life Expectancy in Pleural and Peritoneal Mesothelioma. Lung Cancer Int. 2017;2017:2782590.
15. Neumann V, Loseke S, Nowak D, Herth FJ, Tannapfel A. Malignant pleural mesothelioma: incidence, etiology, diagnosis, treatment, and occupational health. Dtsch Arztebl Int. 2013;110(18):319-26.
16. Robinson BW, Lake RA. Advances in malignant mesothelioma. N Engl J Med. 2005;353(15):1591-603.
17. Robinson BW, Musk AW, Lake RA. Malignant mesothelioma. Lancet. 2005;366(9483):397-408.
18. Bianchi C, Bianchi T. Malignant mesothelioma: global incidence and relationship with asbestos. Ind Health. 2007;45(3):379-87.
19. Gregoire M. What's the place of immunotherapy in malignant mesothelioma treatments? Cell Adh Migr. 2010;4(1):153-61.
20. Bianchi C, Bianchi T. Global mesothelioma epidemic: Trend and features. Indian J Occup Environ Med. 2014;18(2):82-8.

21. Bibby AC, Tsim S, Kanellakis N, Ball H, Talbot DC, Blyth KG, et al. Malignant pleural mesothelioma: an update on investigation, diagnosis and treatment. Eur Respir Rev. 2016;25(142):472-86.
22. Inai K. Pathology of mesothelioma. Environ Health Prev Med. 2008;13(2):60-4.
23. Yap TA, Aerts JG, Popat S, Fennell DA. Novel insights into mesothelioma biology and implications for therapy. Nature Reviews Cancer. 2017;17(8):475-88.
24. Nabavi N, Bennewith KL, Churg A, Wang Y, Collins CC, Mutti L. Switching off malignant mesothelioma: exploiting the hypoxic microenvironment. Genes Cancer. 2016;7(11-12):340-54.
25. Bakker E, Guazzelli A, Ashtiani F, Demonacos C, Krstic-Demonacos M, Mutti L. Immunotherapy advances for mesothelioma treatment. Expert Rev Anticancer Ther. 2017;17(9):799-814.
26. Thomas A, Hassan R. Immunotherapies for non-small-cell lung cancer and mesothelioma. Lancet Oncol. 2012;13(7):e301-10.
27. Starnes CO. Coley's toxins in perspective. Nature. 1992;357(6373):11-2.
28. Parish CR. Cancer immunotherapy: the past, the present and the future. Immunol Cell Biol. 2003;81(2):106-13.
29. Restifo NP, Dudley ME, Rosenberg SA. Adoptive immunotherapy for cancer: harnessing the T cell response. Nat Rev Immunol. 2012;12(4):269-81.
30. Jackaman C, Dye DE, Nelson DJ. IL-2/CD40-activated macrophages rescue age and tumor-induced T cell dysfunction in elderly mice. Age (Dordr). 2014;36(3):9655.
31. Malek TR, Castro I. Interleukin-2 receptor signaling: at the interface between tolerance and immunity. Immunity. 2010;33(2):153-65.
32. Olejniczak K, Kasprzak A. Biological properties of interleukin 2 and its role in pathogenesis of selected diseases--a review. Med Sci Monit. 2008;14(10):RA179-89.
33. Smith KA. Interleukin-2: inception, impact, and implications. Science. 1988;240(4856):1169-76.
34. Bazan JF. Unraveling the structure of IL-2. Science. 1992;257(5068):410-3.
35. Jen EY, Poindexter NJ, Farnsworth ES, Grimm EA. IL-2 regulates the expression of the tumor suppressor IL-24 in melanoma cells. Melanoma Res. 2012;22(1):19-29.
36. Clark EA, Ledbetter JA. Activation of human B cells mediated through two distinct cell surface differentiation antigens, Bp35 and Bp50. Proceedings of the National Academy of Sciences. 1986;83(12):4494-8.
37. Paulie S, Ehlin-Henriksson B, Mellstedt H, Koho H, Ben-Aissa H, Perlmann P. A p50 surface antigen restricted to human urinary bladder carcinomas and B lymphocytes. Cancer Immunol Immunother. 1985;20(1):23-8.
38. Banchereau J, Bazan F, Blanchard D, Briere F, Galizzi JP, van Kooten C, et al. The CD40 antigen and its ligand. Annu Rev Immunol. 1994;12:881-922.
39. Grewal IS, Flavell RA. The role of CD40 ligand in costimulation and T-cell activation. Immunol Rev. 1996;153:85-106.
40. Stout RD, Suttles J. The many roles of CD40 in cell-mediated inflammatory responses. Immunol Today. 1996;17(10):487-92.
41. Van Kooten C, Banchereau J. CD40-CD40 ligand: a multifunctional receptor-ligand pair. Adv Immunol. 1996;61:1-77.
42. Kawabe T, Matsushima M, Hashimoto N, Imaizumi K, Hasegawa Y. CD40/CD40 ligand interactions in immune responses and pulmonary immunity. Nagoya J Med Sci. 2011;73(3-4):69-78.
43. Nelson D, Fisher S, Robinson B. The "Trojan Horse" approach to tumor immunotherapy: targeting the tumor microenvironment. J Immunol Res. 2014;2014:789069.

44. Chiodoni C, Iezzi M, Guiducci C, Sangaletti S, Alessandrini I, Ratti C, et al. Triggering CD40 on endothelial cells contributes to tumor growth. J Exp Med. 2006;203(11):2441-50.
45. Killeen SD, Wang JH, Andrews EJ, Redmond HP. Exploitation of the Toll-like receptor system in cancer: a doubled-edged sword? Br J Cancer. 2006;95(3):247-52.
46. Lotze MT, Zeh HJ, Rubartelli A, Sparvero LJ, Amoscato AA, Washburn NR, et al. The grateful dead: damage-associated molecular pattern molecules and reduction/oxidation regulate immunity. Immunol Rev. 2007;220:60-81.
47. Cherfils-Vicini J, Platonova S, Gillard M, Laurans L, Validire P, Caliandro R, et al. Triggering of TLR7 and TLR8 expressed by human lung cancer cells induces cell survival and chemoresistance. J Clin Invest. 2010;120(4):1285-97.
48. Gantier MP, Tong S, Behlke MA, Xu D, Phipps S, Foster PS, et al. TLR7 is involved in sequence-specific sensing of single-stranded RNAs in human macrophages. The Journal of Immunology. 2008;180(4):2117-24.
49. Cervantes JL, Weinerman B, Basole C, Salazar JC. TLR8: the forgotten relative revindicated. Cell Mol Immunol. 2012;9(6):434-8.
50. Gonzalez S, Gonzalez-Rodriguez AP, Suarez-Alvarez B, Lopez-Soto A, Huergo-Zapico L, Lopez-Larrea C. Conceptual aspects of self and nonself discrimination. Self Nonself. 2011;2(1):19-25.
51. Kawai T, Akira S. The role of pattern-recognition receptors in innate immunity: update on Toll-like receptors. Nat Immunol. 2010;11(5):373-84.
52. Pandya PH, Murray ME, Pollok KE, Renbarger JL. The Immune System in Cancer Pathogenesis: Potential Therapeutic Approaches. J Immunol Res. 2016;2016:4273943.
53. Schnare M, Barton GM, Holt AC, Takeda K, Akira S, Medzhitov R. Toll-like receptors control activation of adaptive immune responses. Nat Immunol. 2001;2(10):947-50.
54. Lanca T, Silva-Santos B. The split nature of tumor-infiltrating leukocytes: Implications for cancer surveillance and immunotherapy. Oncoimmunology. 2012;1(5):717-25.
55. Sasieni P, Shelton J, Ormiston-Smith N, Thomson C, Silcocks P. What is the lifetime risk of developing cancer?: the effect of adjusting for multiple primaries. British journal of cancer. 2011;105(3):460-5.
56. Shankaran V, Ikeda H, Bruce AT, White JM, Swanson PE, Old LJ, et al. IFNgamma and lymphocytes prevent primary tumour development and shape tumour immunogenicity. Nature. 2001;410(6832):1107-11.
57. Dunn GP, Old LJ, Schreiber RD. The three Es of cancer immunoediting. Annu Rev Immunol. 2004;22:329-60.
58. Schreiber RD, Old LJ, Smyth MJ. Cancer immunoediting: integrating immunity's roles in cancer suppression and promotion. Science. 2011;331(6024):1565-70.
59. Hanahan D, Weinberg RA. Hallmarks of cancer: the next generation. Cell. 2011;144(5):646-74.
60. Arum CJ, Anderssen E, Viset T, Kodama Y, Lundgren S, Chen D, et al. Cancer immunoediting from immunosurveillance to tumor escape in microvillus-formed niche: a study of syngeneic orthotopic rat bladder cancer model in comparison with human bladder cancer. Neoplasia. 2010;12(6):434-42.
61. Dunn GP, Bruce AT, Ikeda H, Old LJ, Schreiber RD. Cancer immunoediting: from immunosurveillance to tumor escape. Nat Immunol. 2002;3(11):991-8.
62. Zou W. Immunosuppressive networks in the tumour environment and their therapeutic relevance. Nature reviews cancer. 2005;5(4):263-74.
63. Merien F. A Journey with Elie Metchnikoff: From Innate Cell Mechanisms in Infectious Diseases to Quantum Biology. Front Public Health. 2016;4:125.
64. Ginhoux F, Lim S, Hoeffel G, Low D, Huber T. Origin and differentiation of microglia. Front Cell Neurosci. 2013;7:45.

65. Ginhoux F, Greter M, Leboeuf M, Nandi S, See P, Gokhan S, et al. Fate mapping analysis reveals that adult microglia derive from primitive macrophages. Science. 2010;330(6005):841-5.
66. Fan X, Zhang H, Cheng Y, Jiang X, Zhu J, Jin T. Double roles of macrophages in human neuroimmune diseases and their animal models. Mediators of inflammation. 2016;2016.
67. Murray PJ, Wynn TA. Protective and pathogenic functions of macrophage subsets. Nat Rev Immunol. 2011;11(11):723-37.
68. Gordon S, Taylor PR. Monocyte and macrophage heterogeneity. Nat Rev Immunol. 2005;5(12):953-64.
69. Huang X, Li Y, Fu M, Xin HB. Polarizing Macrophages In Vitro. Methods Mol Biol. 2018;1784:119-26.
70. Biswas SK, Mantovani A. Macrophage plasticity and interaction with lymphocyte subsets: cancer as a paradigm. Nature immunology. 2010;11(10):889-96.
71. Jain A, Pasare C. Innate Control of Adaptive Immunity: Beyond the Three-Signal Paradigm. J Immunol. 2017;198(10):3791-800.
72. Sansom D. CD28, CTLA-4 and their ligands: who does what and to whom? Immunology. 2000;101(2):169.
73. Chen L, Flies DB. Molecular mechanisms of T cell co-stimulation and co-inhibition. Nat Rev Immunol. 2013;13(4):227-42.
74. Howland KC, Ausubel LJ, London CA, Abbas AK. The roles of CD28 and CD40 ligand in T cell activation and tolerance. J Immunol. 2000;164(9):4465-70.
75. Elgueta R, Benson MJ, de Vries VC, Wasiuk A, Guo Y, Noelle RJ. Molecular mechanism and function of CD40/CD40L engagement in the immune system. Immunol Rev. 2009;229(1):152-72.
76. Marigo I, Zilio S, Desantis G, Mlecnik B, Agnellini AH, Ugel S, et al. T Cell Cancer Therapy Requires CD40-CD40L Activation of Tumor Necrosis Factor and Inducible Nitric-Oxide-Synthase-Producing Dendritic Cells. Cancer Cell. 2016;30(4):651.
77. Lum HD, Buhtoiarov IN, Schmidt BE, Berke G, Paulnock DM, Sondel PM, et al. Tumoristatic effects of anti-CD40 mAb-activated macrophages involve nitric oxide and tumour necrosis factor-alpha. Immunology. 2006;118(2):261-70.
78. Smyth CM, Logan G, Boadle R, Rowe PB, Smythe JA, Alexander IE. Differential subcellular localization of CD86 in human PBMC-derived macrophages and DCs, and ultrastructural characterization by immuno-electron microscopy. Int Immunol. 2005;17(2):123-32.
79. Lim W, Gee K, Mishra S, Kumar A. Regulation of B7. 1 costimulatory molecule is mediated by the IFN regulatory factor-7 through the activation of JNK in lipopolysaccharide-stimulated human monocytic cells. The Journal of Immunology. 2005;175(9):5690-700.
80. Alegre ML, Frauwirth KA, Thompson CB. T-cell regulation by CD28 and CTLA-4. Nat Rev Immunol. 2001;1(3):220-8.
81. Bugeon L, Dallman MJ. Costimulation of T cells. Am J Respir Crit Care Med. 2000;162(4 Pt 2):S164-8.
82. Krummel MF, Allison JP. CD28 and CTLA-4 have opposing effects on the response of T cells to stimulation. The Journal of experimental medicine. 1995;182(2):459-65.
83. Krummel MF, Allison JP. CTLA-4 engagement inhibits IL-2 accumulation and cell cycle progression upon activation of resting T cells. The Journal of experimental medicine. 1996;183(6):2533-40.
84. Burnstock G, Boeynaems JM. Purinergic signalling and immune cells. Purinergic Signal. 2014;10(4):529-64.
85. Cekic C, Linden J. Purinergic regulation of the immune system. Nat Rev Immunol. 2016;16(3):177-92.

86. Petit-Jentreau L, Tailleux L, Coombes JL. Purinergic signaling: a common path in the macrophage response against Mycobacterium tuberculosis and toxoplasma gondii. Frontiers in Cellular and Infection Microbiology. 2017;7:347.
87. Al-Taei S, Salimu J, Spary LK, Clayton A, Lester JF, Tabi Z. Prostaglandin E2-mediated adenosinergic effects on CD14(+) cells: Self-amplifying immunosuppression in cancer. Oncoimmunology. 2017;6(2):e1268308.
88. d'Almeida SM, Kauffenstein G, Roy C, Basset L, Papargyris L, Henrion D, et al. The ecto-ATPDase CD39 is involved in the acquisition of the immunoregulatory phenotype by M-CSF-macrophages and ovarian cancer tumor-associated macrophages: regulatory role of IL-27. Oncoimmunology. 2016;5(7):e1178025.
89. Allard B, Longhi MS, Robson SC, Stagg J. The ectonucleotidases CD39 and CD73: Novel checkpoint inhibitor targets. Immunol Rev. 2017;276(1):121-44.
90. Ohta A. A Metabolic Immune Checkpoint: Adenosine in Tumor Microenvironment. Front Immunol. 2016;7:109.
91. Jiang X, Wang J, Deng X, Xiong F, Ge J, Xiang B, et al. Role of the tumor microenvironment in PD-L1/PD-1-mediated tumor immune escape. Mol Cancer. 2019;18(1):10.
92. Schalper KA, Carvajal-Hausdorf D, McLaughlin J, Velcheti V, Chen L, Sanmamed M, et al. Clinical significance of PD-L1 protein expression on tumor-associated macrophages in lung cancer. Journal for immunotherapy of cancer. 2015;3(Suppl 2).
93. Türeci Ö, Schmitt H, Fadle N, Pfreundschuh M, Sahin U. Molecular definition of a novel human galectin which is immunogenic in patients with Hodgkin's disease. Journal of Biological Chemistry. 1997;272(10):6416-22.
94. Ungerer C, Quade-Lyssy P, Radeke HH, Henschler R, Königs C, Köhl U, et al. Galectin-9 is a suppressor of T and B cells and predicts the immune modulatory potential of mesenchymal stromal cell preparations. Stem cells and development. 2014;23(7):755-66.
95. Enninga EA, Nevala WK, Holtan SG, Leontovich AA, Markovic SN. Galectin-9 modulates immunity by promoting Th2/M2 differentiation and impacts survival in patients with metastatic melanoma. Melanoma Res. 2016;26(5):429-41.
96. Monney L, Sabatos CA, Gaglia JL, Ryu A, Waldner H, Chernova T, et al. Th1-specific cell surface protein Tim-3 regulates macrophage activation and severity of an autoimmune disease. Nature. 2002;415(6871):536-41.
97. Zhu C, Anderson AC, Schubart A, Xiong H, Imitola J, Khoury SJ, et al. The Tim-3 ligand galectin-9 negatively regulates T helper type 1 immunity. Nat Immunol. 2005;6(12):1245-52.
98. Anderson AC, Anderson DE, Bregoli L, Hastings WD, Kassam N, Lei C, et al. Promotion of tissue inflammation by the immune receptor Tim-3 expressed on innate immune cells. Science. 2007;318(5853):1141-3.
99. Canton J, Neculai D, Grinstein S. Scavenger receptors in homeostasis and immunity. Nat Rev Immunol. 2013;13(9):621-34.
100. Graversen JH, Madsen M, Moestrup SK. CD163: a signal receptor scavenging haptoglobin-hemoglobin complexes from plasma. Int J Biochem Cell Biol. 2002;34(4):309-14.
101. Azad AK, Rajaram MV, Metz WL, Cope FO, Blue MS, Vera DR, et al. gamma-Tilmanocept, a New Radiopharmaceutical Tracer for Cancer Sentinel Lymph Nodes, Binds to the Mannose Receptor (CD206). J Immunol. 2015;195(5):2019-29.
102. Stein M, Keshav S, Harris N, Gordon S. Interleukin 4 potently enhances murine macrophage mannose receptor activity: a marker of alternative immunologic macrophage activation. J Exp Med. 1992;176(1):287-92.

103. Bouhlel M, Derudas B, Rigamonti E, Dièvart R, Brozek J, Haulon S, et al. PPARgamma activation primes human monocytes into alternative M2 macrophages with anti-inflammatory properties, Cell Metabol. 6 (2007) 137–143.
104. Li W, Katz BP, Spinola SM. Haemophilus ducreyi-induced interleukin-10 promotes a mixed M1 and M2 activation program in human macrophages. Infect Immun. 2012;80(12):4426-34.
105. Zhi Y, Gao P, Xin X, Li W, Ji L, Zhang L, et al. Clinical significance of sCD163 and its possible role in asthma (Review). Mol Med Rep. 2017;15(5):2931-9.
106. Rőszer T. Understanding the mysterious M2 macrophage through activation markers and effector mechanisms. Mediators of inflammation. 2015;2015.
107. Etzerodt A, Moestrup SK. CD163 and inflammation: biological, diagnostic, and therapeutic aspects. Antioxid Redox Signal. 2013;18(17):2352-63.
108. Etzerodt A, Maniecki MB, Moller K, Moller HJ, Moestrup SK. Tumor necrosis factor alpha-converting enzyme (TACE/ADAM17) mediates ectodomain shedding of the scavenger receptor CD163. J Leukoc Biol. 2010;88(6):1201-5.
109. Rittig N, Svart M, Jessen N, Moller N, Moller HJ, Gronbaek H. Macrophage activation marker sCD163 correlates with accelerated lipolysis following LPS exposure: a human-randomised clinical trial. Endocr Connect. 2018;7(1):107-14.
110. Timmermann M, Buck F, Sorg C, Högger P. Interaction of soluble CD163 with activated T lymphocytes involves its association with non-muscle myosin heavy chain type A. Immunology and cell biology. 2004;82(5):479-87.
111. Bi J, Zeng X, Zhao L, Wei Q, Yu L, Wang X, et al. miR-181a Induces Macrophage Polarized to M2 Phenotype and Promotes M2 Macrophage-mediated Tumor Cell Metastasis by Targeting KLF6 and C/EBPalpha. Mol Ther Nucleic Acids. 2016;5(9):e368.
112. Smith TD, Tse MJ, Read EL, Liu WF. Regulation of macrophage polarization and plasticity by complex activation signals. Integrative Biology. 2016;8(9):946-55.
113. Scodeller P, Simon-Gracia L, Kopanchuk S, Tobi A, Kilk K, Saalik P, et al. Precision Targeting of Tumor Macrophages with a CD206 Binding Peptide. Sci Rep. 2017;7(1):14655.
114. Burt BM, Rodig SJ, Tilleman TR, Elbardissi AW, Bueno R, Sugarbaker DJ. Circulating and tumor-infiltrating myeloid cells predict survival in human pleural mesothelioma. Cancer. 2011;117(22):5234-44.
115. Byeon SE, Lee J, Kim JH, Yang WS, Kwak YS, Kim SY, et al. Molecular mechanism of macrophage activation by red ginseng acidic polysaccharide from Korean red ginseng. Mediators Inflamm. 2012;2012:732860.
116. Hu X, Chen J, Wang L, Ivashkiv LB. Crosstalk among Jak-STAT, Toll-like receptor, and ITAM-dependent pathways in macrophage activation. J Leukoc Biol. 2007;82(2):237-43.
117. Martinez-Nunez RT, Louafi F, Sanchez-Elsner T. The interleukin 13 (IL-13) pathway in human macrophages is modulated by microRNA-155 via direct targeting of interleukin 13 receptor α1 (IL13Rα1). Journal of Biological Chemistry. 2011;286(3):1786-94.
118. Heusinkveld M, van der Burg SH. Identification and manipulation of tumor associated macrophages in human cancers. J Transl Med. 2011;9:216.
119. Brower V. Macrophages: cancer therapy's double-edged sword. J Natl Cancer Inst. 2012;104(9):649-52.
120. Kim J, Bae JS. Tumor-Associated Macrophages and Neutrophils in Tumor Microenvironment. Mediators Inflamm. 2016;2016:6058147.
121. Zhang M, He Y, Sun X, Li Q, Wang W, Zhao A, et al. A high M1/M2 ratio of tumor-associated macrophages is associated with extended survival in ovarian cancer patients. Journal of ovarian research. 2014;7(1):19.
122. Ruffell B, Affara NI, Coussens LM. Differential macrophage programming in the tumor microenvironment. Trends Immunol. 2012;33(3):119-26.

123. Schmid MC, Varner JA. Myeloid cells in the tumor microenvironment: modulation of tumor angiogenesis and tumor inflammation. J Oncol. 2010;2010:201026.
124. Bremnes RM, Al-Shibli K, Donnem T, Sirera R, Al-Saad S, Andersen S, et al. The role of tumor-infiltrating immune cells and chronic inflammation at the tumor site on cancer development, progression, and prognosis: emphasis on non-small cell lung cancer. Journal of Thoracic Oncology. 2011;6(4):824-33.
125. Yang L, Zhang Y. Tumor-associated macrophages: from basic research to clinical application. J Hematol Oncol. 2017;10(1):58.
126. Ryder M, Ghossein RA, Ricarte-Filho JC, Knauf JA, Fagin JA. Increased density of tumor-associated macrophages is associated with decreased survival in advanced thyroid cancer. Endocrine-related cancer. 2008;15(4):1069-74.
127. Zhu X-D, Zhang J-B, Zhuang P-Y, Zhu H-G, Zhang W, Xiong Y-Q, et al. High expression of macrophage colony-stimulating factor in peritumoral liver tissue is associated with poor survival after curative resection of hepatocellular carcinoma. Journal of clinical oncology. 2008;26(16):2707-16.
128. Lin EY, Nguyen AV, Russell RG, Pollard JW. Colony-stimulating factor 1 promotes progression of mammary tumors to malignancy. J Exp Med. 2001;193(6):727-40.
129. Sapi E, Kacinski BM. The role of CSF-1 in normal and neoplastic breast physiology. Proc Soc Exp Biol Med. 1999;220(1):1-8.
130. Allavena P, Piemonti L, Longoni D, Bernasconi S, Stoppacciaro A, Ruco L, et al. IL-10 prevents the differentiation of monocytes to dendritic cells but promotes their maturation to macrophages. European journal of immunology. 1998;28(1):359-69.
131. Sica A, Saccani A, Bottazzi B, Polentarutti N, Vecchi A, van Damme J, et al. Autocrine production of IL-10 mediates defective IL-12 production and NF-kappa B activation in tumor-associated macrophages. J Immunol. 2000;164(2):762-7.
132. Klimp AH, Hollema H, Kempinga C, van der Zee AG, de Vries EG, Daemen T. Expression of cyclooxygenase-2 and inducible nitric oxide synthase in human ovarian tumors and tumor-associated macrophages. Cancer Res. 2001;61(19):7305-9.
133. Franklin RA, Li MO. Ontogeny of Tumor-associated Macrophages and Its Implication in Cancer Regulation. Trends Cancer. 2016;2(1):20-34.
134. Lewis CE, Pollard JW. Distinct role of macrophages in different tumor microenvironments. Cancer Res. 2006;66(2):605-12.
135. Sultan M, Coyle KM, Vidovic D, Thomas ML, Gujar S, Marcato P. Hide-and-seek: the interplay between cancer stem cells and the immune system. Carcinogenesis. 2017;38(2):107-18.
136. Mantovani A, Sozzani S, Locati M, Allavena P, Sica A. Macrophage polarization: tumor-associated macrophages as a paradigm for polarized M2 mononuclear phagocytes. Trends in immunology. 2002;23(11):549-55.
137. Curiel TJ, Coukos G, Zou L, Alvarez X, Cheng P, Mottram P, et al. Specific recruitment of regulatory T cells in ovarian carcinoma fosters immune privilege and predicts reduced survival. Nat Med. 2004;10(9):942-9.
138. Rodriguez PC, Quiceno DG, Zabaleta J, Ortiz B, Zea AH, Piazuelo MB, et al. Arginase I production in the tumor microenvironment by mature myeloid cells inhibits T-cell receptor expression and antigen-specific T-cell responses. Cancer Res. 2004;64(16):5839-49.
139. Winograd R, Byrne KT, Evans RA, Odorizzi PM, Meyer AR, Bajor DL, et al. Induction of T-cell Immunity Overcomes Complete Resistance to PD-1 and CTLA-4 Blockade and Improves Survival in Pancreatic Carcinoma. Cancer Immunol Res. 2015;3(4):399-411.
140. Benazzi C, Al-Dissi A, Chau CH, Figg WD, Sarli G, de Oliveira JT, et al. Angiogenesis in spontaneous tumors and implications for comparative tumor biology. ScientificWorldJournal. 2014;2014:919570.

141. Sundfør K, Lyng H, Rofstad E. Tumour hypoxia and vascular density as predictors of metastasis in squamous cell carcinoma of the uterine cervix. British journal of cancer. 1998;78(6):822-7.
142. Hasan J, Byers R, Jayson GC. Intra-tumoural microvessel density in human solid tumours. Br J Cancer. 2002;86(10):1566-77.
143. Leek RD, Landers RJ, Harris AL, Lewis CE. Necrosis correlates with high vascular density and focal macrophage infiltration in invasive carcinoma of the breast. Br J Cancer. 1999;79(5-6):991-5.
144. Koide N, Nishio A, Sato T, Sugiyama A, Miyagawa S. Significance of macrophage chemoattractant protein-1 expression and macrophage infiltration in squamous cell carcinoma of the esophagus. Am J Gastroenterol. 2004;99(9):1667-74.
145. Ohta M, Kitadai Y, Tanaka S, Yoshihara M, Yasui W, Mukaida N, et al. Monocyte chemoattractant protein-1 expression correlates with macrophage infiltration and tumor vascularity in human gastric carcinomas. Int J Oncol. 2003;22(4):773-8.
146. Saji H, Koike M, Yamori T, Saji S, Seiki M, Matsushima K, et al. Significant correlation of monocyte chemoattractant protein-1 expression with neovascularization and progression of breast carcinoma. Cancer. 2001;92(5):1085-91.
147. Guo C, Buranych A, Sarkar D, Fisher PB, Wang XY. The role of tumor-associated macrophages in tumor vascularization. Vasc Cell. 2013;5(1):20.
148. Lewis CE, Hughes R. Inflammation and breast cancer. Microenvironmental factors regulating macrophage function in breast tumours: hypoxia and angiopoietin-2. Breast Cancer Res. 2007;9(3):209.
149. Schoppmann SF, Birner P, Stockl J, Kalt R, Ullrich R, Caucig C, et al. Tumor-associated macrophages express lymphatic endothelial growth factors and are related to peritumoral lymphangiogenesis. Am J Pathol. 2002;161(3):947-56.
150. Vignaud JM, Marie B, Klein N, Plenat F, Pech M, Borrelly J, et al. The role of platelet-derived growth factor production by tumor-associated macrophages in tumor stroma formation in lung cancer. Cancer Res. 1994;54(20):5455-63.
151. Balkwill F. Cancer and the chemokine network. Nat Rev Cancer. 2004;4(7):540-50.
152. Strieter RM, Belperio JA, Burdick MD, Sharma S, Dubinett SM, Keane MP. CXC chemokines: angiogenesis, immunoangiostasis, and metastases in lung cancer. Ann N Y Acad Sci. 2004;1028:351-60.
153. Strieter RM, Belperio JA, Phillips RJ, Keane MP. CXC chemokines in angiogenesis of cancer. Semin Cancer Biol. 2004;14(3):195-200.
154. Murdoch C, Giannoudis A, Lewis CE. Mechanisms regulating the recruitment of macrophages into hypoxic areas of tumors and other ischemic tissues. Blood. 2004;104(8):2224-34.
155. Poltavets V, Kochetkova M, Pitson SM, Samuel MS. The Role of the Extracellular Matrix and Its Molecular and Cellular Regulators in Cancer Cell Plasticity. Front Oncol. 2018;8:431.
156. Locati M, Deuschle U, Massardi ML, Martinez FO, Sironi M, Sozzani S, et al. Analysis of the gene expression profile activated by the CC chemokine ligand 5/RANTES and by lipopolysaccharide in human monocytes. J Immunol. 2002;168(7):3557-62.
157. Hagemann T, Robinson SC, Schulz M, Trümper L, Balkwill FR, Binder C. Enhanced invasiveness of breast cancer cell lines upon co-cultivation with macrophages is due to TNF-α dependent up-regulation of matrix metalloproteases. Carcinogenesis. 2004;25(8):1543-9.
158. Donaldson K, Murphy FA, Duffin R, Poland CA. Asbestos, carbon nanotubes and the pleural mesothelium: a review of the hypothesis regarding the role of long fibre retention in the parietal pleura, inflammation and mesothelioma. Particle and fibre toxicology. 2010;7(1):5.

159. Murphy FA, Schinwald A, Poland CA, Donaldson K. The mechanism of pleural inflammation by long carbon nanotubes: interaction of long fibres with macrophages stimulates them to amplify pro-inflammatory responses in mesothelial cells. Particle and fibre toxicology. 2012;9(1):8.
160. Demetri GD, Zenzie BW, Rheinwald JG, Griffin JD. Expression of colony-stimulating factor genes by normal human mesothelial cells and human malignant mesothelioma cells lines in vitro. Blood. 1989;74(3):940-6.
161. Schmitter D, Lauber B, Fagg B, Stahel RA. Hematopoietic growth factors secreted by seven human pleural mesothelioma cell lines: interleukin-6 production as a common feature. International journal of cancer. 1992;51(2):296-301.
162. Genard G, Lucas S, Michiels C. Reprogramming of Tumor-Associated Macrophages with Anticancer Therapies: Radiotherapy versus Chemo- and Immunotherapies. Front Immunol. 2017;8:828.
163. Chene AL, d'Almeida S, Blondy T, Tabiasco J, Deshayes S, Fonteneau JF, et al. Pleural Effusions from Patients with Mesothelioma Induce Recruitment of Monocytes and Their Differentiation into M2 Macrophages. J Thorac Oncol. 2016;11(10):1765-73.
164. Haroon ZA, Raleigh JA, Greenberg CS, Dewhirst MW. Early wound healing exhibits cytokine surge without evidence of hypoxia. Annals of surgery. 2000;231(1):137.
165. Henze AT, Mazzone M. The impact of hypoxia on tumor-associated macrophages. J Clin Invest. 2016;126(10):3672-9.
166. Dace DS, Khan AA, Kelly J, Apte RS. Interleukin-10 promotes pathological angiogenesis by regulating macrophage response to hypoxia during development. PLoS One. 2008;3(10):e3381.
167. Li XB, Gu JD, Zhou QH. Review of aerobic glycolysis and its key enzymes - new targets for lung cancer therapy. Thorac Cancer. 2015;6(1):17-24.
168. Bergman O, Ben-Shachar D. Mitochondrial Oxidative Phosphorylation System (OXPHOS) Deficits in Schizophrenia: Possible Interactions with Cellular Processes. Can J Psychiatry. 2016;61(8):457-69.
169. Cazzaniga M, Bonanni B. Relationship between metabolic reprogramming and mitochondrial activity in cancer cells. Understanding the anticancer effect of metformin and its clinical implications. Anticancer research. 2015;35(11):5789-96.
170. Fu Y, Liu S, Yin S, Niu W, Xiong W, Tan M, et al. The reverse Warburg effect is likely to be an Achilles' heel of cancer that can be exploited for cancer therapy. Oncotarget. 2017;8(34):57813.
171. Liberti MV, Locasale JW. The Warburg effect: how does it benefit cancer cells? Trends in biochemical sciences. 2016;41(3):211-8.
172. Li S, Li J, Dai W, Zhang Q, Feng J, Wu L, et al. Genistein suppresses aerobic glycolysis and induces hepatocellular carcinoma cell death. Br J Cancer. 2017;117(10):1518-28.
173. Ganapathy-Kanniappan S, Geschwind J-FH. Tumor glycolysis as a target for cancer therapy: progress and prospects. Molecular cancer. 2013;12(1):1-11.
174. Aparicio LM, Villaamil VM, Calvo MB, Rubira LV, Rois JM, Valladares-Ayerbes M, et al. Glucose transporter expression and the potential role of fructose in renal cell carcinoma: A correlation with pathological parameters. Mol Med Rep. 2010;3(4):575-80.
175. Anderson NM, Mucka P, Kern JG, Feng H. The emerging role and targetability of the TCA cycle in cancer metabolism. Protein Cell. 2018;9(2):216-37.
176. Barron CC, Bilan PJ, Tsakiridis T, Tsiani E. Facilitative glucose transporters: Implications for cancer detection, prognosis and treatment. Metabolism. 2016;65(2):124-39.
177. Zhao Y, Butler EB, Tan M. Targeting cellular metabolism to improve cancer therapeutics. Cell Death Dis. 2013;4:e532.

178. Wang F, Zhang S, Jeon R, Vuckovic I, Jiang X, Lerman A, et al. Interferon Gamma Induces Reversible Metabolic Reprogramming of M1 Macrophages to Sustain Cell Viability and Pro-Inflammatory Activity. EBioMedicine. 2018;30:303-16.
179. Qiu X, Guo H, Yang J, Ji Y, Wu CS, Chen X. Down-regulation of guanylate binding protein 1 causes mitochondrial dysfunction and cellular senescence in macrophages. Sci Rep. 2018;8(1):1679.
180. Del Rey MJ, Valín Á, Usategui A, García-Herrero CM, Sánchez-Aragó M, Cuezva JM, et al. Hif-1α knockdown reduces glycolytic metabolism and induces cell death of human synovial fibroblasts under normoxic conditions. Scientific reports. 2017;7(1):1-10.
181. Diskin C, Palsson-McDermott EM. Metabolic Modulation in Macrophage Effector Function. Front Immunol. 2018;9:270.
182. Rabold K, Netea MG, Adema GJ, Netea-Maier RT. Cellular metabolism of tumor-associated macrophages - functional impact and consequences. FEBS Lett. 2017;591(19):3022-41.
183. Corcoran SE, O'Neill LA. HIF1alpha and metabolic reprogramming in inflammation. J Clin Invest. 2016;126(10):3699-707.
184. Galvan-Pena S, O'Neill LA. Metabolic reprograming in macrophage polarization. Front Immunol. 2014;5:420.
185. Jeong H, Kim S, Hong B-J, Lee C-J, Kim Y-E, Bok S, et al. Tumor-associated macrophages enhance tumor hypoxia and aerobic glycolysis. Cancer research. 2019;79(4):795-806.
186. Pugsley MK, Tabrizchi R. The vascular system. An overview of structure and function. J Pharmacol Toxicol Methods. 2000;44(2):333-40.
187. Klagsbrun M, Moses MA. Molecular angiogenesis. Chem Biol. 1999;6(8):R217-24.
188. Patan S. Vasculogenesis and angiogenesis as mechanisms of vascular network formation, growth and remodeling. Journal of neuro-oncology. 2000;50(1-2):1-15.
189. Mentzer SJ, Konerding MA. Intussusceptive angiogenesis: expansion and remodeling of microvascular networks. Angiogenesis. 2014;17(3):499-509.
190. Carmeliet P. Angiogenesis in life, disease and medicine. Nature. 2005;438(7070):932-6.
191. Kolte D, McClung JA, Aronow WS. Vasculogenesis and angiogenesis. Translational Research in Coronary Artery Disease: Elsevier; 2016. p. 49-65.
192. Watnick RS. The role of the tumor microenvironment in regulating angiogenesis. Cold Spring Harb Perspect Med. 2012;2(12):a006676.
193. Folkman J. Tumor angiogenesis: therapeutic implications. N Engl J Med. 1971;285(21):1182-6.
194. Hillen F, Griffioen AW. Tumour vascularization: sprouting angiogenesis and beyond. Cancer Metastasis Rev. 2007;26(3-4):489-502.
195. Holmgren L, O'Reilly MS, Folkman J. Dormancy of micrometastases: balanced proliferation and apoptosis in the presence of angiogenesis suppression. Nat Med. 1995;1(2):149-53.
196. Vilanova G, Colominas I, Gomez H. A mathematical model of tumour angiogenesis: growth, regression and regrowth. J R Soc Interface. 2017;14(126).
197. Goel S, Duda DG, Xu L, Munn LL, Boucher Y, Fukumura D, et al. Normalization of the vasculature for treatment of cancer and other diseases. Physiol Rev. 2011;91(3):1071-121.
198. Jain RK. Taming vessels to treat cancer. Sci Am. 2008;298(1):56-63.
199. Nagy J, Chang S, Dvorak A, Dvorak H. Why are tumour blood vessels abnormal and why is it important to know? British journal of cancer. 2009;100(6):865-9.
200. Chaplin DJ, Olive PL, Durand RE. Intermittent blood flow in a murine tumor: radiobiological effects. Cancer Res. 1987;47(2):597-601.

201. Martin TA, Jiang WG. Loss of tight junction barrier function and its role in cancer metastasis. Biochim Biophys Acta. 2009;1788(4):872-91.
202. Mai J, Virtue A, Shen J, Wang H, Yang X-F. An evolving new paradigm: endothelial cells–conditional innate immune cells. Journal of hematology & oncology. 2013;6(1):61.
203. Koyama S, Matsunaga S, Imanishi M, Maekawa Y, Kitano H, Takeuchi H, et al. Tumour blood vessel normalisation by prolyl hydroxylase inhibitor repaired sensitivity to chemotherapy in a tumour mouse model. Sci Rep. 2017;7:45621.
204. Schaaf MB, Garg AD, Agostinis P. Defining the role of the tumor vasculature in antitumor immunity and immunotherapy. Cell Death Dis. 2018;9(2):115.
205. Mak IW, Evaniew N, Ghert M. Lost in translation: animal models and clinical trials in cancer treatment. Am J Transl Res. 2014;6(2):114-8.
206. Nunes AS, Barros AS, Costa EC, Moreira AF, Correia IJ. 3D tumor spheroids as in vitro models to mimic in vivo human solid tumors resistance to therapeutic drugs. Biotechnology and bioengineering. 2019;116(1):206-26.
207. Chatzinikolaidou M. Cell spheroids: the new frontiers in in vitro models for cancer drug validation. Drug Discov Today. 2016;21(9):1553-60.
208. Menshykau D. Emerging technologies for prediction of drug candidate efficacy in the preclinical pipeline. Drug Discov Today. 2017;22(11):1598-603.
209. Weiswald LB, Bellet D, Dangles-Marie V. Spherical cancer models in tumor biology. Neoplasia. 2015;17(1):1-15.
210. Pampaloni F, Reynaud EG, Stelzer EH. The third dimension bridges the gap between cell culture and live tissue. Nature reviews Molecular cell biology. 2007;8(10):839-45.
211. Spencer VA, Xu R, Bissell MJ. Gene expression in the third dimension: the ECM-nucleus connection. J Mammary Gland Biol Neoplasia. 2010;15(1):65-71.
212. Jacks T, Weinberg RA. Taking the study of cancer cell survival to a new dimension. Cell. 2002;111(7):923-5.
213. Manning LS, Whitaker D, Murch AR, Garlepp MJ, Davis MR, Musk AW, et al. Establishment and characterization of five human malignant mesothelioma cell lines derived from pleural effusions. International journal of cancer. 1991;47(2):285-90.
214. Pegg DE. Principles of cryopreservation. Methods Mol Biol. 2007;368:39-57.
215. Cohen AB. The interaction of α-1-antitrypsin with chymotrypsin, trypsin and elastase. Biochimica et Biophysica Acta (BBA)-Enzymology. 1975;391(1):193-200.
216. Jaffe EA, Nachman RL, Becker CG, Minick CR. Culture of human endothelial cells derived from umbilical veins. Identification by morphologic and immunologic criteria. J Clin Invest. 1973;52(11):2745-56.
217. Baker RL, Mallevaey T, Gapin L, Haskins K. T cells interact with T cells via CD40-CD154 to promote autoimmunity in type 1 diabetes. Eur J Immunol. 2012;42(3):672-80.
218. Brutkiewicz RR. Cell signaling pathways that regulate antigen presentation. The journal of immunology. 2016;197(8):2971-9.
219. Porcheray F, Viaud S, Rimaniol AC, Leone C, Samah B, Dereuddre-Bosquet N, et al. Macrophage activation switching: an asset for the resolution of inflammation. Clinical & Experimental Immunology. 2005;142(3):481-9.
220. Shi L, Chen S, Yang L, Li Y. The role of PD-1 and PD-L1 in T-cell immune suppression in patients with hematological malignancies. J Hematol Oncol. 2013;6(1):74.
221. Huang S, Apasov S, Koshiba M, Sitkovsky M. Role of A2a extracellular adenosine receptor-mediated signaling in adenosine-mediated inhibition of T-cell activation and expansion. Blood. 1997;90(4):1600-10.
222. Kuchroo VK, Dardalhon V, Xiao S, Anderson AC. New roles for TIM family members in immune regulation. Nat Rev Immunol. 2008;8(8):577-80.

223. Muller WA. Getting leukocytes to the site of inflammation. Vet Pathol. 2013;50(1):7-22.
224. Kevil CG, Orr AW, Langston W, Mickett K, Murphy-Ullrich J, Patel RP, et al. Intercellular adhesion molecule-1 (ICAM-1) regulates endothelial cell motility through a nitric oxide-dependent pathway. Journal of Biological Chemistry. 2004;279(18):19230-8.
225. Huang WC, Chan ST, Yang TL, Tzeng CC, Chen CC. Inhibition of ICAM-1 gene expression, monocyte adhesion and cancer cell invasion by targeting IKK complex: molecular and functional study of novel alpha-methylene-gamma-butyrolactone derivatives. Carcinogenesis. 2004;25(10):1925-34.
226. Ramos TN, Bullard DC, Barnum SR. ICAM-1: isoforms and phenotypes. J Immunol. 2014;192(10):4469-74.
227. Barthel SR, Gavino JD, Descheny L, Dimitroff CJ. Targeting selectins and selectin ligands in inflammation and cancer. Expert Opin Ther Targets. 2007;11(11):1473-91.
228. Nassiri F, Cusimano MD, Scheithauer BW, Rotondo F, Fazio A, Yousef GM, et al. Endoglin (CD105): a review of its role in angiogenesis and tumor diagnosis, progression and therapy. Anticancer Res. 2011;31(6):2283-90.
229. Gavard J. Endothelial permeability and VE-cadherin: a wacky comradeship. Cell Adh Migr. 2014;8(2):158-64.
230. Lei X, Guan CW, Song Y, Wang H. The multifaceted role of CD146/MCAM in the promotion of melanoma progression. Cancer Cell Int. 2015;15(1):3.
231. Liu Z, Qi L, Li Y, Zhao X, Sun B. VEGFR2 regulates endothelial differentiation of colon cancer cells. BMC Cancer. 2017;17(1):593.
232. Koenen RR, Pruessmeyer J, Soehnlein O, Fraemohs L, Zernecke A, Schwarz N, et al. Regulated release and functional modulation of junctional adhesion molecule A by disintegrin metalloproteinases. Blood. 2009;113(19):4799-809.
233. Goetsch L, Haeuw JF, Beau-Larvor C, Gonzalez A, Zanna L, Malissard M, et al. A novel role for junctional adhesion molecule-A in tumor proliferation: modulation by an anti-JAM-A monoclonal antibody. Int J Cancer. 2013;132(6):1463-74.
234. Symersky J, Osowski D, Walters DE, Mueller DM. Oligomycin frames a common drug-binding site in the ATP synthase. Proc Natl Acad Sci U S A. 2012;109(35):13961-5.
235. Terada H. Uncouplers of oxidative phosphorylation. Environ Health Perspect. 1990;87:213-8.
236. Trotta AP, Gelles JD, Serasinghe MN, Loi P, Arbiser JL, Chipuk JE. Disruption of mitochondrial electron transport chain function potentiates the pro-apoptotic effects of MAPK inhibition. Journal of Biological Chemistry. 2017;292(28):11727-39.
237. Tidmarsh GF, Tanner LI, O'Connor J, Eng C, Mordec K. Effect of 2-Deoxyglucose, a Glycolytic Inhibitor, on the ATP Levels and Viability of B Lymphocytes from Subjects with Chronic Lymphocytic Leukemia (CLL). American Society of Hematology; 2004.
238. Condeelis J, Pollard JW. Macrophages: obligate partners for tumor cell migration, invasion, and metastasis. Cell. 2006;124(2):263-6.
239. Quail DF, Joyce JA. Microenvironmental regulation of tumor progression and metastasis. Nat Med. 2013;19(11):1423-37.
240. Marcq E, Siozopoulou V, De Waele J, van Audenaerde J, Zwaenepoel K, Santermans E, et al. Prognostic and predictive aspects of the tumor immune microenvironment and immune checkpoints in malignant pleural mesothelioma. Oncoimmunology. 2017;6(1):e1261241.
241. Schürch CM, Forster S, Brühl F, Yang SH, Felley-Bosco E, Hewer E. The "don't eat me" signal CD47 is a novel diagnostic biomarker and potential therapeutic target for diffuse malignant mesothelioma. Oncoimmunology. 2018;7(1):e1373235.
242. Kowal J, Kornete M, Joyce JA. Re-education of macrophages as a therapeutic strategy in cancer. Immunotherapy. 2019;11(8):677-89.

243. Muz B, de la Puente P, Azab F, Azab AK. The role of hypoxia in cancer progression, angiogenesis, metastasis, and resistance to therapy. Hypoxia (Auckl). 2015;3:83-92.
244. Corzo CA, Condamine T, Lu L, Cotter MJ, Youn JI, Cheng P, et al. HIF-1alpha regulates function and differentiation of myeloid-derived suppressor cells in the tumor microenvironment. J Exp Med. 2010;207(11):2439-53.
245. Doedens AL, Stockmann C, Rubinstein MP, Liao D, Zhang N, DeNardo DG, et al. Macrophage expression of hypoxia-inducible factor-1α suppresses T-cell function and promotes tumor progression. Cancer research. 2010;70(19):7465-75.
246. Jackaman C, Yeoh TL, Acuil ML, Gardner JK, Nelson DJ. Murine mesothelioma induces locally-proliferating IL-10(+)TNF-alpha(+)CD206(-)CX3CR1(+) M3 macrophages that can be selectively depleted by chemotherapy or immunotherapy. Oncoimmunology. 2016;5(6):e1173299.
247. Del Rey MJ, Valin A, Usategui A, Garcia-Herrero CM, Sanchez-Arago M, Cuezva JM, et al. Hif-1alpha Knockdown Reduces Glycolytic Metabolism and Induces Cell Death of Human Synovial Fibroblasts Under Normoxic Conditions. Sci Rep. 2017;7(1):3644.
248. Francis RJ, Segard T, Morandeau L, Lee YG, Millward MJ, Segal A, et al. Characterization of hypoxia in malignant pleural mesothelioma with FMISO PET-CT. Lung Cancer. 2015;90(1):55-60.
249. Ong SM, Tan YC, Beretta O, Jiang D, Yeap WH, Tai JJ, et al. Macrophages in human colorectal cancer are pro-inflammatory and prime T cells towards an anti-tumour type-1 inflammatory response. Eur J Immunol. 2012;42(1):89-100.
250. Hoves S, Ooi CH, Wolter C, Sade H, Bissinger S, Schmittnaegel M, et al. Rapid activation of tumor-associated macrophages boosts preexisting tumor immunity. J Exp Med. 2018;215(3):859-76.
251. Mathur RK, Awasthi A, Saha B. The conundrum of CD40 function: host protection or disease promotion? Trends Parasitol. 2006;22(3):117-22.
252. Nakajima A, Kodama T, Morimoto S, Azuma M, Takeda K, Oshima H, et al. Antitumor effect of CD40 ligand: elicitation of local and systemic antitumor responses by IL-12 and B7. J Immunol. 1998;161(4):1901-7.
253. Turbitt WJ, Demark-Wahnefried W, Peterson CM, Norian LA. Targeting Glucose Metabolism to Enhance Immunotherapy: Emerging Evidence on Intermittent Fasting and Calorie Restriction Mimetics. Front Immunol. 2019;10:1402.
254. Wegiel B, Vuerich M, Daneshmandi S, Seth P. Metabolic Switch in the Tumor Microenvironment Determines Immune Responses to Anti-cancer Therapy. Front Oncol. 2018;8:284.
255. Wang T, Liu H, Lian G, Zhang S-Y, Wang X, Jiang C. HIF1α-induced glycolysis metabolism is essential to the activation of inflammatory macrophages. Mediators of inflammation. 2017;2017.
256. Van den Bossche J, Baardman J, de Winther MP. Metabolic characterization of polarized M1 and M2 bone marrow-derived macrophages using real-time extracellular flux analysis. JoVE (Journal of Visualized Experiments). 2015(105):e53424.
257. Carmeliet P, Jain RK. Angiogenesis in cancer and other diseases. Nature. 2000;407(6801):249-57.
258. Vaupel P, Harrison L. Tumor hypoxia: causative factors, compensatory mechanisms, and cellular response. Oncologist. 2004;9 Suppl 5:4-9.
259. Guo S, Deng CX. Effect of Stromal Cells in Tumor Microenvironment on Metastasis Initiation. Int J Biol Sci. 2018;14(14):2083-93.
260. Riabov V, Gudima A, Wang N, Mickley A, Orekhov A, Kzhyshkowska J. Role of tumor associated macrophages in tumor angiogenesis and lymphangiogenesis. Front Physiol. 2014;5:75.

261. Hida K, Maishi N, Annan DA, Hida Y. Contribution of Tumor Endothelial Cells in Cancer Progression. Int J Mol Sci. 2018;19(5).
262. Jain RK, Martin JD, Stylianopoulos T. The role of mechanical forces in tumor growth and therapy. Annual review of biomedical engineering. 2014;16:321-46.
263. Shibuya M. Vascular Endothelial Growth Factor (VEGF) and Its Receptor (VEGFR) Signaling in Angiogenesis: A Crucial Target for Anti- and Pro-Angiogenic Therapies. Genes Cancer. 2011;2(12):1097-105.
264. Miettinen M, Rikala M-S, Rysz J, Lasota J, Wang Z-F. Vascular endothelial growth factor receptor 2 (VEGFR2) as a marker for malignant vascular tumors and mesothelioma–immunohistochemical study of 262 vascular endothelial and 1640 nonvascular tumors. The American journal of surgical pathology. 2012;36(4):629.
265. Bellon A, Luchino J, Haigh K, Rougon G, Haigh J, Chauvet S, et al. VEGFR2 (KDR/Flk1) signaling mediates axon growth in response to semaphorin 3E in the developing brain. Neuron. 2010;66(2):205-19.
266. Olsson AK, Dimberg A, Kreuger J, Claesson-Welsh L. VEGF receptor signalling - in control of vascular function. Nat Rev Mol Cell Biol. 2006;7(5):359-71.
267. Peng FW, Liu DK, Zhang QW, Xu YG, Shi L. VEGFR-2 inhibitors and the therapeutic applications thereof: a patent review (2012-2016). Expert Opin Ther Pat. 2017;27(9):987-1004.
268. Falcon BL, Chintharlapalli S, Uhlik MT, Pytowski B. Antagonist antibodies to vascular endothelial growth factor receptor 2 (VEGFR-2) as anti-angiogenic agents. Pharmacology & therapeutics. 2016;164:204-25.
269. Parveen A, Subedi L, Kim HW, Khan Z, Zahra Z, Farooqi MQ, et al. Phytochemicals targeting VEGF and VEGF-related multifactors as anticancer therapy. Journal of clinical medicine. 2019;8(3):350.
270. Ishigami S, Arii S, Furutani M, Niwano M, Harada T, Mizumoto M, et al. Predictive value of vascular endothelial growth factor (VEGF) in metastasis and prognosis of human colorectal cancer. British journal of cancer. 1998;78(10):1379-84.
271. O'Byrne KJ, Koukourakis MI, Giatromanolaki A, Cox G, Turley H, Steward WP, et al. Vascular endothelial growth factor, platelet-derived endothelial cell growth factor and angiogenesis in non-small-cell lung cancer. Br J Cancer. 2000;82(8):1427-32.
272. Inoue K, Slaton JW, Davis DW, Hicklin DJ, McConkey DJ, Karashima T, et al. Treatment of human metastatic transitional cell carcinoma of the bladder in a murine model with the anti-vascular endothelial growth factor receptor monoclonal antibody DC101 and paclitaxel. Clin Cancer Res. 2000;6(7):2635-43.
273. Warren RS, Yuan H, Matli MR, Gillett NA, Ferrara N. Regulation by vascular endothelial growth factor of human colon cancer tumorigenesis in a mouse model of experimental liver metastasis. J Clin Invest. 1995;95(4):1789-97.
274. Ramos TN, Bullard DC, Barnum SR. ICAM-1: isoforms and phenotypes. The Journal of Immunology. 2014;192(10):4469-74.
275. Evans CE, Branco-Price C, Johnson RS. HIF-mediated endothelial response during cancer progression. Int J Hematol. 2012;95(5):471-7.
276. Radisavljevic Z, Avraham H, Avraham S. Vascular endothelial growth factor up-regulates ICAM-1 expression via the phosphatidylinositol 3 OH-kinase/AKT/Nitric oxide pathway and modulates migration of brain microvascular endothelial cells. J Biol Chem. 2000;275(27):20770-4.
277. Roebuck KA, Finnegan A. Regulation of intercellular adhesion molecule-1 (CD54) gene expression. J Leukoc Biol. 1999;66(6):876-88.
278. Kevil CG, Orr AW, Langston W, Mickett K, Murphy-Ullrich J, Patel RP, et al. Intercellular adhesion molecule-1 (ICAM-1) regulates endothelial cell motility through a nitric oxide-dependent pathway. J Biol Chem. 2004;279(18):19230-8.

279. Minajeva A, Kase M, Saretok M, Adamson-Raieste A, Kase S, Niinepuu K, et al. Impact of Blood Vessel Quantity and Vascular Expression of CD133 and ICAM-1 on Survival of Glioblastoma Patients. Neurosci J. 2017;2017:5629563.
280. Usami Y, Ishida K, Sato S, Kishino M, Kiryu M, Ogawa Y, et al. Intercellular adhesion molecule-1 (ICAM-1) expression correlates with oral cancer progression and induces macrophage/cancer cell adhesion. Int J Cancer. 2013;133(3):568-78.
281. Clark PR, Manes TD, Pober JS, Kluger MS. Increased ICAM-1 expression causes endothelial cell leakiness, cytoskeletal reorganization and junctional alterations. Journal of Investigative Dermatology. 2007;127(4):762-74.
282. Sumagin R, Kuebel JM, Sarelius IH. Leukocyte rolling and adhesion both contribute to regulation of microvascular permeability to albumin via ligation of ICAM-1. American Journal of Physiology-Cell Physiology. 2011;301(4):C804-C13.
283. Sarelius IH, Glading AJ. Control of vascular permeability by adhesion molecules. Tissue Barriers. 2015;3(1-2):e985954.
284. Kopczynska E, Makarewicz R. Endoglin - a marker of vascular endothelial cell proliferation in cancer. Contemp Oncol (Pozn). 2012;16(1):68-71.
285. Li C, Issa R, Kumar P, Hampson IN, Lopez-Novoa JM, Bernabeu C, et al. CD105 prevents apoptosis in hypoxic endothelial cells. Journal of cell science. 2003;116(13):2677-85.
286. Fonsatti E, Nicolay HJ, Altomonte M, Covre A, Maio M. Targeting cancer vasculature via endoglin/CD105: a novel antibody-based diagnostic and therapeutic strategy in solid tumours. Cardiovasc Res. 2010;86(1):12-9.
287. Sánchez-Elsner T, Botella LM, Velasco B, Langa C, Bernabéu C. Endoglin expression is regulated by transcriptional cooperation between the hypoxia and transforming growth factor-β pathways. Journal of Biological Chemistry. 2002;277(46):43799-808.
288. Li C, Issa R, Kumar P, Hampson IN, Lopez-Novoa JM, Bernabeu C, et al. CD105 prevents apoptosis in hypoxic endothelial cells. J Cell Sci. 2003;116(Pt 13):2677-85.
289. Fonsatti E, Altomonte M, Nicotra MR, Natali PG, Maio M. Endoglin (CD105): a powerful therapeutic target on tumor-associated angiogenetic blood vessels. Oncogene. 2003;22(42):6557-63.
290. Behrem S, Žarković K, Eškinja N, Jonjić N. Endoglin is a better marker than CD31 in evaluation of angiogenesis in glioblastoma. Croatian medical journal. 2005;46(3).
291. Taskiran C, Erdem O, Onan A, Arisoy O, Acar A, Vural C, et al. The prognostic value of endoglin (CD105) expression in ovarian carcinoma. Int J Gynecol Cancer. 2006;16(5):1789-93.
292. Salvesen HB, Gulluoglu MG, Stefansson I, Akslen LA. Significance of CD 105 expression for tumour angiogenesis and prognosis in endometrial carcinomas. APMIS. 2003;111(11):1011-8.
293. White J, Jiang Z, Diamond M, Saed G. Hypoxia induces transforming growth factor beta 1 (TGFβ1) in human macrophages through a hypoxia inducible factor 1α (HIF-1α)–dependent mechanism. Fertility and Sterility. 2009;92(3):S124.
294. Gory-Faure S, Prandini MH, Pointu H, Roullot V, Pignot-Paintrand I, Vernet M, et al. Role of vascular endothelial-cadherin in vascular morphogenesis. Development. 1999;126(10):2093-102.
295. Corada M, Mariotti M, Thurston G, Smith K, Kunkel R, Brockhaus M, et al. Vascular endothelial–cadherin is an important determinant of microvascular integrity in vivo. Proceedings of the National Academy of Sciences. 1999;96(17):9815-20.
296. Gavard J. Endothelial permeability and VE-cadherin: a wacky comradeship. Cell adhesion & migration. 2013;7(6):465-71.
297. Azzi S, Hebda JK, Gavard J. Vascular permeability and drug delivery in cancers. Front Oncol. 2013;3:211.

298. Zhao Y, Ting KK, Li J, Cogger VC, Chen J, Johansson-Percival A, et al. Targeting Vascular Endothelial-Cadherin in Tumor-Associated Blood Vessels Promotes T-cell-Mediated Immunotherapy. Cancer Res. 2017;77(16):4434-47.
299. Bartolome RA, Torres S, Isern de Val S, Escudero-Paniagua B, Calvino E, Teixido J, et al. VE-cadherin RGD motifs promote metastasis and constitute a potential therapeutic target in melanoma and breast cancers. Oncotarget. 2017;8(1):215-27.
300. Gavard J. Endothelial permeability and VE-cadherin: a wacky comradeship. Cell Adh Migr. 2013;7(6):455-61.
301. Dejana E, Orsenigo F, Lampugnani MG. The role of adherens junctions and VE-cadherin in the control of vascular permeability. J Cell Sci. 2008;121(Pt 13):2115-22.
302. Lehmann JM, Riethmüller G, Johnson JP. MUC18, a marker of tumor progression in human melanoma, shows sequence similarity to the neural cell adhesion molecules of the immunoglobulin superfamily. Proceedings of the National Academy of Sciences. 1989;86(24):9891-5.
303. Shih IM, Elder DE, Speicher D, Johnson JP, Herlyn M. Isolation and functional characterization of the A32 melanoma-associated antigen. Cancer Res. 1994;54(9):2514-20.
304. Bardin N, Frances V, Lesaule G, Horschowski N, George F, Sampol J. Identification of the S-Endo 1 endothelial-associated antigen. Biochem Biophys Res Commun. 1996;218(1):210-6.
305. Wallez Y, Huber P. Endothelial adherens and tight junctions in vascular homeostasis, inflammation and angiogenesis. Biochim Biophys Acta. 2008;1778(3):794-809.
306. Dejana E, Orsenigo F, Molendini C, Baluk P, McDonald DM. Organization and signaling of endothelial cell-to-cell junctions in various regions of the blood and lymphatic vascular trees. Cell and tissue research. 2009;335(1):17-25.
307. Espagnolle N, Guilloton F, Deschaseaux F, Gadelorge M, Sensébé L, Bourin P. CD 146 expression on mesenchymal stem cells is associated with their vascular smooth muscle commitment. Journal of cellular and molecular medicine. 2014;18(1):104-14.
308. Maier CL, Shepherd BR, Yi T, Pober JS. Explant outgrowth, propagation and characterization of human pericytes. Microcirculation. 2010;17(5):367-80.
309. Jiang T, Zhuang J, Duan H, Luo Y, Zeng Q, Fan K, et al. CD146 is a coreceptor for VEGFR-2 in tumor angiogenesis. Blood, The Journal of the American Society of Hematology. 2012;120(11):2330-9.
310. Bardin N, Blot-Chabaud M, Despoix N, Kebir A, Harhouri K, Arsanto JP, et al. CD146 and its soluble form regulate monocyte transendothelial migration. Arterioscler Thromb Vasc Biol. 2009;29(5):746-53.
311. Simon GC, Martin RJ, Smith S, Thaikoottathil J, Bowler RP, Barenkamp SJ, et al. Up-regulation of MUC18 in airway epithelial cells by IL-13: implications in bacterial adherence. Am J Respir Cell Mol Biol. 2011;44(5):606-13.
312. Tsuchiya S, Tsukamoto Y, Taira E, LaMarre J. Involvement of transforming growth factor-beta in the expression of gicerin, a cell adhesion molecule, in the regeneration of hepatocytes. Int J Mol Med. 2007;19(3):381-6.
313. Yan X, Lin Y, Yang D, Shen Y, Yuan M, Zhang Z, et al. A novel anti-CD146 monoclonal antibody, AA98, inhibits angiogenesis and tumor growth. Blood. 2003;102(1):184-91.
314. Kratzer A, Chu HW, Salys J, Moumen Z, Leberl M, Bowler R, et al. Endothelial cell adhesion molecule CD146: implications for its role in the pathogenesis of COPD. J Pathol. 2013;230(4):388-98.
315. Riazy M, Chen JH, Steinbrecher UP. VEGF secretion by macrophages is stimulated by lipid and protein components of OxLDL via PI3-kinase and PKCζ activation and is independent of OxLDL uptake. Atherosclerosis. 2009;204(1):47-54.

316. Wu W-K, Llewellyn OP, Bates DO, Nicholson LB, Dick AD. IL-10 regulation of macrophage VEGF production is dependent on macrophage polarisation and hypoxia. Immunobiology. 2010;215(9-10):796-803.
317. Obeid E, Nanda R, Fu YX, Olopade OI. The role of tumor-associated macrophages in breast cancer progression (review). Int J Oncol. 2013;43(1):5-12.
318. Waltenberger J, Mayr U, Pentz S, Hombach V. Functional upregulation of the vascular endothelial growth factor receptor KDR by hypoxia. Circulation. 1996;94(7):1647-54.
319. Zund G, Uezono S, Stahl GL, Dzus AL, McGowan FX, Hickey PR, et al. Hypoxia enhances induction of endothelial ICAM-1: role for metabolic acidosis and proteasomes. Am J Physiol. 1997;273(5):C1571-80.
320. Clark PR, Manes TD, Pober JS, Kluger MS. Increased ICAM-1 expression causes endothelial cell leakiness, cytoskeletal reorganization and junctional alterations. J Invest Dermatol. 2007;127(4):762-74.
321. Ruco LP, de Laat PA, Matteucci C, Bernasconi S, Sciacca FM, van der Kwast TH, et al. Expression of ICAM-1 and VCAM-1 in human malignant mesothelioma. J Pathol. 1996;179(3):266-71.
322. Podgrabinska S, Kamalu O, Mayer L, Shimaoka M, Snoeck H, Randolph GJ, et al. Inflamed lymphatic endothelium suppresses dendritic cell maturation and function via Mac-1/ICAM-1-dependent mechanism. J Immunol. 2009;183(3):1767-79.
323. Gong L, Mi HJ, Zhu H, Zhou X, Yang H. P-selectin-mediated platelet activation promotes adhesion of non-small cell lung carcinoma cells on vascular endothelial cells under flow. Mol Med Rep. 2012;5(4):935-42.
324. Dymicka-Piekarska V, Kemona H. Does colorectal cancer clinical advancement affect adhesion molecules (sP-selectin, sE-selectin and ICAM-1) concentration? Thrombosis research. 2009;124(1):80-3.
325. Basoglu M, Atamanalp S, Yildirgan M, Aydinli B, Öztürk G, Akçay F, et al. Correlation between the serum values of soluble intercellular adhesion molecule-1 and total sialic acid levels in patients with breast cancer. European Surgical Research. 2007;39(3):136-40.
326. Dowlati A, Gray R, Sandler AB, Schiller JH, Johnson DH. Cell adhesion molecules, vascular endothelial growth factor, and basic fibroblast growth factor in patients with non-small cell lung cancer treated with chemotherapy with or without bevacizumab--an Eastern Cooperative Oncology Group Study. Clin Cancer Res. 2008;14(5):1407-12.
327. Laurent VM, Duperray A, Sundar Rajan V, Verdier C. Atomic force microscopy reveals a role for endothelial cell ICAM-1 expression in bladder cancer cell adherence. PLoS One. 2014;9(5):e98034.
328. Sipos E, Chen L, Andras IE, Wrobel J, Zhang B, Pu H, et al. Proinflammatory adhesion molecules facilitate polychlorinated biphenyl-mediated enhancement of brain metastasis formation. Toxicol Sci. 2012;126(2):362-71.
329. Iida T, Mine S, Fujimoto H, Suzuki K, Minami Y, Tanaka Y. Hypoxia-inducible factor-1alpha induces cell cycle arrest of endothelial cells. Genes Cells. 2002;7(2):143-9.
330. Funamoto K, Yoshino D, Matsubara K, Zervantonakis IK, Funamoto K, Nakayama M, et al. Endothelial monolayer permeability under controlled oxygen tension. Integr Biol (Camb). 2017;9(6):529-38.
331. Bidlingmaier S, He J, Wang Y, An F, Feng J, Barbone D, et al. Identification of MCAM/CD146 as the target antigen of a human monoclonal antibody that recognizes both epithelioid and sarcomatoid types of mesothelioma. Cancer research. 2009;69(4):1570-7.
332. Wragg JW, Finnity JP, Anderson JA, Ferguson HJ, Porfiri E, Bhatt RI, et al. MCAM and LAMA4 are highly enriched in tumor blood vessels of renal cell carcinoma and predict patient outcome. Cancer research. 2016;76(8):2314-26.

333. Ma J, Xu H, Wang S. Immunosuppressive Role of Myeloid-Derived Suppressor Cells and Therapeutic Targeting in Lung Cancer. J Immunol Res. 2018;2018:6319649.
334. Benner B, Scarberry L, Suarez-Kelly LP, Duggan MC, Campbell AR, Smith E, et al. Generation of monocyte-derived tumor-associated macrophages using tumor-conditioned media provides a novel method to study tumor-associated macrophages in vitro. Journal for immunotherapy of cancer. 2019;7(1):1-14.
335. Biswas SK, Sica A, Lewis CE. Plasticity of macrophage function during tumor progression: regulation by distinct molecular mechanisms. J Immunol. 2008;180(4):2011-7.
336. Sica A, Larghi P, Mancino A, Rubino L, Porta C, Totaro MG, et al., editors. Macrophage polarization in tumour progression. Seminars in cancer biology; 2008: Elsevier.
337. Long KB, Beatty GL. Harnessing the antitumor potential of macrophages for cancer immunotherapy. Oncoimmunology. 2013;2(12):e26860.
338. Ren F, Fan M, Mei J, Wu Y, Liu C, Pu Q, et al. Interferon-γ and celecoxib inhibit lung-tumor growth through modulating M2/M1 macrophage ratio in the tumor microenvironment. Drug design, development and therapy. 2014;8:1527.
339. Torroella-Kouri M, Silvera R, Rodriguez D, Caso R, Shatry A, Opiela S, et al. Identification of a subpopulation of macrophages in mammary tumor–bearing mice that are neither M1 nor M2 and are less differentiated. Cancer research. 2009;69(11):4800-9.
340. Jackaman C, Lew AM, Zhan Y, Allan JE, Koloska B, Graham PT, et al. Deliberately provoking local inflammation drives tumors to become their own protective vaccine site. International immunology. 2008;20(11):1467-79.
341. Rolny C, Mazzone M, Tugues S, Laoui D, Johansson I, Coulon C, et al. HRG inhibits tumor growth and metastasis by inducing macrophage polarization and vessel normalization through downregulation of PlGF. Cancer cell. 2011;19(1):31-44.
342. Huang Y, Yuan J, Righi E, Kamoun WS, Ancukiewicz M, Nezivar J, et al. Vascular normalizing doses of antiangiogenic treatment reprogram the immunosuppressive tumor microenvironment and enhance immunotherapy. Proc Natl Acad Sci U S A. 2012;109(43):17561-6.
343. Chen P, Bonaldo P. Role of macrophage polarization in tumor angiogenesis and vessel normalization: implications for new anticancer therapies. Int Rev Cell Mol Biol. 2013;301:1-35.
344. Cully M. Cancer: Tumour vessel normalization takes centre stage. Nat Rev Drug Discov. 2017;16(2):87.
345. Li W, Quan YY, Li Y, Lu L, Cui M. Monitoring of tumor vascular normalization: the key points from basic research to clinical application. Cancer Manag Res. 2018;10:4163-72.
346. Jackaman C, Cornwall S, Graham PT, Nelson DJ. CD40-activated B cells contribute to mesothelioma tumor regression. Immunology and cell biology. 2011;89(2):255-67.
347. Nelson D, Fisher S, Robinson B. The "Trojan Horse" approach to tumor immunotherapy: targeting the tumor microenvironment. Journal of immunology research. 2014;2014.
348. Jackaman C, Nelson DJ. Intratumoral interleukin-2/agonist CD40 antibody drives CD4+-independent resolution of treated-tumors and CD4+-dependent systemic and memory responses. Cancer Immunology, Immunotherapy. 2012;61(4):549-60.
349. Jackaman C, Lansley S, Allan JE, Robinson BW, Nelson DJ. IL-2/CD40-driven NK cells install and maintain potency in the anti-mesothelioma effector/memory phase. Int Immunol. 2012;24(6):357-68.
350. Langston PK, Shibata M, Horng T. Metabolism Supports Macrophage Activation. Front Immunol. 2017;8:61.
351. Viola A, Munari F, Sanchez-Rodriguez R, Scolaro T, Castegna A. The Metabolic Signature of Macrophage Responses. Front Immunol. 2019;10:1462.

352. Edmondson R, Broglie JJ, Adcock AF, Yang L. Three-dimensional cell culture systems and their applications in drug discovery and cell-based biosensors. Assay Drug Dev Technol. 2014;12(4):207-18.
353. Kaku Y, Imaoka H, Morimatu Y, Matsuoka M, Natori H, Suetomo M, et al. M2 macrophage marker CD163, CD204 and CD206 expression on alveolar macrophages in the lung of patients with chronic obstructive pulmonary. European Respiratory Journal. 2014;44(Suppl 58).
354. Mantovani A, Biswas SK, Galdiero MR, Sica A, Locati M. Macrophage plasticity and polarization in tissue repair and remodelling. J Pathol. 2013;229(2):176-85.
355. Mak IW, Evaniew N, Ghert M. Lost in translation: animal models and clinical trials in cancer treatment. American journal of translational research. 2014;6(2):114-8.
356. Gong X, Lin C, Cheng J, Su J, Zhao H, Liu T, et al. Generation of Multicellular Tumor Spheroids with Microwell-Based Agarose Scaffolds for Drug Testing. PLoS One. 2015;10(6):e0130348.
357. Horning JL, Sahoo SK, Vijayaraghavalu S, Dimitrijevic S, Vasir JK, Jain TK, et al. 3-D tumor model for in vitro evaluation of anticancer drugs. Molecular pharmaceutics. 2008;5(5):849-62.
358. Gurski LA, Jha AK, Zhang C, Jia X, Farach-Carson MC. Hyaluronic acid-based hydrogels as 3D matrices for in vitro evaluation of chemotherapeutic drugs using poorly adherent prostate cancer cells. Biomaterials. 2009;30(30):6076-85.
359. Loessner D, Stok KS, Lutolf MP, Hutmacher DW, Clements JA, Rizzi SC. Bioengineered 3D platform to explore cell–ECM interactions and drug resistance of epithelial ovarian cancer cells. Biomaterials. 2010;31(32):8494-506.
360. Charoen KM, Fallica B, Colson YL, Zaman MH, Grinstaff MW. Embedded multicellular spheroids as a biomimetic 3D cancer model for evaluating drug and drug-device combinations. Biomaterials. 2014;35(7):2264-71.
361. Talukder MA, Menyuk CR, Kostov Y. Distinguishing between whole cells and cell debris using surface plasmon coupled emission. Biomed Opt Express. 2018;9(4):1977-91.
362. Duong L, Radley-Crabb HG, Gardner JK, Tomay F, Dye DE, Grounds MD, et al. Macrophage Depletion in Elderly Mice Improves Response to Tumor Immunotherapy, Increases Anti-tumor T Cell Activity and Reduces Treatment-Induced Cachexia. Frontiers in Genetics. 2018;9(526).
363. Marcq E, Siozopoulou V, De Waele J, van Audenaerde J, Zwaenepoel K, Santermans E, et al. Prognostic and predictive aspects of the tumor immune microenvironment and immune checkpoints in malignant pleural mesothelioma. Oncoimmunology. 2016;6(1):e1261241-e.
364. Yella VR, Bansal M. In silico Identification of Eukaryotic Promoters. Systems and synthetic biology: Springer; 2015. p. 63-75.
365. Javan B, Shahbazi M. Hypoxia-inducible tumour-specific promoters as a dual-targeting transcriptional regulation system for cancer gene therapy. ecancermedicalscience. 2017;11.
366. Domènec Farré RR, Mario Huerta, José E. Adsuara, Llorenç Roselló, M.Mar Albà, Xavier Messeguer. Identification of patterns in biological sequences at the ALGGEN server: PROMO and MALGEN. Nucleic Acids Res,. 2003; 31,(13,):3651-3,.
367. Kaelin WG, Jr., Ratcliffe PJ. Oxygen sensing by metazoans: the central role of the HIF hydroxylase pathway. Mol Cell. 2008;30(4):393-402.
368. Bruegge K, Jelkmann W, Metzen E. Hydroxylation of hypoxia-inducible transcription factors and chemical compounds targeting the HIF-alpha hydroxylases. Curr Med Chem. 2007;14(17):1853-62.
369. Wigerup C, Påhlman S, Bexell D. Therapeutic targeting of hypoxia and hypoxia-inducible factors in cancer. Pharmacology & therapeutics. 2016;164:152-69.

370. Chen L, Endler A, Shibasaki F. Hypoxia and angiogenesis: regulation of hypoxia-inducible factors via novel binding factors. Experimental & Molecular Medicine. 2009;41(12):849-57.
371. Zhao X, Liu L, Li R, Wei X, Luan W, Liu P, et al. Hypoxia-Inducible Factor 1-α (HIF-1α) Induces Apoptosis of Human Uterosacral Ligament Fibroblasts Through the Death Receptor and Mitochondrial Pathways. Medical science monitor : international medical journal of experimental and clinical research. 2018;24:8722-33.
372. Elks PM, van Eeden FJ, Dixon G, Wang X, Reyes-Aldasoro CC, Ingham PW, et al. Activation of hypoxia-inducible factor-1α (Hif-1α) delays inflammation resolution by reducing neutrophil apoptosis and reverse migration in a zebrafish inflammation model. Blood. 2011;118(3):712-22.
373. Girgis CM, Cheng K, Scott CH, Gunton JE. Novel links between HIFs, type 2 diabetes, and metabolic syndrome. Trends in Endocrinology & Metabolism. 2012;23(8):372-80.
374. Skuli N, Liu L, Runge A, Wang T, Yuan L, Patel S, et al. Endothelial deletion of hypoxia-inducible factor-2alpha (HIF-2alpha) alters vascular function and tumor angiogenesis. Blood. 2009;114(2):469-77.
375. Fordel E, Geuens E, Dewilde S, De Coen W, Moens L. Hypoxia/ischemia and the regulation of neuroglobin and cytoglobin expression. IUBMB life. 2004;56(11-12):681-7.
376. Rashid I, Pathak AK, Kumar R, Srivastava P, Singh M, Murali S, et al. Genome-Wide comparative analysis of HIF binding sites in Cyprinus carpio for in silico identification of functional hypoxia response elements. Frontiers in genetics. 2019;10.
377. Riethoven J-JM. Regulatory regions in DNA: promoters, enhancers, silencers, and insulators. Computational biology of transcription factor binding: Springer; 2010. p. 33-42.
378. Butler JE, Kadonaga JT. The RNA polymerase II core promoter: a key component in the regulation of gene expression. Genes & development. 2002;16(20):2583-92.
379. Sarda S, Das A, Vinson C, Hannenhalli S. Distal CpG islands can serve as alternative promoters to transcribe genes with silenced proximal promoters. Genome research. 2017;27(4):553-66.
380. Roeder RG. The complexities of eukaryotic transcription initiation: regulation of preinitiation complex assembly. Trends in biochemical sciences. 1991;16:402-8.
381. Rius J, Guma M, Schachtrup C, Akassoglou K, Zinkernagel AS, Nizet V, et al. NF-kappaB links innate immunity to the hypoxic response through transcriptional regulation of HIF-1alpha. Nature. 2008;453(7196):807-11.
382. Frede S, Stockmann C, Freitag P, Fandrey J. Bacterial lipopolysaccharide induces HIF-1 activation in human monocytes via p44/42 MAPK and NF-κB. Biochemical Journal. 2006;396(3):517-27.
383. D'Ignazio L, Rocha S. Hypoxia Induced NF-κB. Cells. 2016;5(1):10.
384. Mayr B, Montminy M. Transcriptional regulation by the phosphorylation-dependent factor CREB. Nat Rev Mol Cell Biol. 2001;2(8):599-609.
385. Nakayama K. cAMP-response element-binding protein (CREB) and NF-kappaB transcription factors are activated during prolonged hypoxia and cooperatively regulate the induction of matrix metalloproteinase MMP1. J Biol Chem. 2013;288(31):22584-95.
386. Nakayama K, Kataoka N. Regulation of Gene Expression under Hypoxic Conditions. International journal of molecular sciences. 2019;20(13):3278.
387. Toth RK, Warfel NA. Strange Bedfellows: Nuclear Factor, Erythroid 2-Like 2 (Nrf2) and Hypoxia-Inducible Factor 1 (HIF-1) in Tumor Hypoxia. Antioxidants (Basel). 2017;6(2).
388. Levy DE, Darnell JE, Jr. Stats: transcriptional control and biological impact. Nat Rev Mol Cell Biol. 2002;3(9):651-62.
389. Lee MY, Joung YH, Lim EJ, Park JH, Ye SK, Park T, et al. Phosphorylation and activation of STAT proteins by hypoxia in breast cancer cells. Breast. 2006;15(2):187-95.

390. Nakayama K, Kataoka N. Regulation of Gene Expression under Hypoxic Conditions. Int J Mol Sci. 2019;20(13).
391. Tansey WP. Mammalian MYC Proteins and Cancer. New Journal of Science. 2014;2014:757534.
392. Dang CV, Le A, Gao P. MYC-Induced Cancer Cell Energy Metabolism and Therapeutic Opportunities. Clinical Cancer Research. 2009;15(21):6479-83.
393. Zhang Q, Xu P, Lu Y, Dou H. Correlation of MACC1/c-Myc expression in endometrial carcinoma with clinical/pathological features or prognosis. Medical science monitor: international medical journal of experimental and clinical research. 2018;24:4738.
394. Haeussler M, Zweig AS, Tyner C, Speir ML, Rosenbloom KR, Raney BJ, et al. The UCSC genome browser database: 2019 update. Nucleic acids research. 2019;47(D1):D853-D8.
395. Schmid CD, Praz V, Delorenzi M, Périer R, Bucher P. The Eukaryotic Promoter Database EPD: the impact of in silico primer extension. Nucleic acids research. 2004;32(suppl_1):D82-D5.
396. Messeguer X, Escudero R, Farré D, Nuñez O, Martínez J, Albà MM. PROMO: detection of known transcription regulatory elements using species-tailored searches. Bioinformatics. 2002;18(2):333-4.
397. Briones-Orta MA, Avendaño-Vázquez SE, Ivette Aparicio-Bautista D, Coombes JD, Weber GF, Syn W-K. Prediction of transcription factor bindings sites affected by SNPs located at the osteopontin promoter. Data Brief. 2017;14:538-42.
398. Messeguer X, Escudero R, Farré D, Núñez O, Martínez J, Albà MM. PROMO: detection of known transcription regulatory elements using species-tailored searches. Bioinformatics. 2002;18(2):333-4.
399. Klabatsa A, Sheaff M, Steele J, Evans M, Rudd R, Fennell D. Expression and prognostic significance of hypoxia-inducible factor 1α (HIF-1α) in malignant pleural mesothelioma (MPM). Lung cancer. 2006;51(1):53-9.
400. Kim M-C, Hwang S-H, Kim N-Y, Lee H-S, Ji S, Yang Y, et al. Hypoxia promotes acquisition of aggressive phenotypes in human malignant mesothelioma. BMC Cancer. 2018;18(1):819.
401. Abhinand CS, Raju R, Soumya SJ, Arya PS, Sudhakaran PR. VEGF-A/VEGFR2 signaling network in endothelial cells relevant to angiogenesis. J Cell Commun Signal. 2016;10(4):347-54.
402. Sunitha P, Raju R, Sajil CK, Abhinand CS, Nair AS, Oommen OV, et al. Temporal VEGFA responsive genes in HUVECs: Gene signatures and potential ligands/receptors fine-tuning angiogenesis. Journal of cell communication and signaling. 2019;13(4):561-71.
403. Zagórska A, Dulak J. HIF-1: the knowns and unknowns of hypoxia sensing. Acta Biochim Pol. 2004;51(3):563-85.
404. Wenger RH, Stiehl DP, Camenisch G. Integration of oxygen signaling at the consensus HRE. Sci STKE. 2005;2005(306):re12.
405. Semenza GL. Regulation of oxygen homeostasis by hypoxia-inducible factor 1. Physiology (Bethesda). 2009;24:97-106.
406. Majmundar AJ, Wong WJ, Simon MC. Hypoxia-inducible factors and the response to hypoxic stress. Mol Cell. 2010;40(2):294-309.
407. Qiu Y-Q. KEGG Pathway Database. In: Dubitzky W, Wolkenhauer O, Cho K-H, Yokota H, editors. Encyclopedia of Systems Biology. New York, NY: Springer New York; 2013. p. 1068-9.
408. Holmes K, Roberts OL, Thomas AM, Cross MJ. Vascular endothelial growth factor receptor-2: structure, function, intracellular signalling and therapeutic inhibition. Cellular signalling. 2007;19(10):2003-12.

409. Liang X, Arullampalam P, Yang Z, Ming X-F. Hypoxia Enhances Endothelial Intercellular Adhesion Molecule 1 Protein Level Through Upregulation of Arginase Type II and Mitochondrial Oxidative Stress. Frontiers in physiology. 2019;10:1003-.
410. Lee J, Chuang TH, Redecke V, She L, Pitha PM, Carson DA, et al. Molecular basis for the immunostimulatory activity of guanine nucleoside analogs: activation of Toll-like receptor 7. Proc Natl Acad Sci U S A. 2003;100(11):6646-51.
411. Ito T, Amakawa R, Kaisho T, Hemmi H, Tajima K, Uehira K, et al. Interferon-alpha and interleukin-12 are induced differentially by Toll-like receptor 7 ligands in human blood dendritic cell subsets. J Exp Med. 2002;195(11):1507-12.
412. Heil F, Ahmad-Nejad P, Hemmi H, Hochrein H, Ampenberger F, Gellert T, et al. The Toll-like receptor 7 (TLR7)-specific stimulus loxoribine uncovers a strong relationship within the TLR7, 8 and 9 subfamily. Eur J Immunol. 2003;33(11):2987-97.
413. Lu M, Perez VL, Ma N, Miyamoto K, Peng HB, Liao JK, et al. VEGF increases retinal vascular ICAM-1 expression in vivo. Invest Ophthalmol Vis Sci. 1999;40(8):1808-12.
414. Kim I, Moon SO, Kim SH, Kim HJ, Koh YS, Koh GY. Vascular endothelial growth factor expression of intercellular adhesion molecule 1 (ICAM-1), vascular cell adhesion molecule 1 (VCAM-1), and E-selectin through nuclear factor-kappa B activation in endothelial cells. J Biol Chem. 2001;276(10):7614-20.
415. Semenza GL. Oxygen sensing, hypoxia-inducible factors, and disease pathophysiology. Annu Rev Pathol. 2014;9:47-71.
416. Kopczyńska E, Makarewicz R. Endoglin - a marker of vascular endothelial cell proliferation in cancer. Contemporary oncology (Poznan, Poland). 2012;16(1):68-71.
417. Mineo TC, Ambrogi V, Baldi A, Rabitti C, Bollero P, Vincenzi B, et al. Prognostic impact of VEGF, CD31, CD34, and CD105 expression and tumour vessel invasion after radical surgery for IB-IIA non-small cell lung cancer. J Clin Pathol. 2004;57(6):591-7.
418. Ilhan N, Gungor H, Gul HF, Eroksuz H. Expression of endoglin and vascular endothelial growth factor as prognostic markers in experimental colorectal cancer. Anticancer research. 2016;36(8):3953-9.
419. Bishop GA, Moore CR, Xie P, Stunz LL, Kraus ZJ. TRAF proteins in CD40 signaling. Adv Exp Med Biol. 2007;597:131-51.
420. Säemann MD, Diakos C, Kelemen P, Kriehuber E, Zeyda M, Böhmig GA, et al. Prevention of CD40-triggered dendritic cell maturation and induction of T-cell hyporeactivity by targeting of Janus kinase 3. Am J Transplant. 2003;3(11):1341-9.
421. Säemann MD, Kelemen P, Zeyda M, Böhmig G, Staffler G, Zlabinger GJ. CD40 triggered human monocyte-derived dendritic cells convert to tolerogenic dendritic cells when JAK3 activity is inhibited. Transplant Proc. 2002;34(5):1407-8.
422. Liao W, Lin JX, Leonard WJ. Interleukin-2 at the crossroads of effector responses, tolerance, and immunotherapy. Immunity. 2013;38(1):13-25.
423. Liu KD, Gaffen SL, Goldsmith MA, Greene WC. Janus kinases in interleukin-2-mediated signaling: JAK1 and JAK3 are differentially regulated by tyrosine phosphorylation. Curr Biol. 1997;7(11):817-26.
424. Gaffen SL, LAi SY, Xu W, Gouilleux F, Groner B, Goldsmith MA, et al. Signaling through the interleukin 2 receptor beta chain activates a STAT-5-like DNA-binding activity. Proceedings of the National Academy of Sciences. 1995;92(16):7192-6.
425. Gilmour KC, Pine R, Reich NC. Interleukin 2 activates STAT5 transcription factor (mammary gland factor) and specific gene expression in T lymphocytes. Proceedings of the National Academy of Sciences. 1995;92(23):10772-6.
426. Matsumoto A, Masuhara M, Mitsui K, Yokouchi M, Ohtsubo M, Misawa H, et al. CIS, a cytokine inducible SH2 protein, is a target of the JAK-STAT5 pathway and modulates STAT5 activation. Blood. 1997;89(9):3148-54.

427. Minami Y, Nakagawa Y, Kawahara A, Miyazaki T, Sada K, Yamamura H, et al. Protein tyrosine kinase Syk is associated with and activated by the IL-2 receptor: possible link with the c-myc induction pathway. Immunity. 1995;2(1):89-100.
428. Endo K, Takeshita T, Kasai H, Sasaki Y, Tanaka N, Asao H, et al. STAM2, a new member of the STAM family, binding to the Janus kinases. FEBS letters. 2000;477(1-2):55-61.
429. Schulze-Luehrmann J, Ghosh S. Antigen-receptor signaling to nuclear factor κB. Immunity. 2006;25(5):701-15.
430. Bai D, Ueno L, Vogt PK. Akt-mediated regulation of NFkappaB and the essentialness of NFkappaB for the oncogenicity of PI3K and Akt. International journal of cancer. 2009;125(12):2863-70.
431. Jain J, Loh C, Rao A. Transcriptional regulation of the IL-2 gene. Current opinion in immunology. 1995;7(3):333-42.
432. Hegmans JP, Hemmes A, Hammad H, Boon L, Hoogsteden HC, Lambrecht BN. Mesothelioma environment comprises cytokines and T-regulatory cells that suppress immune responses. European Respiratory Journal. 2006;27(6):1086-95.
433. Jackaman C, Cornwall S, Lew AM, Zhan Y, Robinson BW, Nelson DJ. Local effector failure in mesothelioma is not mediated by CD4+ CD25+ T-regulator cells. European Respiratory Journal. 2009;34(1):162-75.
434. del Barrio IM, Penski C, Schlahsa L, Stein RG, Diessner J, Wöckel A, et al. Adenosine-generating ovarian cancer cells attract myeloid cells which differentiate into adenosine-generating tumor associated macrophages–a self-amplifying, CD39-and CD73-dependent mechanism for tumor immune escape. Journal for immunotherapy of cancer. 2016;4(1):1-16.
435. Sek K, Molck C, Stewart GD, Kats L, Darcy PK, Beavis PA. Targeting Adenosine Receptor Signaling in Cancer Immunotherapy. Int J Mol Sci. 2018;19(12).
436. Cekic C, Day YJ, Sag D, Linden J. Myeloid expression of adenosine A2A receptor suppresses T and NK cell responses in the solid tumor microenvironment. Cancer Res. 2014;74(24):7250-9.
437. Jackaman C, Yeoh TL, Acuil ML, Gardner JK, Nelson DJ. Murine mesothelioma induces locally-proliferating IL-10+ TNF-α+ CD206− CX3CR1+ M3 macrophages that can be selectively depleted by chemotherapy or immunotherapy. Oncoimmunology. 2016;5(6):e1173299.
438. Van den Bossche J, O'Neill LA, Menon D. Macrophage immunometabolism: where are we (going)? Trends in immunology. 2017;38(6):395-406.
439. Iida T, Mine S, Fujimoto H, Suzuki K, Minami Y, Tanaka Y. Hypoxia-inducible factor-1α induces cell cycle arrest of endothelial cells. Genes to Cells. 2002;7(2):143-9.
440. Kowanetz M, Ferrara N. Vascular endothelial growth factor signaling pathways: therapeutic perspective. Clin Cancer Res. 2006;12(17):5018-22.